DIASTEREOSELECTIVE CONJUGATE ADDITION REACTIONS USING DIVERSE NUCLEOPHILES ON A VARIETY OF MORITA-BAYLIS-HILLMAN (MBH) ADDUCTS

by

Nafisa Bhom

A dissertation submitted to the Faculty of Science

University of the Witwatersrand

Johannesburg

in fulfilment of the requirements for the degree of Master of Science

7th SEPTEMBER 2023

DECLARATION

I declare that this dissertation is my own work under the supervision of Professor Moira L. Bode. It is being submitted for the degree of Master of Science at the University of the Witwatersrand, Johannesburg. It has not been submitted before for any degree or examination at any other University.

Nafisa

7th SEPTEMBER 2023

ABSTRACT

The Morita-Baylis-Hillman (MBH) reaction involves the formation of a new carbon-carbon bond, generating an MBH adduct. These MBH adducts are multi-functional molecules, which can be used as synthons for the generation of complex and diverse compounds.

The first part of the work described here involved the synthesis of a series of diverse ester and nitrile MBH adducts obtained as racemic mixtures. The MBH adducts were protected using different protecting groups, which could potentially control the diastereoselectivity and the formation of alternative products in the subsequent conjugate addition reaction. Conjugate addition reactions were performed on the protected MBH adducts using different nucleophiles to obtain the product as diastereomers. These reactions were monitored to detect whether diastereomers were obtained or not. The diastereomeric ratios obtained using different substrates, protecting groups and nucleophiles were determined.

The best diastereomeric ratio was 3:1, obtained for the piperidine and benzylamine addition on the TBDMS protected nitrile adducts **192a/b** and **196a/b**. The addition of sulfur nucleophiles gave the conjugate addition product only and the addition of nitrogen nucleophiles gave both conjugate addition and allylic substitution products. It was found that the protecting groups did not have an effect on the diastereomeric ratio obtained, nor on the formation of alternative products. The last step performed in the sequence was the deprotection of the conjugate addition products. The configuration of the major and the minor diastereomers were determined, the major product was assigned as the *syn* diastereomer. The major:minor diastereomeric ratio for compound **208a/b** was 3:1 and for compound **209a/b**, a ratio of 2:1 was obtained.

The next part of the work involved the synthesis of MBH adducts with amide as the electron withdrawing group. The originally proposed route involved the synthesis of MBH esters and their conversion into amides. The conjugate addition reactions were attempted on these amide adducts, but were unsuccessful. A number of alternative routes were attempted for the synthesis of amide adducts and conjugate addition products resulting from these adducts. From all the alternative routes, the best route was the originally proposed route.

ACKNOWLEDGEMENTS

I would like to express my sincere gratitude to my supervisor, Prof Moira L. Bode, for her diligence and her faith in me. Her guidance and significant support carried me through all the stages of my research. I would also like to thank NRF and PMA for their financial assistance and my lab mates for their continuous support. I am extremely thankful to my family and my husband, for their constant encouragement in every part of my research.

LIST OF ABBREVIATIONS

CALB	Lipase B from *candida antarctica*
COSY	Correlation spectroscopy
DABCO	1,4-diazabicyclo[2.2.2]octane
DCM	Dichloromethane
de	Diastereomeric excess
DMAP	4-Dimethylaminopyridine
DMF	Dimethyl formamide
DMSO	Dimethyl sulfoxide
ee	Enantiomeric excess
EWG	Electron withdrawing group
HMBC	Heteronuclear multiple bond correlation
HSQC	Heteronuclear multiple quantum coherence
IR	Infrared
MBH	MORITA-BAYLIS-HILLMAN
MVK	Methyl vinyl ketone
NMR	Nuclear magnetic resonance
TBAF	Tetra-*n*-butylammonium fluoride
TBDMS	*Tert*-butyldimethylsilyl
THF	Tetrahydrofuran
TLC	Thin layer chromatography
TMS	Trimethylsilyl

U.S.	Ultrasound

TABLE OF CONTENTS

CHAPTER ONE

1. INTRODUCTION

1.1. Morita-Baylis-Hillman reaction

1.1.1. General aspects

The formation of a carbon-carbon bond is one of the most essential approaches to obtain diverse molecular frameworks. In fact, it has become one of the most useful tools in modern organic chemistry. Formation of these carbon-carbon bonds remains a fundamental challenge in organic synthesis.[1] Constructing carbon-carbon bonds only at specific positions, in the presence of several competing sites is the current requirement. A number of carbon-carbon bond forming reactions have been discovered and utilized in organic synthesis.[2] Advancement in organic chemistry has confirmed that the effective development of a reaction depends on its atom-economy and selectivity.[3] Among all the fascinating work done on the generation of carbon-carbon bonds, the Morita-Baylis-Hillman (MBH) reaction has become one of the very important and exponentially developing carbon-carbon bond forming reactions.

The MBH reaction occurs by coupling a carbon electrophile **1** and the α-position of an activated alkene **2** through a condensation reaction to generate highly functionalized allylic alcohols **3** (**Scheme 1**).[4] Different carbon electrophiles carrying an electron-deficient sp^2 carbon such as an aldehyde or a ketone have been used for this reaction. This reaction is usually catalyzed by a nucleophilic catalyst such as a tertiary amine or a phosphine catalyst.[5] Significant advancements of the MBH reaction have occurred, due to its ability to generate C-C bonds in an extremely atom economical manner. These advancements include incorporating enantioselectivity, as well as implementing a variation of the MBH reaction, the aza-MBH reaction.[6]

The aza-MBH reaction is very similar to the MBH reaction except that it involves reacting electron deficient alkenes **2** with an imine **1** instead of an aldehyde or a ketone as the carbon electrophile, to generate highly functionalized allylic amines **3** (**Scheme 1**).[7] This aza-MBH reaction has been receiving great attention lately from various organic chemists, since it generates building blocks that are very useful in medicinal chemistry.[8] Development in the aza-MBH reaction involves the application of different imines derived from ketones (ketimines) and aldehydes (aldimines) to

perform this reaction as well as implementing an asymmetric version of the reaction.[6] The scheme below shows the MBH and the aza-MBH reaction.

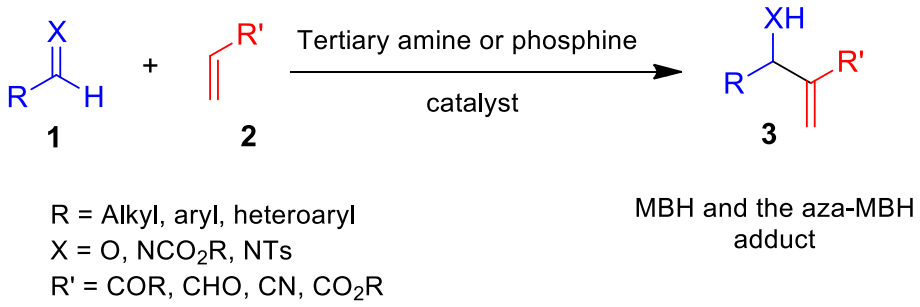

Scheme 1: The Morita-Baylis-Hillman reaction and its variant, the aza-MBH reaction.

The MBH and the aza-MBH reaction results in the formation of a multi-functionalized product known as the MBH and the aza-MBH adduct **3**, respectively (**Scheme 1**). These are very important synthons for the synthesis of natural and unnatural products since they are comprised of different functional groups within close proximity which allows its further transformation.[9] The MBH reaction allows a very convenient and simple approach to obtain highly functionalized molecules, thus emerging as a very important synthetic tool.

1.1.2. Origin and development

The MBH reaction first originated in 1968 in a publication by Morita, and later in 1972 in a German patent by Baylis and Hillman. Morita reported the reaction between an aldehyde **4** and acrylonitriles or acrylates **2** using a phosphine **5** as a catalyst.[10] Later, Baylis and Hillman reported similar type of reactions between aldehydes **4** and different activated alkenes **2** including amides, esters, nitriles and ketones in the presence of a tertiary amine **6** as a catalyst **(Scheme 2)**. Despite the versatility of this reaction, unfortunately, it remained ignored by organic chemists for a very long time after its discovery. However, since the mid-1990s, the reaction and its application have acquired an increasing interest as have its mechanistic details, which have been thoroughly researched and documented.[10,11] This is due to its ability to convert very cheap starting materials in the presence of a suitable catalyst into multifunctional molecules, which can be transformed further.

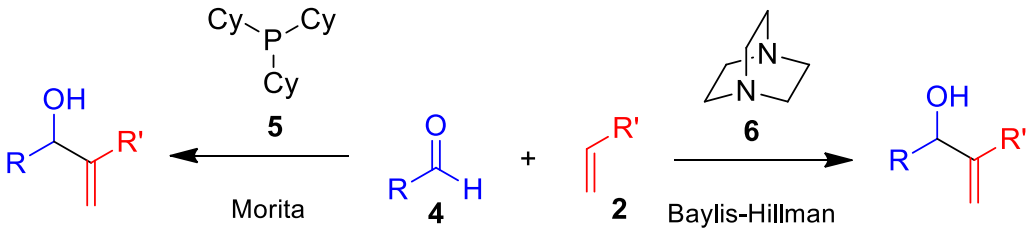

Scheme 2: The Morita Baylis Hillman reaction performed by Morita and Baylis and Hillman, reacting aldehydes with different activated alkenes in the presence of different catalysts.

The MBH reaction plays a very important role in organic synthesis due to its key characteristics such as high atom economy, its eco-friendly nature and the ability for the reaction to be carried out under aqueous medium or solvent-free conditions. It also requires only mild reaction conditions, and it requires starting materials that are commercially available. The product obtained is multifunctional and the reaction is organocatalytic and does not require any heavy metals.[1,3,12,13] The only limitation of the Morita-Baylis Hillman reaction is its long reaction times. However, over the years different experimental protocols have been reported to improve its reaction times and yields, such as using different ionic liquids, using ultrasound, altering catalysts, using high pressure, microwave irradiation, as well as other methods.[14,15]

1.2. Morita Baylis Hillman reaction mechanism

1.2.1. Amine catalyzed mechanism

The MBH mechanism was initially investigated in 1983 by Hoffmann and Rabe.[16] Later, a mechanism was reported by Hills and Isaacs based on rate, pressure dependence and kinetic isotope effect data, which was taken as the most plausible mechanism for a very long time **(Scheme 3)**.[11] This mechanism is comprised of a series of addition-elimination steps. For the reaction between a benzaldehyde **7** and a methyl vinyl ketone **8** in the presence of a DABCO **9** catalyst, the mechanism initiates with the Michael addition of the DABCO **9** to the alkene **8** (**Scheme 3, step 1**), forming a zwitterionic 3-ammonium enolate **10**, followed by an aldol reaction where the enolate **10** adds onto the benzaldehyde **7** (**Scheme 3, step 2**) generating a second zwitterionic intermediate **11**, which goes through an intramolecular proton transfer to form intermediate three, **12** (**Scheme 3, step 3**).[15] This is followed by an E2 or E1cB elimination, releasing product **13** and reforming the catalyst **9** which goes back to the catalytic cycle (**Scheme 3, step 4**).[15,17] The rate determining step in the mechanism was thought to be the aldol reaction step (**Scheme 3, step 2**).

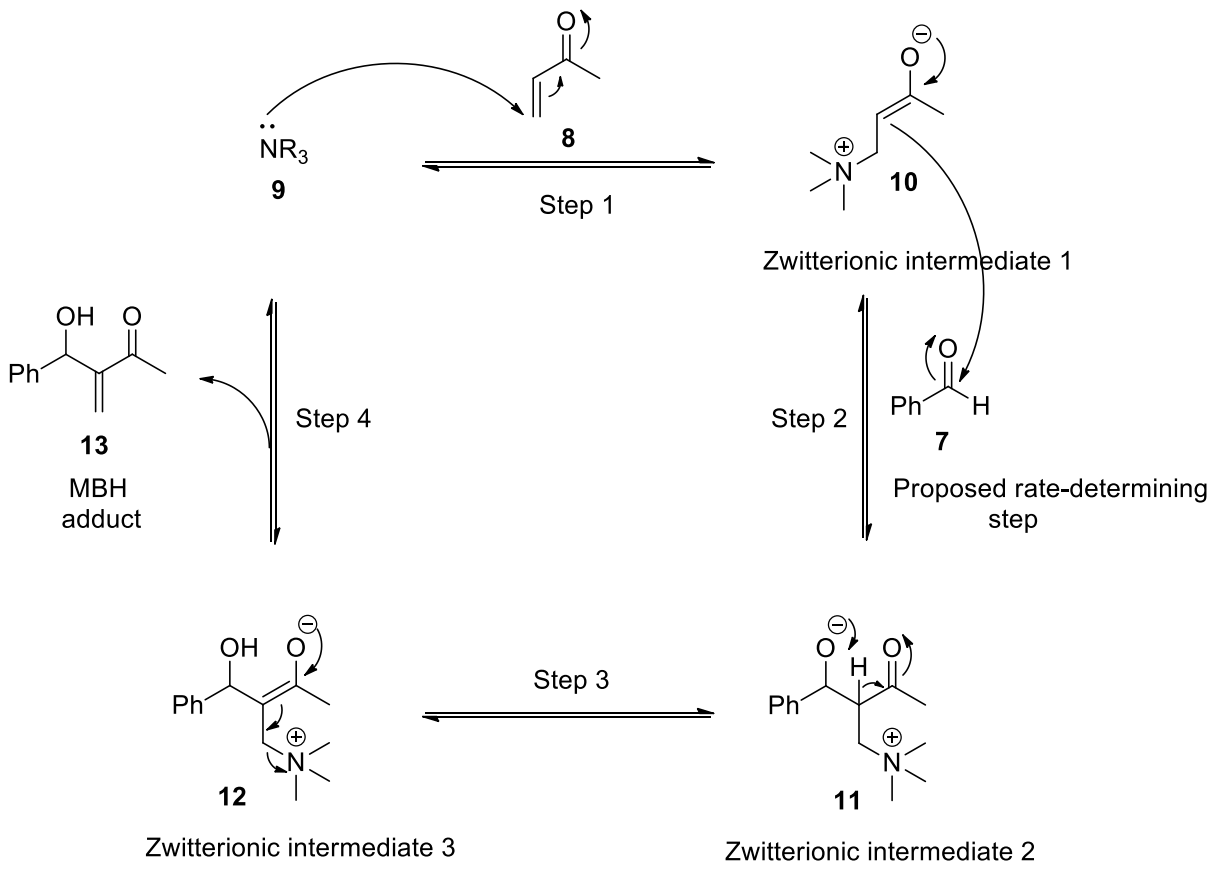

Scheme 3: MBH reaction mechanism proposed by Hill and Isaacs using amine as a catalyst.[15]

This mechanism could explain many observations made in the MBH reaction; however, it was unsuccessful in some cases. For example, the mechanism could not explain why the control of stereochemistry is so difficult in the MBH reaction, the substantial formation of dioxanone as the byproduct and the rate acceleration as the product formed, could not be explained using the above mechanism.[18] Recently, the MBH mechanism involving a hemiacetal intermediate **14** was suggested by McQuade *et al.* based on the reaction rate data obtained in aprotic solvents (**Scheme 4)**.[19] The mechanism was based on the findings that the rate-determining step is first order in the DABCO and the acrylate and second order in the aldehyde.[19,20]

For the McQuade's proposed mechanism in the absence of a protic species, the first step is the addition of amine catalyst **9** on activated alkene **8** to generate the first enolate intermediate **10**.[21] This intermediate **10** then reacts with aldehyde **7** to form a second intermediate **11**, which then reacts with a second molecule of the aldehyde **7** to form a hemiacetal intermediate 1 (**14**). Which undergoes an intramolecular proton transfer by forming a six-membered transition state **15**. Amine

catalyst **9** is then eliminated to generate hemiacetal intermediate 2 (**16**).[11] This intermediate decomposes to generate product **13** and aldehyde **7**. McQuade reported the rate determining step to be the proton transfer step through the hemiacetal intermediate 1 (**14**) (**Scheme 4, step 4** (McQuade's proposal)).[19,20]

Based on their kinetic studies, Aggarwal *et al.* also reported the proton transfer step to be the rate determining step (**Scheme 4, step 4** (Aggarwal's proposal)) however, only for the early (≤ 20%) conversion, and as the reaction proceeded the aldol step (**Scheme 4, step 2** ((Aggarwal's proposal)) becomes the rate determining step, confirmed by the loss of the isotopic effect.[22] Evidently, the MBH adducts can help with the proton-transfer step by acting as a proton-donor through a six-membered intermediate (**Scheme 4**). Aggarwal *et al.* suggested a proton-shuttle mechanism which is aided by a proton source, such as a protic solvent or an alcohol product. The proton transfer occurs from the α-position of intermediate **11** to the alkoxide through the formation of a six-membered transition state **17** (**Scheme 4, step 3 and step 4** (Aggarwal's proposal)).[23,24]

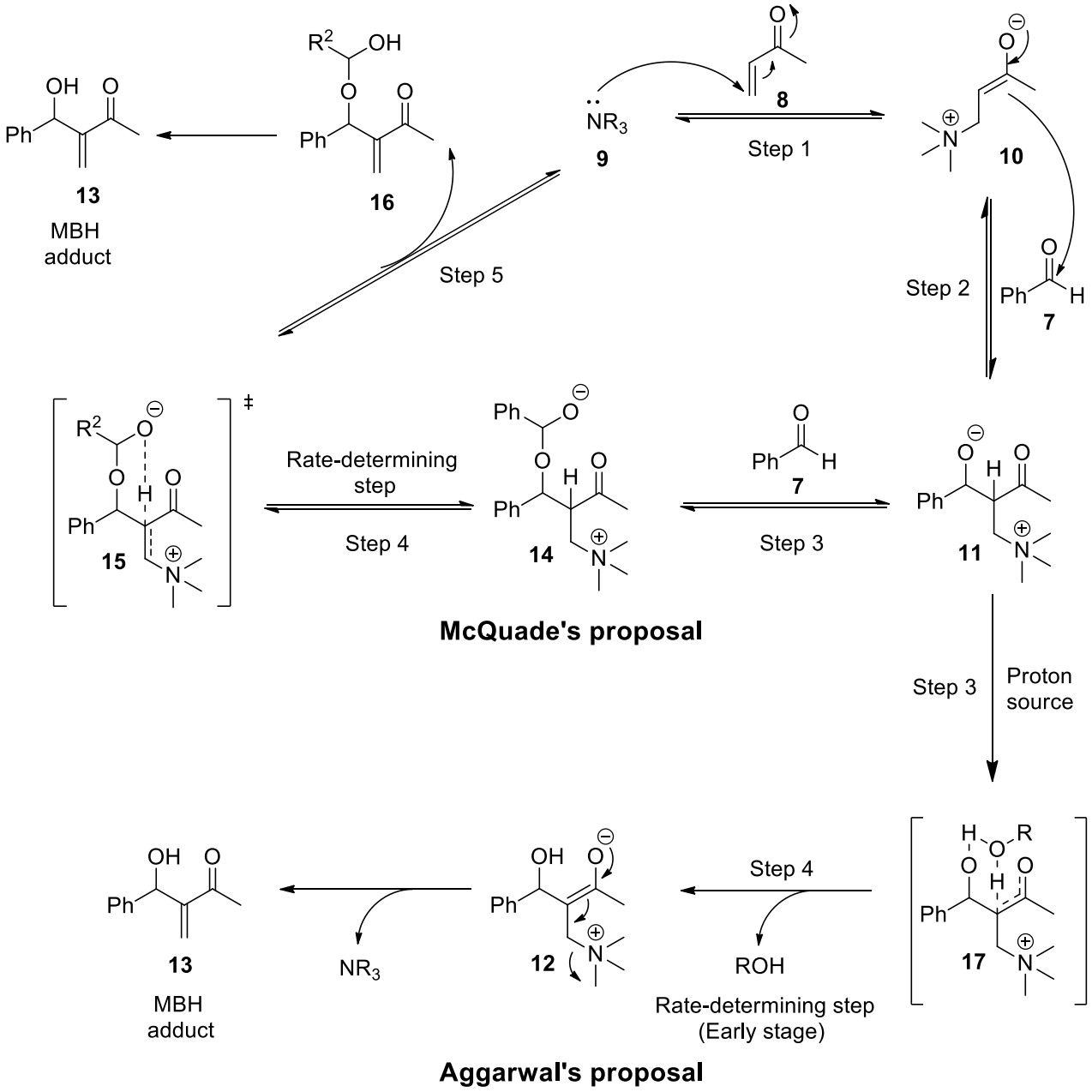

Scheme 4: MBH reaction mechanism proposed by McQuade and Aggarwal.

Lately, a comprehensive theoretical study was also conducted by Aggarwal which confirmed their own kinetic findings as well as those of McQuade's regarding the proton-transfer step. They suggested that two pathways can be involved in the proton transfer step: 1. Hemiacetal alkoxide can be formed by adding an extra molecule of aldehyde accompanied by a rate-limiting proton transfer as suggested by McQuade and 2. A proton transfer by the alcohol which serves as a carrier from the α-position to the alkoxide can occur.[25]

Coelho and Eberlin have also investigated the MBH mechanism by using electrospray ionization mass spectrometry to distinguish MBH reaction intermediates and also to elucidate the co-catalytic function of ionic liquids in the MBH reaction.[15] Cantillo and Kappe also conducted an experimental and computational analysis of the mechanism and the thermodynamic properties of the MBH adducts, reporting that the reaction of benzaldehyde and methyl acrylate is reversible at 120 ˚C, showing that the temperature is dependent on the equilibrium of the reaction.[15,22]

More recently, a thorough analysis of the prototypical MBH reaction mechanism was performed by Singleton and Plata, where they used *p*-nitrobenzaldehyde **18**, methyl acrylate **19** and DABCO **9** in methanol for both theoretical and experimental studies. They generated a complete free-energy profile of the MBH reaction, including all the transition states and intermediates.[23] This free-energy profile was based on the kinetic and thermodynamic measurements, kinetic isotope effect, and independent intermediate generation. Singleton and Plata proposed a stepwise proton transfer through an acid-base mechanism where the protonation of oxygen in **20** and the consecutive deprotonation of **21** to form zwitterionic intermediate **22** are assisted by the solvent (**Scheme 5)**.[22,25]

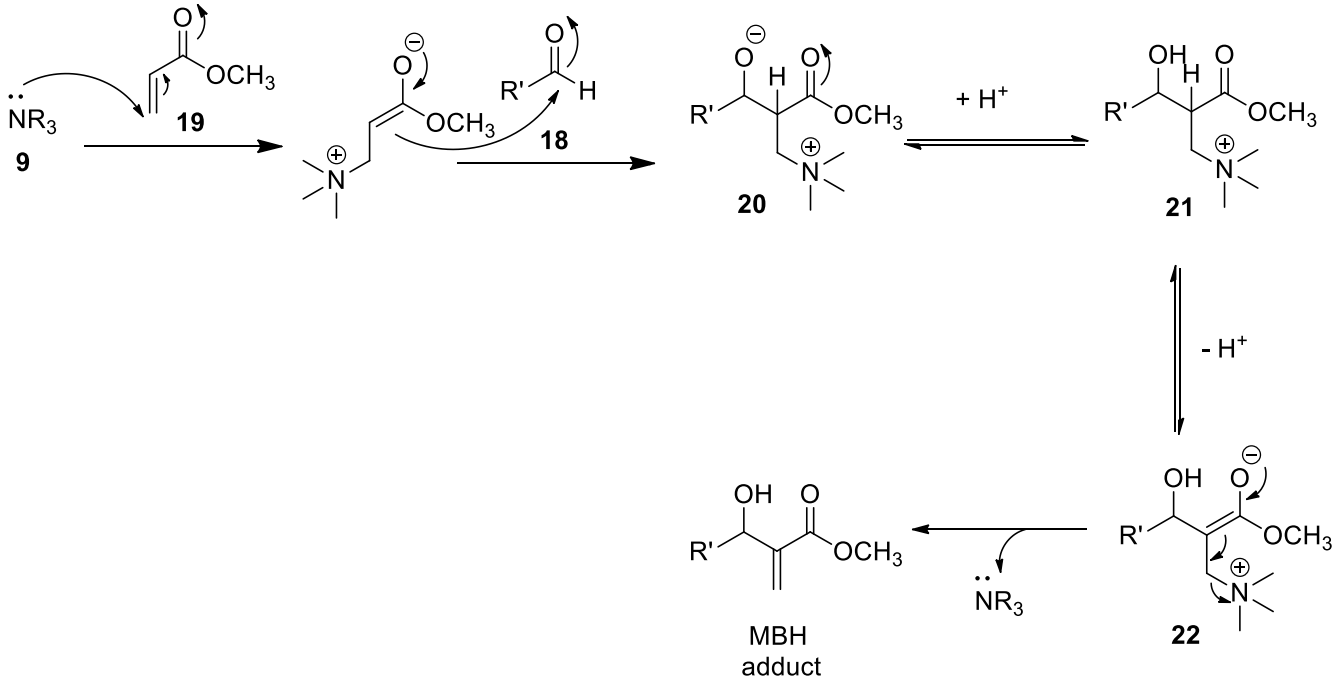

Scheme 5: MBH reaction mechanism proposed by Singleton and Plata.[23]

1.2.2. Phosphine catalyzed mechanism

The most plausible MBH mechanism catalyzed by a phosphine catalyst **23** is almost identical to the amine catalyzed **9** mechanism shown in the schemes above, the only difference is that the intermediate **24** formed can isomerize to a phosphorus ylide **25**. A zwitterionic intermediate **24** is formed through the reaction between an activated alkene **26** and a tertiary phosphine catalyst **23**. The intermediate can isomerize into a phosphorus ylide **25** which can then undergo a Wittig reaction to give alkene **27** shown in **Scheme 6**.[18]

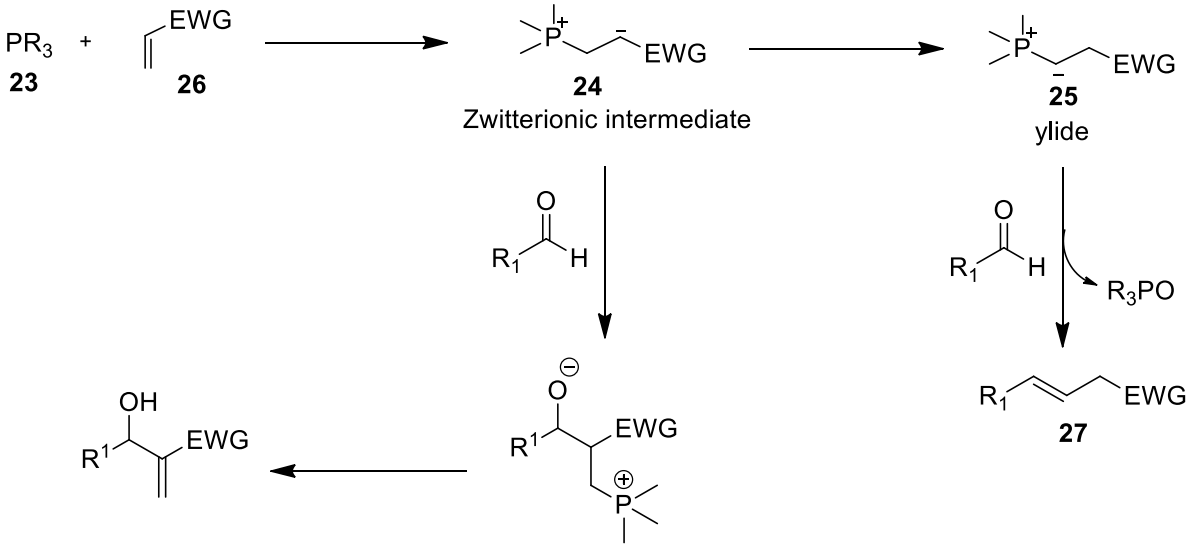

Scheme 6: Phosphine catalyzed MBH reaction mechanism

Xu and Sanoj also conducted further theoretical studies on the MBH mechanism. Xu performed a density functional theory calculation to investigate the MBH mechanism for the reaction catalyzed by PMe_3.[11]

1.3. Components of the Morita Baylis hillman reaction

Since its discovery, different activated alkenes, aldehydes, and catalysts have been used to perform the MBH reaction. There has been exponential growth of the MBH reaction with regards to all three components. Different allenes, cyclic and acyclic activated alkenes, electrophiles, amines and non-amine catalysts have been conveniently used for this reaction.[2] Although not resolved completely, considerable improvement in selectivity and substrate compatibility have been seen.

1.3.1. Activated alkenes

A wide range of activated alkenes have been used for the MBH reaction.[2] The reactivity of the activated alkene depends on the electronegativity of the activating group attached.[26] As the electronegativity increases the reactivity increases, except for the phenyl vinyl sulfonate **28** which has unusually high reactivity. Based on the MBH reaction mechanism, the expected order would be phenyl vinyl sulfoxide **29** = acrylamides **30** < phenyl vinyl sulfone **31** < acrylic esters **32** = ethyl vinyl phosphonate **33** < acrylonitrile **34** < α,β-unsaturated ketones **35** < α-acrolein **36** = phenyl vinylsulfonate **28** (**Figure 1**). [26] The reactivity order is independent of the type of catalyst used.

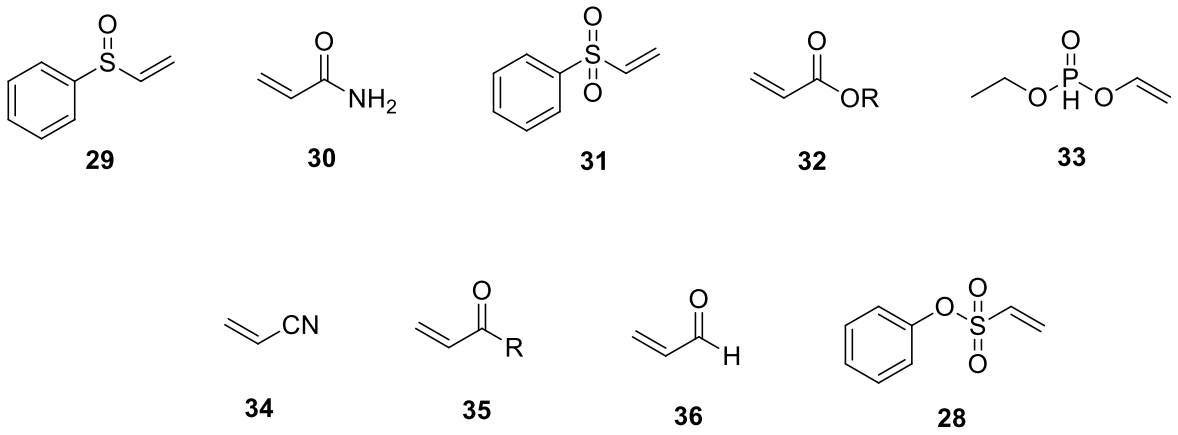

Figure 1: Different types of activated alkenes that are used in the MBH reaction

So far, acrylates **32** make up the largest group of alkenes used for the MBH reaction.[18] This might be due to the flexibility of the ester group for additional reactions. Although a wide range of activated alkenes have been successfully used for the MBH reaction, the use of various β-substituted alkenes such as the nitriles, sulfones, vinyl aldehydes, β-substituted acrylic esters and ketones still needs to be studied in detail (**Figure 2**). There are only a few publications reported for these alkenes using high pressure and with particular electrophiles only.[2]

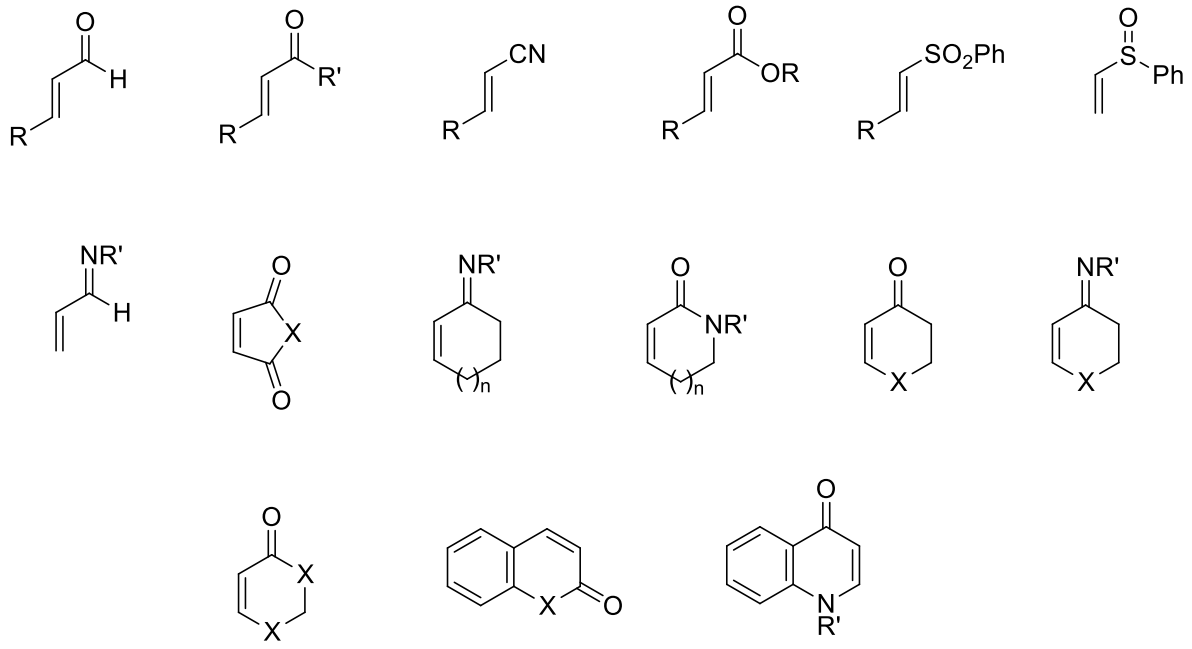

Figure 2: Activated alkenes that need to be studied in detail.

1.3.2. Electrophiles

Although a variety of electrophiles have been used for this reaction such as the aldehydes and imines, many other electrophiles such as ketones, simple allyl and alkyl halides, triflates, mesylates, epoxides, aziridines and acid chlorides have not yet been explored (**Figure 3**).[2] Only a few reports have been published reporting the usage of these electrophiles in the MBH reaction. This might be due to the difficulty of carrying out the reaction in the presence of these electrophiles. For example, ketones do not react easily and normally require high pressures in order for them to react. Therefore, the existing methods have to be altered and developed to accommodate these electrophiles under normal conditions.[27]

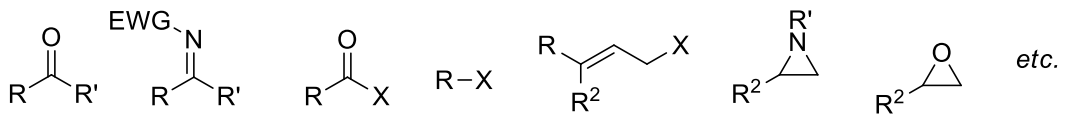

R, R' = Alkyl, Alkenyl, Alkynyl, Aryl, *etc.*
R^2 = H, R
X = Halogen, OMs, OTs, OTf, *etc.*
EWG = electron withdrawing group

Figure 3: Electrophiles that need to be studied further in the MBH reaction.

1.3.2.1. Aldehydes

Aldehydes have been the main type of electrophile used for the MBH reaction since its discovery. In terms of steric and electronic effects, they are highly active compared to ketones.[18] α-Branched aldehydes and aliphatic aldehydes with long chains react very slowly compared to aldehydes with six or fewer carbons. Aliphatic aldehydes with six or fewer carbons have only slightly lower reactivity compared to formaldehydes.[18]

Scheme 7, Table 1 shows the reaction duration obtained from the MBH reaction of differently substituted aldehydes **37** with methyl acrylates **38** in the presence of DABCO at room temperature.[18] The table shows that aldehydes carrying long carbon chains (R = *n*-Bu) and the α-branched aldehydes (R = *i*-Pr) react very slowly compared to aldehydes carrying small carbon chains (R = Me) and that no reaction occurs when α-branched aldehydes such as 2,2-dimethylpropanal (R = *t*-Bu) are used under normal conditions using DABCO. It also shows that electron withdrawing groups (Cl_3C and CO_2Me) present on the α-carbon increase the reactivity, decreasing the reaction duration.

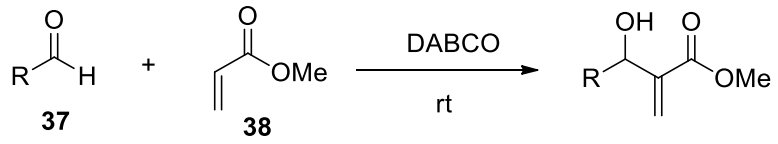

Scheme 7: Comparison of reaction duration of differently substituted aldehydes and methyl acrylate in an MBH reaction.

Table 1: The reaction duration and the yields obtained from the different aldehydes applied in the above reaction (**Scheme 7**).

R	**Time**	**Yield (%)**
Me	7 days	88
n-Bu	9 days	72
i-Pr	13 weeks	68
t-Bu	-	-
Cl_3C	20 h	> 55
CO_2Me	48 h	74

1.3.2.2. Ketones

The MBH reaction does not occur in the presence of unreactive ketones under atmospheric conditions. Very low yields and long reaction times have been reported for reactions using ketones in the presence of catalysts at high temperatures. For example, a reaction between acetone **39** and *n*-butyl acrylate **40** in DABCO at 120 ˚C yields only 7% after being reacted for 4-6 days (**Scheme 8**).[28]

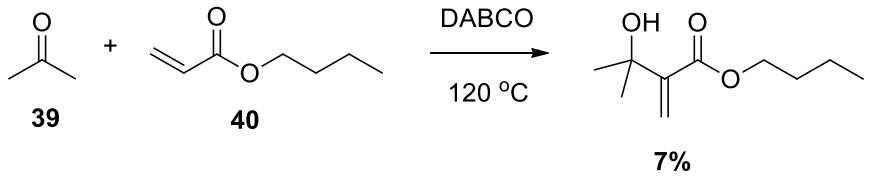

Scheme 8: The MBH reaction between acetone and *n*-butyl acrylate.

Reactions with ketones that are sterically hindered such as the aryl alkyl ketone and diisopropyl ketone do not occur even under high pressures.[29] However, both hindered and unhindered halogenated ketones react very well with acrylonitriles, acroleins and ethyl acrylates (**Scheme 9**). Thus, the problem with the MBH reaction of ketones seems to be more electronic than steric.[30]

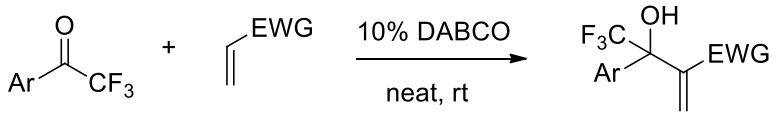

Ar = Ph; EWG = CO_2Et, 70%
Ar = Ph; EWG = CN, 94%
Ar = 2-Thiophene; EWG = CO_2Et, 65%
Ar = 2-Thiophene; EWG = CN, 82%

Scheme 9: MBH reaction of halogenated ketones with different activated alkenes.

1.3.3. Catalysts

The MBH reaction is a very slow reaction, requiring very long reaction times, generally up to several days. In order to enhance the rate of the reaction and improve the reaction yields, different alternatives to the original reaction conditions have been applied. Heating the reaction mixture has been reported to accelerate the reaction, however, it increases the side reactions such as alkene polymerization.

According to the MBH reaction mechanism proposed by Hill and Isaacs shown above in Scheme 3, the rate determining step is the reaction between the zwitterionic intermediate 1 (**10**) and the aldehyde (**7**). Based on this mechanism, the reaction rate can be increased by increasing the amount of the ammonium enolate (**10**), activating the aldehyde (**7**) or stabilizing the zwitterionic intermediate 2 (**11**).[31,32] Stabilization of the zwitterionic intermediate 2 (**11**) occurs through hydrogen bonding by using protic or polar solvents (DMF, DMSO, alcohols) or using phenol additives (**Scheme 10**).[33,32] Kim *et al.* reported the acceleration of the reaction rates by stabilizing zwitterionic intermediate 2 (**11**) using different proton donors and Lewis acids.[31] They also reported high yields for MBH adducts of α,β-unsaturated aldehydes using excess amounts of DABCO and phenol additive which would stabilize intermediate 2. [31]

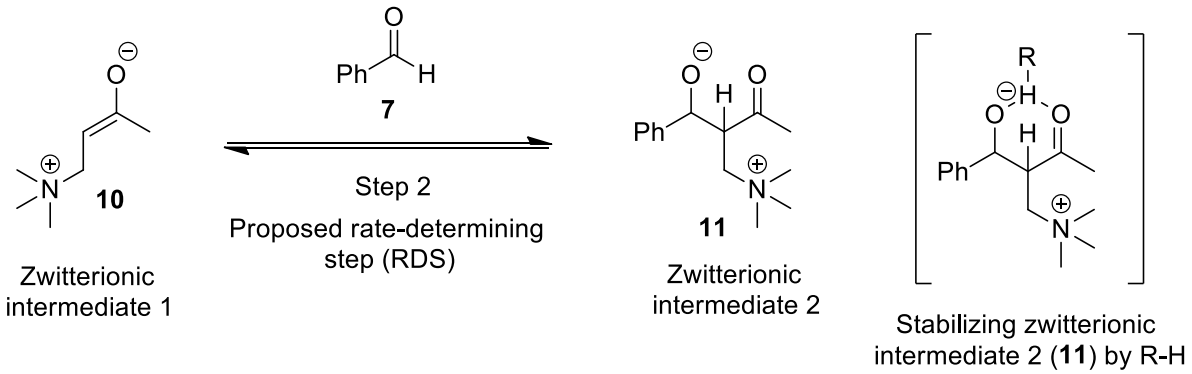

Scheme 10: Step 2 from the Hill and Isaacs proposed reaction mechanism and the stabilization of intermediate 2.[31]

Catalysts have also been used to enhance the rate of the MBH reaction. This reaction is normally catalyzed by Lewis bases including the tertiary amine or phosphine catalysts. DABCO and tricyclohexylphosphine catalysts were the originally used catalysts for the MBH reaction. DABCO has still been used for the MBH reaction and improvements to its catalytic activity as well as its easy recovery has since been made.[20] Many other Lewis bases have also been used to catalyze the reaction including the 1,8-diazabicyclo(5.4.0)undec-7-ene (DBU), quinuclidine, DMAP, imidazole etc. as well as chalcogenide-centered Lewis bases have also been used to catalyze the MBH reaction.

Xu and Shi investigated the MBH reaction in the presence of various Michael acceptors and Lewis base catalysts in an attempt to accelerate the reaction rate by easily forming the ammonium or phosphonium enolate intermediates **10** obtained from the conjugate addition reaction of Lewis base **9** on an α,β-unsaturated enones **8**.[34] This allows the zwitterionic phosphonium or ammonium enolates **10** to be maintained in higher concentration, shifting the equilibrium forward to achieve the nucleophilic attack of the enolate **10** on the electrophile **7**, forming the MBH adduct **13**, leading to an increase in the reaction rate (**Scheme 3**).[34]

Lewis acids have also been used to catalyze the MBH reaction,[35] they enhance the reaction rate through hydrogen bonding by stabilizing the enolate intermediate thereby increasing its concentration or by activating the aldehyde.[36] Lewis acids such as $TiCl_4$, $BF_3.OEt_2$, $Sc(OTf)_3$ and $Ti(OEt)_4$ have been used along with DABCO in the reaction.[30,33]

1.3.3.1. Tertiary amine catalysts

The first MBH reaction using a tertiary amine catalyst was reported in 1972 by Baylis and Hillman, where they used various activated alkenes such as α, β-unsaturated ketones, amides, esters, and nitriles with different aldehydes. The reactions were performed using a bicyclic tertiary amine catalyst such as DABCO (1,4-diazabicyclo [2.2.2] octane), quinuclidine or indolizine **(Figure 4)**.[37]

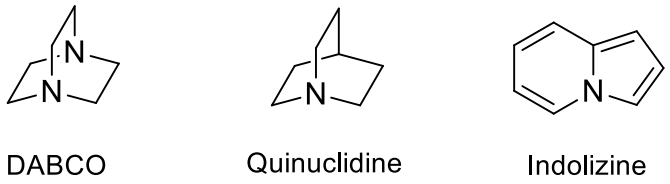

Figure 4: Tertiary amine catalysts used in the first MBH reaction reported by Baylis and Hillman in 1972.

Since then, many reports have been published reporting MBH reactions using these catalysts. In 1982, a reaction between acetaldehyde **41** and ethyl acrylate **42** in the presence of DABCO was reported by Drewes and Emslie, the adduct **43** was further used to synthesize Integerrinecic acid **44** (**Scheme 11**).[38]

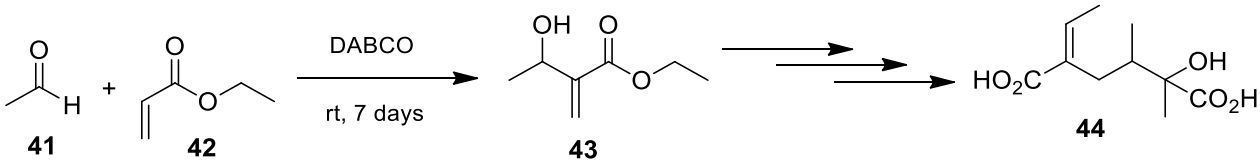

Scheme 11: The MBH reaction between acetaldehyde and ethyl acrylate in the presence of DABCO reported by Drewes and Emslie, which was further transformed into integerrinecic acid.[38]

Shortly after, an MBH reaction between methyl and *tert*-butyl acrylates with aldehydes in the presence of DABCO was developed by Hoffman *et al.* (**Scheme 12**).[39]

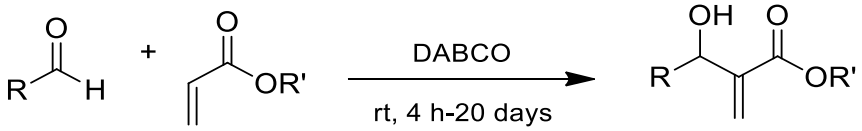

Scheme 12: Reaction between methyl and *tert*-butyl acrylates with aldehydes in the presence of DABCO reported by Hoffman *et al.*[39]

Another nitrogen-based catalyst used for the MBH reaction is the DBU catalyst. In a report published in 2022 by Dai *et al.*, they reported a DBU catalyzed MBH-type cyclization reaction to

generate 3-ethynylcoumarins. The coumarin derivatives were easily obtained at room temperature in half an hour. Electron-rich aldehydes gave very good yields, however, electron-poor aldehydes gave poor yields (**Scheme 13**).[40]

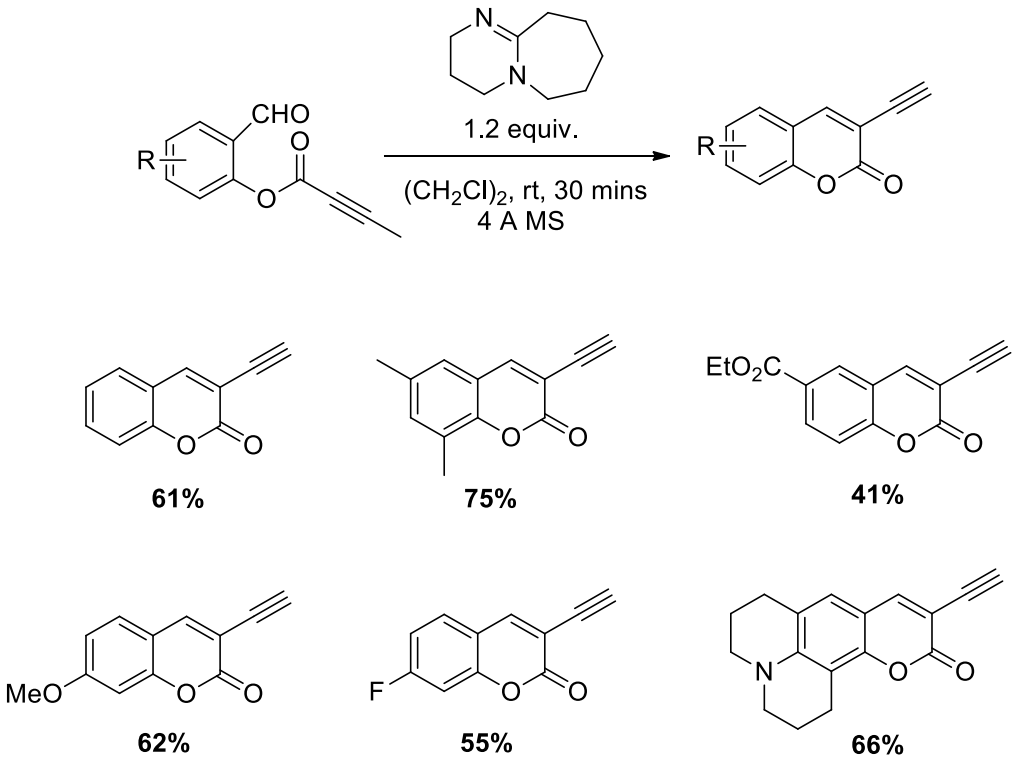

Scheme 13: MBH cyclization reaction in the presence of DBU catalyst to generate 3-ethynylcoumarins and the yields obtained from different coumarin derivatives.[40]

Numerous tertiary amines have been explored in an attempt to find more effective catalysts. Amongst all the bicyclic amine catalysts shown in Figure 5, only 3-hydroxyquiniclidine (3-HQD) has been reported to be more efficient than DABCO. 3-Hydroxyquiniclidine has now been used frequently in the MBH reaction since it reduces the half-life by four to tenfold.[33,41]

Drewes *et al*. reported a significant increase in the reaction rate for the reaction between strong electrophilic aldehydes and methyl acrylates by using 3-hydroxyquiniclidine rather than DABCO as a catalyst.[42] The reduction in the reaction half-life occurs as a result of the hydrogen-bonding stabilization between the catalyst and the acrylate adduct through the hydroxyl group present on the catalyst.[43] This hypothesis was later confirmed by the fact that the acetylated derivative of 3-hydroxyquiniclidine was a poor catalyst compared to 3-hydroxyquiniclidine.[42]

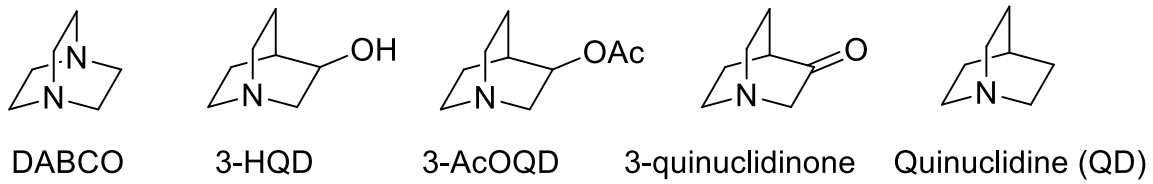

Figure 5: Tertiary amine catalysts used for the MBH reaction.

The amines basicity is directly related to the p*K*a of its conjugate acid. Without the presence of any steric effects, there is a good correlation between the reaction rate and the p*K*a value, since the presence of amines that has higher p*K*a values must provide ammonium enolate **10** (**Scheme 3**) with higher concentrations.[44,41]

Aggarwal *et al.* reported the correlation between the pK_a values of different quinuclidine-based catalysts and their reactivities in the MBH reaction (**Scheme 14, Table 2**).[41] The MBH reaction was performed using 2-pyridinecarboxaldehyde **45** and methyl acrylate **46** in the presence of different quinuclidine catalysts and the p*K*a's were determined in water. 3-hydroxyquinicludine had the least solubility with only 5 mol % dissolved. Aggarwal *et al.* reported a direct correlation between the pK_a and the reaction rate. They reported that quinuclidine had the highest pKa value in protic solvents and hence, it was the most active catalyst. Additionally, they reported that quinuclidine with methanol is the best combination for catalyzing the MBH reaction.[41] The lowest reaction rate was obtained for the quinuclidinone catalyst, which had the lowest p*K*a value. DABCO did not show a correlation between its pKa and the reaction rate. It showed a higher rate based on its pKa, this might be due to the presence of two nitrogen atoms present on it which gave higher effective molarity.[41]

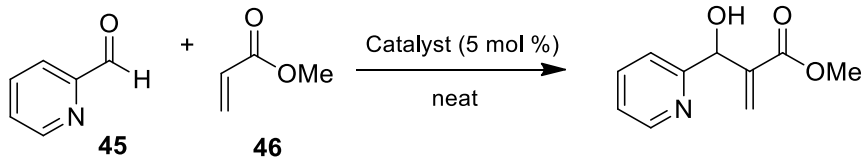

Scheme 14: The MBH reaction between 2-pyridinecarboxaldehyde and methyl acrylate in the presence of different quinuclidine catalysts shown in Table 2.

Table 2: The correlation between the pK_a values of different tertiary amine catalysts and their reactivities in the MBH reaction as reported by Aggarwal *et al*.

	DABCO	**3-HQD**	**3-AcOQD**	**3-quinuclidinone**	**Quinuclidine (QD)**
pK_a (H_2O)	8.5	9.9	9.3	6.9	11.3
Rate (%/min)	0.21	0.88	0.031	0.0013	1.8
K_{rel}	1.0	4.3	0.15	0.006	9.0

Mayr and coworkers examined the nucleophilic effects of quinuclidine, DABCO and DMAP. They suggested that quinuclidine and DABCO had a much better nucleophilic effect and were much better leaving groups than DMAP, making them better catalysts.[45]

1.3.3.2. Tertiary phosphine catalysts

The MBH reaction emerged from the dimerization reaction of activated alkenes using phosphine as catalysts, reported by Rauhut and Currier, Balzer and Anderson, and McClure.[46] Phosphine catalysts that are applicable in the MBH reaction are tributylphosphane **47**, tricyclohexylphosphane **48**, triphenylphosphine **49**, triethylphosphane **50**, and diethylphenylphosphane **51 (Figure 6)**.[33] Phosphane-centered Lewis bases are highly nucleophilic and have weak proton basicity compared to their amine-centered analogues; this is due to the low electron density and greater polarizability of the phosphorus atom.[33]

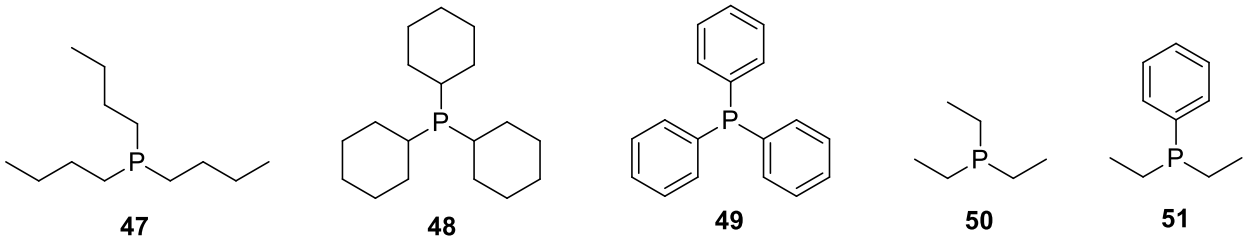

Figure 6: Phosphine catalysts that have been used in the MBH reaction.

Morita *et al.* used tricyclohexylphosphine **48** as a catalyst in the Morita Baylis Hillman reaction between activated alkenes and fumaric esters or aldehydes (**Scheme 15**).[47] Since then, a variety of phosphines have been applied as catalysts to couple aldehydes and activated alkenes in different reactions.

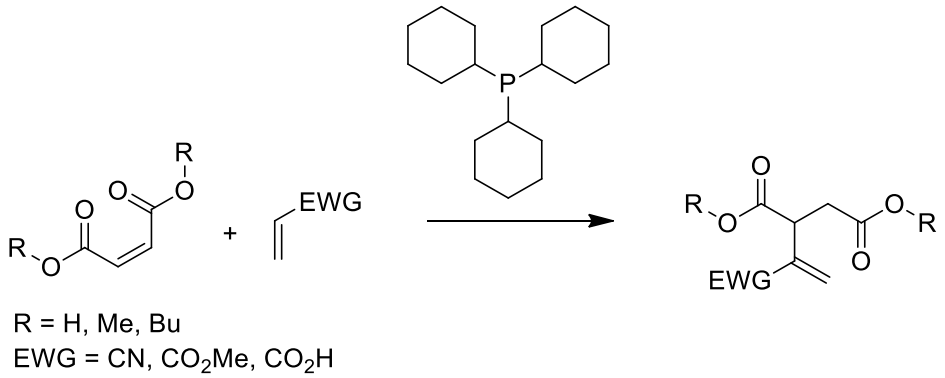

Scheme 15: MBH Reaction between fumaric esters or aldehydes and different activated alkenes using tricyclohexylphosphine as a catalyst as reported by Morita *et al*.[47]

Aldehydes which have an enolizable carbonyl can undergo a self-aldol reaction, which can be avoided by using trialkylphosphines. This is particularly helpful for hindered aldehydes that react slowly. Different trialkylphosphines have been used in the non-asymmetric reactions. Amongst these phosphines, tributylphosphine has been found to be the most effective. Leahy *et al.* reported the MBH reaction between propionaldehyde **52** and methyl acrylate **53** in the presence of tributylphosphine as a catalyst. Using tributylphosphine instead of an amine catalyst increased the rate of the reaction and also prevented the occurrence of the aldol reaction that would normally occur in an amine catalyzed MBH reaction at room temperature (**Scheme 16, Table 3**).[48]

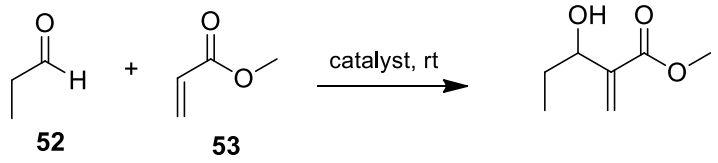

Scheme 16: MBH reaction between a propionaldehyde **52** and methyl acrylate **53** in the presence of different catalysts.

Table 3: Reaction duration and the yield obtained by applying different catalysts in the above reaction shown in Scheme 15.

Catalyst	DABCO			Me_3P	Bu_3P
Time	10 d	2 d	No reaction	No reaction	2 d
Yield (%)	84 %	< 10%			80

1.3.3.3 $TiCl_4$-Lewis acid promoted Morita-Baylis-Hillman reaction.

Lewis acids can be used to promote the MBH reaction, it enhances the rate of the reaction by stabilizing the zwitterionic intermediate and also by conveying better electrophilicity on the aldehyde.[45] Lewis acids can be utilized with or without other any additives. A variety of Lewis acids have been used for the MBH reaction, such as $TiCl_4$, $ZnCl_2$ and $AlCl_3$ in the absence of a base. Other Lewis acids, such as $EtAlCl_3$, $SnCl_4$, $SmCl_3$, $BF_3.Et_2O$ have been used in a base-catalyzed MBH reaction medium.[45] $TiCl_4$ is of utmost importance amongst all the other Lewis acids as it has been successfully employed to enhance the MBH reaction rate, it has the ability to achieve high diastereoselectivity and to tolerate other Lewis bases and promoters.[45,49]

Patra *et al.* reported an MBH reaction between substituted 5-isoxazolecarboxaldehydes **54** and cyclohexanone **55** in DCM using $TiCl_4$ as the Lewis acid, this reaction gave the desired MBH adduct **56** along with hemiacetals **57** as the byproducts. However, when they used cyclopentanone **58** instead of cyclohexanone **55**, the desired MBH adducts **59** were formed in a good yield and only trace amounts of α-chloromethyl enones **60** were obtained (**Scheme 17**).[36] They also tested the same reaction using $TiCl_4$ in the presence of different bases (DBU, 3-HQN and DABCO), which led to formation of phenols in minor quantities along with the desired MBH adduct.[36]

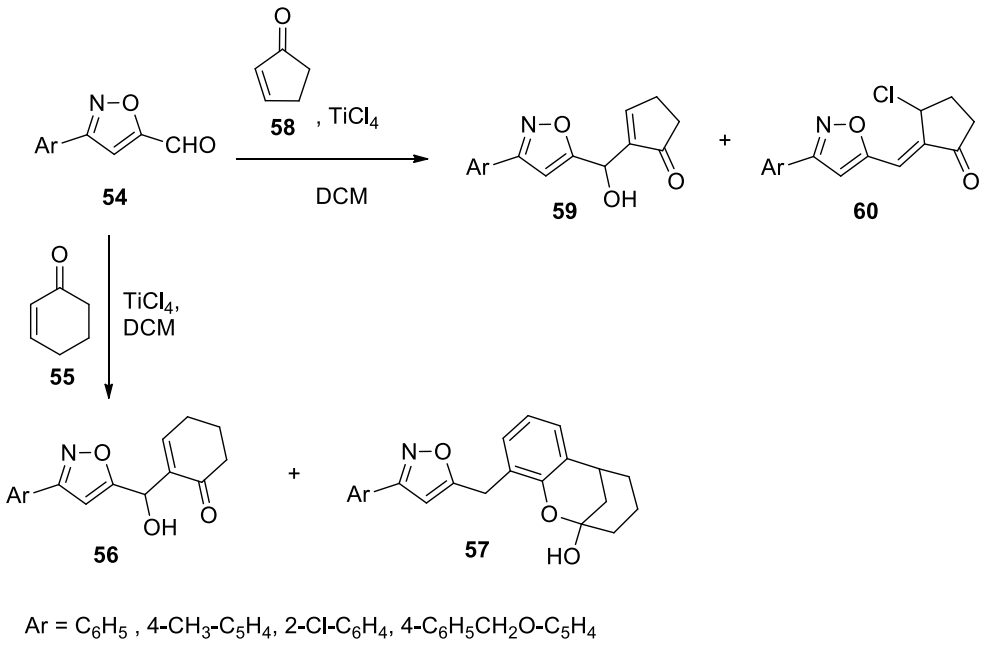

Scheme 17: MBH reaction between substituted 5-isoxazolecarboxaldehydes **54** and unsaturated ketone, **55** and **58** in DCM using $TiCl_4$ as the Lewis acid.[36]

1.4. Asymmetric MBH reaction

One of the most crucial characteristics of the MBH reaction is the generation of a stereogenic centre when using a prochiral electrophile. This provides chemists with an opportunity to generate an asymmetric form of the reaction.[50,51] There are five different ways in which an asymmetric form of the reaction can be obtained: 1) utilizing a chiral electrophile, 2) employing a chiral catalyst, 3) using a chiral activated alkene, 4) Choosing a suitable chiral medium, 5) Utilizing various mixtures of one/two/three/four of chiral electrophiles/activated alkenes/ medium and a chiral catalyst. The presence of an asymmetric centre on either or both electrophile and the activated alkene leads to the formation of two or more diastereomers.[2,51]

1.4.1. Chiral electrophile

A number of studies have been performed reporting the use of chiral electrophiles to form an asymmetric form of the reaction. The diastereoselectivity of the MBH reaction between methyl vinyl ketones and methyl acrylates have been reported in many publications using a variety of non-racemic and racemic aldehydes in the presence of a tertiary amine catalyst.[20] In 1988, Roos *et al.* reported the formation of diastereomers from the reaction between *(S)*-*O*-(methoxymethyl) lactaldehyde **61** with either methyl vinyl ketone **62** or methyl acrylate **62** in the presence of 3-hydroxy quinuclidine or DABCO as a catalyst.[52] *Anti*-diastereomer **63** was obtained as the major diastereomer (**Scheme 18**). Similar diastereoselectivity was obtained for both tertiary amine catalysts.[20,53]

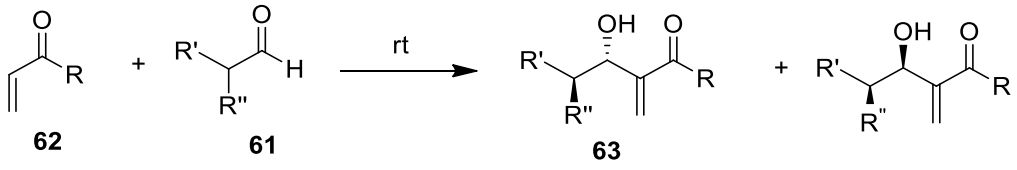

62 **61** **63**

R = Me or OMe

≥ 70 ≤ 30

Scheme 18: A reaction between *(S)*-*O*-(methoxymethyl)lactaldehyde **61** with methyl vinyl ketone **62** or methyl acrylate **62** in the presence of 3-hydroxyquinuclidine or DABCO as a catalyst.

K.R. Luna-Freire *et al*. reported the total synthesis of pyrrolizidines **64** using asymmetric substrate-controlled MBH reaction. MBH adduct **65** generated from chiral amino aldehyde **66** and methyl

acrylate **67** was used as a substrate for the synthesis of pyrrolizidine **64**. The chiral amino aldehyde **66** was synthesized using commercially available chiral hydroxyproline **68** (**Scheme 19**).[64]

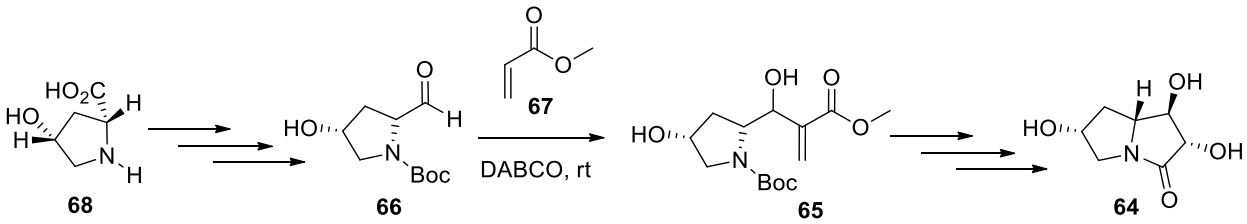

Scheme 19: The total synthesis of pyrrolizidines **64** using asymmetric MBH reaction.

A comprehensive study was performed on enantiopure α-branched aldehydes **61** reacting with methyl acrylate **67** (**Scheme 20**). NMR spectroscopy and x-ray crystallography were performed to obtain the *syn/anti* ratios, the results are shown in Table 4. The type of catalyst used did not have an influence on the *syn/anti* ratio, it only affected the rate of the reaction (Entry **1** and **2**, **Table 4**). In the same way, the amount of catalyst used only had an effect on the rate of the reaction. For most of the reactions *anti* isomer was obtained as the major isomer.[55] The *anti/syn* ratio might be affected by the size of the groups attached to the aldehyde (R' and R''). Bulky groups (R'') attached to the aldehyde gives the *anti*-product in a higher ratio compared to the *syn* product, since it prevents the enolate intermediate from attacking on the same side as the group (R''), forcing it to attack on the opposite side forming the *anti*-product.

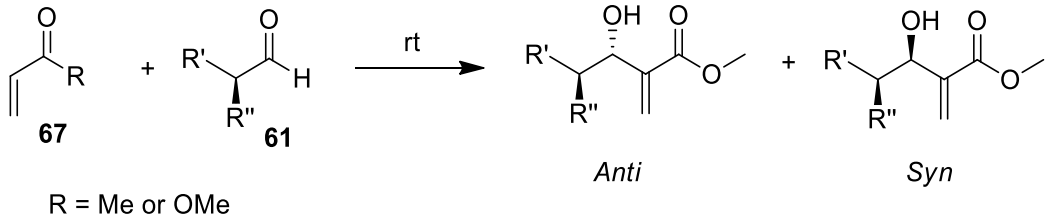

Scheme 20: A reaction between differently substituted α-branched aldehydes **61** and methyl acrylate **67** using different conditions.

Table 4: The different substituents used on the aldehyde in the above reaction shown in Scheme **20**, and the results obtained under different conditions.

	R'	**R''**	**Conditions**	**Yield (%)**	***Anti: Syn***
1	Me	$MeOCH_2O$-	DABCO, 4 d	55	70:30
2	Me	$MeOCH_2O$-	3-Quinuclidinol, 1.5 d	60	72:28
3	Me	$BnOCH_2O$-	DABCO, 6 d	42	70:30
4	Ph	$MeOCH_2O$-	DABCO, > 10 d	42	37:63
5	*n*-Pr	Me	3-Quinuclidinol, 60 d	30	35:65
6	-$CH_2OC(Me)_2O$-		DABCO, 55 d	62	69:31
7	Me	-$NHCO_2$Bu-*t*	DABCO, 7 d	80	26:74
8	Me	*N*-Phthalimidyl	DABCO, 3.5 d	28	46:54
9	-$CH_2OC(Me)_2N(CO_2$Bu-*t*)-		DABCO, < 11 d	43	89:11

1.4.2. Chiral activated alkene

Different optically active acrylates have been used as activated alkenes in the asymmetric MBH reaction. An initial attempt to perform this kind of reaction was carried out by Brown *et al.* in 1986 involving acetaldehyde **69** and (1)-menthyl acrylate **70** in the presence of a DABCO as a catalyst. The diastereomeric excess obtained was 16% (**Scheme 21**).[20,30]

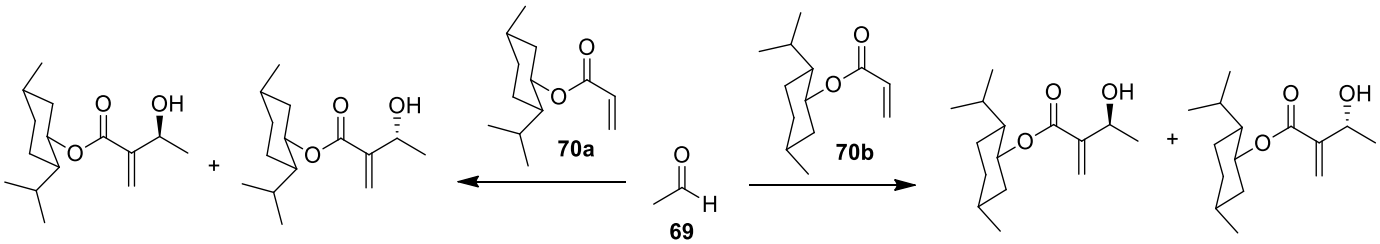

Scheme 21: An asymmetric MBH reaction using acetaldehyde and (1)-menthyl acrylate in the presence of DABCO as a catalyst.

1.4.3. Chiral catalyst

1.4.3.1. Chiral amine catalyst

The catalyst most often used in the MBH reaction is the tertiary amine catalyst. The proposed reaction mechanism suggests the involvement of the amine catalyst throughout the reaction, including the step that involves the formation of the stereogenic centre.[56] If a chiral amine is used, it should lead to the formation of a chiral product. Various chiral tertiary amine catalysts have been used in the MBH reaction including quinidine, quinine, retronecine, and cinchonidine.[56] Due to the proton donating ability of the catalyst in the selectivity and the rate enhancement of the MBH reaction, much consideration has been given to β-amino alcohols, such as the cinchona catalyst.[57]

Enantioselective MBH reactions using aldehydes and methyl vinyl ketones in the presence of a β-amino alcohol were initially investigated by Marko *et al.*[57,58] Different β-hydroxy amines were investigated for the MBH reaction between a methyl vinyl ketone **71** and cyclohexyl carboxaldehyde **72.** From all the β-hydroxy amines, the greatest enantioselectivity was displayed for the cinchona alkaloids **73**, this is followed by the ephedrine **74** and proline derivatives **75** (**Scheme 22**).[58]

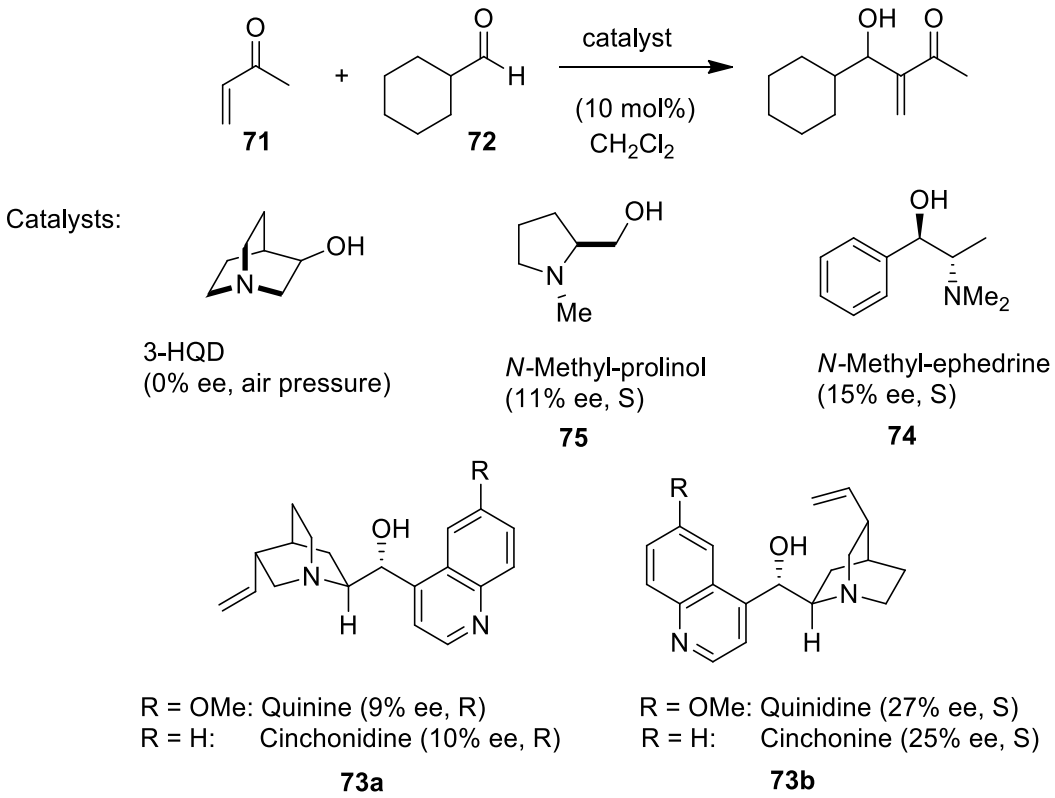

Scheme 22: MBH reaction between a methyl vinyl ketone and cyclohexylcarboxaldehyde in the presence of different β-hydroxy amines as catalysts.

Hirama coupled benzaldehyde and methyl acrylate using a chiral DABCO derivative at high pressure forming the adduct in a high yield of 93% and an ee value of 47%.[58]

1.4.3.2. Chiral phosphine catalyst

Compared to the chiral amine catalysts, chiral phosphine catalysts have been less investigated for the enantioselective MBH reaction. The initial enantioselective cycloisomerization intramolecular MBH reaction was performed using a cyclopentenol derivative **76** in the presence of a (-)-CAMP catalyst **77** (**Scheme 23**).[59] An ee value of 14% was obtained; the low enantiomeric excess obtained was a result of a reversible cyclization.

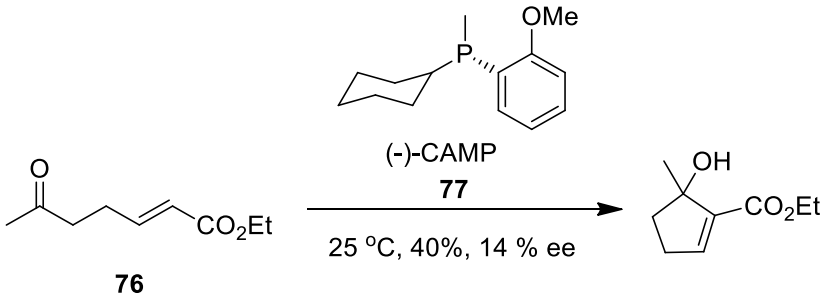

Scheme 23: An enantioselective intramolecular MBH reaction using a cyclopentenol derivative **76** in the presence of (-)-CAMP **77** as a catalyst.[59]

A variety of chiral phosphine catalysts have been investigated for the intermolecular MBH reaction of methyl acrylate **53** and pyrimidine 5-carboxaldehyde **78** (**Scheme 24**).[60] Amongst all the phosphine catalysts examined, 2,2'-bis(diphenylphosphino)-1,1'-binaphthyl (BINAP) **79** was found to be the best catalyst, where the product was obtained with a 44% enantiomeric excess. The yield and ee of the products in the MBH reaction between pyrimidine 5-carboxaldehyde **78** and other acrylates depended on the bulkiness of the acrylate used.[58,61]

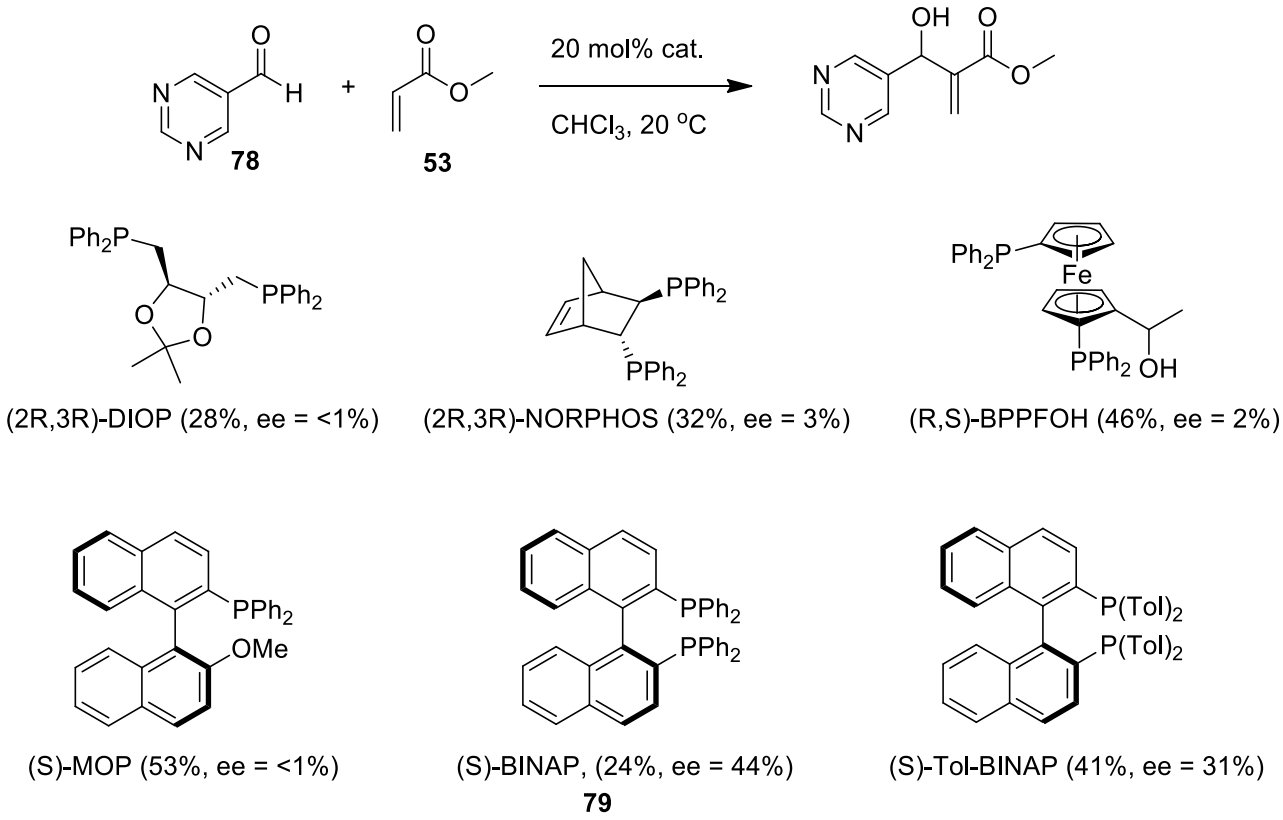

Scheme 24: Intermolecular MBH reaction of methyl acrylate and pyrimidine 5-carboxaldehyde in the presence of various chiral phosphine catalysts.

All the above approaches lead to the formation of enantioselective MBH adducts. Using chiral electrophiles and activated alkenes lead to the formation of diastereomers, whereas a chiral catalyst generates enantiomers.

1.5. Transformation of the MBH adducts

A highly functionalized molecule is obtained from the MBH reaction, carrying three functional groups in close proximity. These groups allow for the application of MBH adducts in numerous organic reactions and their further transformations.[62] Chemists have comprehensively examined and developed new strategies and approaches to obtain heterocyclic, carbocyclic, and trisubstituted alkenes. Different types of natural products and bioactive molecules have been generated from the MBH adducts.

The MBH adduct contain a minimum of three functional groups, an alkene, a hydroxy and an electron withdrawing group (EWG).[62] These functional groups can undergo numerous

chemoselective transformations and due to their close proximity, different stereo- and regioselective transformations can take place through the reaction of an individual or a combination of functional groups (**Figure 7**). A series of cyclic compounds can be obtained from these transformations.

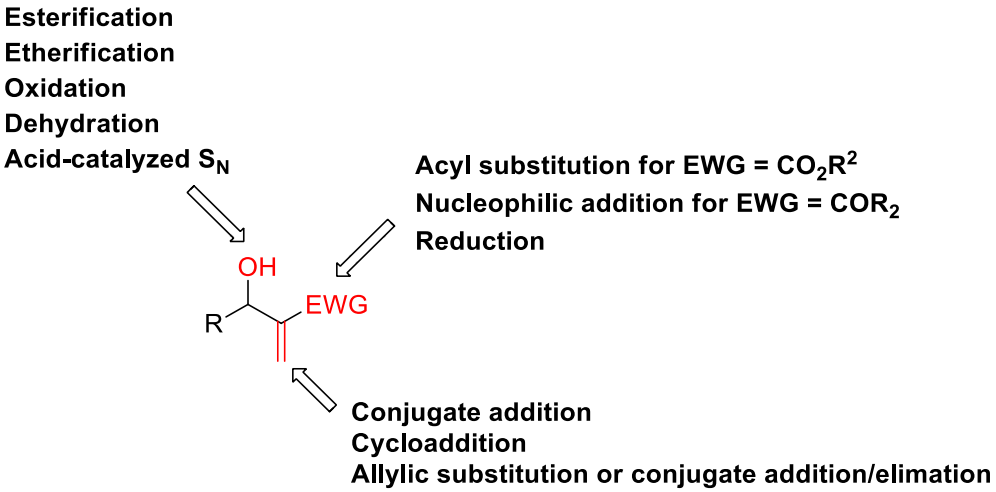

Figure 7: Different reactions that are possible on the three functional groups present on the MBH adduct.

The MBH adduct is electrophilic at the terminal of the alkene which is attached to an electron withdrawing group. Modified MBH adducts **80**, where the allylic hydroxy group is transformed into a leaving group such as the tert-butoxycarbonyloxy or an acetoxy group, have an electrophilic allylic position.[63] However, a direct nucleophilic attack at the allylic position is disfavoured, partly due to the steric hindrance present at that position. In fact, an S_N2' type reaction occurs on the modified MBH adducts by various nucleophiles, favouring a nucleophilic substitution reaction at the terminal alkene site (**Scheme 25**).[63]

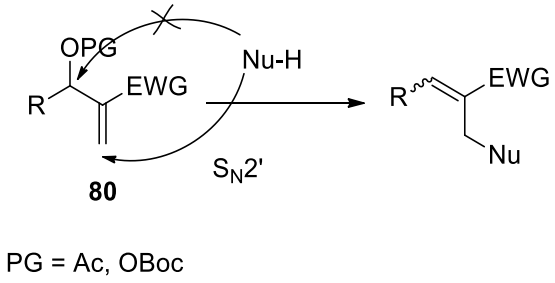

Scheme 25: Reaction of the modified MBH adducts with nucleophiles.

1.5.1. Reactions of the hydroxyl group

1.5.1.1. Esterification or etherification

The hydroxy group present on the MBH adduct can be transformed into an acetate through reaction of an acetyl chloride using a base or by using acetic anhydride in concentrated H_2SO_4. Acetates obtained from an aromatic aldehyde can isomerize, generating a more stable state through intramolecular rearrangement or by using DABCO as a nucleophilic catalyst or using other reagents (**Scheme 26**).[64]

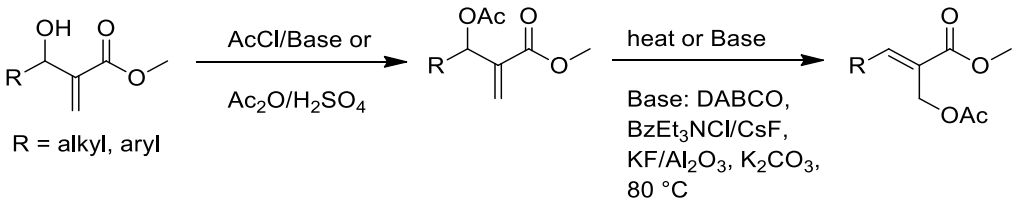

Scheme 26: The conversion of the hydroxy group using acetyl chloride and a base or by using acetic anhydride in concentrated sulfuric acid and the conversion of acetate into a more stable state.

Regioselective synthesis of MBH acetates **81** has been reported by Sa *et al.* using acetic anhydride and a suitable solid catalyst in the absence of any solvent. The type of product obtained depends on both the catalyst and the substrate used. Basic catalysis led to the selective generation of unrearranged acetate product **81** whilst the acid catalysis and substrate with an electron donor group led to the isomerized product **82** (**Scheme 27**).[64]

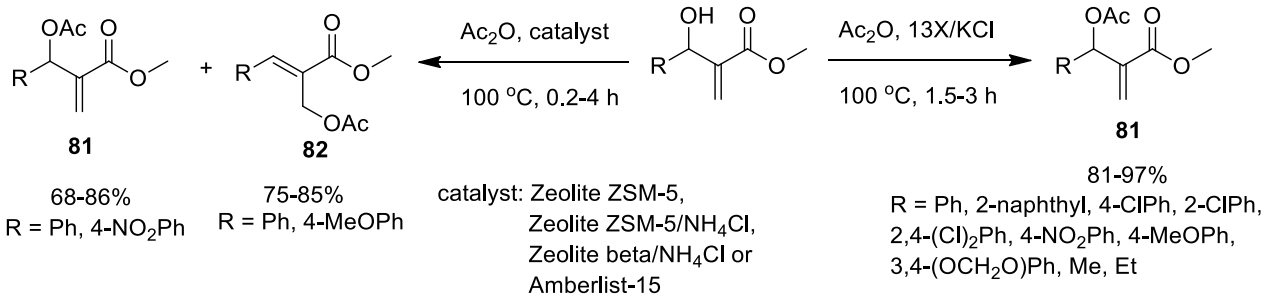

Scheme 27: Regioselective synthesis of MBH acetates using acetic anhydride and different catalysts.

1.5.1.2. Oxidation

Many papers have been published reporting the oxidation of primary alcohols using various oxidants. Some of these methods have major drawbacks, for example, Cr(VI) containing reagents (used in Jones oxidation) are highly toxic and have difficult workups; IBX has low solvent solubility; TEMPO as an oxidant has no tolerance for certain functional groups and some oxidants create acidic byproducts which are not good for the catalytic activity of the catalyst. Many of these reagents have been used to oxidize the MBH adduct.[65]

Jones reagents have been used to transform hydroxy groups in MBH adducts, synthesizing doubly activated alkenes. Pyridinium chlorochromate on silica has been shown to be a less effective oxidant for the oxidation of the MBH adducts. Lawrence *et al.* reported a direct oxidation of alkyl 2-hydroxyarylacrylates **83** by Dess-Martin periodinane, which resulted in product **84**. However, when Swern oxidation was performed on the same adduct **83**, it led to the formation of the S_N2'substitution product **85** (**Scheme 28**).[66]

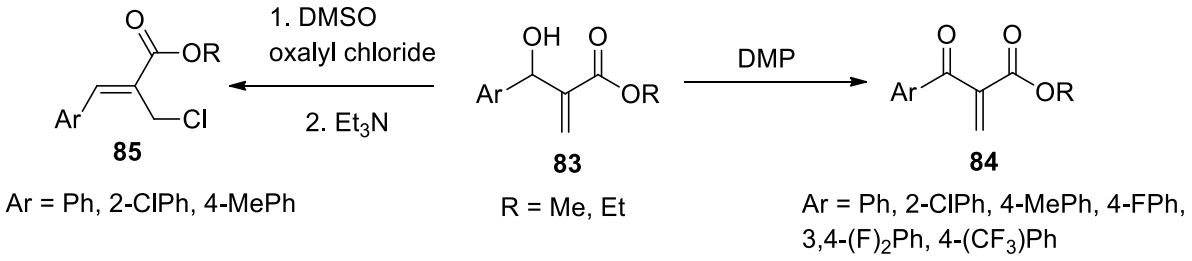

Scheme 28: Oxidation of alkyl 2-hydroxyarylacrylates **83** reported by Lawrence *et al.*

1.5.2. Reactions of the double bond

1.5.2.1. Conjugate addition reactions on the MBH adducts.

Unmodified MBH adducts can act as Michael acceptors in a Michael addition reaction with different nucleophiles such as carbon, nitrogen, sulfur, and oxygen. Bhuniya et al. reported the conjugate addition of oximes **86** onto the MBH adducts **87** catalyzed by triphenyl phosphine, which led to the formation of aldol products **88** (**Scheme 29**).[67]

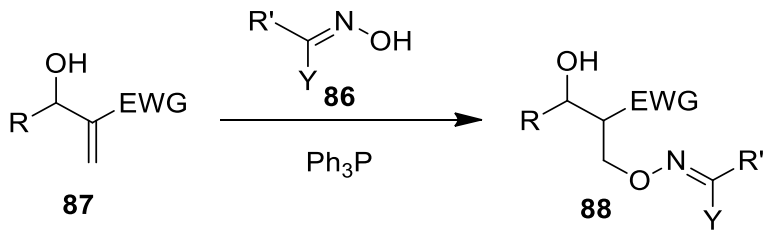

Scheme 29: Conjugate addition of oxime **86** on MBH adduct **87**.

Conjugate addition reactions have also been performed on oxidized MBH adducts. Silva *et al.* reported a reaction involving the sequential one-pot IBX oxidation of the MBH adduct **89** followed by the conjugate addition of indolizines **90** on the oxidized adduct in the absence of a catalyst (**Scheme 30**).[64]

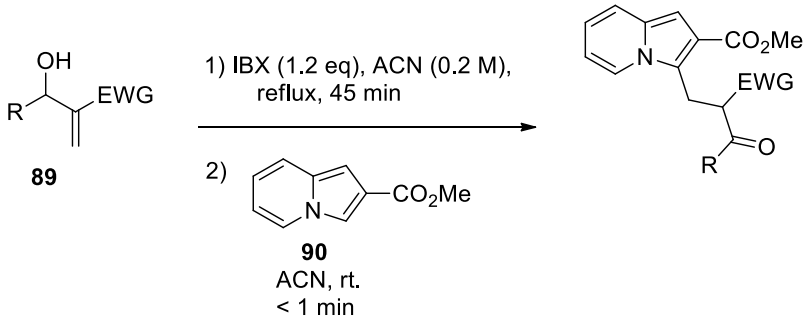

Scheme 30: Conjugate addition of indolizines **90** on oxidized MBH adducts.

Kamimura *et al.* reported the conjugate addition of ethanthiol to TBS protected MBH adducts (TBS ether) **91** to synthesize *syn*-β-hydroxy-α-thiomethyl carbonyl compounds using lithium thiolate in catalytic amounts (**Scheme 31**).[68] These products were further converted into β-lactams. The conjugate addition reactions were performed with very good diastereoselectivity on the MBH adducts synthesized using acetaldehyde and methyl acrylate. However, when acrylonitrile was used instead of methyl acrylate for the synthesis of MBH adducts, the conjugate addition reaction led to the loss of stereoselectivity for the diastereomers formed (**Scheme 31, Table 5**).[68]

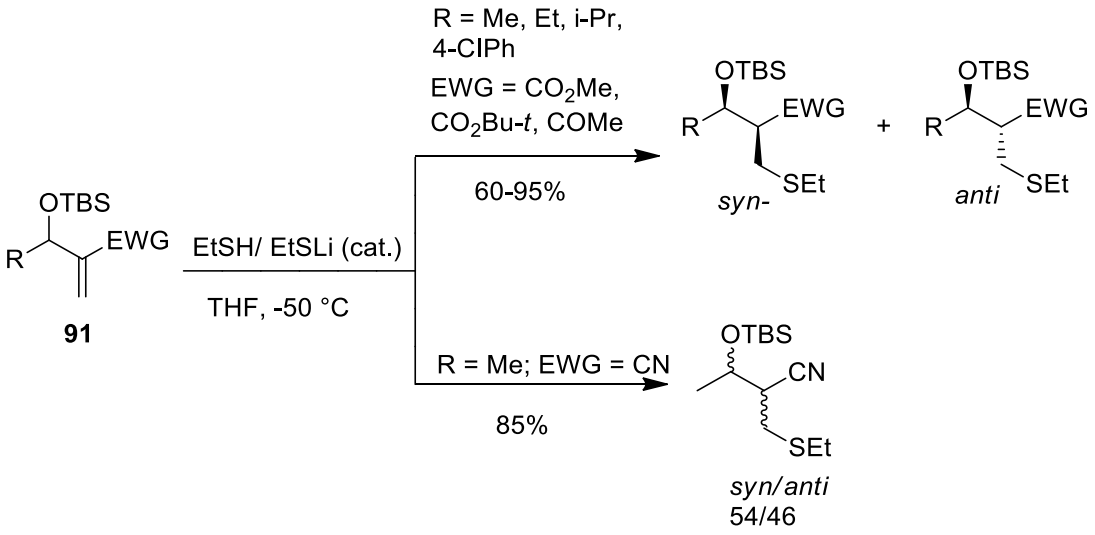

Scheme 31: Conjugate addition to a TBS protected MBH adduct using ethanethiol to synthesize *syn*-β-hydroxy-α-thiomethyl carbonyl compounds and their conversion into β-lactams.

Table 5: Conjugate addition reaction to different TBS protected MBH adducts using ethanethiol and their diastereomeric ratios.

EWG	**R**	**Thiol**	**Protecting group**	***Syn/anti***
CO_2Me	Me	EtSH	TBS	97/3
CO_2Bu-*t*	Me	EtSH	TBS	92/8
CO_2Me	Et	EtSH	TBS	94/6
CO_2Me	*i*-Pr	EtSH	TBS	92/8
CO_2Me	*p*-Cl-C_6H_4	EtSH	TBS	99/1
COMe	Me	EtSH	TBS	90/10
CN	Me	EtSH	TBS	54/46

The presence of the bulky TBS group also controls the stereoselectivity. The *syn* diastereomer was obtained as the major product during the addition reaction. This is explained by the following proposed mechanism. The conjugate addition reaction involves the formation of an enolate intermediate that can take on one of two conformations, where one conformer is favoured over the other. In the mechanism shown in Scheme 32, conformer A is favoured, this is due to the absence

of any unfavourable steric interactions between the groups R'' and OMe present on the enolate. The *syn* product is obtained as the major product as a result of the presence of the bulky TBS group in the favoured conformer A, which blocks the top side and only allows the incoming proton to approach from the bottom. Low diastereoselectivity is obtained in the absence of a bulky protecting group, as the proton can approach from either the top or the bottom direction (**Scheme 32**).[68,69]

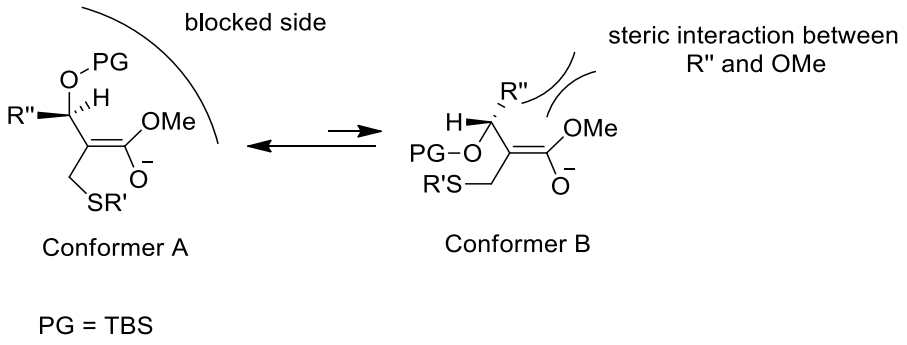

Scheme 32: Mechanism showing the formation of the *syn* product as the major diastereomer.

MBH adducts **92** obtained from iminium salts **93** and methyl acrylate **94** in the presence of DBU in catalytic amounts can undergo a conjugate addition reaction using (trimethylsilyl)dialkylamine to produce diamines **95** (**Scheme 33**).[64]

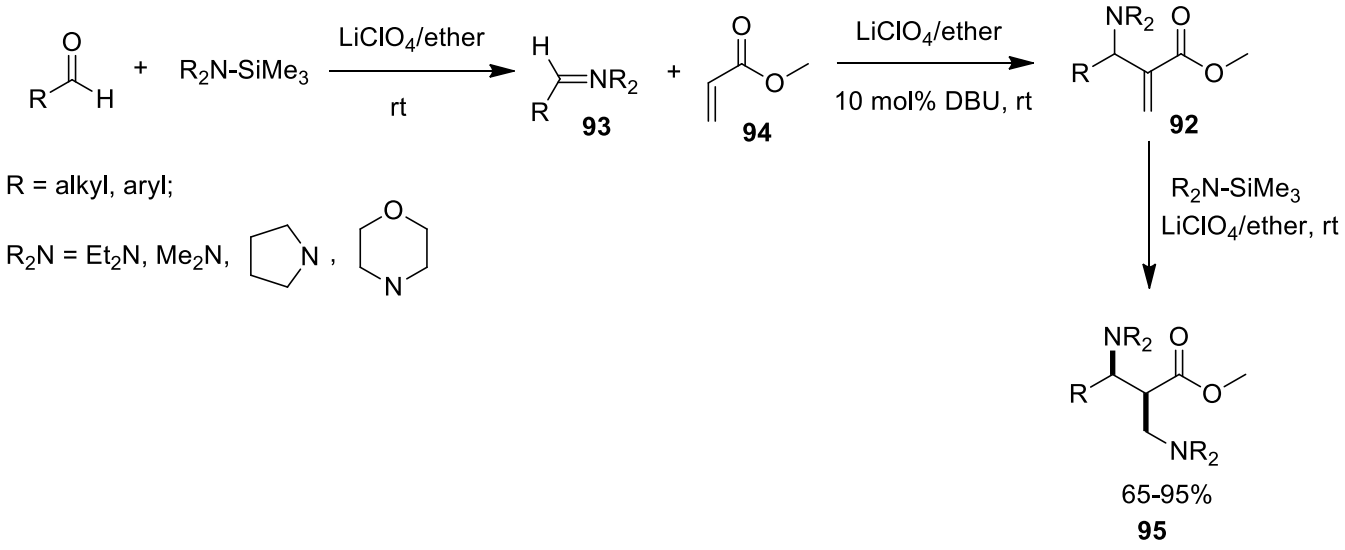

Scheme 33: Conjugate addition reaction of (trimethylsilyl)dialkylamine on MBH adducts **92** obtained from iminium salts **93** and methyl acrylate **94** to produce diamines **95**.

A one-pot method has been reported by Wang *et al.* for the successive MBH and Michael addition reaction to generate two C-C bonds. The reaction involves an α, β-unsubstituted acrylate **96**, an aromatic aldehyde **97** and methide **98** as a nucleophile in the presence of DBU to generate a multi-functional product (**Scheme 34**).[70]

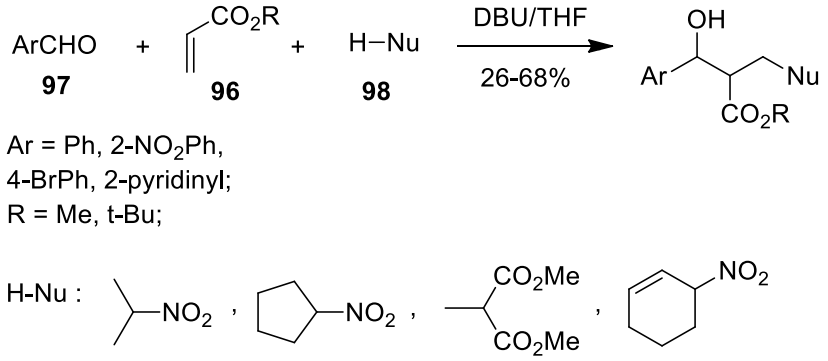

Scheme 34: A one-pot method for the successive Morita Baylis hillman and Michael addition reaction reported by Wang *et al.*[70]

1.5.2.2. Allylic substitution reaction (S_N2')

An allylic substitution reaction can be done on MBH adducts by changing the hydroxy group present on the adduct into a good leaving group. The allylic substitution reaction on MBH adducts with a protected alcohol group has been widely performed, proceeding via the S_N2' mechanism.[63] The S_N2' type substitution reaction can be performed on acetates using different nucleophiles, such as the C-, O-, N-, S-, and P- nucleophiles, generating multi-substituted alkenes. The MBH adduct can undergo a conjugate addition, an S_N2' substitution or S_N2'- S_N2' substitution depending on the structure of the MBH adduct as well as the conditions under which the reaction was performed.[71]

In the presence of a primary MBH adduct, an allyl alcohol **99** Michael addition reaction occurs. Where the nucleophile adds on to the terminal carbon of an activated alkene (**Scheme 35A**).[72] When the hydroxy group on the MBH adduct is converted into a good leaving group (acetoxy group), an S_N2' substitution or S_N2'- S_N2' substitution occurs depending on the reaction conditions. Performing the reaction in organic solvents under organocatalytic conditions, S_N2' substitution occurs by sequential addition-elimination reaction. This reaction occurs on the MBH acetate **100**, by the substitution of the alkene position and the rearrangement of the double bond (**Scheme 35B**).[72] S_N2'- S_N2' substitution occurs when a Lewis base is used in an aqueous medium, substitution occurs at the leaving acetoxy group. This reaction occurs by the addition of the base

on the MBH acetate **100**, which results in the elimination of the leaving group, forming an intermediate **101** which is attacked by the nucleophile (**Scheme 35C**).[72]

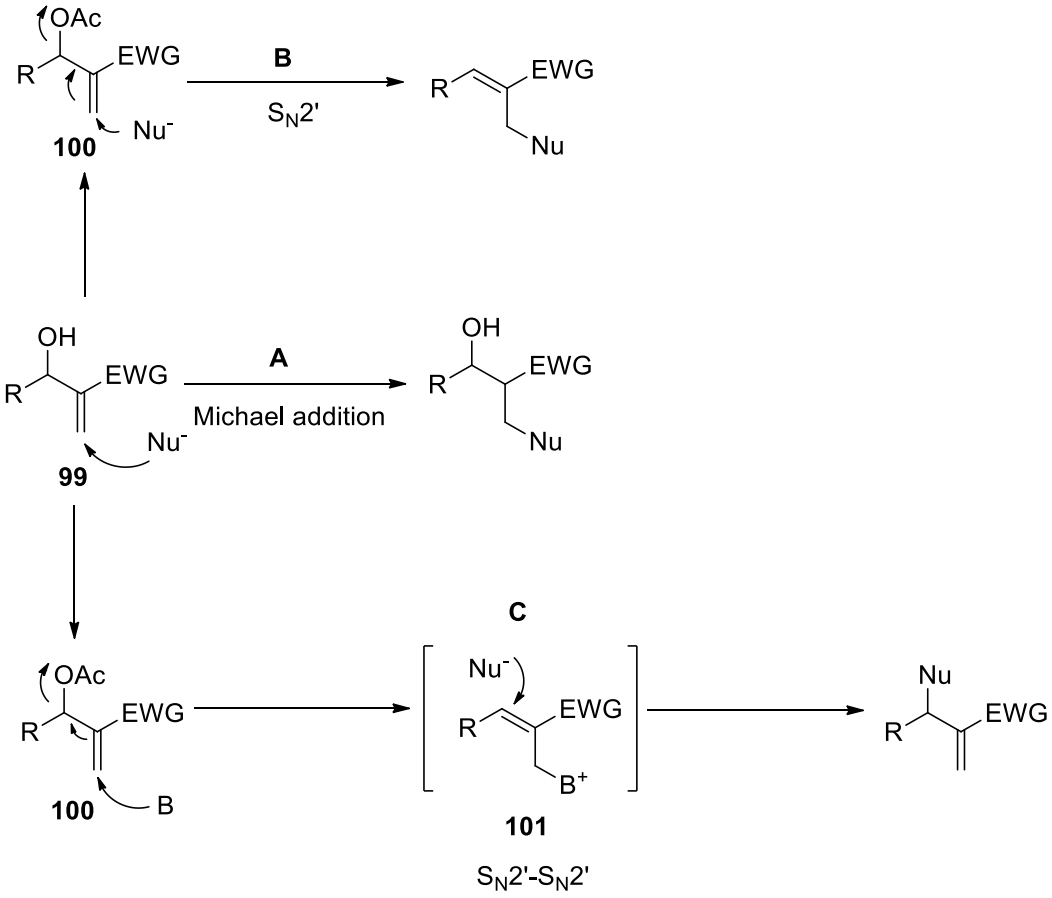

Scheme 35: Nucleophilic substitution reactions on the MBH adduct and acetates.

1.5.2.2.1. Nitrogen nucleophiles

Nitrogen nucleophiles have been used to convert MBH acetates **102** stereoselectively into (*E*)-allyl amines **103**. Substitution reactions of MBH acetates using primary or secondary amines primarily formed (*E*)-allyl amines. Treating the MBH acetate **102** with sodium azide and doing a reduction on the azide product **104** produces the primary (*E*)-allyl amine **105** (**Scheme 36**).[64]

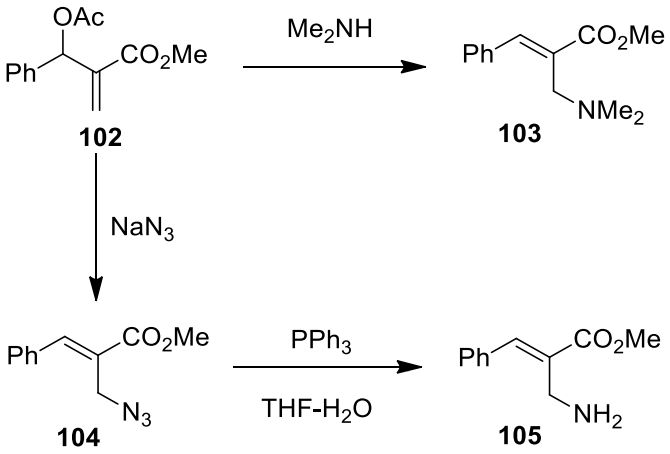

Scheme 36: Stereoselective conversion of MBH acetates **102** into (*E*)-allyl amines **103** and **105** using nitrogen nucleophiles.

Drewes *et al.* reported the reaction between MBH acetates **106** and formyl imidazole **107**, where changing the reaction conditions gave either the allylic substitution **108** or the rearrangement product **109**. By controlling the reaction conditions the desired product could be obtained. Allylic substitution product **108** was obtained when DABCO was used in THF and performing same reaction without DABCO in methanol gave the rearrangement product **109** (**Scheme 37**).[73]

The allylic substitution product **108** forms by the attack of the DABCO nucleophilic catalyst at the α-allyl position of the MBH acetate **106**, leading to the elimination of the acetate leaving group. The nucleophile, which is the formyl imidazole **107** then adds on the alkene formed from the elimination of the acetate group, which is activated by the ester electron withdrawing group. In the absence of a catalyst, the formyl imidazole **107** attacks the α-allyl position directly, leading to the elimination of the leaving group and forming the rearrangement product **109** (**Scheme 37**).

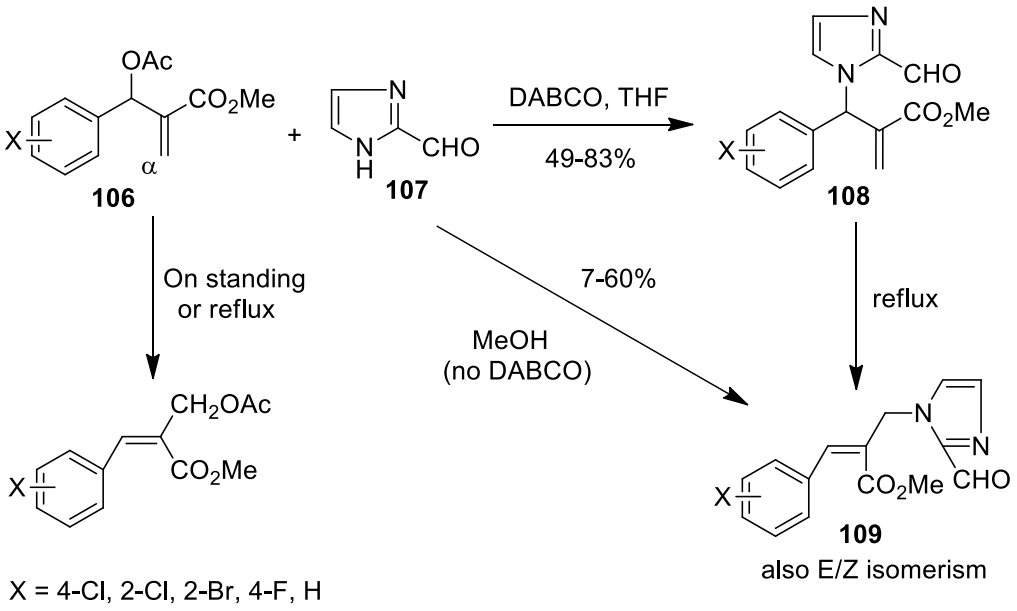

Scheme 37: A reaction between MBH acetates and formyl imidazole reported by Drewes *et al.*[73]

The reaction between MBH acetates **110** and different amines **111** has been reported by Xia *et al.* using both ultrasound irradiation and conventional stirring. Using ultrasound afforded the target products **112** with improved reaction yields, shorter reaction times and without forming any byproducts (**Scheme 38**). The DABCO catalyst attacks the α-allyl position on the MBH acetate **110** eliminating the acetate group, the amine **111** then attacks the alkene generated, forming product **112.**[74]

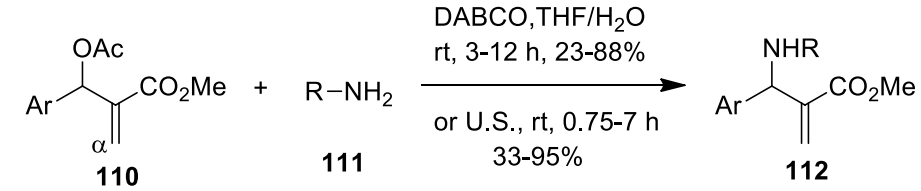

Ar = Ph, 2-pyridyl, 4-ClPh, 2-ClPh, 4-FPh, 4-CF_3Ph, 4-BrPh, 4-MePh, 2,4-Cl_2Ph;
R = Ph, 4-MeOPh, 4-MePh, 2-MePh, 4-ClPh, 2,5-$(Me)_2$Ph, Bn, i-Pr, 2-(H_2N)Ph,
3-ClPh, 2-naphthyl, 4-HOPh,

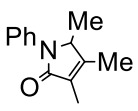

Scheme 38: A reaction between MBH acetate **110** and different amines **111** using both ultrasound irradiation and conventional stirring reported by Xia *et al.*[74]

1.5.2.2.2. Carbon nucleophiles

Yadav *et al.* reported an allylic substitution reaction of MBH acetates **113** with tosylmethyl isocyanide **114** using boron trifluoride diethyl etherate (BF_3OEt_2) as a Lewis acid, affording trisubstituted olefin products **115** (**Scheme 39**).[64]

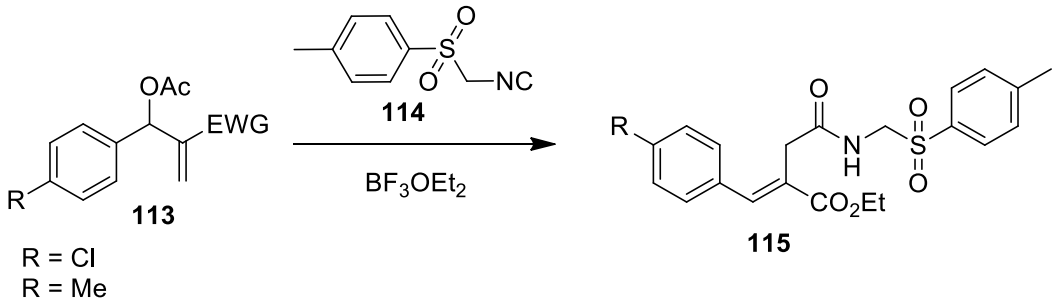

Scheme 39: An allylic substitution reaction of MBH acetates **113** with tosylmethyl isocyanide **114** using boron trifluoride diethyl etherate (BF_3OEt_2).

1.5.2.2.3. Phosphorus nucleophiles

Basaviah and Pandiaraju reported an allylic substitution reaction between trialkyl phosphite and the MBH acetate **116**. The MBH acetates **116** were prepared from aromatic or aliphatic aldehydes. Allyl phosphonates **117** were obtained in a very good yield and excellent diastereoselectivity. The *Z* isomer formed as the predominant isomer (**Scheme 40**).[72]

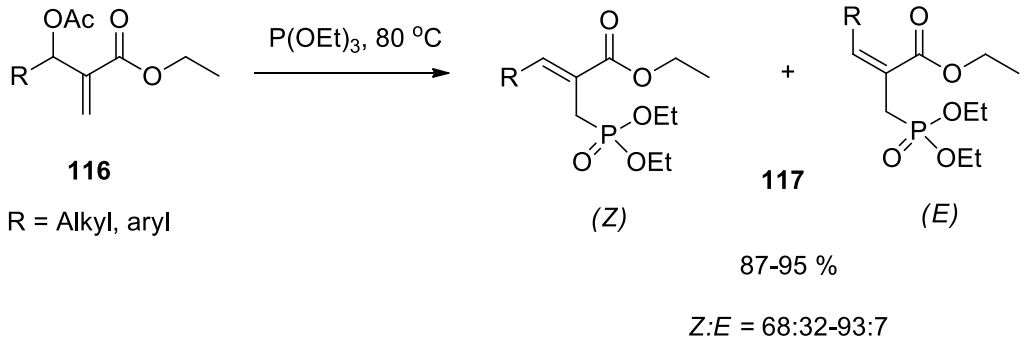

Scheme 40: Reaction of the MBH acetate **116** with the trialkyl phosphite.

The type of reaction occurring, whether conjugate addition or allylic substitution depends on the type of MBH adduct present. The primary MBH adduct, with a hydroxyl leaving group will give a conjugate addition product upon the attack by a nucleophile since the hydroxyl group is a poor

leaving group. Converting the hydroxyl group to a better leaving group such as the acetoxy group, increases its chances for allylic substitution reaction.

1.6. Applications of MBH adducts

MBH adducts are very important synthons since they contain at least three distinctive functional groups in proximity. They can be used to generate complex and diverse compounds, imparting new aspects to organic chemistry. The initial application of these adducts was reported in 1982 by Drewes and Emslie to synthesize integerrinecic acid **118**, later in 1983 Hoffman and Rabe applied the MBH adduct in the synthesis of mikanecic acid **119** (**Scheme 41**).[27]

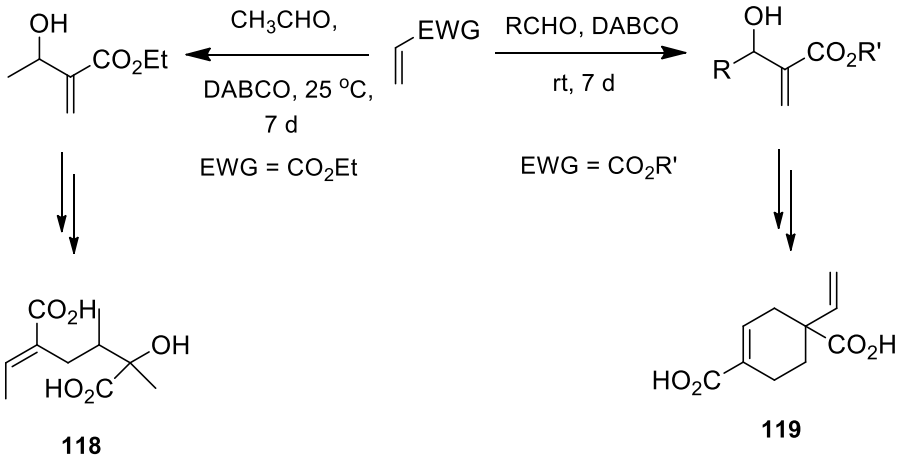

Scheme 41: Using the MBH adducts to synthesize integerrinecic acid and mikanecic acid.

In 2018, Basaviah and Naganoboina also reported the synthesis of naphthyridine **120**, piperidin-2-one **121** and piperidine-2,6-dione **122** frameworks from the alkenoates obtained from the Johnson-Claisen rearrangement of the MBH adducts (**Scheme 42**).[50]

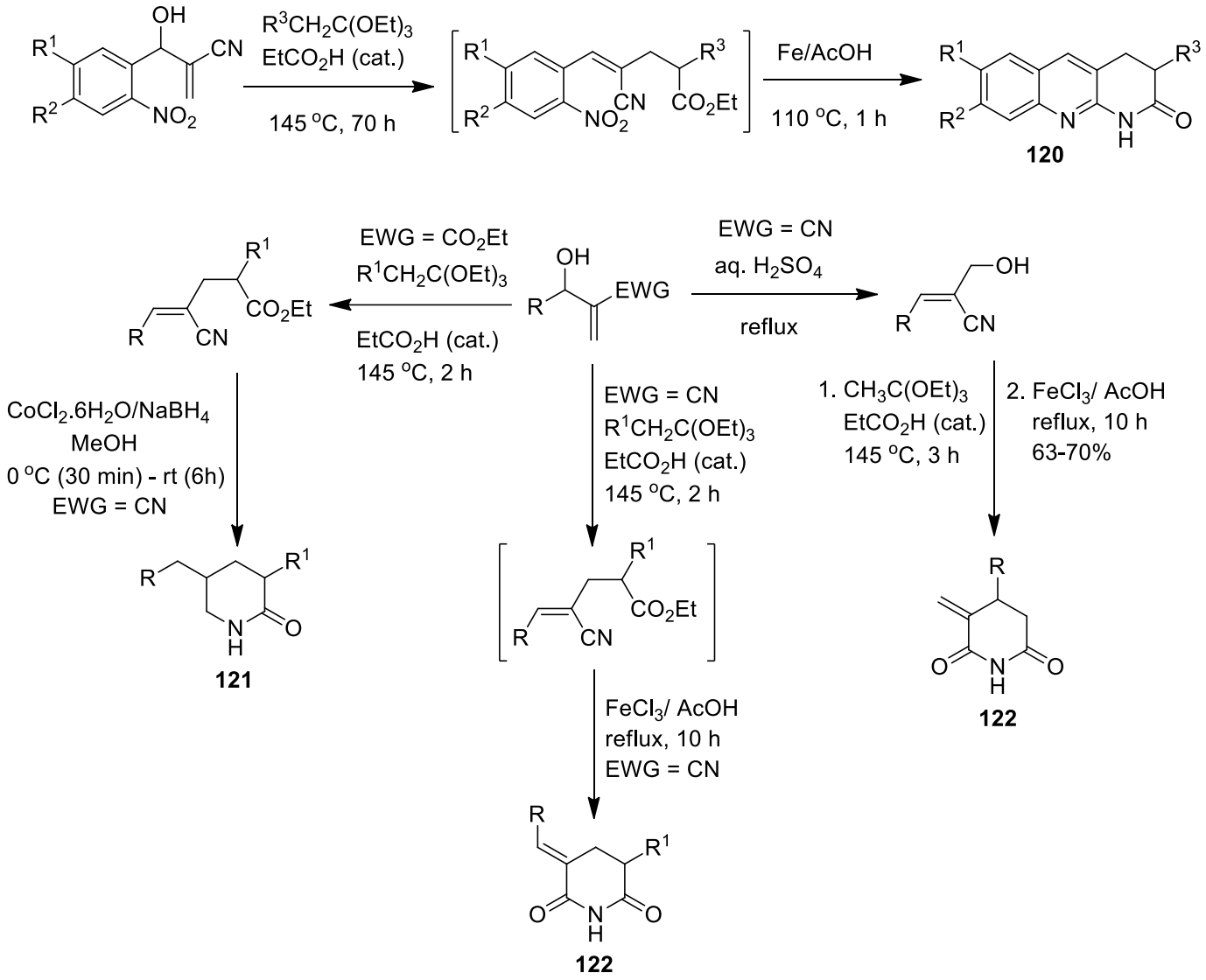

Scheme 42: Synthesis of naphthyridine, piperidin-2-one and piperidine-2,6-dione frameworks reported by Basaviah and Naganoboina.

(+)-Arnicenone **123**, an angular triquinane sesquiterpene, and (-)-pentenomycin I **124**, a cyclopentanoid antibiotic have been synthesized by Ogasawara *et al.* by transforming the resulting adducts **125** obtained from the MBH coupling of formalin **126** and chiral bicyclic enones (-)-KDP **127** and (+)-KDP **128**, respectively (**Scheme 43**).[75]

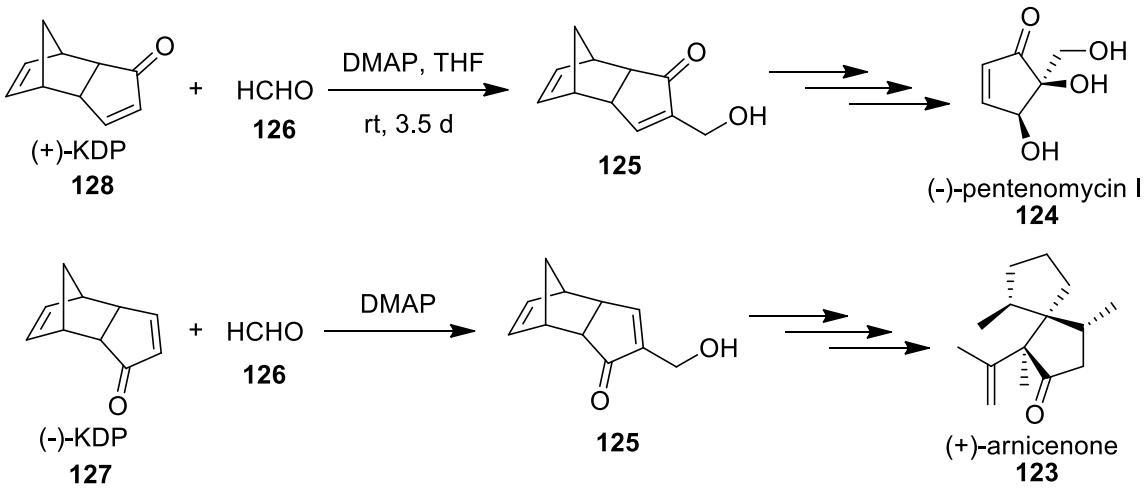

Scheme 43: Synthesis of (+)-arnicenone and (-)-pentenomycin I by Ogasawara *et al*.

Oxazolidin-2-one **129** has been synthesized by Coelho and Rossi by transforming the MBH adduct **130** obtained from piperonal **131**. This molecule was then used to synthesize derivatives of β-chloramphenicol **132** and substituted amino alcohols (**Scheme 44**).[76]

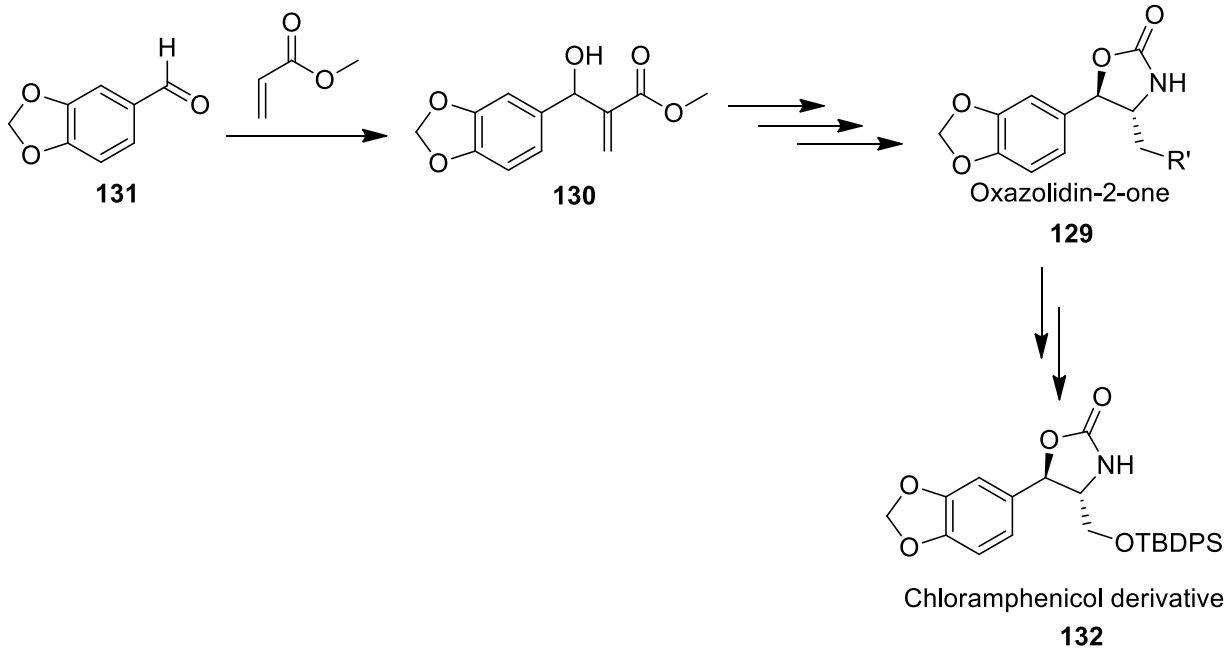

Scheme 44: Synthesis of β-chloramphenicol derivative **132** using Oxazolidin-2-one **129** by transforming the MBH adduct **130** obtained from piperonal **131**.

A methyl acrylate **133** and octanal **134** derived MBH adduct **135** has been used to synthesize a very crucial natural product, (-)-acaterin **136**, as reported by Singh *et al.* (**Scheme 45**).[77]

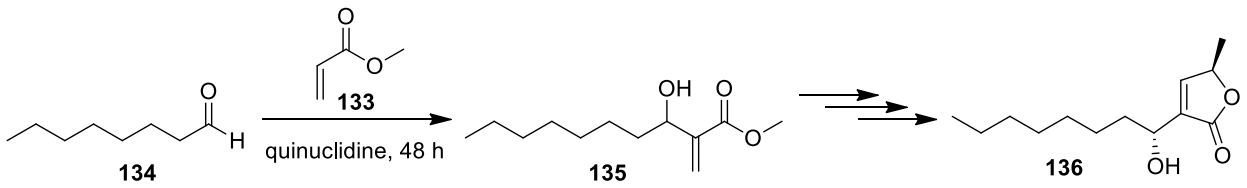

Scheme 45: A methyl acrylate **133** and octanal **134** derived MBH adduct **135** used to synthesize (-)-acaterin **136**.

Many bioactive molecules and natural products have been obtained by different research groups using the derivatives of MBH adducts, such as bromides, acetates and carbonates. The first total synthesis of (±)-floribundane B **137** was achieved by Souza and coworkers through a Johnson-Claisen rearrangement of MBH adducts **138** in 2019 (**Scheme 46**).[78]

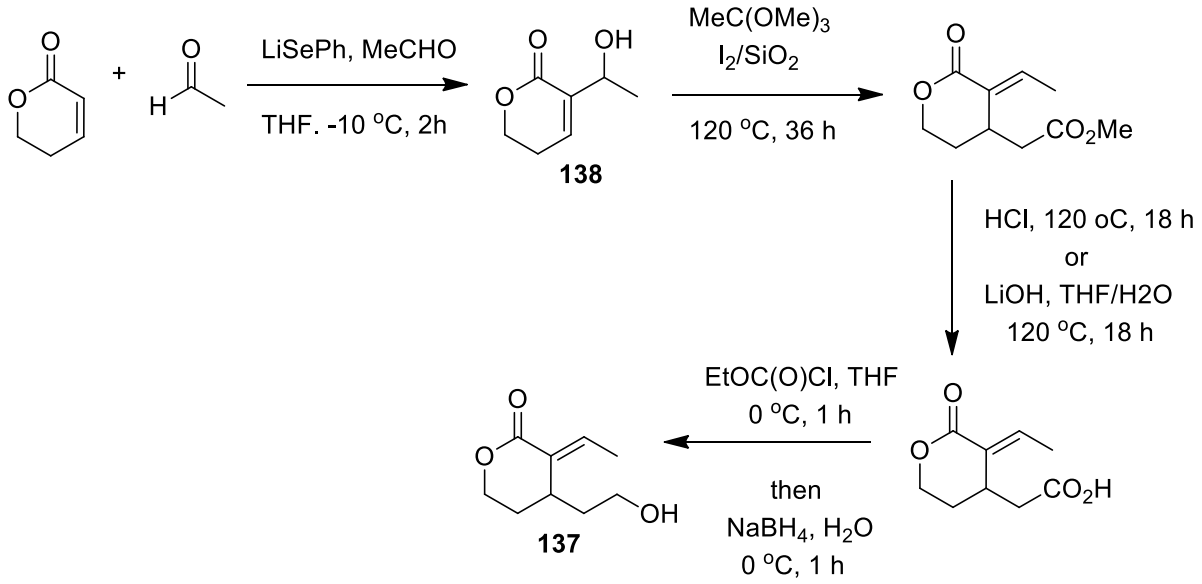

Scheme 46: The first total synthesis of (±)-floribundane B through a Johnson-Claisen rearrangement of MBH adducts.

CHAPTER 2

2. AIMS AND OBJECTIVES

2.1. Aim

The main aim of this project was to perform the Morita-Baylis-Hillman (MBH) reaction on differently substituted benzaldehydes and various activated alkenes and then to react the products with different nucleophiles to examine the effect of different MBH adducts and nucleophiles on the conjugate addition reaction. In addition, the aim was to prepare a diverse range of products with multiple possible applications.

2.2. Objectives

- To obtain racemic MBH adducts by performing an MBH reaction between different benzaldehydes and activated alkenes carrying different electron withdrawing groups: ester and nitrile group (**Scheme 47**).

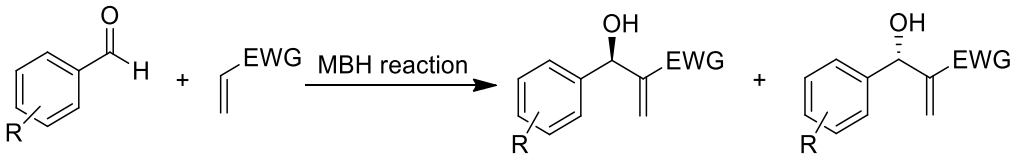

R = H, 4-Cl, 4-NO_2, 2-Br, 2-Cl
EWG = CO_2Me, CO_2Et, CN

Scheme 47: The MBH reaction using differently substituted benzaldehydes and activated alkenes.

- To protect the alcohol on the MBH adducts with different protecting groups, TBDMS and TMS.
- To synthesize a range of derivatives by performing a conjugate addition reaction of amine and thiol nucleophiles on the MBH adducts (**Scheme 48**).

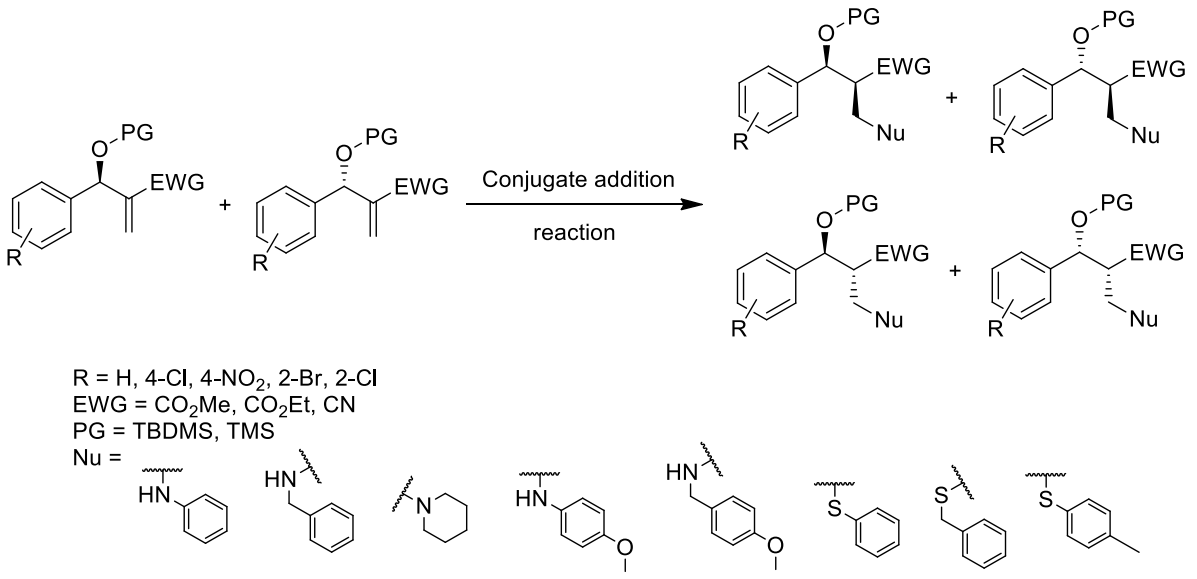

Scheme 48: The addition of different nucleophiles on the MBH adducts.

- To deprotect the MBH adducts.
- To determine the effect of the protecting and electron withdrawing groups on the nucleophilic addition reaction.
- To determine the diastereomeric ratio of the products.
- To explore methods for obtaining amide MBH adducts.

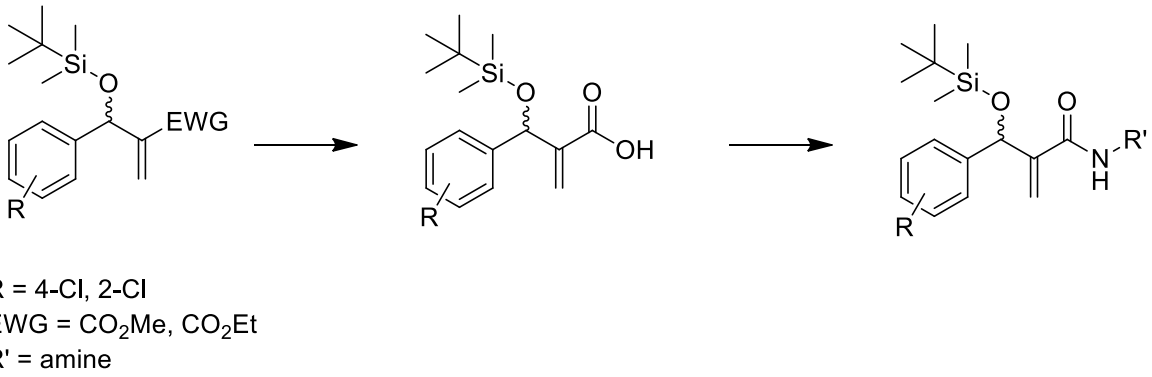

Scheme 49: Original route for the synthesis of amide MBH adducts.

- To perform nucleophilic addition on the amide containing adducts.

CHAPTER 3

3. RESULTS AND DISCUSSION

The first goal was to prepare MBH adducts from different substituted benzaldehydes and activated alkenes in the presence of DABCO. DABCO acts as a catalyst and drives the reaction by increasing its reaction rate.

Activated alkenes with different electron withdrawing groups were used. These electron withdrawing groups decrease the electron density on the alkene, making it more electrophilic, thereby improving its reactivity towards the catalyst. Methyl acrylate **139**, acrylonitrile **140** and methyl vinyl ketone **141** were used as the activated alkenes. These activated alkenes were commercially available (**Figure 8**).

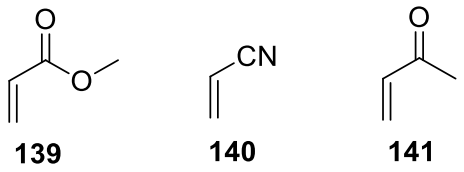

Figure 8: The activated alkenes used in the MBH reaction.

Substituted and unsubstituted benzaldehydes were used for the MBH reaction. *p*-chloro **142**, *p*-nitro **143**, *o*-cloro **144** and *o*-bromo **145** substituted benzaldehydes were used (**Figure 9**). The type of substituted benzaldehydes used were randomly chosen based on their availability. Most of the MBH adducts were synthesized using the substituted benzaldehydes since they have been proven to increase the rate of the MBH reaction compared to the unsubstituted ones due to their electron withdrawing nature.

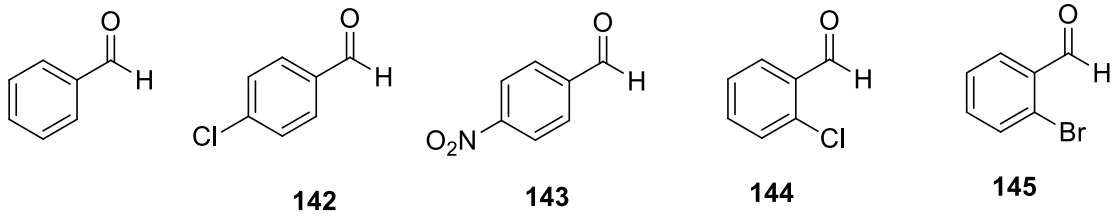

Figure 9: Substituted and unsubstituted benzaldehydes used for the MBH reaction.

Once the MBH adducts were prepared, the next goal was to protect the hydroxyl group with different protecting groups, TBDMS and TMS groups were used. The protection of the hydroxyl group was important to control the stereoselectivity during the subsequent nucleophilic addition reaction. Different protecting groups were used, to determine their effect on the diastereoselectivity of the addition reaction.

The next phase of the project was to react the protected adducts with different nucleophiles to prepare diastereomers where possible, the aim was to isolate the diastereomers, and to determine the ratio of the different diastereomers obtained. Different nitrogen and sulfur nucleophiles were used in order to compare their diastereomeric ratios and determine the best nucleophile for the addition on the MBH adducts (**Figure 10**).

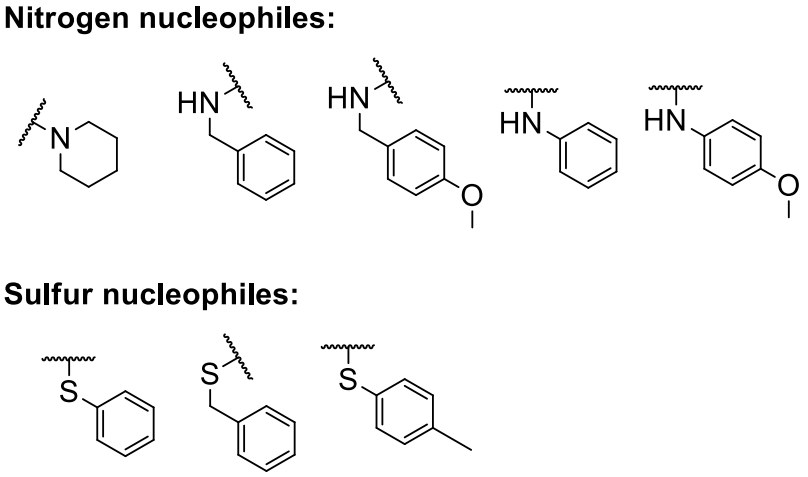

Figure 10: Nucleophiles used for the conjugate addition reaction of protected MBH adducts.

The last step was to deprotect the diastereomers to obtain the final product.

The next goal was to prepare amide derivatives using different methods. Attempts were made to synthesize MBH adducts carrying amide as the electron withdrawing group. A simple MBH reaction using commercially available acrylamides and benzaldehydes was not performed since, they have been reported to give very low yields for the MBH amide product along with the formation of byproducts. Hence, alternative routes were attempted.

Finally, the goal was to add long alkyl chain containing nitrogen nucleophiles to the MBH amides. The aim was to synthesize compounds that would mimic the natural antibacterial peptides that are produced by living organisms as antibacterial agents (**Figure 11**).[79]

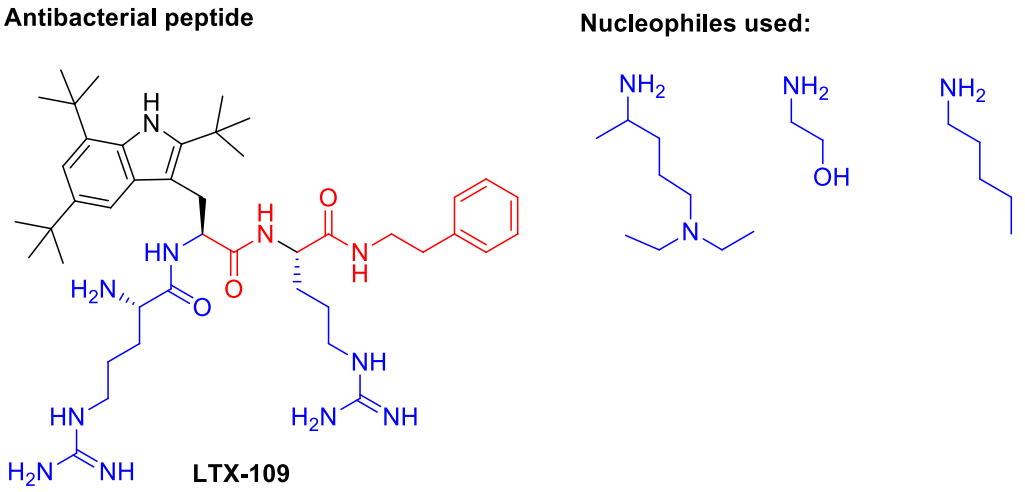

Figure 11: The nucleophiles used for the addition reaction on the MBH adducts carrying amide group and the antibacterial agent the products were meant to mimic.[79]

3.1. Preparation and characterization of MBH ester, nitrile and ketone adducts and their conjugate addition products.

The first step was to prepare ester, nitrile and ketone adducts **146**. These adducts **146** were then protected using TBDMSCl and TMSCl to give compound **147**, which were then reacted with different nucleophiles forming conjugate addition product **148.** Followed by a deprotection step using TBAF in THF to give the final product **149 (Scheme 50)**.

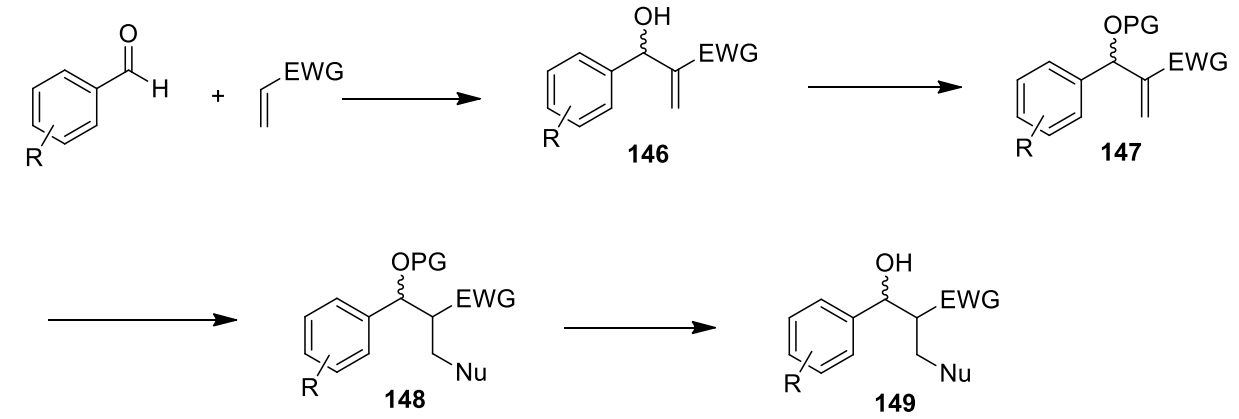

R = H, 4-Cl, 4-NO_2, 2-Br, 2-Cl
EWG = CO_2Me, CN, COMe
PG = TBDMS, TMS
Nu = amine and sulfur Nu

Scheme 50: The proposed synthesis to obtain the diastereomers by performing a conjugate addition reaction on the MBH adducts.

3.1.1. Preparation and characterization of the MBH ester, nitrile and ketone adducts.

The first step involved the formation of the MBH adducts **146**. The MBH ester, nitrile and ketone adducts were easily prepared by reacting different benzaldehydes **150** with commercially available methyl acrylate, acrylonitrile, and methyl vinyl ketone **151**, respectively. The reaction was done at room temperature, in the presence of 1,4-diazabicyclo[2.2.2.]octane (DABCO) as a catalyst (**Scheme 51**). The product obtained from the reaction was then extracted and purified using column chromatography. The method used was based on that reported by Juma *et al.*[69] with only a slight change, as the reaction was performed at room temperature and not at 0 ˚C.

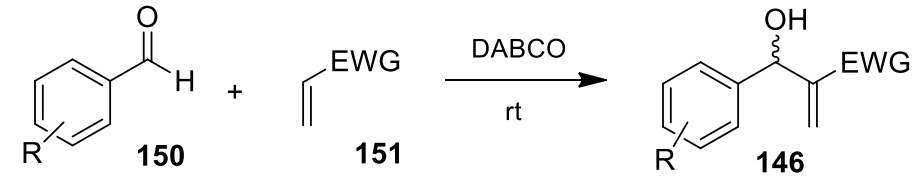

R = H, 4-Cl, 4-NO_2, 2-Br, 2-Cl
EWG = CO_2Me, CN, COMe

Scheme 51: The Morita Baylis Hillman reaction on the substituted benzaldehydes and activated alkenes using DABCO at room temperature.

The reaction duration varied depending on the type of starting material used. Substituted benzaldehydes normally gave a shorter reaction time compared to the unsubstituted ones. The substituents present on the benzaldehydes were chlorine, bromine and nitro groups; these are electron withdrawing groups, pulling electrons away from the reacting carbon, making it more electrophilic and readily available for reaction. Yields of the product also varied depending on the starting materials used and on the duration of the reaction.

Table 6 shows the different combinations of substituted benzaldehydes and activated alkenes carrying different electron withdrawing groups used in the MBH reaction and the yields that were obtained from those reactions. All the products obtained from the MBH reaction gave very good yields, with the best yield obtained for the unsubstituted nitrile adduct, followed by the *para*-chloro substituted ester adduct. Most of the yields were in the 70-80% range. The formation of these adducts was confirmed using different characterization techniques such as ^{1}H NMR, ^{13}C NMR, IR spectroscopy and determining the melting point.

Table 6: The differently substituted benzaldehydes and activated alkenes used in the MBH reaction and the yields of **146** obtained from the different reactions.

R	**EWG**	**Yield (%) of 146**
H	CO_2CH_3	59
4-Cl	CO_2CH_3	84
4-NO_2	CO_2CH_3	71
2-Br	CO_2CH_3	78
H	CN	87

2-Cl	CN	77
2-Br	CN	83
H	$COCH_3$	61

3.1.1.1. Characterization of the MBH esters.

Esters **152-155** (**Figure 12**) were prepared, and their characterization is discussed below.

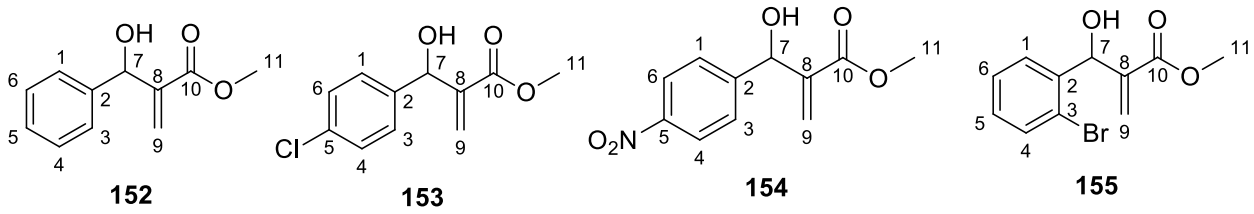

Figure 12: The Morita Baylis Hillman ester adducts that were synthesized.

Table 7: The IR and the NMR data obtained for the MBH esters shown in Figure 12.

Compound No.	**IR** (neat, cm^{-1})	**NMR**
152	3318 (OH), 2958 (C-H), 1714 (C=O)	**^{1}H NMR (400 MHz, $CDCl_3$)** δ 7.40-7.25 (5H, m, Ar-H), 6.34 (1H, s, H-9a), 5.84 (1H, s, H-9b), 5.57 (1H, d, *J* = 5.6 Hz, H-7), 3.73 (3H, s, H-11), 3.05 (1H, d, *J* = 5.6 Hz, OH); **^{13}C NMR (101 MHz, $CDCl_3$)** δ 166.8 (C-10), 141.9 (C-2), 141.2 (C-8), 128.4 (C-1,3), 127.8 (C-5), 126.5 (C-4,6), 126.2 (C-9), 73.3 (C-7), 52.0 (C-11).
153	3331 (OH), 2942 (C-H), 1721 (C=O)	**^{1}H NMR (400 MHz, $CDCl_3$)** δ 7.34-7.31 (4H, m, Ar-H), 6.35 (1H, s, H-9a), 5.83 (1H, s, H-9b), 5.53 (1H, d, *J* = 5.7 Hz, H-7), 3.74 (3H, s, H-11), 3.08 (1H, d, *J* = 4.0 Hz, OH); **^{13}C NMR (101 MHz, $CDCl_3$)** δ 166.7 (C-10), 141.6 (C-2), 139.8 (C-8), 133.6 (C-5), 128.6 (C-1,3), 128.0 (C-4,6), 126.5 (C-9), 72.8 (C-7), 52.1 (C-11).

154	3508 (OH), 2981 (C-H), 1695 (C=O)	**^{1}H NMR (400 MHz, $CDCl_3$)** δ 8.21 (2H, d, *J* = 6.7 Hz, H-4,6), 7.58 (2H, d, *J* = 6.8 Hz, H-1,3), 6.39 (1H, s, H-9a), 5.87 (1H, s, H-9b), 5.63 (1H, d, *J* = 6.2 Hz, H-7), 3.75 (3H, s, H-11), 3.29 (1H, d, *J* = 6.1 Hz, OH); **^{13}C NMR (101 MHz, $CDCl_3$)** δ 166.4 (C-10), 148.6 (C-5), 147.5 (C-8), 141.0 (C-2), 127.33 (C-1,3), 127.26 (C-9), 123.6 (C-4,6), 72.8 (C-7), 52.2 (C-11).
155	2951 (C-H), 1708 (C=O)	**^{1}H NMR (400 MHz, $CDCl_3$)** δ 7.55 (2H, d, *J* = 7.7 Hz, H-1,4), 7.36 (1H, t, *J* = 7.6 Hz, H-5), 7.17 (1H, t, *J* = 7.6 Hz, H-6), 6.35 (1H, s, H-9a), 5.95 (1H, s, H-7), 5.56 (1H, s, H-9b), 3.79 (3H, s, H-11), 3.33 (1H, m, OH). **^{13}C NMR (101 MHz, $CDCl_3$)** δ 167.0 (C-10), 140.6 (C-8), 139.8 (C-3), 132.8 (C-4), 129.4 (C-6), 128.4 (C-1), 127.7 (C-5), 127.2 (C-9), 123.1 (C-2), 71.5 (C-7), 52.2 (C-11).

Table 7 shows the characterization data obtained for the MBH esters **152-155** (**Figure 12**). The IR spectra showed the presence of all the characteristic functional groups observed in a methyl acrylate derivative, which confirmed the formation of the product. IR spectroscopy showed the presence of a hydroxyl, carbonyl, and an alkene functional group. The IR spectra of the methyl acrylate adducts showed the presence of a broad stretch at around 3000 cm^{-1}, which belonged to the hydroxyl group. The presence of this stretch confirmed the formation of the adduct since it implied that a reaction had occurred between the aldehyde and the activated alkene to form a new functional group, a hydroxyl group. The IR spectra also showed the presence of a strong carbonyl stretch around 1700 cm^{-1}. These stretches are expected to be present in a typical methyl acrylate adduct, confirming the formation of these adducts.

The ^{1}H and ^{13}C NMR spectra also confirmed the formation of these adducts due to the presence of key signals in the spectra. Figure 13 shows the ^{1}H NMR spectrum of MBH adduct **153**. The most deshielded peaks belong to the aromatic protons, integrating for 5 protons in an unsubstituted

adduct and for 4 protons in all the substituted ones. All the aromatic peaks appeared in the 7-8 ppm range, confirming the presence of an aromatic ring. The terminal vinylic protons (H-9a and H-9b) appeared at around 5 and 6 ppm. There was no geminal coupling observed between H-9a and H-9b as they appeared as singlets in the proton NMR spectra.

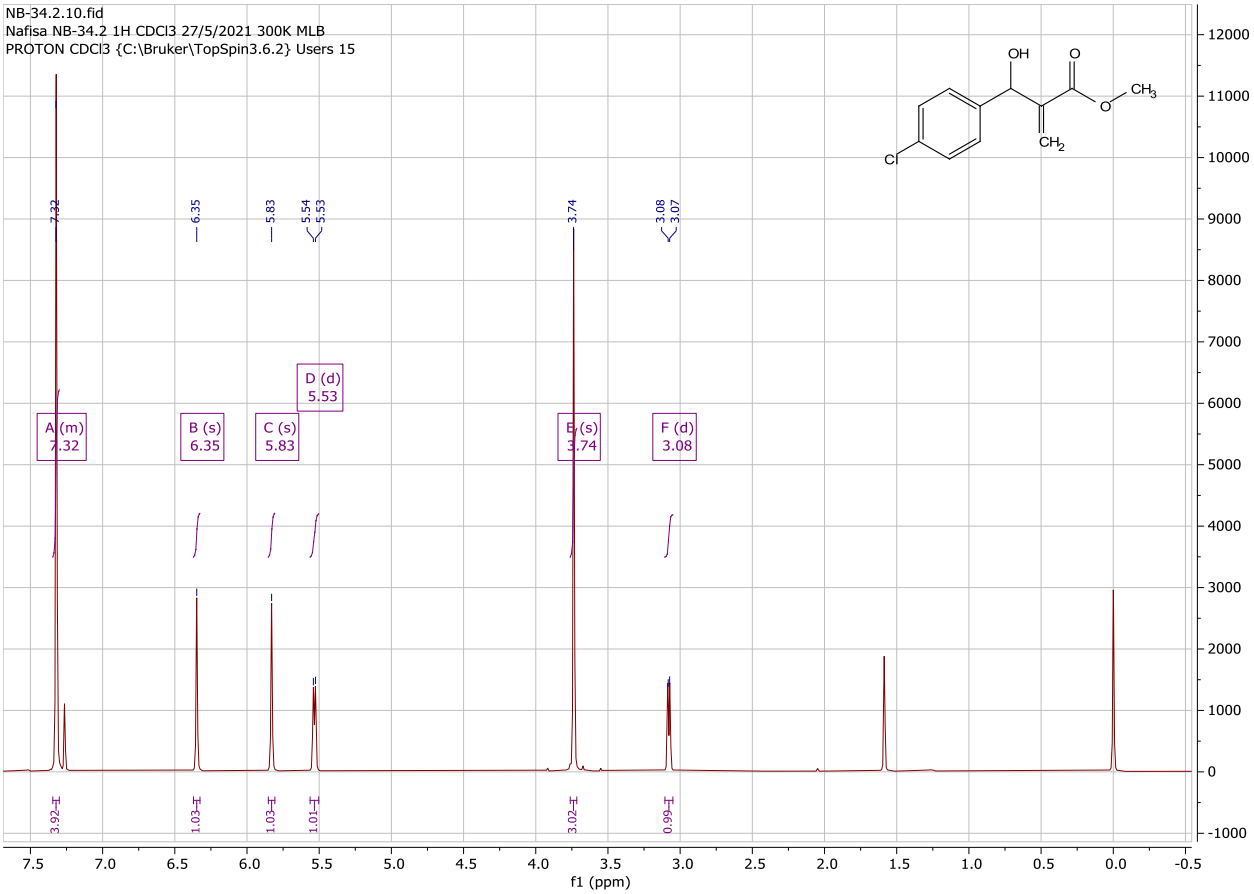

Figure 13: The ^{1}H NMR spectrum of MBH adduct **153**.

These H-9 protons appeared more deshielded compared to H-7 for all the adducts except for the *ortho*-bromo adduct **155**. The electronegative bromine in the *ortho* position appears to pull electrons away from H-7, making it more deshielded compared to one of the H-9 protons. The H-7 proton signal was found around 5 ppm, integrating for 1 proton, and appearing as a doublet, coupling to the neighbouring OH proton. Methyl protons were present at around 3 ppm for all the adducts, confirming the presence of a methyl ester group. The appearance of an OH signal at around 3 ppm also confirmed the formation of the methyl acrylate adducts. The OH peak appeared as a doublet or a multiplet, showing coupling to the neighbouring H-7 proton.

The ^{13}C NMR spectra also confirmed the formation of the expected product. All the important peaks were present in the spectra, such as the carbonyl peak, which was seen around 166 ppm, as well as all the aromatic carbon signals around 120-140 ppm. The carbon attached to the hydroxyl group (C-7) was also present at around 70 ppm, and the most shielded peak belonged to the carbon of the CH_3 group. The peak around 126 ppm belonged to C-9, which appeared negative on the DEPT135 spectrum, confirming the presence of two terminal alkene protons.

All of these compounds have been reported in literature, with very similar IR and NMR data reported. Compound **154** has been reported before by Vieira *et al.*[80] and the NMR data reported is very similar to the data obtained here.

3.1.1.2. Characterization of the MBH nitriles.

Nitriles **156-158** (**Figure 14**) were prepared following the same procedure as the methyl acrylate adducts, except that acrylonitrile was used as the activated alkene. All the compounds shown in Figure 14 were obtained in an exceptionally good yield. The expected compounds were obtained, as verified by different characterization techniques.

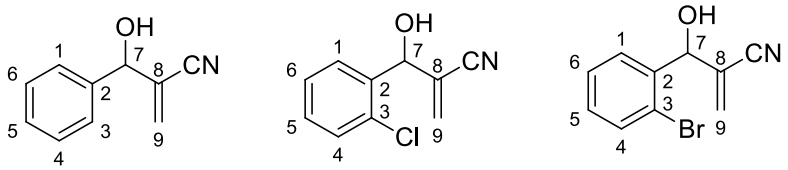

156 **157** **158**

Figure 14: The Morita Baylis Hillman nitrile adducts synthesized.

Table 8: The IR and the NMR data obtained for the MBH nitriles shown above in figure 14.

Compound No.	**IR** (neat, cm^{-1})	**NMR**
156	3450 (OH), 2981 (C-H), 2229 (CN)	**^{1}H NMR (400 MHz, $CDCl_3$)** δ 7.43-7.35 (5H, m, Ar-H), 6.12 (1H, s, H-9a), 6.04 (1H, s, H-9b), 5.32-5.30 (1H, m, H-7), 2.42-2.36 (1H, m, OH). **^{13}C NMR (101 MHz, $CDCl_3$)** δ 139.2 (C-2), 129.8 (C-9), 129.1 (C-4,6), 129.0 (C-1,3), 126.6 (C-5), 126.3 (C-8), 116.9 (CN), 74.3 (C-7).

157	3450 (OH), 2949 (C-H), 2229 (CN)	**^{1}H NMR (400 MHz, $CDCl_3$)** δ 7.61 (1H, d, *J* = 7.7 Hz, H-4), 7.41-7.28 (3H, m, H-1,5,6), 6.07 (2H, s, H-9), 5.77 (1H, d, *J* = 4.6 Hz, H-7), 2.59-2.56 (1H, m, OH). **^{13}C NMR (101 MHz, $CDCl_3$)** δ 136.4 (C-2), 132.6 (C-3), 131.3 (C-9), 130.1 (C-5), 129.8 (C-6), 128.0 (C-4), 127.6 (C-1), 124.6 (C-8), 116.7 (CN), 70.6 (C-7).
158	3420 (OH), 2238 (CN)	**^{1}H NMR (400 MHz, $CDCl_3$)** δ 7.64-7.56 (2H, m, H-1,4), 7.41 (1H, t, *J* = 7.6 Hz, H-5), 7.27-7.21 (1H, m, H-6), 6.09 (2H, s, H-9), 5.76 (1H, s, H-7), 2.53-2.51 (1H, m, OH). **^{13}C NMR (101 MHz, $CDCl_3$)** δ 138.0 (C-2), 133.1 (C-4), 131.5 (C-9), 130.4 (C-6), 128.3 (C-1), 128.2 (C-5), 124.6 (C-3), 122.8 (C-8), 116.6 (CN), 72.8 (C-7).

^{1}H NMR, ^{13}C NMR, and IR spectra (**Table 8**) were used to verify the identity of the compounds. IR spectra showed the presence of characteristic stretches which were very similar to the methyl acrylate adducts, except for the nitrile stretch instead of the carbonyl stretch, which was present at around 2229 cm^{-1}. Proton NMR spectra also confirmed the formation of the adducts. These spectra showed the presence of the aromatic proton peaks in the aromatic region between 7-8 ppm, as well as the terminal vinylic protons (H-9) appearing as singlets at around 6 ppm. Signals at around 5 ppm belonged to the H-7 proton. The presence of the OH proton at around 2.5 ppm, also confirmed the formation of the adducts. These OH signals appeared as multiplets, coupling to the neighbouring H-7 proton.

^{13}C NMR also showed the presence of all the key signals required to confirm the formation of the products. These spectra showed the presence of the CN peak at around 116 ppm, the aromatic carbons in the aromatic region between 140-125 ppm, as well as the C-8 peak in the 120 ppm region. The carbon atom attached to the nitrile group (C-8) present in the acrylonitrile adduct appeared more upfield compared to the same carbon present in the methyl acrylate adduct. This

might be due to the delocalization of the electrons in the α,β-unsaturated nitrile occurring more than for the ester, this delocalization shields the proton by increasing the electron density. The terminal alkene carbon signals (C-9) were also observed at around 120-130 ppm.

All the above compounds have been reported before and very similar IR data and NMR shift values were reported, confirming the formation of the anticipated product.

3.1.1.3. Characterization of the MBH ketone.

Methyl vinyl ketone adduct **159** (**Figure 15**) was prepared using the same procedure as the other adducts except that methyl vinyl ketone was used as the activated alkene. Methyl vinyl ketone containing MBH adducts were more difficult to prepare compared to the other MBH adducts.

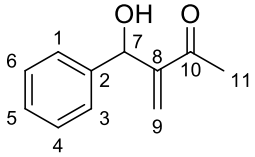

159

Figure 15: The Morita Baylis Hillman ketone adduct synthesized.

Table 9: The NMR data obtained for the MBH ketone shown in Figure 15.

Compound No.	**NMR**
159	**^{1}H NMR (400 MHz, $CDCl_3$)** δ 7.39 -7.21 (5H, m, Ar-H), 6.19 (1H, s, H-9a), 5.97 (1H, s, H-9b), 5.66-5.59 (1H, m. H-7), 3.12-3.06 (1H, m, OH), 2.34 (3H, s, H-12). **^{13}C NMR (101 MHz, $CDCl_3$)** δ 200.3 (C-10), 150.0 (C-8), 141.5 (C-2), 128.4 (C-4,6), 127.7 (C-5), 126.7 (C-9), 126.5 (C-1,3), 72.9 (C-7), 26.5 (C-11).

The ^{1}H and ^{13}C NMR spectra (**Table 9**) confirmed the formation of the product. These spectra showed the presence of all the significant signals to verify the formation of adduct **159**. Signals in the aromatic region between 7-8 ppm integrated for 5 protons as expected; terminal vinylic protons were present (H-9) at around 6 ppm, appearing as singlets. The signal at around 3 ppm integrating for 1 proton belonged to the hydroxyl functional group, confirming the formation of the adduct.

This shows that the reaction between the aldehyde and the activated alkene occured to give the new hydroxy functional group, which verified the formation of the adduct. H-7 was also present at around 5 ppm, which appeared as a multiplet and like rest of the adducts coupled to the neighbouring OH proton. The methyl group was also present around 2 ppm, appearing as a singlet, as expected, and integrating for three protons.

All the expected carbon signals were also present, including the ketone carbonyl signal at around 200 ppm. All the aromatic carbon signals were also present in the aromatic region between 120-140 ppm. The carbon attached to the hydroxyl group (C-7) was also present at around 70 ppm and the methyl carbon appeared around 27 ppm.

The same methyl vinyl ketone MBH adduct has been synthesized before by Mathias *et al*.[67] and very similar NMR data was obtained. For example, the aromatic protons appeared as a single signal integrating for 5 protons. The terminal alkene protons and the other protons gave very similar shift values to those obtained here.

The methyl vinyl ketone adduct **159** was not used in the next step since the ketone adducts were difficult to work with and their purification was also difficult. Only ester and nitrile adducts were used for further reactions.

3.1.2. Preparation and characterization of the protected adducts.

The second step was the protection of the hydroxyl group of the MBH adducts **146** (**Scheme 52**). The adducts were protected in an attempt to control the diastereoselectivity during the subsequent nucleophilic addition reaction. The presence of the bulky protecting group is expected to block the top side of the favoured conformer, allowing the incoming proton to approach from the bottom side only (**Scheme 32**). From the literature, it was reported that the *syn* product was obtained as the major diastereomer during the addition reaction.[69]

The adducts were protected using TMSCl or TBDMSCl as protecting groups in the presence of imidazole as a base (**Scheme 52**). The reaction was done in anhydrous DMF under nitrogen at room temperature. After the reaction was complete, the mixture was diluted with hexane and washed with brine solution. The product was purified using 20% ethyl acetate: hexane. This procedure has been reported before by Kohn *et al*.[81] and was followed exactly as reported.

Different protecting groups (TBDMS and TMS) were used to compare the diastereomeric ratios obtained from the subsequent nucleophilic addition reaction.

The expected products were obtained, and their identities were confirmed using IR, ^{1}H NMR and ^{13}C NMR spectroscopy.

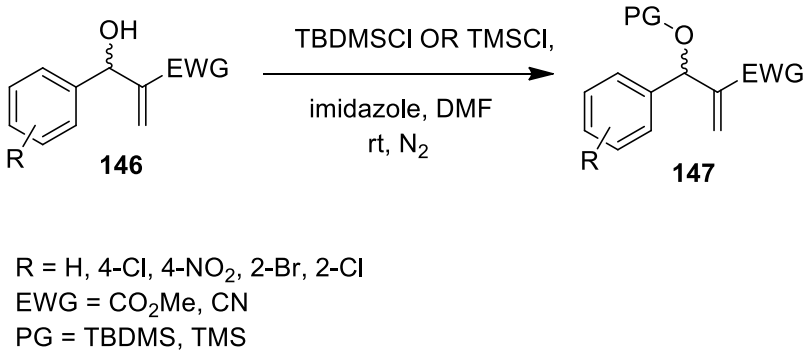

Scheme 52: The protection of the alcohol group on the MBH adduct obtained from the MBH reaction.

Table 10 shows all the yields obtained from the protecting step. The yields were independent of the type of protecting group used, as both protecting groups generally gave very good yields. The best overall yield from both the protecting groups was obtained for the TBDMS protected *para*-chloro substituted ester MBH adduct, which was 93%. From the TMS adducts only, it was the *ortho*-bromo substituted nitrile adduct that gave the best yield. The lowest yield was obtained for the unsubstituted nitrile TBDMS protected adduct, which was 18%. This might be due to slow reactions, not allowing enough time to complete the reaction and the loss of product during purification.

Table 10: The yields obtained from the alcohol protection reaction for all the different MBH adducts using both TBDMS and TMS protecting groups.

Protecting group	**R**	**EWG**	**Yield (%) of 147**
TBDMS	H	CO_2CH_3	69
	2-Br	CO_2CH_3	53
	4-Cl	CO_2CH_3	93
	2-Br	CN	75

	H	CN	18
	4-Cl	CN	64
TMS	4-Cl	CO_2CH_3	41
	2-Br	CO_2CH_3	79
	2-Br	CN	31
	H	CN	70
	4-Cl	CN	72

3.1.2.1. Characterization of TBDMS protected ester and nitrile adducts.

3.1.2.1.1. Ester adducts.

Characterization data (**Table 11**) for the ester adducts **160-162** (**Figure 16**) are presented and discussed below.

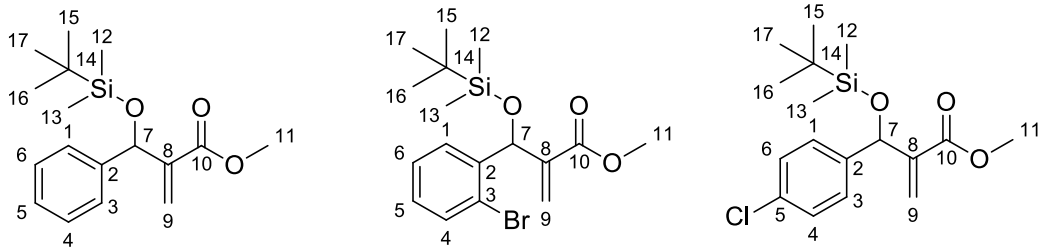

Figure 16: The *tert*-butyldimethylsilyl (TBDMS) protected ester adducts.

Table 11: The IR and the NMR data obtained for the TBDMS protected ester adducts **160-162** shown in Figure 16.

Compound No.	**IR** (neat, cm^{-1})	**NMR**
160	2953 (C-H), 1720 (C=O), 840 (Si-O)	**^{1}H NMR (400 MHz, $CDCl_3$)** δ 7.37 – 7.32 (2H, m, H-1,3), 7.31 – 7.27 (2H, m, H-4,6), 7.24 – 7.19 (1H, m, H-5), 6.24 (1H, s, H-9a), 6.06 (1H, s, H-9b), 5.60 (1H, s, H-7), 3.67 (3H, s, H-11), 0.87 (9H, s, H-15,16,17), 0.05 (3H, s, H-12), -

		0.12 (3H, s, H-13); **^{13}C NMR (101 MHz, $CDCl_3$)** δ 166.4 (C-10), 144.0 (C-8), 142.6 (C-2), 128.0 (C-4,6), 127.4 (C-5), 127.0 (C-1,3), 123.8 (C-9), 72.7 (C-7), 51.6 (C-11), 25.8 (C-15,16,17), 18.2 (C-14), -4.9 (C-12), -5.1 (C-13).
161	2937 (C-H), 1726 (C=O), 840 (Si-O),	**^{1}H NMR (400 MHz, $CDCl_3$)** δ 7.52 – 7.43 (2H, m, H-1,4), 7.32 – 7.26 (1H, m, H-5), 7.14 – 7.08 (1H, m, H-6), 6.28 (1H, s, H-9a), 6.00 (1H, s, H-7), 5.75 (1H, s, H-9b), 3.71 (3H, s, H-11), 0.86 (9H, s, H-15,16,17), 0.11 (3H, s, H-12), -0.10 (3H, s, H-13); **^{13}C NMR (101 MHz, $CDCl_3$)** δ 166.4 (C-10), 143.0 (C-8), 141.4 (C-2), 132.6 (C-4), 129.5 (C-1), 128.9 (C-6), 127.3 (C-5), 125.5 (C-9), 122.9 (C-3), 71.5 (C-7), 51.7 (C-11), 25.8 (C-15,16,17), 18.1 (C-14), -4.8 (C-12), -5.0 (C-13).
162	2930 (C-H), 1719 (C=O), 835 (Si-O)	**^{1}H NMR (400 MHz, $CDCl_3$)** δ 7.31 – 7.23 (4H, m, Ar-H), 6.25 (1H, s, H-9a), 6.08 (1H, s, H-9b), 5.56 (1H, s, H-7), 3.67 (3H, s, H-11), 0.87 (9H, s, H-15,16,17), 0.05 (3H, s, H-12), -0.10 (3H, s, H-13). **^{13}C NMR (101 MHz, $CDCl_3$)** δ 166.2 (C-10), 143.6 (C-5), 141.3 (C-8), 133.1 (C-2), 128.4 (C-4,6), 128.2 (C-1,3), 124.0 (C-9), 72.1 (C-7), 51.7 (C-11), 25.7 (C-15,16,17), 18.2 (C-14), -4.9 (C-12), -5.1 (C-13).

The IR signals for all the methyl ester adducts with different substituents on the aromatic ring were very similar. The signals present in the IR spectra confirmed the formation of the products. All the IR spectra showed the expected stretches, including the carbonyl at around 1700 ppm and the Si-O stretch. The absence of the OH band and the presence of the Si-O band around 840 cm^{-1} confirms the protection of the adducts.

The ^{1}H NMR spectra showed the presence of the characteristic signals, such as the aromatic protons in the most deshielded aromatic region between 6-7.52 ppm. H-9a and H-9b also appeared as singlets around 6 ppm. H-7 was also present at around 5 ppm, and the methyl group at around 3 ppm, integrating for three protons. It appears as a singlet, showing no coupling as it has no protons on the neighbouring carbon atom. The absence of the OH proton signal also confirmed the protection of the hydroxyl group. The presence of the TBDMS signals confirmed the protection of the alcohol.

The signal present at around 0.8 ppm, integrating for 9 protons belonged to the three methyl groups present on the TBDMS group. The signal present at around 0.1 and -0.1 ppm belonged to the protons from the two methyl groups attached to the Si atom. Similar to the unprotected adduct, the 2-bromo substituted adduct had the H-7 proton shifted downfield compared to the rest of the protected methyl ester adducts, this might be due to the electronegativity of the bromine atom which pulls electrons away from it, deshielding it. The presence of the bromine atom also shields one of the H-9 protons, making it appear more upfield compared to the rest of the adducts.

The ^{13}C NMR data also verified the formation of the product. The spectra showed the presence of all the important signals such as the carbonyl group, which was the most deshielded peak present in the spectra, appearing at around 166 ppm, which is typical of the ester carbonyl group. All the aromatic carbon signals were also present in the aromatic region between 125-145 ppm. Due to the symmetry present in the unsubstituted adduct **160**, the aromatic carbons C1 and C3 had the same chemical environment and appeared as a single signal; the same applied to C4 and C6.

C-7 appeared at around 70 ppm, which is the same as for the unprotected adducts. C-8 appeared downfield relative to the aromatic carbons, this might be due to the presence of the carbonyl group adjacent to C-8 which pulls electrons away, deshielding it. All the carbons present in the TBDMS group appeared far upfield in the most shielded region. C-15, 16 and 17 have the same chemical environment and make up a single signal in both the ^{13}C and the ^{1}H NMR spectra. C-14 appeared at around 18 ppm and the other two methyl groups attached to the silicon atom also appeared upfield at around -4.9 and -5.1 ppm.

The DEPT spectra also confirmed the protection of the adduct. It showed the C-15, 16 and 17 signal at around 25 ppm appearing as a positive peak, which confirms that it belongs to the methyl

groups. It also showed a signal in the negative region, confirming the presence of a C-9 carbon attached to two protons.

All the compounds **160-162** have been reported before. Compounds **160** and **162** were reported before by Coelho *et al*.[82] These compounds were obtained in very good yields. The IR and the NMR data were compared to verify the formation of these adducts, and very similar data were obtained to that previously reported.

3.1.2.1.2. Characterization of nitrile adducts.

The TBDMS protected nitrile adducts **163** and **165** (**Figure 17**) were obtained in a very good yield of 75% and 64%, respectively. The anticipated products were obtained as verified by IR, ^{1}H and ^{13}C NMR spectra. Characterization data (**Table 12**) for the nitrile adducts **163-165** (**Figure 17**) are presented and discussed below.

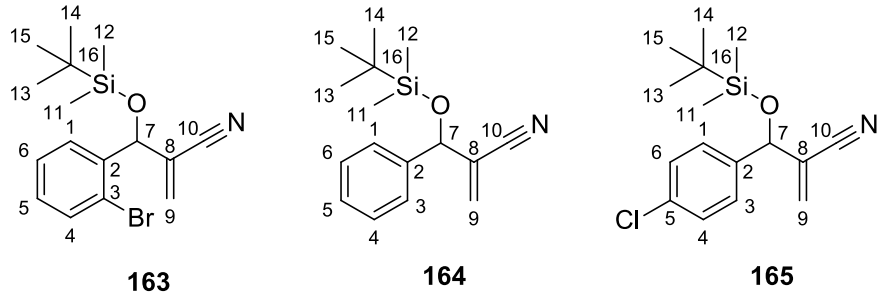

Figure 17: The *tert*-butyldimethylsilyl (TBDMS) protected nitrile adducts.

Table 12: The IR and the NMR data obtained for the TBDMS protected nitrile adducts shown in figure 17.

Compound No.	**IR** (neat, cm^{-1})	**NMR**
163	3007 (C-H), 2223 (CN), 845 (Si-O)	**^{1}H NMR (400 MHz, $CDCl_3$)** δ 7.65 – 7.61 (1H, d, H-4), 7.55 – 7.52 (1H, d, H-1), 7.41 – 7.36 (1H, t, H-5), 7.22 – 7.17 (1H, t, H-6), 5.98 (1H, d, *J* = 1.3 Hz, H-9a), 5.95 (1H, d, *J* = 1.0 Hz, H-9b), 5.68 (1H, br s, H-7), 0.91 (9H, s, H-13,14,15), 0.13 (3H, s, H-11), -0.03 (3H, s, H-12); **^{13}C NMR (101 MHz, $CDCl_3$)** δ 139.1 (C-3), 132.6 (C-1), 129.9 (C-9), 129.8

		(C-4), 128.9 (C-5), 128.0 (C-6), 126.2 (C-8), 122.0 (C-2), 116.8 (C-10), 73.3 (C-7), 25.6 (C-13,14,15), 18.2 (C-16), -5.0 (C-11), -5.1 (C-12).
164	2957 (C-H), 2225 (CN), 860 (Si-O)	**^{1}H NMR (400 MHz, $CDCl_3$)** δ 7.37 – 7.29 (5H, m, Ar-H), 6.03 (1H, d, *J* = 1.6 Hz, H-9a), 5.93 (1H, br s, H-9b), 5.23 (1H, t, H-7), 0.91 (9H, s, H-13,14,15), 0.10 (3H, s, H-11), -0.05 (3H, s, H-12); **^{13}C NMR (101 MHz, $CDCl_3$)** δ 140.1 (C-2), 128.6 (C-4,6), 128.42 (C-8), 128.35 (C-9), 127.9 (C-5), 126.4 (C-1,3), 117.1 (C-10), 75.0 (C-7), 25.7 (C-13,14,15), 18.2 (C-16), -4.9 (C-11), -5.1 (C-12).
165	2981 (C-H), 2229 (CN), 834 (Si-O)	**^{1}H NMR (400 MHz, $CDCl_3$)** δ 7.37 – 7.35 (1H, m, H-4), 7.35 – 7.33 (1H, m, H-6), 7.32 – 7.30 (1H, m, H-1), 7.30 – 7.27 (1H, m, H-3), 6.04 (1H, d, H-9a), 5.96 – 5.94 (1H, m, H-9b), 5.20 (1H, t, H-7), 0.91 (9H, s, H-13,14,15), 0.10 (3H, s, H-11), -0.04 (3H, s, H-12). ^{13}C **NMR (101 MHz, $CDCl_3$)** δ 138.7 (C-5), 134.3 (C-2), 128.9 (C-4,6), 128.6 (C-9), 127.7 (C-1,3), 127.5 (C-8), 116.9 (C-10), 74.3 (C-7), 25.6 (C-13,14,15), 18.2 (C-16), -4.9 (C-11), -5.1 (C-12).

The IR spectra for all the nitrile adducts confirmed the formation of the product as they showed the presence of all the important stretches, and the absence of the OH stretch at around 3000 cm^{-1}, which confirms the alcohol protection. The nitrile and the Si-O stretches were visible in the IR spectra. All the IR spectra showed the presence of the nitrile stretch at around 2200 cm^{-1}, as well as the Si-O stretch around 840 cm^{-1}. The presence of the Si-O stretch also confirmed the protection of the hydroxyl group.

The ^{1}H NMR spectra of the three nitrile adducts confirmed the formation of the products. The spectra showed the presence of all the important signals that should be present in the protected

acrylonitrile adduct. The aromatic protons were seen in the aromatic region between 7.17-7.65 ppm. In the 2-bromo substituted adduct (**163**), the aromatic protons, H-4 and H-1 appeared as doublets showing coupling to the adjacent protons H-5 and H-6, respectively. H-5 appeared as a triplet in the ^{1}H NMR spectrum, showing coupling to H-4 and H-6 with almost equal coupling constants. H-6 also appeared as a triplet coupling to H-1 and H-5 with very similar coupling constants. In the same adduct, H-9a and H-9b appeared as doublets, showing vinylic geminal coupling, with a coupling constant of ~1 Hz. H-7 appeared as a singlet, showing no coupling.

In the ^{1}H NMR spectrum of unsubstituted adduct (**164**) shown in figure 18, the aromatic protons appeared as a single signal, while H-9a appeared as a doublet, showing coupling to the H-7 proton in the COSY spectrum. H-9b appeared as a broad singlet, while H-7 appeared as a triplet, coupling to both H-9 protons. In the 4-Cl substituted adduct (**165**) all the aromatic signals appeared as multiplets, showing coupling to each other. The H-9 and H-7 signals showed coupling to each other, as for the unsubstituted adduct. For all the acrylonitrile alcohol protected adducts, the three methyl groups attached to the carbon of the TBDMS groups appeared at around 1 ppm, integrating for 9 protons. These signals appeared as singlets showing no coupling, as there no adjacent protons. The other two methyl groups attached to the silicon atom appeared below 1 ppm, in the most shielded region. The presence of these signals confirmed the protection of the alcohol group.

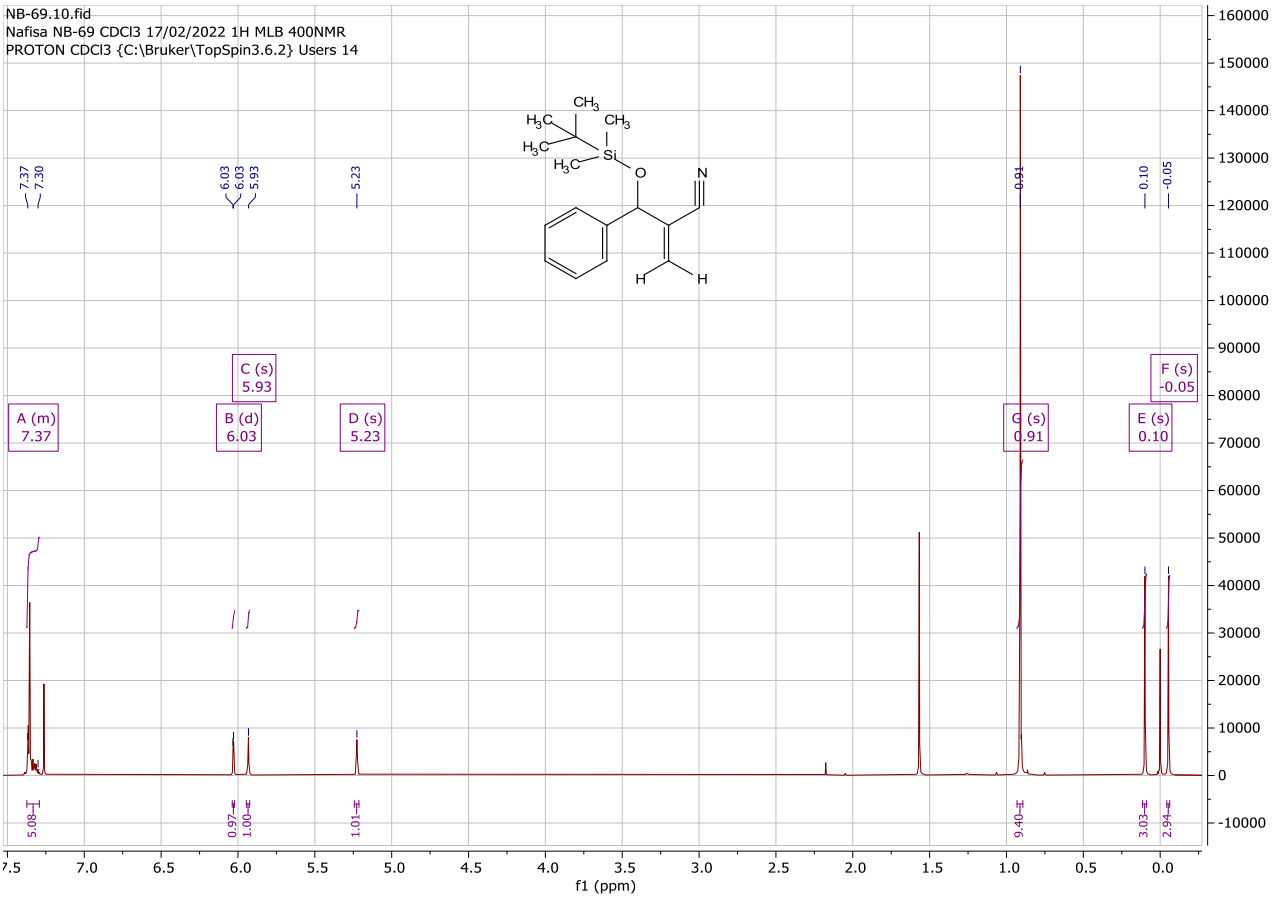

Figure 18: The ^{1}H NMR spectrum of compound **164**.

The ^{13}C NMR spectra also confirmed the formation of these adducts. These spectra showed the presence of all the expected aromatic carbon signals, as well as the alkene carbon signals. The nitrile carbon signal appeared around 117 ppm for all three protected adducts (**163-165**). C-7 was also present at around 70 ppm for all three adducts, and all the TBDMS carbon signals were present in the most shielded region for all three adducts. C-13, 14 and 15 appeared at around 26 ppm in the three adducts, and C-16 appeared at 18.2 ppm. The signal around 26 ppm appeared as a positive peak in the DEPT spectra confirming that it belongs to the methyl groups of the TBDMS group. The DEPT spectra also showed the C-9 CH_2 signal in the negative region.

3.1.2.2. Characterization of the TMS protected ester and nitrile adducts.

The TMS protected adducts were synthesized in a very similar manner to the TBDMS protected adducts, except that TMSCl was used instead of TBDMSCl in the presence of imidazole in anhydrous DMF.

3.1.2.2.1. Characterization of ester adducts.

Characterization data (**Table 13**) for the ester adducts **166** and **167** (**Figure 19**) are presented and discussed below. The TMS protected ester adducts were characterized by IR and NMR spectroscopy (**Table 13**).

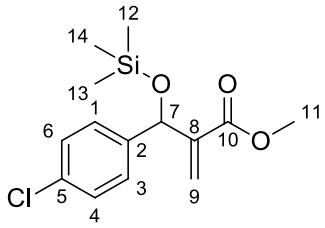

166

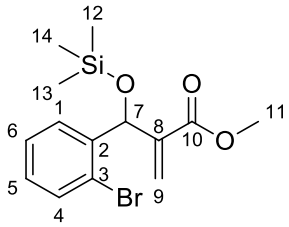

167

Figure 19: The trimethylsilyl (TMS) protected ester adducts **166** and **167**.

Table 13: The IR and the NMR data obtained for the TMS protected ester adducts **166** and **167** shown in Figure 19.

Compound No.	**IR** (neat, cm^{-1})	**NMR**
166	2922 (C-H), 1719 (C=O), 840 (Si-O)	**^{1}H NMR (400 MHz, $CDCl_3$)** δ 7.31 – 7.23 (4H, m, Ar-H), 6.28 (1H, s, H-9a), 6.01 (1H, s, H-9b), 5.57 (1H, s, H-7), 3.68 (3H, s, H-11), 0.06 (9H, br s, H-12,13,14); **^{13}C NMR (101 MHz, $CDCl_3$)** δ 166.2 (C-10), 143.3 (C-8), 141.1 (C-2), 133.2 (C-5), 128.5 (C-4,6), 128.4 (C-1,3), 124.6 (C-9), 71.9 (C-7), 51.7 (C-11), 0.0 (C-12,13,14).
167	2966 (C-H), 1724 (C=O), 840 (Si-O)	**^{1}H NMR (400 MHz, $CDCl_3$)** δ 7.51 (1H, d, *J* = 8.0 Hz, H-4), 7.46 (1H, d, *J* = 8.8 Hz, H-1), 7.30 (1H, t, *J* = 7.5 Hz, H-5), 7.13 (1H, t, *J* = 8.4 Hz, H-6), 6.30 (1H, s, H-9a), 6.01 (1H, s, H-7), 5.65 (1H, s, H-9b), 3.73 (3H, s, H-11), 0.10 (9H, s, H-12,13,14); **^{13}C NMR (101 MHz, $CDCl_3$)** δ 166.3 (C-10), 142.7 (C-8), 141.2 (C-2), 132.6 (C-1), 129.2 (C-4),

		129.0 (C-5), 127.4 (C-6), 125.9 (C-9), 123.0 (C-3), 71.5 (C-7), 51.8 (C-11), 0.1 (C-12,13,14).

The IR spectra were very similar to the corresponding TBDMS protected adducts, with the same carbonyl (~1720 cm^{-1}) and Si-O stretches. The presence of the Si-O stretch at around 840 cm^{-1} and the absence of the OH stretch at 3000 cm^{-1} confirmed the protection of the hydroxyl group.

The ^{1}H NMR spectra also showed all the important signals such as the aromatic proton signals at around 7.13-7.51 ppm and the terminal alkene proton (H-9) signals which appeared as singlets at around 6 ppm and showed no coupling to the nearby protons. Figure 20 shows the ^{1}H NMR spectrum of compound **166**.

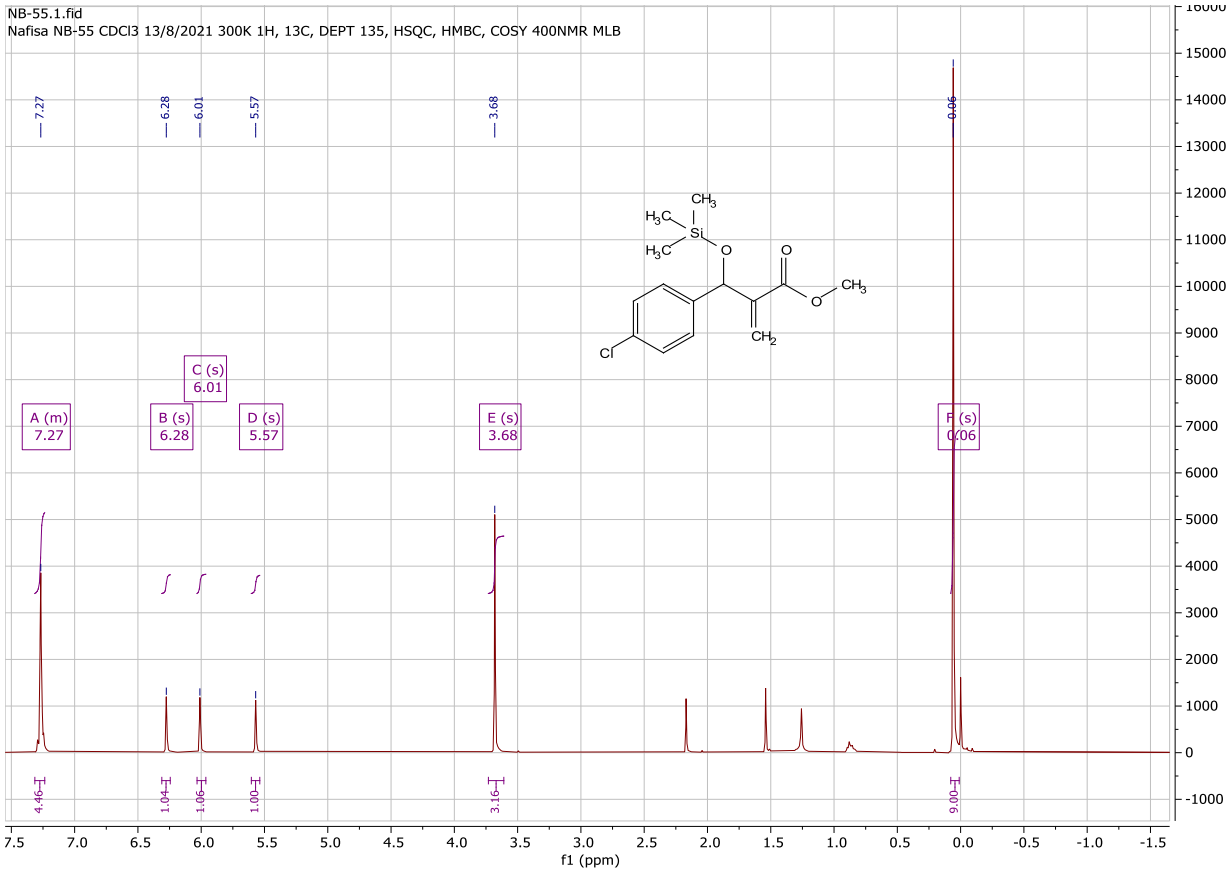

Figure 20: The ^{1}H NMR spectrum of compound **166**.

The H-7 signal was visible at around 5-6 ppm, also showed no coupling, as it appeared as a singlet. As observed for the other 2-bromo substituted adducts, in 2-bromo substituted adduct **167**, the H-7 appeared more downfield compared to the 4-chloro adduct **166**, due to the bromine atom pulling electrons away and deshielding it. The signal present at around 0.1 ppm confirmed the protection of the alcohol using TMS, as it integrated for 9 protons and appeared as a singlet showing no coupling to any other protons.

^{13}C NMR showed the presence of all the important signals, such as the carbonyl signal at around 166 ppm, aromatic carbon signals at around 140-127 ppm and the terminal alkene carbon signal (C-9) at around 124 ppm. The C-7 and C-11 signals appeared at around 71 and 51 ppm, respectively. The TMS carbon signal was also present around 0.1 ppm, it appeared as a positive peak in the DEPT spectra, as expected.

Both compound **166** and **167** have been reported before. Compound **166** was reported by Coelho *et al*.[82] and the data were compared to verify the formation of the adduct. Very similar shift values were obtained to those previously reported.

3.1.2.2.2. **Characterization of nitrile adducts**.

Characterization data (**Table 14**) for the nitrile adducts **168-170** (**Figure 21**) are presented and discussed below.

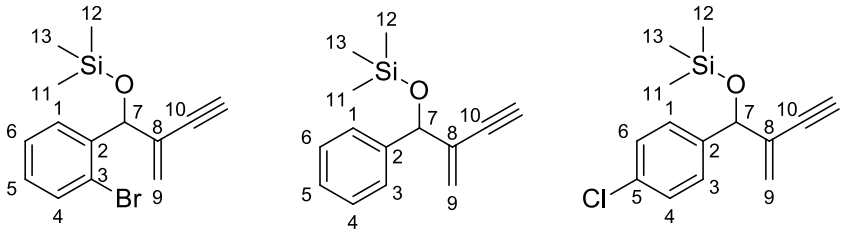

Figure 21: The trimethylsilyl (TMS) protected nitrile adducts.

Table 14: The IR and the NMR data obtained for the TMS protected nitrile adducts **168-170** shown in Figure 21.

Compound No.	**IR** (neat, cm^{-1})	**NMR**

168	-	**^{1}H NMR (400 MHz, $CDCl_3$)** δ 7.64 – 7.60 (1H, d, H-4), 7.55 – 7.52 (1H, d, H-1), 7.41 – 7.35 (1H, m, H-5), 7.23 – 7.17 (1H, m, H-6), 5.96 (2H, dd, *J* = 4.6 Hz, H-9), 5.67 (1H, br s, H-7), 0.13 (9H, s, H-11, 12, 13); **^{13}C NMR (101 MHz, $CDCl_3$)** δ 138.9 (C-3), 132.7 (C-1), 130.02 (C-9), 129.95 (C-4), 128.9 (C-5), 128.0 (C-6), 126.1 (C-8), 122.1 (C-2), 116.9 (C-10), 73.1 (C-7), -0.1 (C-11, 12, 13).
169	2229 (CN), 847 (Si-O);	**^{1}H NMR (400 MHz, $CDCl_3$)** δ 7.38 – 7.31 (5H, m, Ar-H), 6.03 – 6.01 (1H, m, H-9a), 5.96 – 5.94 (1H, m, H-9b), 5.25 – 5.20 (1H, m, H-7) , 0.11 (9H, s, H-11 ,12, 13); **^{13}C NMR (101 MHz, $CDCl_3$)** δ 139.9 (C-2), 128.7 (C-9), 128.6 (C-4,6), 128.5 (C-5), 127.6 (C-8), 126.5 (C-1,3), 117.2 (C-10), 74.7 (C-7), -0.1 (C-11, 12, 13).
170	2981 (C-H), 2229 (CN), 834 (Si-O)	**^{1}H NMR (400 MHz, $CDCl_3$)** δ 7.37 – 7.35 (1H, m, H-4), 7.35 – 7.33 (1H, m, H-6), 7.32 – 7.30 (1H, m, H-1), 7.29 – 7.28 (1H, m, H-3), 6.05 – 6.02 (1H, m, H-9a), 5.98 – 5.95 (1H, m, H-9b), 5.20 (1H, t, *J*=1.5 Hz, H-7), 0.13 (9H, s, H-11,12,13). **^{13}C NMR (101 MHz, $CDCl_3$)** δ 138.6 (C-5), 134.5 (C-2), 129.0 (C-4,6), 129.0 (C-1,3), 128.0 (C-9), 127.4 (C-8), 117.0 (C-10), 74.2 (C-7), 0.00 (C-11,12,13).

The TMS protected nitrile adducts **168-170** (**Figure 21**) were also characterized using IR and NMR spectroscopy (**Table 14**). The IR spectra showed all the important stretches, such as the nitrile and the Si-O stretches around 2200 and 840 cm^{-1}, respectively. The presence of the Si-O stretch and the absence of the OH stretch confirmed the protection of the alcohol group.

Comparing compounds 166 and 170, the only difference is the electron withdrawing groups (ester or nitrile group) attached to the double bond. These electron withdrawing groups have an effect on

the chemical shift values of the neighboring protons (H-9), depending on their ability to pull the electron density away from the nucleus. Esters are more electron withdrawing compared to nitrile groups hence, pulling more electrons away from the nucleus, deshielding them and increasing their chemical shift values. These is shown in table **13** and **14**, where H-9a and H-9b of compound **166** have a larger chemical shift values (6.28 and 6.01 ppm) compared to those of compound **170** (6.03 and 5.96 ppm). The same applies to compounds **167** and **168**. The protons belonging to silane methyl groups appear far upfield, because these proton atoms are highly shielded by the metallic silicon atom.

The ^{1}H NMR spectra confirmed the protection of the hydroxyl group, as it showed the absence of the OH proton peak, and all the peaks present also confirmed the formation of the expected product. The aromatic protons were found in the typical deshielded region between 7.17-7.64 ppm for all three TMS protected nitrile adducts. Aromatic protons integrated for four or five protons, depending on the substituent present. The terminal alkene protons, H-9 appeared as separate peaks for adducts **169** and **170**. These signals appeared as multiplets, while for adduct **168**, the signal appeared as a doublet of doublets, with these protons coupling to each other and to the H-7 proton. H-7 was found at around 5 ppm for all three adducts. These signals appeared as multiplets coupling to the neighbouring H-9 protons. The most shielded peak around 0.1 ppm belonged to the TMS protons.

The ^{13}C NMR spectra also showed all the important signals, with the aromatic carbon signals at 125-140 ppm, the C-9 carbon signal in the 130 ppm region and the C-8 carbon signal in the 127 ppm region. The nitrile carbon signal was also present around 117 ppm and the C-7 signal at around 74 ppm for all three adducts. The most shielded peak at around 0 ppm belonged to the three equivalent TMS carbon atoms. All these peaks were confirmed using the HSQC and the DEPT spectra.

3.1.3. Preparation and characterization of the conjugate addition products

The third step was to conduct conjugate addition reactions on the protected MBH adducts using different nucleophiles. The addition reaction involves a nucleophilic attack on the alkene group of the MBH adduct **171** converting it into an alkane, generating a second stereogenic centre leading to the formation of diastereomers **172** and **173** (**Scheme 53**). The objective was to perform the

addition reactions and monitor whether diastereomers could be observed or not and if so, in what ratio were they obtained. In addition, the reactions were also monitored to detect the formation of alternative products. The addition reactions were done using different nitrogen and sulfur nucleophiles. Piperidine **174**, benzylamine **175**, methoxybenzylamine **176**, aniline **177** and methoxyaniline **178** were used as the nitrogen nucleophiles. Benzyl mercaptan **179**, 4-methylbenzenethiol **180** and benzenethiol **181** were used as the sulfur nucleophiles (**Scheme 53**).

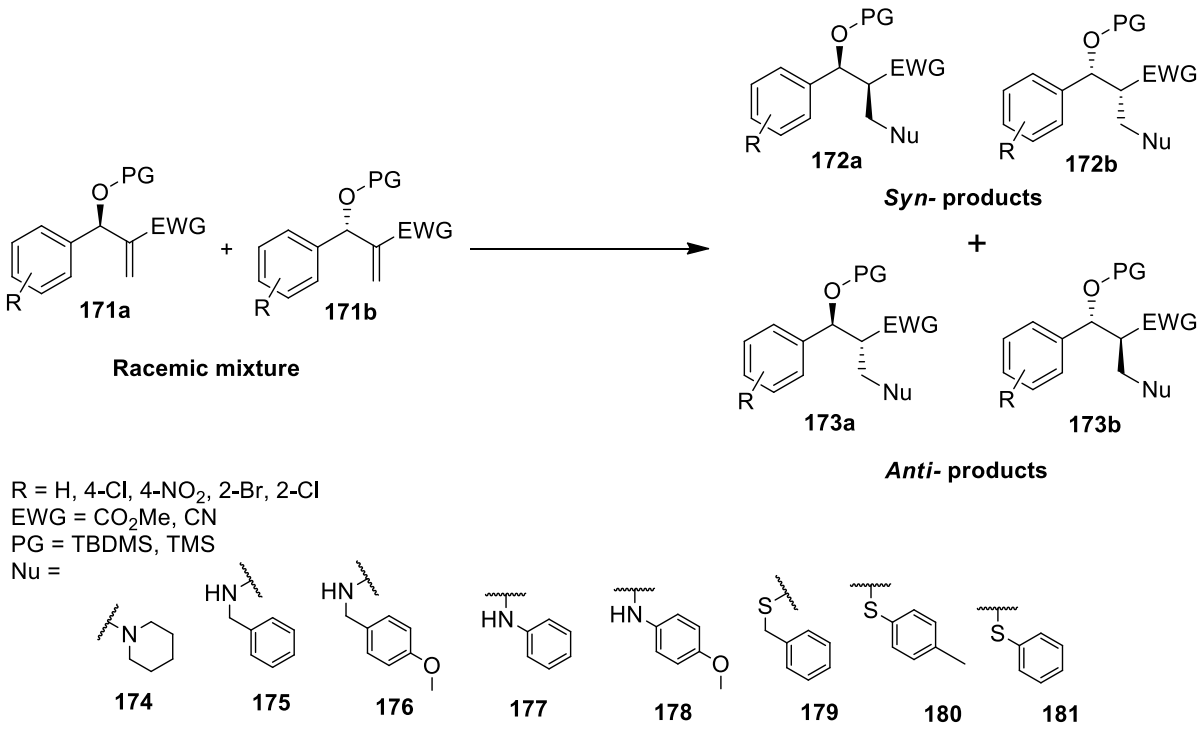

Scheme 53: The formation of diastereomers **172** and **173** by the conjugate addition reaction of different nucleophiles **174-181** on the MBH adduct **171.**

Many papers have been published reporting the formation of alternative products in the conjugate addition reaction of the MBH adducts. Under certain conditions, allylic substitution products may be obtained when conducting conjugate addition reactions. A good leaving group may give the allylic substitution product and the type of nucleophile might also have an effect on the type of product obtained. Juma *et al.*[63] reported the occurrence of allylic substitution reaction along with the nucleophilic addition reaction on MBH ethyl esters in the presence of the bulky silyl groups. A nucleophilic addition reaction on the MBH adduct with acetate as the alcohol protecting group have also been reported by S. Ghosh *et al.*, where they reported the occurrence of allylic

substitution reaction upon the addition of different amines, as the acetate acts as a good leaving group.[83] A similar type of reaction has also been reported by P. Srihari *et al.*, where they formed 1,5-disubstituted tetrazoles from MBH acetates as potential TNF-α inhibitor by performing a nucleophilic addition reaction on the adducts using different amines, forming allylic substitution products.[84]

The conjugate addition reaction occurs on the MBH adduct **182** by the attack of the nucleophile on the terminal carbon of the alkene, forming a new carbon-carbon bond generating intermediate **183**, which is then protonated giving the final product **184**. The allylic substitution occurs due to presence of a good leaving group, where the nucleophile attacks the terminal carbon, eliminating the leaving group and giving the final substitution product **185** (**Scheme 54**).[85]

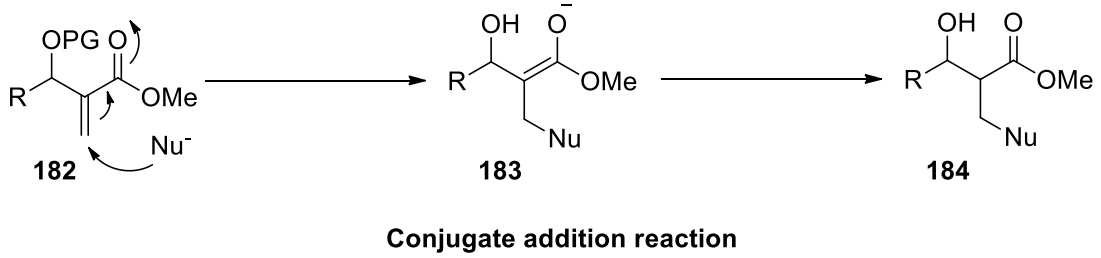

Scheme 54: The reaction mechanism for the formation of conjugate addition and allylic substitution product

For the ^{1}H NMR spectra belonging to products obtained as mixtures of two diastereomers, the partial integrations values from the two diastereomers are combined to give the total expected integration values shown in the tables below. The integrations of all the signals belonging to both diastereomers were determined by combining the partial integrations of the H-7 proton signals and taking them as the reference integration. For the ^{13}C NMR, the tentative assignments for the two

diastereomers are based on signal height differences which can be indicative of which signals belong to which diastereomer.

The diastereomeric ratio of the two diastereomers that appear as mixtures, were determined by comparing the height intensity of the peaks in the ^{1}H NMR and for diastereomers that were separated, the ratios were determined by comparing the mass differences. The ratio of the allylic substitution: conjugate addition product was determined by comparing the mass of the allylic substitution product with the total mass of the diastereomers of the conjugate addition product.

3.1.3.1. Conjugate addition reaction using nitrogen nucleophiles.

The conjugate addition reactions of nitrogen nucleophiles to the protected adducts **147** were done in methanol at room temperature in the absence of any catalyst. The crude product obtained was purified using column chromatography to obtain the desired product **148**. This method was used as previously reported in our laboratory (**Scheme 55**).[69] This reaction was also performed in dichloromethane; however poor yields were obtained.

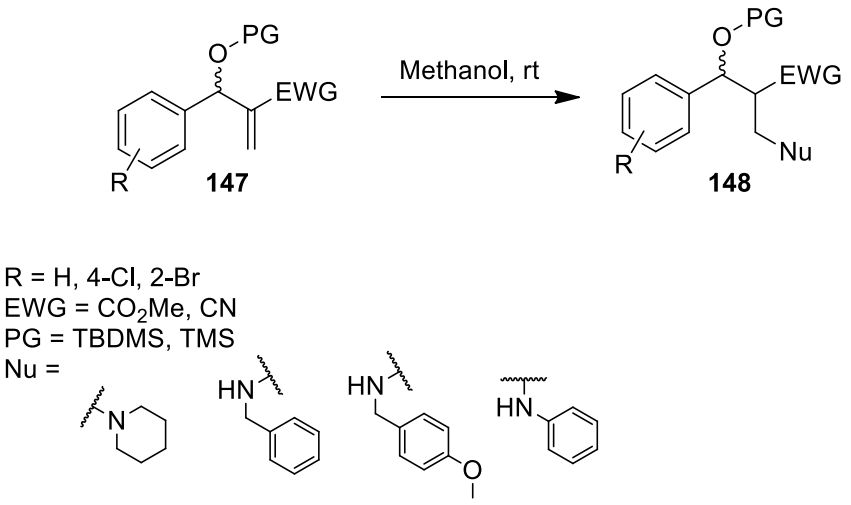

Scheme 55: The conjugate addition reaction on the protected adducts **147** using different nucleophiles.

3.1.3.1.1. Piperidine nucleophile.

3.1.3.1.1.1. Addition of piperidine to the TMS protected ester adduct 166.

The first reaction was the addition of piperidine to the TMS protected adduct **166**. The reaction worked well. It gave the desired product **186**, however in a low yield. Three different products

were obtained, the desired addition product **186**, the deprotected addition product **187** and the allylic substitution product **188** (**Figure 22**). The desired product was obtained with a poor yield of 31%. These is likely due to the deprotection of some of the anticipated product, as well as the side reaction that occured along with it. The expected product might have deprotected during the reaction or during purification on silica gel. Only one diastereomeric product was observed from this reaction this may be because of loss of one diastereomer during purification or heavy dominance of one diastereomer over the other, making the other diastereomer undetectable.

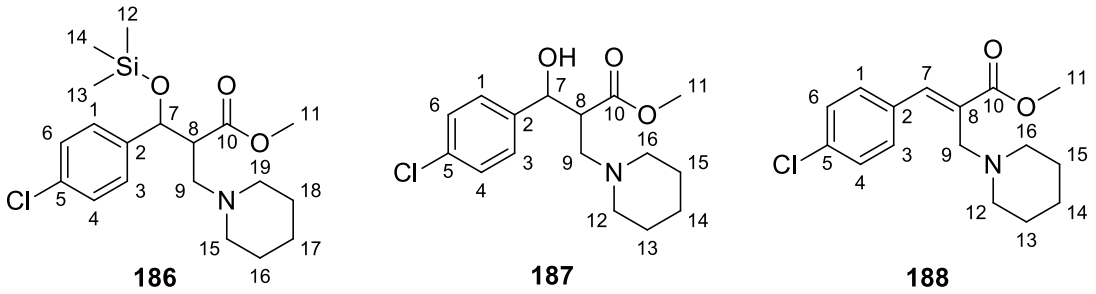

Figure 22: Conjugate addition reaction of piperidine nucleophile to the TMS protected ester adduct to form **186** and the byproducts **187** and **188** obtained from the reaction.

Table 15: The IR and the NMR data for the products obtained from the conjugate addition reaction using piperidine on the TMS protected ester adduct.

Compound No.	**IR** (neat, cm^{-1})	**NMR**
186	2949 (C-H), 1731 (C=O), 820 (Si-O)	**^{1}H NMR (400 MHz, $CDCl_3$)** δ 7.30 – 7.27 (4H, m, Ar-H), 4.96 (1H, d, *J* = 12.0 Hz, H-7), 3.41 (3H, s, H-11), 3.10 – 2.99 (1H, m , H-9a), 2.92 – 2.83 (1H, m, H-8), 2.78 – 2.63 (3H, m, H-9b,15a,19a), 2.43 – 2.41 (2H, m, H-15b,19b), 1.65 – 1.63 (4H, m, H-16,18) , 1.53 (2H, s, H-17), 0.00 (9H, s, H-12,13,14). **^{13}C NMR (400 MHz, $CDCl_3$)** δ 171.8 (C-10), 140.8 (Ar-C), 133.4 (Ar-C), 128.3 (Ar-C), 128.0 (Ar-C), 77.2 (C-7), 61.2 (C-9), 54.9 (C-15,19), 51.6 (C-11), 49.8 (C-8), 25.9 (C-16,18), 23.9 (C-17), 0.0 (C-12,13,14).

187	3665 (OH), 1731 (C=O)	**^{1}H NMR (400 MHz, $CDCl_3$)** δ 7.31 – 7.26 (4H, m, Ar-H), 4.96 (1H, d, *J* = 9.0 Hz, H-7), 3.41 (3H, s, H-11), 3.09 – 2.98 (1H, m, H-9a), 2.92 – 2.81 (1H, m, H-8), 2.76 – 2.63 (3H, m, H-9b,12a,16a), 2.43 – 2.41 (2H, m, H-12b,16b), 1.70 – 1.55 (4H, m, H-13,15), 1.53 – 1.43 (2H, m, H-14). **^{13}C NMR (101 MHz, $CDCl_3$)** δ 171.8 (C-10), 140.8 (Ar-C), 133.4 (Ar-C), 128.3 (Ar-C), 128.0 (Ar-C), 77.5 (C-7), 61.3 (C-9), 54.9 (C-12,16), 51.6 (C-11), 49.8 (C-8), 25.9 (C-13,15), 23.9 (C-14).
188	2933 (C-H), 1710 (C=O)	**^{1}H NMR (400 MHz, $CDCl_3$)** δ 7.76 (1H, s, H-7), 7.69 (2H, d, *J* = 7.7 Hz, Ar-H), 7.36 (2H, d, *J* = 7.9 Hz, Ar-H), 3.82 (3H, s, H-11), 3.25 (2H, s, H-9), 2.40 – 2.38 (4H, m, H-12,16), 1.55 – 1.53 (4H, m, H-13,15), 1.27 – 1.25 (2H, m, H-14). **^{13}C NMR (101 MHz, $CDCl_3$)** δ 169.1 (C-10), 141.8 (C-7), 134.9 (Ar-C), 134.0 (Ar-C), 132.1 (Ar-C), 130.8 (C-8), 128.5 (Ar-C), 54.0 (C-9), 53.9 (C-12,16), 52.1 (C-11), 26.2 (C-13,15), 24.4 (C-14).

The identity of all the products was verified using ^{1}H and ^{13}C NMR and IR spectroscopy (**Table 15**). The deprotected adduct **187** gave very similar IR signals to the protected adduct **186**, however it showed the appearance of an extra stretch in the OH region around 3665 cm^{-1}, implying the removal of the TMS protecting group. The IR spectra for all three products showed the presence of a carbonyl stretch around 1720 cm^{-1}, confirming the presence of the carbonyl functional group.

The ^{1}H and ^{13}C NMR spectra of the deprotected adduct **187** also showed very similar signals to the protected version **186** except for the absence of the TMS signal around 0.00 ppm. The ^{1}H NMR spectrum showed a single signal in the aromatic region around 7.3 ppm for both protected and the deprotected adducts, integrating for four protons, confirming the presence of the aromatic ring. This signal appears as a multiplet, showing coupling of the protons to one another. There was a

signal present at 4.96 ppm for **186** and **187** integrating for 1 proton, which belongs to H-7, appearing as a doublet through coupling to the neighbouring H-8 proton.

The H-8 signal appeared as a multiplet around 2.9 ppm, showing coupling to both H-7 and H-9 protons. H-9 is divided into two signals for H-9a and 9b, as these two diastereotopic protons are not chemically equivalent. Both H-9 signals appeared as a multiplet coupling to H-8 and to each other. The H-11 signal was also present at 3.41 ppm, integrating for three protons. The piperidine protons give signals in the shielded region. In the protected adduct **186**, the signal at 2.78 ppm integrated for 3 protons, from the H-9b proton, as well as the H-15a and H-19a protons. The H-15b and H-19b protons were more shielded and appeared around 2.43 ppm. Both appeared as multiplets coupling to each other and to neighbouring protons.

Piperidine can adopt a chair conformation, and signals belonging to equatorial and axial protons of the piperidine ring can be differentiated using coupling constants. However, from the ^{1}H NMR spectrum shown in figure 23, it is difficult to differentiate between the two, since both signals appear as poorly resolved multiplets for which the coupling constants could not be measured. In the protected adduct, H-16 and H-18 appeared as a single signal integrating for 4 protons and H-17 appeared as a separate signal around 1.53 ppm. The TMS signal was found in the most shielded region, which was absent in the deprotected adduct **187**. The COSY spectrum clearly showed coupling of H-7 and H-8 protons.

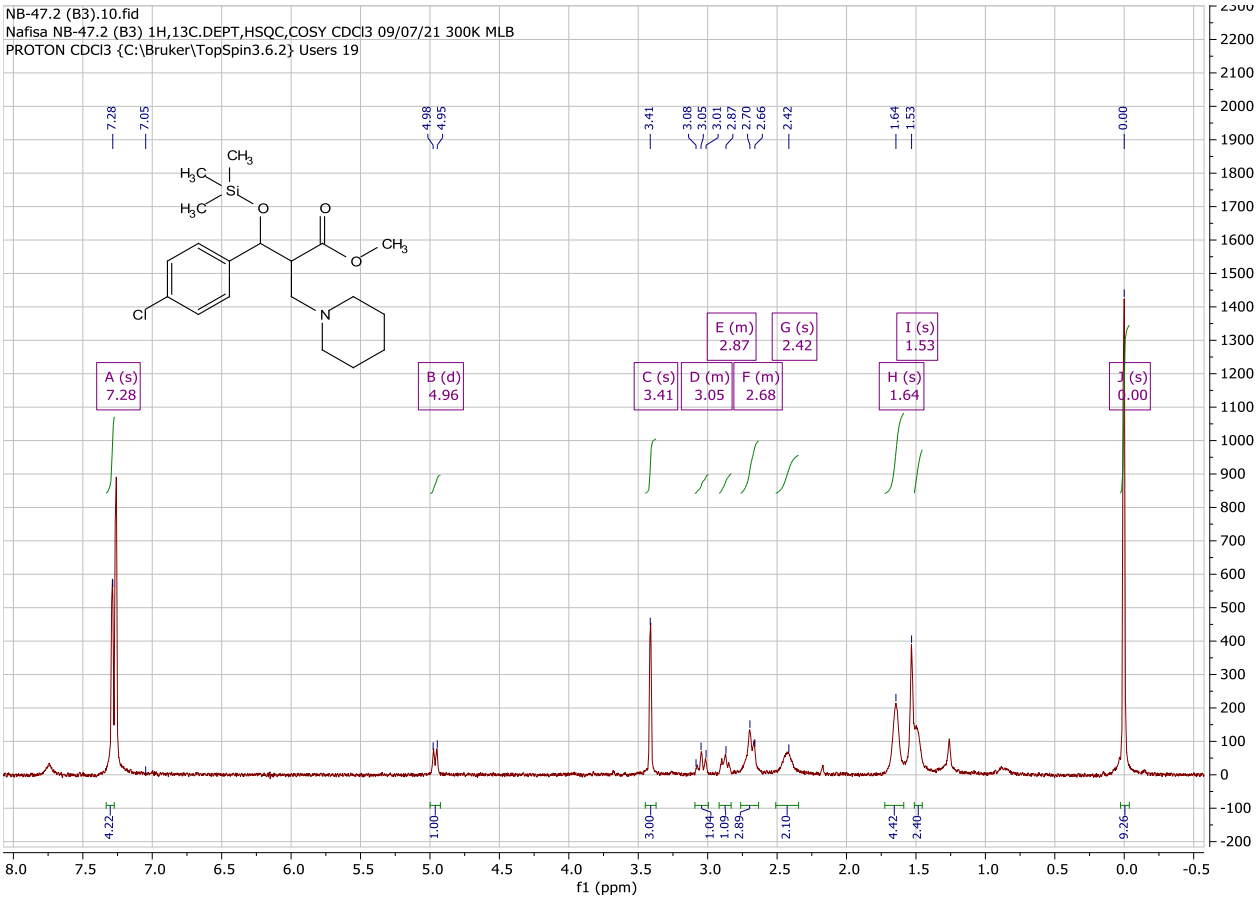

Figure 23: The ^{1}H NMR spectrum of compound **186**.

For the protected and the deprotected adducts, **186** and **187**, the ^{13}C NMR spectrum showed all the important signals such as the carbonyl signal around 171.8 ppm, the aromatic signals in the aromatic region between 128-140 ppm, C-7 at around 70 ppm and C-9 at around 61 ppm. All the piperidine carbon signals were also found in the shielded region between 24-55 ppm with the C-15 and C-19 appearing in the same chemical environment, as well as C-16 and C-18. The only difference between the adducts was the absence of the TMS carbon signals in the deproteced adduct. For compound **187**, the value obtained from the mass spectrum corresponded very well with the expected mass. Calculated [M+H^{+}]: 312.1303, found: 312:1303.

The allylic substitution product **188** was obtained in a low yield of 14%. In the proton NMR spectrum, the aromatic signals were also present in the 7.4-7.7 ppm region; in this adduct the signals were split into two with each appearing as a doublet coupling to the other. The ^{1}H NMR spectrum integrated for fewer protons compared to the desired product, showing the absence of the TMS group. The proton attached to the alkene group gave the most deshielded peak around

7.76 ppm (H-7). The signal at 3.83 ppm belonging to the methyl group (H-11). integrated for 3 protons. The next signal integrated for two protons and belong to the H-9 protons. The rest of the signals between 1.3-2.4 ppm belong to the piperidine ring.

The carbon signals were assigned using the HSQC spectrum, by matching the proton signals with the corresponding carbon signals. These were confirmed using the DEPT spectra, which showed positive peaks in the aromatic region showing that they belonged to the C-H protons and the negative peaks in the shielded region implying that they belonged to CH_2 protons of the piperidine ring as well as H-9.

3.1.3.1.1.2.Addition of piperidine to the TBDMS protected ester adduct 160 and the unprotected adduct 152.

A nucleophilic addition reaction was done on the TBDMS protected adduct **160** to obtain **189** and the unprotected adduct **152** to obtain **190**, to compare the diastereomeric ratios, as the purpose of the protecting group was to control the diastereoselectivity. However, only a single diastereomer was observed for both reactions, it could have been a result of losing the minor diastereomer during purification or due to high diasteroeselectivity. *Syn* product is more likely to form due to the presence of the bulky TBDMS group, which could block one side of the double bond and in turn control the addition of the nucleophile, as well as the incoming proton.

The expected products, **189** and **190** were obtained as confirmed using IR and NMR spectroscopy (**Figure 24, Table 16**). Both compounds were obtained in a fair yield, **189** was obtained in a yield of 54% and **190** in a yield of 59%.

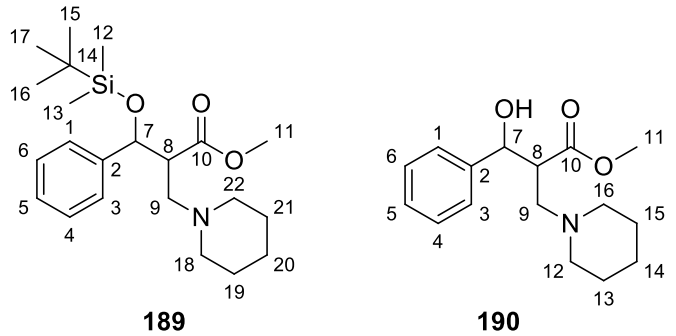

Figure 24: Conjugate addition reaction of piperidine nucleophile on the TBDMS protected ester adduct and the unprotected adduct.

Table 16: The IR and the NMR data for products **189** and **190**

Compound No.	**IR** (neat, cm^{-1})	**NMR**
189	2936 (C-H), 1736 (C=O), 840 (Si-O)	**^{1}H NMR (400 MHz, $CDCl_3$)** δ 7.34 – 7.24 (5H, m, Ar-H), 4.75 (1H, d, *J* = 7.7 Hz, H-7), 3.41 (3H, s, H-11), 2.98 – 2.90 (1H, m, H-8), 2.87 – 2.79 (1H, m, H-9a), 2.71 (1H, dd, *J*=12.4, 3.6 Hz, H-9b), 2.46-2.36 (2H, m, H-18,22), 2.27-2.19 (2H, m, H-18,22), 1.54 – 1.45 (4H, m, H-19,21), 1.42 – 1.32 (2H, m, H-20), 0.86 (9H, s, H-15,16,17), 0.01 (3H, s, H-12), -0.26 (3H, s, H-13). **^{13}C NMR (101 MHz, $CDCl_3$)** δ 173.8 (C-10), 142.7 (Ar-C), 127.9 (Ar-C), 127.5 (Ar-C), 126.5 (Ar-C), 75.4 (C-7), 58.2 (C-9), 54.4 (C-18,22), 53.7 (C-8), 51.2 (C-11), 30.9 (C-19,21), 26.1 (C-20), 25.8 (C-15,16,17), 18.1 (C-14), -4.6 (C-12), -5.2 (C-13).
190	3708 (OH), 2952 (C-H), 1731 (C=O)	**^{1}H NMR (400 MHz, $CDCl_3$)** δ 7.37 – 7.28 (4H, m, Ar-H), 7.25 – 7.21 (1H, m, Ar-H), 4.98 (1H, d, *J*=9.1 Hz, H-7), 3.38 (3H, s, H-11), 3.10 – 3.01 (1H, m, H-9a), 2.98 – 2.88 (1H, m, H-8), 2.79 – 2.62 (3H, m, H-9b,12a,16a), 2.49 – 2.36 (2H, m, H-12b,16b), 1.70 – 1.62 (4H, m, H-13,15), 1.52 – 1.45 (2H, m, H-14) **^{13}C NMR (101 MHz, $CDCl_3$)** δ 172.0 (C-10), 142.2 (C-2), 128.2 (C-4,6), 127.8 (C-5), 126.6 (C-1,3), 78.2 (C-7), 61.3 (C-9), 54.9 (C-12,16), 51.5 (C-11), 49.9 (C-8), 25.9 (C-13,15), 24.0 (C-14).

The IR spectra for both compounds showed signals similar to those of TMS protected adduct **186**. They showed all the important signals, such as the carbonyl stretch that was present around 1730

cm^{-1} for both adducts **189** and **190**. For the unprotected adduct **190**, the OH stretch was found in its typical region around 3708 cm^{-1}, appearing as a broad band.

The ^{1}H and ^{13}C NMR spectra also showed the formation of the anticipated products. The spectra were very similar to the TMS protected adduct **186**. The ^{1}H NMR spectra showed all the significant signals with the aromatic proton signals appearing between 7.21-7.37 ppm. The absence of the two terminal alkene proton signals in the 5-6 ppm region showed that addition of piperidine had occured on the alkene. The spectrum also showed the appearance of H-7 in its typical region around 4-5 ppm, integrating for 1 proton. These peaks appeared as doublets, coupling to the H-8 proton as confirmed using the COSY spectrum. The next signal at around 3.41 ppm integrated for 3 protons, belonging to the methyl protons H-11. This was also confirmed using the HMBC spectrum as it showed coupling to the carbonyl carbon peak at around 172 ppm. For both adducts **189** and **190**, this methyl proton signal corresponded to the carbon signal at 51 ppm as shown in the HSQC spectrum and also confirmed from the DEPT spectrum where it appeared as a positive peak.

The H-8 signal was found at around 3 ppm for both adducts, appearing as a multiplet coupling to the peak at 53.7 and 49.9 ppm in the HSQC for the protected **189** and the unprotected **190** adduct, respectively. The two proton signals that belong to the H-9 protons were present between 2.5-3 ppm. These two signals couple to the same carbon signal on the HSQC spectrum showing that these signals belong to protons attached to a single carbon. For adducts **189** and **190**, the next four signals belong to the piperidine ring, where the most deshielded amongst these signals belongs to the protons on the carbon atom directly attached to the nitrogen, which pulls electron density towards itself. They appeared as multiplets coupling to each other. In the protected adduct **189**, the signals around 0 ppm belong to the TBDMS group. All the carbon signals were assigned using the HSQC spectra and confirmed using the DEPT spectra.

Compound **190** has been synthesized before as reported in a communication by Kundu and Bhat.[86] Very similar NMR data was obtained with a few minor changes in the shift values, integrations, as well as multiplicities.

3.1.3.1.1.3.Addition of piperidine to the TMS protected nitrile adduct 170.

Piperidine was also added to the TMS protected nitrile adduct **170**. However, the TMS group was lost during the addition reaction or purification. This might be due to the instability of the TMS group, which can be removed easily under acidic conditions such as in the presence of silica gel. The product **191** was obtained as a mixture of diastereomers **191a** and **191b** (**Figure 25**). The presence of diastereomers is due to the formation of a new stereogenic centre as the alkene is converted into an alkane group through the addition reaction. C-7 and C-8 are both stereogenic centres, giving rise to diastereomers which can be distinguished by their different chemical shift values in the NMR spectra. The mixture of diastereomers **191a/b** were obtained in a very good yield of 80%.

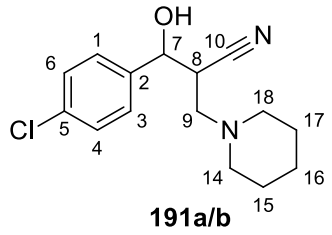

191a/b

Figure 25: Conjugate addition reaction of piperidine nucleophile on the TMS protected nitrile adduct **170** to form compound **191a/b**.

Table 17: The approximate chemical shift and integration values obtained from the ^{1}H NMR spectrum for both the major and minor diastereomer **191a/b.**

Major and Minor diastereomer combined (**191a/b**)			
Assignment	**Approximate chemical shift values (ppm)**	**Combining partial integrations**	**Overall integration**
Ar-H	7.44-7.33	4H	4H
H-7	5	0.58H + 0.24H	1H
H-8	3.05	0.60H + 0.24H	1H
H-9	3	0.04H + 0.13H + 0.10H + 0.13H + 0.39H + 0.50H + 0.88H	2H

H-14,18	2.43	4H	4H
H-15,17	1.6	4H	4H
H-16	1.43	2H	2H

Table 18: The ^{13}C NMR data for both the major and minor diastereomer of **191a/b**

Assignment	Major diastereomer	**Assignment**	Minor diastereomer
Ar-C	138.6	**Ar-C'**	139.2
Ar-C	134.0	**Ar-C'**	134.3
Ar-C	128.7	**Ar-C'**	128.7
Ar-C	127.5	**Ar-C'**	127.9
C-10	118.6	**C-10'**	118.1
C-7	73.9	**C-7'**	76.6
C-9	58.3	**C-9'**	60.6
C-14,18	55.4	**C-14',18'**	54.7
C-8	36.1	**C-8'**	35.8
C-15,17	26.0	**C-15',17'**	25.8
C-16	23.7	**C-16'**	25.9

The piperidine addition was verified by IR and the NMR spectroscopy. Compound **191a/b** showed the OH signal at 3416 cm^{-1}, as well as the CN signal at 2255 cm^{-1}.

The ^{1}H NMR spectrum also showed all the expected signals, and the absence of the terminal alkene protons confirmed the addition of piperidine. The ^{1}H NMR spectrum showed the signals for both diastereomers. All the signals were integrated against the H-7 signal, where the H-7 signals for both diastereomers were combined and integrated together for one proton. All the corresponding signals for both diastereomers were combined, to ensure they integrated for the correct number of protons. The diastereomers were assigned based on the HSQC spectrum. The signals at 3.15 ppm and 2.90 ppm combined integrated for 1 proton which belongs to H-8. The HSQC spectrum showed that both signals belong to a proton that is attached to the C-8 carbon for the major and

the minor diastereomers, which means that combining the two will give the H-8 proton. The same applies to the rest of the signals, which were assigned using the HSQC spectrum.

The H-9 signals for both diastereomers were made up from a number of small signals identified using the HSQC spectra, such as the signals at 3.04, 3.01, 2.97. 2.93, 2.89, 2.83, and 2.76 ppm. When the integration values for all these signals were combined, they integrated for 2 protons. The signal at around 2 ppm integrated for 4 protons which belong to the piperidine ring protons on the carbon attached directly to the nitrogen, making them more deshielded compared to the rest of the piperidine protons. The other two signals, in the shielded region between 1.43-1.72 ppm belong to the piperidine protons. The H-9 signals appeared as doublets, and multiplets, showing coupling to each other and the H-8 proton.

The carbon signals for both diastereomers were assigned using the HSQC spectrum. The signals are differentiated using a prime symbol, for example: C-9 and C-9', where the prime symbol shows the carbon belonging to the minor diastereomer (**Table 18**). The ^{13}C NMR spectrum showed a big and a small signal for each of the carbons, belonging to the major and the minor diastereomer, respectively. The DEPT spectrum confirmed the carbon assignments, where all the aromatic protons, carbon 7 and carbon 8 appeared in the positive region and carbon 9 and the piperidine carbon signals appeared in the negative region.

3.1.3.1.1.4. Addition of piperidine to the TBDMS protected nitrile adduct 164.

Piperidine was also added to the TBDMS protected adduct **164**, the product **192a/b** was obtained as a mixture of diastereomers. The allylic substitution product **193** was obtained as a byproduct. The diastereomers were obtained in a very good yield of 80%. The major and minor diastereomer were obtained in a 3:1 ratio determined by comparing the height intensity of the H-7 proton peaks in the ^{1}H NMR spectrum. The ratio of the conjugate addition: allylic substitution was 4:1, determined by comparing the mass of the diastereomers combined and mass of the allylic substitution product. A ratio of 4:1 is very good, as the desired product was obtained in a very good yield compared to the byproduct.

Table 19 shows how the partial integration values observed were combined to confirm the expected total integration values for both diastereomers.

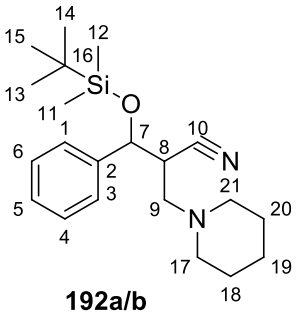

192a/b

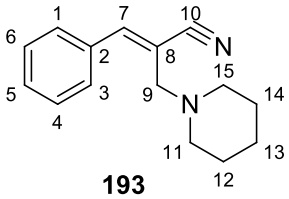

193

Figure 26: Conjugate addition reaction of piperidine nucleophile on the TBDMS protected nitrile adduct to form diasteromers **192a/b** and the byproduct **193** obtained.

Table 19: The integrations obtained from the proton NMR for both the major and minor diastereomer **192a/b**

Major and Minor diastereomer combined (**192a/b**)			
Assignment	**Approximate chemical shift values (ppm)**	**Combining partial integrations**	**Overall integration**
Ar-H	7.33-7.18	5H	5H
H-7	4.8	0.72H + 0.27H	1H
H-8	2.9	0.73H + 0.28H	1H
H-9	2.4	0.29H + 0.32H + 0.74H + 1.08H	2H
H-17,21	2.2	4H	4H
H-18,20	1.5	4H	4H
H-19	1.3	2H	2H
H-13,14,15	0.82	2H + 7H	9H
H-11	-0.03	2.93H + 0.33H	3H
H-12	-0.3	2.18H + 0.70H	3H

Table 20: The carbon NMR data for both the major and minor diastereomer **192a/b**.

Assignment	Major diastereomer	**Assignment**	Minor diastereomer

Ar-C	140.2	**Ar-C'**	141.7
Ar-C	128.3	**Ar-C'**	128.4
Ar-C	128.21	**Ar-C'**	128.17
Ar-C	126.8	**Ar-C'**	126.3
C-10	120.1	**C-10'**	119.6
C-7	72.8	**C-7'**	72.1
C-9	56.6	**C-9'**	57.4
C-17,21	54.5	**C-17',21'**	54.5
C-8	39.9	**C-8'**	40.8
C-18,20	26.0	**C-18',20'**	25.9
C-13,14,15	25.7	**C-13',14',15'**	25.7
C-19	24.19	**C-19'**	24.22
C-16	18.11	**C-16'**	18.13
C-12	-4.7	**C-12'**	-4.5
C-11	-5.3	**C-11'**	-5.2

The desired product **192a/b** was obtained as verified by IR and NMR spectroscopy (**Table 19** and **20**). The stretches obtained in the IR spectrum were very similar to those seen for the unprotected adduct **191a/b**, such as the C-H stretch at around 2934 cm^{-1} and the nitrile stretch at around 2230 cm^{-1}. The diastereomers displayed similar stretches as the allylic substitution product **193** except for the presence of the O-Si bend at 836 cm^{-1} for the diastereomers **192a/b** and the presence of a double bond stretch for product **193**.

The NMR spectra also verified the formation of the desired product **192a/b** and also clearly showed presence of the two diastereomers. The diastereomers were assigned by adding the partial integrations; combining the signals for the two diastereomers allowed the full integrations for a specific proton to be obtained (**Table 19**). The integration of the protons was referenced against the H-7 proton, where the two peaks were combined and assigned an integration value of one.

All five of the expected aromatic protons were found in the aromatic region between 7.18-7.33 ppm. H-7 peaks appeared as a multiplet at around 4.8 ppm showing coupling to the neighbouring H-8 proton. The H-8 proton signals belonging to both diastereomers appeared around 3.00 and

2.81 ppm, appearing as a doublet of triplets and a multiplet, respectively. The H-8 proton couples to the H-7 as well as the H-9 protons, giving a doublet of triplets. The HSQC spectrum confirmed that both the signals at 3.00 and 2.81 ppm belong to the H-8 proton as they showed cross-peaks to the carbon 8 signals that are adjacent and belong to both the major and the minor diastereomer. Adding the partial integration values gave the two H-9 protons. All of these signals had cross-peaks to two carbon signals for the major and the minor diastereomer in the HSQC spectrum.

The other signals in the shielded 1.28-2.32 ppm region belonged to piperidine protons for both diastereomers. All the piperidine signals formed a single peak for both the major and the minor diastereomer, with the same chemical shift values for both the major and the minor diastereomers being obtained. The rest of the signals in the shielded region -0.30-0.82 ppm belonged to the TBDMS protons. The HSQC spectrum was used to combine the partial integrations to assign them to a specific proton belonging to both the major and the minor diastereomer.

The carbon signals for both the major and the minor diastereomers were also assigned using the HSQC spectrum (**Table 20**). The signals at 72.8 and 72.1 ppm both belong to carbon 7 for the major and minor diastereomers, as they showed cross-peaks to the H-7 protons. The signals at 56.6 ppm and 57.4 ppm both belong to C-8 for the major and minor diastereomer, respectively. The rest of the signals were assigned in the same way and confirmed using the DEPT spectrum. The DEPT experiment showed positive signals in the aliphatic region, around 70 and 40 ppm, showing that they belong to aliphatic CH protons, H-7 and H-8, respectively.

Table 21: The IR and the NMR data for the allylic substitution product **193**

Compound No.	**IR** (neat, cm^{-1})	**NMR**
193	2936 (C-H) 2220 (CN)	**^{1}H NMR (400 MHz, $CDCl_3$)** δ 7.81 – 7.73 (2H, m, Ar-H), 7.46 – 7.36 (3H, m, Ar-H), 7.09 (1H, s, H-7), 3.26 (2H, s, H-9), 2.54 – 2.43 (4H, m, H-11,15), 1.67 – 1.56 (4H, m, H-12,14), 1.50 – 1.40 (2H, m, H-13). **^{13}C NMR (101 MHz, $CDCl_3$)** δ 145.0 (C-7), 133.4 (Ar-C), 130.2 (Ar-C), 128.9 (Ar-C), 128.8 (Ar-C), 118.9 (C-10), 108.8 (C-8), 63.2 (C-9), 54.1 (C-11,15), 25.9 (C-12,14), 24.2 (C-13).

The allylic substitution product **193** was also obtained along with the addition product. The ^{1}H NMR spectrum showed the absence of the TBDMS group, as well as the absence of the H-8 proton signal (**Table 21**). The ^{1}H NMR spectrum also showed a shift of the H-7 proton to the deshielded region at 7.09 ppm, adjacent to the aromatic protons. The ^{1}H NMR spectrum also showed the presence of the H-9 proton and the piperidine protons in the shielded region between 1.40-3.26 ppm.

^{13}C NMR spectroscopy also confirmed this as it showed the absence of the TBDMS carbon signals (**Table 21**). The carbon signals were assigned using the HSQC spectrum, which showed the direct coupling of the proton and the carbon NMR signal. The most deshielded peak at around 145 ppm belongs to the C-7 carbon, which was confirmed by a DEPT experiment as it was found to give a positive signal together with the aromatic protons. The absence of the peaks at 133.4, 118.9 and 108.8 ppm in the DEPT spectrum showed that they belong to a quaternary carbon. The peak at 133.4 and 108.8 ppm belong to an aromatic carbon and C-8 respectively. The peak at 118.9 ppm belongs to the CN carbon which is its typical region.

Table 22: Overall summary of the nucleophilic addition reaction using piperidine nucleophiles.

Compound no.	**Type of adduct (Ester or nitrile)**	**Protecting group (TBDMS/TMS)**	**Allylic substitution or not**	**Both or single diastereomers and diastereomeric ratios**
186	Ester	TMS	YES	Single
189		TBDMS	NO	Single
190		-	NO	Single
191a/b	Nitrile	TMS	NO	Both (2:1)
192a/b		TBDMS	YES	Both (3:1)

Compounds **186**, **189** and **190** were methyl ester adducts. These three ester adducts were protected with different protecting groups to compare their effect on the nucleophilic addition reaction. The protecting groups affect the formation of the diastereomers and their diastereomeric ratios since

they control the addition of the nucleophile as well as the approach of the incoming proton during the addition reaction. The protecting groups also affect the occurrence of the allylic substitution reaction depending on whether they act as a good leaving group or not.

For compound **186**, allylic substitution occurred which was expected since the TMS group acts as a good leaving group (**Table 22**). The nucleophile attacks the terminal carbon of the alkene and the TMS group leaves. For the TBDMS protected and unprotected adducts (**189** and **190**), allylic substitution did not occur as it would be expected as they are poor leaving groups.

For the three adducts **186**, **189** and **190**, only single diastereomers were obtained (**Table 22**), this might be due to the dominance of one diastereomer over the other. The dominance might occur as a result of the bulky protecting group present, which would block one side of the plane of the double bond, controlling the diastereoselectivity making the other diastereomer almost invisible and undetectable. This would normally be expected for compound **189**, since it has the bulky TBDMS protecting group. However, a single diastereomer was also observed for **186** and **190**, which was unexpected, since this groups are not bulky enough to direct the nucleophile and to control the diastereoselectivity, leading to the formation of both diastereomers in nearly equal ratios. The detection of one diastereomer only, could be due to the loss of the other diastereomer either during the reaction or the purification.

With regards to the nitrile adducts, **191a/b** did not give the allylic substitution product and compound **192a/b** gave the allylic substitution product (**Table 22**). This is the opposite of what was expected. Since TMS group is a good leaving group and would leave easily, giving the allylic substitution product, whereas the TBDMS is a poor leaving group and should not give the allylic substitution product.

For **191a/b** and **192a/b**, both diastereomers were observed. A ratio of 2:1 for TMS protected adduct (**191a/b**) and a ratio of 3:1 for the TBDMS protected adduct (**192a/b**) were obtained (**Table 22**). It shows a greater selectivity for the TBDMS protected adduct than the TMS protected adduct. The greater selectivity might be due to the bulkiness of the TBDMS group, which blocks one side of the double bond, controlling the addition of the nucleophile and the incoming proton from one side forming one diastereomer in a higher ratio.

The nitrile adducts gave both diastereomers whereas, a single diastereomer was observed for the ester adducts. There is no clear reason as to why this occurred (**Table 22**).

3.1.3.1.2. Benzylamine nucleophile

3.1.3.1.2.1. Addition of benzylamine on the TBDMS protected ester adduct 161.

The next addition reactions were done using benzylamine as a nucleophile. The conjugate addition reaction as carried out between benzylamine and TBDMS-protected ester **161** to give expected product **194a/b** as a mixture of diastereomers, together with allylic substitution product **195** (**Figure 27**).

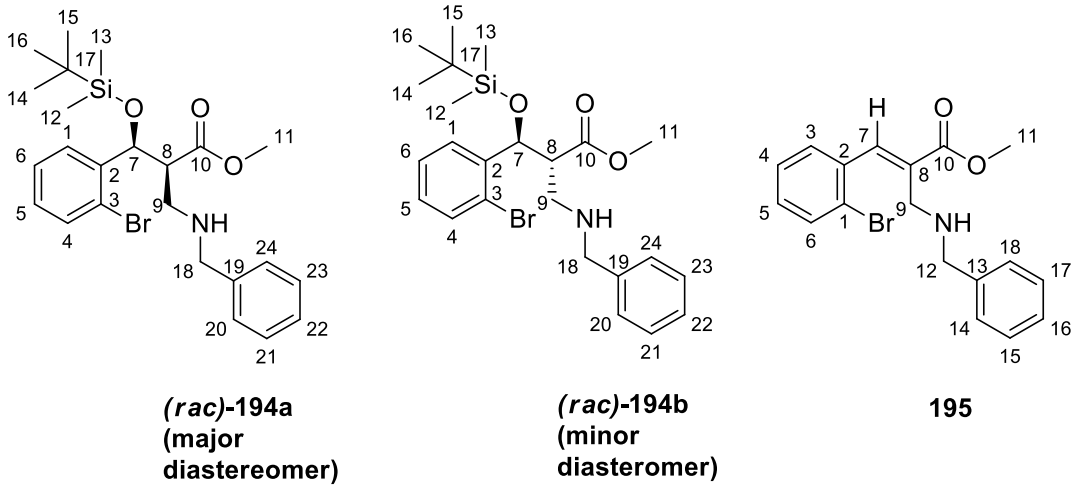

Figure 27: Conjugate addition reaction of the benzylamine nucleophile on the TBDMS protected ester adduct to form diasteromers **194a/b** and the byproduct **195** obtained.

Table 23: The IR and the NMR data for the diastereomers **194a/b** and the allylic substitution product **195**.

Compound No.	**IR** (neat, cm^{-1})	**NMR**
194a (major)	3665 (N-H), 2950 (C-H), 1734 (C=O) 820 (Si-O)	**^{1}H NMR (400 MHz, $CDCl_3$)** δ 7.53 – 7.45 (2H, m, Ar-H), 7.34 – 7.27 (1H, m, Ar-H), 7.26 – 7.21 (2H, m, Ar-H), 7.22 – 7.16 (3H, m, Ar-H), 7.12 – 7.10 (1H, m, Ar-H), 5.31 (1H, d, *J*=7.5 Hz, H-7), 3.70 (3H, s, H-11), 3.68 (1H, m, H-18a), 3.59 (1H, m, H-18b), 2.99 (2H, m, H-8,9a), 2.44 (1H, s, H-

		9b), 1.53 (1H, s, NH), 0.81 (9H, s, H-14,15,16), 0.02 (3H, s, H-12), -0.28 (3H, s, H-13). **^{13}C NMR (101 MHz, $CDCl_3$)** δ 173.5 (C-10), 142.0 (C-2), 140.8 (C-19), 140.0 (C-22), 132.4 (C-4), 129.2 (C-5), 128.3 (C-21,23), 128.0 (C-20,24), 127.6 (C-1), 126.8 (C-6), 122.5 (C-3), 73.1 (C-7), 56.0 (C-8) 53.4 (C-18), 51.5 (C-11), 47.5 (C-9), 25.6 (C-14,15,16), 17.9 (C-17), -4.8 (C-12), -5.4 (C-13).
194b (minor)	3665 (N-H), 2950 (C-H), 1734 (C=O), 820 (Si-O)	**^{1}H NMR (400 MHz, $CDCl_3$)** δ 7.52 – 7.44 (2H, m, Ar-H), 7.31 – 7.26 (2H, m, Ar-H), 7.25 – 7.16 (4H, m, Ar-H), 7.15 – 7.08 (1H, m, Ar-H), 5.50 (1H, s, H-7), 3.71 – 3.62 (5H, m, H-11,18), 3.19 – 3.12 (1H, m, H-9a), 3.07 – 2.99 (1H, m, H-8), 2.73 – 2.64 (1H, m, H-9b), 0.85 (9H, s, H-14,15,16), 0.01 (3H, s, H-12), -0.24 (3H, s, H-13).**^{13}C NMR (101 MHz, $CDCl_3$)** δ 173.0 (C-10), 141.3 (C-2), 140.2 (C-19), 132.7 (C-22), 129.2 (C-4), 129.0 (C-5), 128.3 (C-21,23), 128.1 (C-20,24), 127.1 (C-1), 126.8 (C-6), 121.6 (C-3), 73.5 (C-7), 53.8 (C-18), 51.72 (C-8), 51.70 (C-11), 45.3 (C-9), 25.7 (C-14,15,16), 18.0 (C-17), -4.8 (C-12), -5.5 (C-13).
195	2950 (C-H), 1714 (C=O)	**^{1}H NMR (400 MHz, $CDCl_3$)** δ 7.84 (1H, s, H-7), 7.59 (2H, m, Ar-H), 7.50 – 7.42 (2H, m, Ar-H), 7.29 – 7.27 (1H, m, Ar-H), 7.24 – 7.13 (4H, m, Ar-H), 3.85 (3H, s, H-11), 3.73 (2H, s, H-12), 3.48 (2H, s, H-9). **^{13}C NMR (101 MHz, $CDCl_3$)** δ 142.0 (Ar-C), 140.9 (Ar-C), 132.6 (Ar-C), 130.9 (Ar-C), 130.0 (Ar-C), 128.3 (Ar-C), 127.2 (Ar-C), 126.9 (Ar-C), 77.2 (C-7), 53.3 (C-12), 52.2 (C-11), 45.0 (C-9)

The diastereomers proved to be separable by column chromatography and were both isolated as yellow oils. The identity of the products was confirmed by IR and NMR spectroscopy (**Table 23**).

The IR spectrum confirmed the formation of the products **194a** and **194b** as it showed all the important stretches, such as the NH signal at 3665 cm^{-1} and carbonyl stretches at 1734 cm^{-1}.

The ^{1}H and ^{13}C NMR spectra also showed all the important signals, such as the aromatic signals integrating for 9 protons in the deshielded region between 7.08-7.53 ppm. They all appeared as multiplets, coupling to each other. H-7 was found at around 5 ppm for both major and the minor diastereomer, integrating for 1 proton. It appeared as a doublet, coupling to the neighbouring H-8 proton. The next peaks belong to H-11 and H-18. The H-11 peak appeared as a singlet, whereas the H-18 peak appeared as a multiplet with the two protons coupling to each other. H-11 appeared in a more deshielded position due to the oxygen atom present next to it. Their corresponding carbon signals were found using the HSQC spectrum, at around 53 ppm for C-18 and 52 ppm for C-11 for both the major and the minor diastereomer. The H-18 peaks showed coupling to the aromatic carbons in the HMBC spectrum.

The peaks between 2-3 ppm belong to H-8 and H-9 for both the major and the minor diastereomers. They appeared as multiplets coupling to each other, and in addition H-8 coupled with the H-7 proton. The corresponding C-8 and C-9 carbon signals were found using the HSQC spectrum and confirmed using the DEPT spectra. The C-8 appeared as a positive signal whereas the C-9 appeared as a negative signal. C-8 appeared in a more deshielded position than C-9. There were only minor differences between the shift values of the major and the minor diastereomer. The NH peak was found around 1.53 in one of the diastereomers, however, it was not clearly visible for the other diastereomer. The rest of the peaks were in the shielded region between -0.24-0.85 ppm and belonged to the TBDMS protons. The corresponding carbon peaks were found using an HSQC experiment and confirmed using the DEPT spectrum. For both compounds (**194a and 194b)**, the values obtained from the mass spectrum corresponded very well with the expected masses. Calculated $[M+H^{+}]$ for compound **194a**: 492.1564, found: 492.1597 and the calculated $[M+H^{+}]$ for compound **194b**: 492.1564, found: 492.1600.

An allylic substitution product **195** was also obtained from the nucleophilic addition reaction where the TBDMS protected OH group leaves giving an alkene group. The product identity was confirmed using IR and NMR spectroscopy (**Table 23**). The IR spectrum showed the carbonyl stretch at 1714 cm^{-1}. The ^{1}H NMR spectrum also showed all the expected signals, such as the aromatic signals between 7.13-7.59 ppm appearing as a multiplet coupling to each other. The peak

at 3.85 ppm belongs to H-11 as it integrated for 3 protons. This was confirmed using the HMBC spectrum as it showed coupling to the carbonyl carbon peak.

The next two peaks which integrated for 2 protons belong to H-12 and H-9, with H-12 being more deshielded. The peak around 3.48 ppm belongs to H-9 as it showed coupling to the carbonyl carbon in the HMBC spectrum. Both peaks appeared as singlets as they do not couple to any other protons. All the peaks were assigned using the HSQC spectrum and confirmed using the DEPT spectrum.

3.1.3.1.2.2. Addition of benzylamine to the TBDMS protected nitrile adduct 163.

The conjugate addition reaction with benzylamine was done using the same method as for the piperidine nucleophile. The product **196a/b** was obtained as diastereomers, together with the allylic substitution product **197**. The diastereomers were inseparable and were obtained in a ratio of 1:3, determined by comparing the H-7 proton peak intensities in the ^{1}H NMR for both the major and minor diastereomers. The products were confirmed using the IR and NMR spectroscopy (**Figure 28, Table 24**).

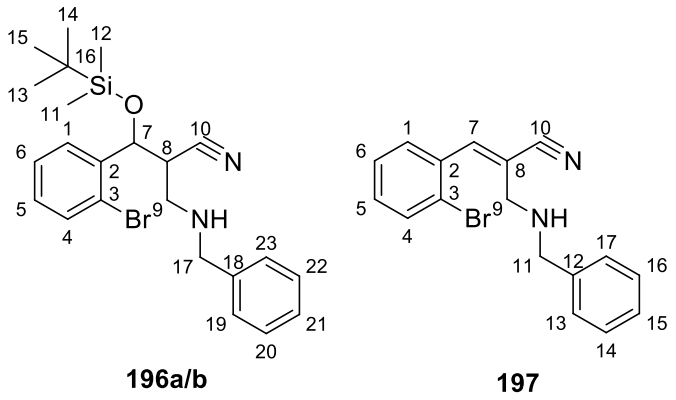

Figure 28: Conjugate addition reaction of the benzylamine nucleophile on the TBDMS protected nitrile adduct to form product **196a/b** and the allylic substitution byproduct **197**.

Table 24: The approximate chemical shift and integration values obtained from the ^{1}H NMR spectrum for both the major and minor diastereomer **196a/b.**

Major and Minor diastereomer combined (**196a/b**)

Assignment	**Approximate chemical shift values (ppm)**	**Combining partial integrations**	**Overall integration**
Ar-H	7.72	0.27H + 1.81H + 3.85H + 3.05H	9H
H-7	5.3	0.72H + 0.22H	1H
H-17	3.8	0.49H + 1.58H	2H
H-8	3.22	1.31H	1H
H-9	2.8	1H + 0.75H	2H
N-H	2.18	1H	1H
H-13,14,15	0.9	2H + 7H	9H
H-11	0.12	2H + 1H	3H
H-12	-0.15	2H + 1H	3H

Table 25: The ^{13}C NMR data for both the major and minor diastereomer **196a/b**

Assignment	Major diastereomer	**Assignment**	Minor diastereomer
Ar-C	139.5	**Ar-C'**	140.2
Ar-C	132.8	**Ar-C'**	132.5
Ar-C	129.82	**Ar-C'**	129.76
Ar-C	128.9	**Ar-C'**	129.1
Ar-C	128.45	**Ar-C'**	128.52
Ar-C	128.10	**Ar-C'**	128.13
Ar-C	127.6	**Ar-C'**	127.8
Ar-C	127.1	**Ar-C'**	127.2
Ar-C	121.8	**Ar-C'**	121.1
C-10	119.8	**C-10'**	119.8
C-7	71.9	**C-7'**	70.6
C-17	53.5	**C-17'**	53.3
C-9	45.7	**C-9'**	48.2

C-8	40.2	**C-8'**	41.4
C-13,14,15	25.7	**C-13',14',15'**	25.7
C-16	18.05	**C-16'**	18.08
C-12	-4.9	**C-12'**	-4.7
C-11	-5.3	**C-11'**	-5.2

The reaction gave a very good yield of 76% for the mixture of both diastereomers. The IR spectra showed all the important signals such as the NH signal around 3347 cm^{-1} and the nitrile signal around 2240 cm^{-1}. The presence of the NH signal confirmed the addition.

The NMR spectra also showed all the important signals. In the ^{1}H NMR spectrum of the diastereomers, the combined H-7 signal peaks were used as the reference for integration; the two signals combined were integrated as 1 proton. The HSQC spectrum was used to find all the signals in the ^{1}H NMR spectrum that belonged to the same proton, so that the partial integration of these peaks could be combined. The peaks at 3.84 ppm and 3.75 ppm belonged to the same two protons, as shown in the HSQC spectrum, as they showed cross-peaks to the carbon signals belonging to the major and the minor diastereomer. These peaks belong to the two H-17 protons. The next peak at around 3.18 ppm belongs to the H-8 proton, as it integrates for 1 proton.

The signals at 2.80 and 2.96 ppm belong to the H-9 protons and show cross-peaks to two adjacent carbon signals in the HSQC spectrum. The rest of the peaks belong to the TBDMS proton signals as the signals combined make up for the right total number of protons. All the ^{13}C NMR peaks were assigned using the HSQC spectrum. All the deshielded peaks above 120 ppm belonged to the aromatic carbons. The peak around 70 ppm belongs to the C-7 carbon as it showed coupling to the H-7 proton. The next peaks around 53 ppm belong to C-17 as they couple to the H-17 proton in the HSQC. The two signals around 48 ppm belong to C-9, and the next two peaks for the major and the minor diastereomer belong to C-8 as determined from the HSQC. The rest of the peaks belong to the TBDMS group.

Table 26: The IR and the NMR data for the allylic substitution product **197**

Compound No.	**IR** (neat, cm^{-1})	**NMR**

197	2927 (C-H), 2215 (CN)	**^{1}H NMR (400 MHz, $CDCl_3$)** δ 7.91 (1H, dd, *J*=8.0, 1.7 Hz, H-7), 7.64 (1H, dd, *J*=8.1, 1.2 Hz, Ar-H), 7.46 – 7.33 (5H, m, Ar-H), 7.32 – 7.27 (1H, m, Ar-H), 7.26 – 7.17 (2H, m, Ar-H), 3.88 (2H, s, H-11), 3.62 (2H, d, *J*=1.4 Hz, H-9), 1.25 (1H, s, N-H). **^{13}C NMR (101 MHz, $CDCl_3$)** δ 143.2 (Ar-C), 139.4 (Ar-C), 133.7 (Ar-C), 133.0 (Ar-C), 131.3 (Ar-C), 129.6 (C-7), 128.6 (Ar-C), 128.3 (Ar-C), 127.8 (Ar-C), 127.3 (Ar-C), 124.3 (Ar-C), 117.7 (C-10), 114.0 (C-8), 52.2 (C-9), 52.1 (C-11).

The allylic substitution product **197** was also obtained from the addition reaction of benzylamine and this product was verified using IR and NMR spectroscopy (**Table 26**). The IR spectrum showed similar stretches to the addition product, except for the absence of the O-Si stretch and the presence of alkene stretch. The ^{1}H and ^{13}C NMR spectra also confirmed product formation, showing all the expected signals. The ^{1}H NMR spectrum showed the most deshielded peak at around 7.91 ppm, belonging to the H-7 proton. This appeared as a doublet of doublets coupling to the neighbouring aromatic proton and H-8 proton as shown in the COSY spectrum.

All the other peaks in the deshielded region between 7.17-6.64 ppm belong to the aromatic protons, where one appeared as a doublet of doublets and the rest as multiplets. The next two peaks at 3.88 and 3.62 ppm belong to H-11 and H-9 and the last peak around 1.25 ppm belongs to the N-H proton. The ^{13}C NMR spectrum was assigned using the HSQC spectrum. All the expected aromatic carbon signals were present in the aromatic region. The CN peak was found in its typical region, around 117 ppm. The next two peaks around 52.2 and 52.1 ppm belong to C-9 and C-11, respectively. The DEPT spectrum was also used to confirm these assignments.

Conjugate addition reaction using benzylamine on both MBH ester and nitrile adducts have been reported before by Kundu and Bhat.[86]

Table 27: Overall summary of the nucleophilic addition reaction using Benzylamine nucleophiles.

Compound no.	**Type of adduct (Ester or nitrile)**	**Protecting group (TBDMS/TMS)**	**Allylic substitution or not**	**Both or single diastereomers and diastereomeric ratios**
194a/b	Ester	TBDMS	YES	Both (2:1)
196a/b	Nitrile			Both (3:1)

Both TBDMS protected ester and nitrile adducts **194a/b** and **196a/b** gave the allylic substitution product (**Table 27**), which was not expected as the TBDMS does not act as a good leaving group. Both diastereomers were obtained for nitrile and ester adducts. The nitrile adducts gave a mixture of diastereomers which were not separable however, for the ester adduct they were easily separated using gravity column chromatography. Compounds **194a/b** were obtained in a 2:1 ratio of major:minor diastereomer, whereas compound **196a/b** were obtained in a 3:1 ratio (**Table 27**). Although both have the same bulky TBDMS protecting group which controls the diastereoselectivity, less selectivity was seen for the ester adduct compared to the nitrile adduct.

3.1.3.1.3. 4-Methoxybenzylamine nucleophile

The next addition reactions were done using methoxybenzylamine on the nitrile and the ester adducts. These products were verified using the IR and the NMR spectra.

3.1.3.1.3.1. Addition of methoxybenzylamine to the TBDMS protected ester adduct 162.

A conjugate addition reaction was performed between methoxybenzylamine and ester **162**. Only one diastereomer of **198** was obtained. No allylic substitution product was obtained from this reaction.

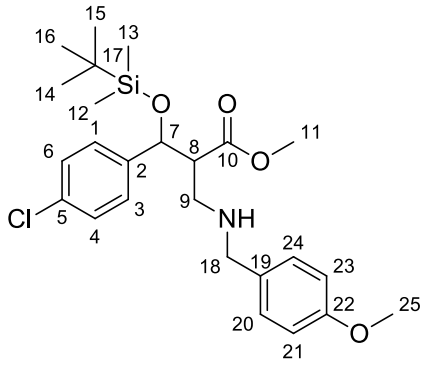

198

Figure 29: Conjugate addition reaction of the methoxybenzylamine nucleophile on the TBDMS protected ester adduct to form **198**.

Table 28: The IR and the NMR data for the conjugate addition product obtained **198.**

Compound No.	**IR** (neat, cm^{-1})	**NMR**
198	31^{87} (N-H), 2952 (C-H), 1727 (C=O), 820 (Si-O)	**^{1}H NMR (400 MHz, $CDCl_3$)** δ 7.31 – 7.26 (2H, m, H-4,6), 7.26 – 7.17 (4H, m, H-1,3,20,24), 6.85 (2H, d, *J*=8.5 Hz, H-21,23), 5.12 (1H, d, *J*=3.7 Hz, H-7), 3.93 – 3.87 (1H, m, H-18a), 3.80 (3H, s, H-25), 3.77 – 3.72 (1H, m, H-18b), 3.64 (3H, s, H-11), 3.20 – 3.08 (2H, m, H-9a,8), 2.85 – 2.78 (1H, m, H-9b), 0.82 (9H, s, H-14,15,16), -0.04 (3H, s, H-12), -0.23 (3H, s, H-13). **^{13}C NMR (101 MHz, $CDCl_3$)** δ 172.4 (C-10), 159.6 (C-22), 140.0 (C-2), 133.6 (C-19), 130.4 (C-20,24), 128.6 (C-4,6), 128.5 (C-5), 127.4 (C-1,3), 114.2 (C-21,23), 73.8 (C-7), 55.3 (C-25), 52.6 (C-8), 52.3 (C-11), 51.9 (C-18), 44.2 (C-9), 25.6 (C-14,15,16), 18.0 (C-17), -4.6 (C-13), -5.5 (C-12).

For the ester adduct **198**, a yield of 69% was obtained. The IR spectrum showed important functional group stretches, such as the ester carbonyl at 1727 cm^{-1} and the NH stretch at cm^{-1}. The ^{1}H NMR spectrum shown in figure 30 shows all the expected signals, such as the eight aromatic

protons signals between 6.5-7.31 ppm. The H-7 peak was found at 5.12 ppm, appearing as a doublet, coupling to the H-8 proton. The C-7 peak was found at 73.8 ppm from the HSQC spectrum. The peaks at 3.90 and 3.80 ppm belong to H-18 as determined from the HSQC as they are attached to the same carbon, and integrate for 2 protons. It was also confirmed from the HMBC spectrum as C-18 showed coupling to the aromatic protons of the methoxybenzene ring. The C-18 peak was found at 51.9 ppm. The peak at 3.80 ppm integrates for 3 protons and belongs to H-25 as it shows coupling to the aromatic carbons of the methoxybenzene ring in the HMBC spectrum. The C-25 peak was found at 55.3 ppm.

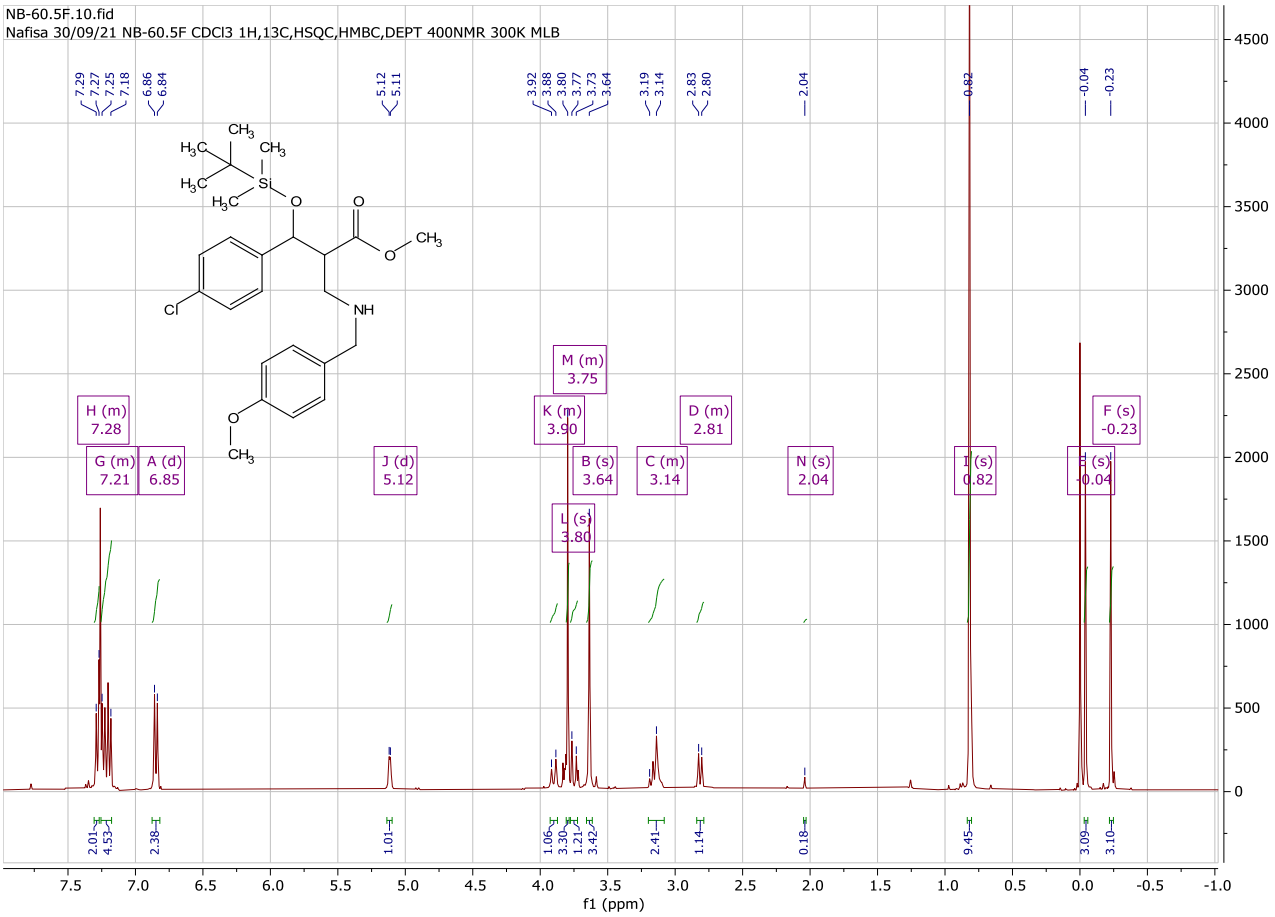

Figure 30: The ^{1}H NMR spectrum of compound **198**.

The next peak at 3.64 ppm belongs to H-11 as it integrates for 3 protons and couples to the carbonyl carbon in the HMBC spectrum. The corresponding carbon peak was found at 52.3 ppm. The next two peaks at 3.2 and 2.9 belong to H-9 and H-8 as determined from the HSQC spectrum. The two H-9 protons each appeared as separate peaks and showed coupling to each other. The peaks

belonging to H-9 was also confirmed using the HMBC spectrum as they couple to the carbonyl carbon. The corresponding C-9 and C-8 peaks were found around 44.2 and 52.6 ppm, respectively. The rest of the ^{1}H NMR peaks belong to the TBMDS protons, and their carbon peaks were found using the HSQC spectrum.

3.1.3.1.3.2. Addition of methoxybenzylamine to the TBDMS protected nitrile adduct 165.

The conjugate addition reaction between methoxybenzylamine and nitrile **165** gave the product **199**. Only a single diastereomer was obtained, this might be due to the loss of the other diastereomer during the reaction or the heavy dominance of one diastereomer over the other. Allylic substitution product **200** was also obtained.

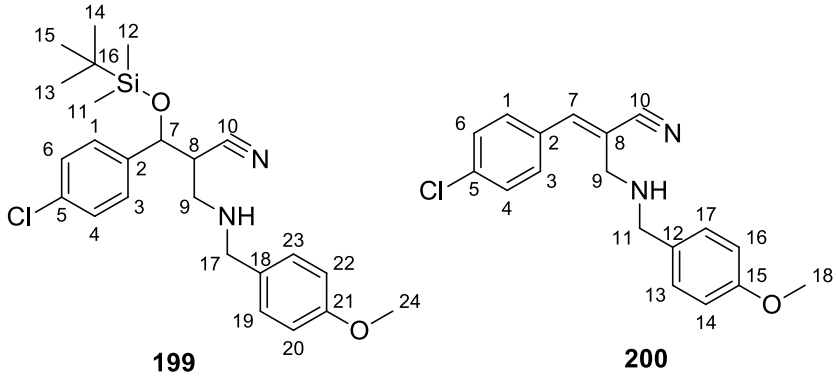

Figure 31: Conjugate addition reaction of the 4-methoxybenzylamine nucleophile on the TBDMS protected nitrile adduct to form product **199** and the allylic substitution byproduct **200** obtained.

Table 29: The IR and the NMR data for the conjugate addition **199** and the allylic substitution product **200**.

Compound No.	**IR** (neat, cm^{-1})	**NMR**
199	2925 (C-H), 2225 (CN), 835 (Si-O)	**^{1}H NMR (400 MHz, $CDCl_3$)** δ 7.34 – 7.24 (4H, m, Ar-H), 7.21-7.16 (2H, m, Ar-H), 6.90 – 6.80 (2H, m, Ar-H), 4.88 (1H, d, *J*=6.5 Hz, H-7), 3.81 (3H, s, H-24), 3.72 (2H, s, H-17), 3.01 – 2.71 (3H, m, H-8,9), 2.21 (1H, s, N-H), 0.89 (3H, s, H-13,14,15), 0.86 (6H, s, H-13,14,15), 0.06 (3H, s, H-11), -0.18 (3H, s, H-12). **^{13}C NMR (101 MHz, $CDCl_3$)** δ 158.9

		(Ar-C), 139.2 (Ar-C), 134.2 (Ar-C), 131.6 (Ar-C), 129.3 (Ar-C), 128.7 (Ar-C), 127.9 (Ar-C), 119.4 (C-10), 113.9 (Ar-C), 72.6 (C-7), 55.3 (C-24), 53.0 (C-17), 46.6 (C-9), 42.6 (C-8), 25.7 (C-13,14,15), 18.0 (C-16), -4.7 (C-12), -5.2 (C-11).
200	2924 (C-H), 2213 (CN)	**^{1}H NMR (400 MHz, $CDCl_3$)** δ 7.69 (2H, d, *J*=8.7 Hz, Ar-H), 7.40 (2H, d, *J*=8.6 Hz, Ar-H), 7.25 – 7.19 (2H, m, Ar-H), 7.03 (1H, s, H-7), 6.90 – 6.87 (2H, m, Ar-H), 3.80 (3H, s, H-18), 3.78 (2H, s, H-11), 3.56 (2H, s, H-9), 2.02 (1H, s, N-H). **^{13}C NMR (101 MHz, $CDCl_3$)** δ 158.9 (Ar-C), 142.6 (C-7), 136.2 (Ar-C), 131.4 (Ar-C), 130.0 (Ar-C), 129.4 (Ar-C), 129.3 (Ar-C), 129.2 (Ar-C), 114.1 (C-10), 113.9 (Ar-C), 111.1 (C-8), 55.3 (C-18), 52.5 (C-9), 51.7 (C-11).

A yield of 91% was obtained, which is a very good yield. For the conjugate addition reaction, the products were verified using IR and NMR spectroscopy (**Table 29**). For both products, the IR spectrum shows the presence of all the important stretches, such as the nitrile at around 2200 cm^{-1} and the C-H stretch at around 2900 cm^{-1}, as well as the Si-O stretch at 835 cm^{-1} for the conjugate addition product.

For the conjugate addition product **199**, the ^{1}H NMR spectrum showed all the expected signals, such as the aromatic signals in the aromatic region between 6.80-7.34 ppm integrating for 8 protons. The H-7 signal was observed at around 4.88 ppm integrating for 1 proton, appearing as a doublet through coupling to the H-8 proton as shown in the COSY spectrum. The next signal at around 3.81 pm belongs to the methoxy group (H-24), appearing as a singlet. H-24 showed a cross-peak to the carbon signal at 55.3 ppm in the HSQC spectrum. The DEPT spectrum also confirmed that the signal appeared as a positive signal. The next peak around 3.72 ppm belongs to H-17 as it integrates for 2 protons, and is attached to a carbon appearing at 53.0 ppm in the HSQC spectrum. In addition, the signal appeared as a negative peak in the DEPT spectrum.

The signal at 2.89 ppm belongs to both H-8 and H-9, as it integrates for three protons. The corresponding carbon peaks for both H-8 and H-9 in the HSQC spectrum were found at 42.6 and 46.6 ppm, respectively. These were also verified by the DEPT spectrum, as the peak at 46.6 ppm was found in the negative region which means that it belongs to a CH_2, whereas the peak at 42.6 ppm was positive and belongs to a CH. The next peak around 2.21 ppm belongs to N-H as it does not couple to any carbon peak in the HSQC spectrum, and the rest of the peaks belong to the TBDMS protons. The nitrile carbon peak appeared in its typical region around 119 ppm, and the DEPT spectrum showed the absence of this peak, which confirms that it belongs to a quaternary carbon such as the nitrile carbon. For compound **199**, the value obtained from the mass spectrum corresponded very well with the expected mass. Calculated [$M+H^+$]: 445.2126, found: 445.2101.

The allylic substitution product **200** was also obtained from this reaction. The ^1H NMR spectrum showed signals such as the aromatic proton signals at 7.19-7.69 ppm, the H-7 proton signal at 7.03 ppm. The methoxy proton signal was found at around 3.80 ppm appearing as a singlet. The HSQC spectrum showed the corresponding carbon peak at 55.3 ppm, which appeared as a positive peak in the DEPT spectrum. The next two peaks at 3.78 and 3.56 ppm belonged to the H-11 and H-9 protons, respectively. Their corresponding carbon peaks were determined by the HSQC spectrum at 51.7 and 52.5 ppm and they appeared as negative peaks in the DEPT spectrum.

The peak in the shielded region at 2.02 ppm belongs to N-H as it integrated for 1 proton and did not show any coupling in any 2D spectra. The nitrile carbon peak also appeared in its typical region at 114 ppm. The peak at 111.1 ppm belongs to the C-8 carbon as it did not appear in the DEPT spectrum and showed coupling to the H-9 protons in the long-range HMBC experiment.

Table 30: Overall summary of the nucleophilic addition reaction using 4-methoxy benzylamine nucleophile.

Compound no.	**Type of adduct (Ester or nitrile)**	**Protecting group (TBDMS/TMS)**	**Allylic substitution or not**	**Both or single diastereomers and diastereomeric ratios**
198	Ester	TBDMS	NO	Single

199	Nitrile		YES	

Allylic substitution product was obtained for the TBDMS protected nitrile adduct **199**, whereas no allylic substitution product formed for the ester adduct **198** protected with the same protecting group (**Table 30**). The protecting group determines whether the allylic substitution reaction occurs or not, as the protecting group which acts as a good leaving group will give a substitution product. Both adducts have the same protecting group, there is no clear reason for the formation of the allylic substitution product for compound **199** and not for compound **198**.

TBDMS protected ester and nitrile compounds **198** and **199** gave a single diastereomer (**Table 30**). This might be due to the heavy dominance of one diastereomer over the other making the other diastereomer invisible. This is due to the presence of the bulky TBDMS protecting group which controls the diastereoselectivity by blocking one side of the plane of the double bond.

3.1.3.1.4. Aniline nucleophile

The next addition reaction was done on the TBDMS protected ester **160** adduct using aniline. This addition reaction gave the desired product **201**, however in a very low yield of 11%. Aniline was added using the same method as the other nitrogen nucleophiles; however, very low yields were obtained as aniline is a very poor nucleophile. This is due to the resonance of the lone pair on the nitrogen, where this electron density is donated to the aromatic ring, which decreases its availability for a nucleophilic attack.[87] The product was obtained as a brown solid, with single diastereomer being observed.

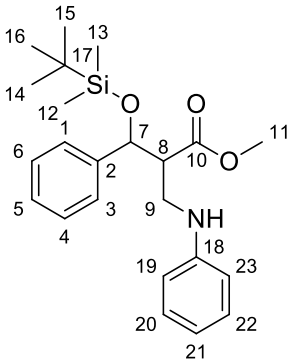

201

Figure 32: Conjugate addition reaction of aniline nucleophile on the TBDMS protected ester adduct to form product **201**.

Table 31: The IR and the NMR data for compound **201**

Compound No.	**IR** (neat, cm^{-1})	**NMR**
201	2955 (C-H), 1735 (C=O), 835 (Si-O)	**^{1}H NMR (400 MHz, $CDCl_3$)** δ 7.38 – 7.29 (5H, m, H-1,3,4,5,6), 7.10 – 7.03 (2H, m, H-20,22), 6.67 – 6.61 (1H, m, H-21), 6.34 (2H, d, *J* = 8.0 Hz, H-19,23), 5.15 (1H, d, *J* = 5.7 Hz, H-7), 3.99 (1H, s, N-H), 3.73 – 3.66 (1H, m, H-9a), 3.56 (3H, s, H-11), 3.48 – 3.41 (1H, m, H-9b), 2.93 (1H, s, H-8), 0.91 (9H, s, H-14,15,16), 0.03 (3H, s, H-12), -0.19 (3H, s, H-13). **^{13}C NMR (101 MHz, $CDCl_3$)** δ 173.1 (C-10), 147.6 (C-18), 142.4 (C-2), 129.2 (20,22), 128.2 (C-4,6), 127.7 (C-5), 126.2 (C-1,3), 117.2 (C-21), 112.7 (C-19,23), 74.7 (C-7), 53.8 (C-8), 51.7 (C-11), 41.0 (C-9), 25.8 (C-14,15,16), 18.1 (C-17), -4.6 (C-12), -5.4 (C-13).

The identity of product **201** (**Figure 32**) was confirmed using IR and NMR spectroscopy (**Table 31**). The IR spectrum showed all the important stretches, such as the carbonyl stretch at 1735 cm^{-1}. The proton NMR spectrum showed 10 aromatic protons in the aromatic region between 6.34-7.38 ppm. The H-7 signal was found at 5.15 ppm. The H-7 signal appeared in its typical region as seen from all the addition products. The signal appeared as a doublet coupling to the neighbouring H-8 proton, this coupling being evident from the COSY spectrum. The corresponding carbon peak was determined using the HSQC spectrum and was found at 74.7 ppm. The peak at 3.99 ppm belongs to the NH proton.

The next peak at 3.68 ppm belongs to one of the H-9 protons and the other H-9 proton was found at 3.44 ppm. The two peaks combined gave an integration of two and their carbon peak was found at 41.0 ppm, as seen from the HSQC spectrum. The peak at 3.56 ppm belongs to the H-11 protons as it integrates for 3 protons and showed coupling to the carbonyl carbon at173.1 ppm in the

HMBC spectrum. The C-11 peak was found at 51.7 ppm from the HSQC spectrum. The peak at 2.93 ppm belongs to the H-8 proton, integrating for 1 proton. This signal showed coupling to H-7 as seen from the COSY spectrum. The C-8 peak was found at 53.8 ppm, as shown in the HSQC spectrum. The rest of the proton peaks belong to the TBDMS protons found in the shielded region between -0.19-0.91 ppm and the TBDMS carbon peaks were assigned using the HSQC spectrum. For compound **201,** the value obtained from the mass spectrum corresponded well with the expected mass. Calculated [$M+H^+$]: 400.2302, found: 400.2238.

Table 32: Overall summary of the nucleophilic addition reaction using aniline nucleophile.

Compound no.	**Type of adduct (Ester or nitrile)**	**Protecting group (TBDMS/TMS)**	**Allylic substitution or not**	**Both or single diastereomers and diastereomeric ratios**
201	Ester	TBDMS	NO	Single

Allylic substitution product was not obtained from the conjugate addition reaction of aniline to form compound **201** (**Table 32**). This might be due to the presence of the bulky TBDMS group, which is a poor leaving group. A single diastereomer was observed, this might be due to the heavy dominance of one diastereomer over the other due to the presence of the bulky TBDMS group, which blocks one side of the plane of the double bond, allowing the aniline nucleophile to approach only from one side, increasing the possibility for the formation of one diastereomer over the other.

3.1.3.1.5. 4-methoxyaniline nucleophile

After the low yield obtained when using aniline in a conjugate addition reaction, a more nucleophilic aniline derivative, *p*-anisidine was tested. The reaction was initially performed under normal conditions shown in scheme 55, however the reaction was sluggish and gave very low yields. A different method was also applied to get a better addition reaction. *p*-Anisidines are more nucleophilic than aniline; this is due to the presence of the methoxy group which acts as an electron donating group, increasing the electron density of the benzene ring, and making the lone pairs on nitrogen more readily available.[88]

p-Anisidine was added to the ester adduct **162** in dichloromethane using triethylamine as a catalyst, in the presence of $ZnCl_2$, and the product **202a/b** (**Scheme 56**) was purified using column chromatography. The method reported by Yamazaki *et al.* was applied with a few alterations such as using triethylamine along with $ZnCl_2$.[89] This gave the product; however, it did not improve the yield, which was 12%. The product was obtained as a mixture of diastereomers.

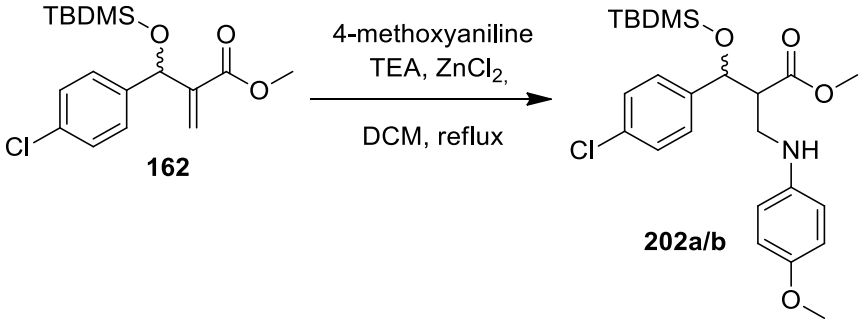

Scheme 56: The conjugate addition reaction on the TBDMS protected ester adduct **162** using 4-methoxyaniline as the nucleophile to form product **202a/b**.

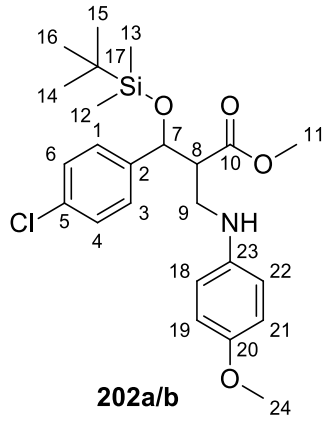

Figure 33: Conjugate addition reaction of 4-methoxyaniline nucleophile on the TBDMS protected ester adduct **162** to form **202a/b**.

The expected product **202a/b** was obtained, which was confirmed using IR and NMR spectroscopy (**Table 33** and **34**).

Table 33: The approximate chemical shift values and integrations obtained from the proton NMR spectrum for both the major and minor diastereomer **202a/b**

Major and Minor diastereomer combined (**202a/b**)

Assignment	**Approximate chemical shift values (ppm)**	**Combining partial integrations**	**Overall integration**
Ar-H	7.4-6.34	2H + 2H + 2H + 2H	8H
H-7	5	0.67H + 0.27H	1H
H-9	3.8	0.05H + 0.11H + 0.30H + 0.66H + 0.7H + 0.20H + 0.44H	2H
H-24	3.73	3H	3H
H-11	3.72	1H + 2H	3H
H-8	2.9	0.44H + 0.21H	1H
H-14,15,16	0.8	6H + 3H	9H
H-12	0.03	2H + 1H	3H
H-13	-0.2	2H + 1H	3H

Table 34: The carbon NMR data for both the major and minor diastereomer **202a/b**

Assignment	Major diastereomer	**Assignment**	Minor diastereomer
C-10	173.0	**C-10'**	173.8
Ar-C	152.1	**Ar-C'**	152.3
Ar-C	141.70	**Ar-C'**	141.67
Ar-C	141.1	**Ar-C'**	140.4
Ar-C	133.4	**Ar-C'**	133.8
Ar-C	128.4	**Ar-C'**	128.6
Ar-C	127.7	**Ar-C'**	128.1
Ar-C	114.9	**Ar-C'**	114.8
C-7	74.1	**C-7'**	74.3
C-24	55.8	**C-24'**	55.8
C-8	53.9	**C-8'**	54.2
C-11	51.7	**C-11'**	51.9

C-9	42.3	**C-9'**	43.2
C-14,15,16	25.7	**C-14',15',16'**	25.6
C-17	18.1	**C-17'**	17.9
C-12	-4.59	**C-12'**	-4.63
C-13	-5.3	**C-13'**	-5.4

The IR spectrum showed all the important signals such as the N-H signal at 3665 cm^{-1}, the carbonyl signal at 1732 cm^{-1}, as well as the C-O signal at 1235 cm^{-1}.

The ^{1}H NMR spectrum also showed the formation of the desired product **202a/b**. It showed all 8 protons belonging to the aromatic ring in the aromatic region between 6.34-7.34 ppm, appearing as multiplets coupling to each other. All the signals were integrated using the H-7 signals as the integration reference signal, for 1 proton. All the signals were assigned using the HSQC spectrum. H-7 signals appear as doublet coupling to H-8 proton as shown in the COSY spectrum. H-7 coupled to the corresponding carbon peaks around 74 ppm for both the major and minor diastereomer from the HSQC spectrum.

Partial integrations of the signals belonging to H-9 were combined using the HSQC spectrum, and their corresponding carbon peaks were also determined from the HSQC spectrum. The coupling of H-9 signals showed their corresponding carbon peaks around 43.2 and 42.3 ppm. The signal at 3.73 ppm integrated for 3 protons and belongs to the methyl protons, H-24. This was also confirmed from the HMBC spectrum as it showed coupling to an aromatic carbon, which is only possible for the methoxy methyl protons and not the ester protons.

The next peak, also integrating for 3 protons at around 3.72 ppm belongs to the H-11 methyl ester protons, and the corresponding carbon peaks were found at around 51 ppm. These assignments were confirmed using the HMBC spectrum as it showed coupling to the carbonyl carbon of the ester group, which was only possible for H-11. H-8 was found around 2.93 ppm, as determined from the HSQC spectrum, and the corresponding carbon peaks were found at 54 ppm. The TBDMS proton signals were found in their typical shielded region between -0.25-0.89. The N-H peak was not visible and might have been obscured by the TBDMS peaks.

Table 35: Overall summary of the nucleophilic addition reaction using 4-methoxyaniline nucleophile.

Compound no.	**Type of adduct (Ester or nitrile)**	**Protecting group (TBDMS/TMS)**	**Allylic substitution or not**	**Both or single diastereomers and diastereomeric ratios**
202a/b	Ester	TBDMS	NO	Both (3:1)

Conjugate addition reaction of 4-methoxyaniline did not give the allylic substitution product, this is due to the presence of the TBDMS protecting group, which acts as a poor leaving group. Both diastereomers were obtained for compound **202a/b** in a ratio of 3:1 (**Table 35**). The compound **202a/b** is obtained with a good selectivity, due to the presence of the TBDMS group which increases the possibility of the formation of one diastereomer over the other by blocking one side of the plane of the double bond controlling the addition of the nucleophile and the incoming proton.

3.1.3.2. Conjugate addition reaction using sulfur nucleophiles.

The next type of compounds to be used in conjugate addition reactions were the thiols. Thiols are strong nucleophiles and good at conjugate addition reaction because the sulfur atoms are more polarisable.[90] The sulfur nucleophiles were added to both nitrile and the ester adducts **147** to synthesize **148** (**Scheme 57**). Different types of sulfur nucleophiles were used. The reaction was performed at room temperature in ethanol using triethylamine as a catalyst. The mixture was left for 1-2 days, and the product was purified using column chromatography. This method has been reported by Kita *et al.* on similar adducts. The method was followed as reported with minor alterations, such as the reactions were performed at room temperature and not at 5 ˚C.[91]

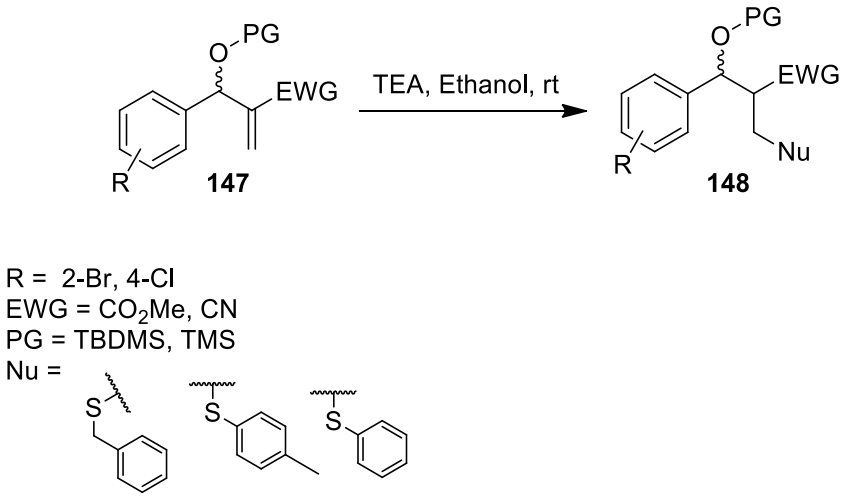

Scheme 57: The conjugate addition reaction on the TBDMS and TMS protected ester and nitrile adducts **147** using sulfur nucleophiles to synthesize **148**.

3.1.3.2.1. Benzyl mercaptan nucleophile

3.1.3.2.1.1. Addition of benzyl mercaptan to the TMS protected ester adduct.

The first reaction was done on the ester adduct **167** using benzylmercaptan to form compound **203a/b**. The product identity was verified using IR and NMR spectroscopy (**Table 36** and **37**).

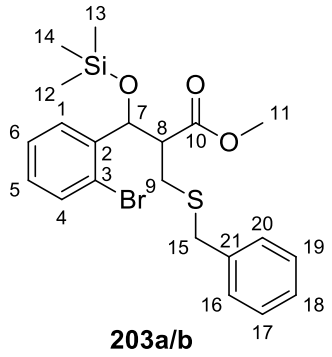

Figure 34: Conjugate addition reaction of benzyl mercaptan nucleophile on the TMS protected ester adduct to synthesize **203a/b**.

Table 36: The approximate chemical shift values and integrations obtained from the ^{1}H NMR spectrum for both the major and minor diastereomer of **203a/b**

Major and Minor diastereomer combined (**203a/b**)			
Assignment	**Approximate chemical shift values (ppm)**	**Combining partial integrations**	**Overall integration**
Ar-H	7.53-6.96	0.56H + 1.30H + 1.25H + 3.79H + 0.73H +1.18H	9H
H-7	5.3	0.54H + 0.36H	1H
H-11	3.7	0.95H + 1.74H	3H
H-15	3.5	0.70H + 0.70H + 0.70H	3H
H-8	2.9	0.59H + 0.42H	1H
H-9	2.7	0.63H + 0.42H + 0.61H + 0.38H	2H
H-12,13,14	-0.03	4.61H + 4.02H	9H

Table 37: The ^{13}C NMR data for both the major and minor diastereomer **203a/b**

Assignment	Major diastereomer	**Assignment**	Minor diastereomer
C-10	172.2	**C-10'**	172.8
Ar-C	140.8	**Ar-C'**	141.3
Ar-C	138.3	**Ar-C'**	137.7
Ar-C	132.8	**Ar-C'**	132.4
Ar-C	129.3	**Ar-C'**	129.18
Ar-C	129.15	**Ar-C'**	128.9
Ar-C	128.7	**Ar-C'**	128.8
Ar-C	128.37	**Ar-C'**	128.42
Ar-C	127.3	**Ar-C'**	127.8
Ar-C	126.7	**Ar-C'**	126.9

Ar-C	121.4	**Ar-C'**	122.5
C-7	73.9	**C-7'**	73.9
C-8	51.7	**C-8'**	55.1
C-11	51.9	**C-11'**	52.1
C-15	36.1	**C-15'**	35.7
C-9	26.5	**C-9'**	28.7
C-12,13,14	-0.3	**C-12',13',14'**	-0.2

The reaction between ester adduct and benzylmercaptan gave two diastereomers **203a/b** that were inseparable. The diastereomers were obtained in a 2:1 ratio, determined by comparing the signal height differences of the H-7 peaks in the ^{1}H NMR spectrum. Integrations for all the peaks were referenced against the H-7 proton peaks, which were found around 5 ppm. Partial integrations of the H-7 peaks were combined to make up 1 proton and integration of the rest of the peaks were referenced against this. Both H-7 peaks for the major and the minor diastereomer appeared as doublets, showing coupling to the neighbouring H-8 proton, as confirmed by the COSY spectrum which also showed where the H-8 proton peaks appeared. The corresponding C-7 carbon peaks were found around 73.9 ppm.

The next two peaks in the ^{1}H NMR spectrum around 3.7 ppm both belong to H-11, as the two partial integrations combined integrated for 3 protons and belonged to adjacent carbon peaks in the HSQC spectrum. These carbon peaks were found around 52 ppm and the assignment was also confirmed using the HMBC spectrum, which showed coupling to the carbonyl carbon peak at 172 around ppm. The next three peaks belonged to H-15, where the partial integrations combined to make up two protons. These three peaks appeared as doublets, showing coupling to each other. Their corresponding carbon peaks were found using the HSQC spectrum, around 36 ppm. This was also confirmed using DEPT spectra as they appeared in the negative region.

The H-9 proton peaks were found between 2.16-2.91 ppm, appearing as four separate peaks belonging to both the major and minor diastereomer. These peaks combined integrated for 2 protons. They all appeared as doublets of doublets, showing coupling to each other, as well as the neighbouring H-8 proton. Their corresponding carbon peaks were found around 28.7 and 26.5 ppm. These were also confirmed using the DEPT spectra as they appeared as negative signals,

showing that they belong to CH_2 protons. The rest of the peaks belonged to the TBDMS protons found in the shielded region between -0.04-(-0.03) ppm The rest of the carbon peaks were assigned using the HSQC spectrum and were confirmed using the DEPT spectrum. The most deshielded peaks at around 172 ppm in the ^{13}C spectrum belonged to the carbonyl carbons.

3.1.3.2.1.2. Addition of benzyl mercaptan to the TMS protected nitrile adduct 168.

The same nucleophile was also added to a TMS protected nitrile adduct **168** but unfortunately the TMS group was lost during the reaction or the purification of the product. TMS groups are very unstable and deprotection happens easily. This reaction also gave a mixture of diastereomers **204a/b** in a 1.4:1 ratio (**Figure 35**). The deprotected product **204a/b** was obtained as verified by IR and NMR spectroscopy (**Table 38** and **39**). The product **204a/b** was obtained in a yield of 95%, which is an excellent yield.

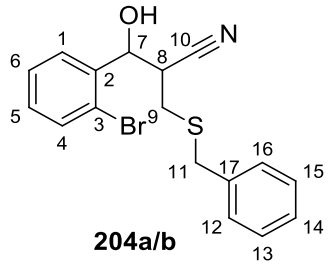

204a/b

Figure 35: Conjugate addition reaction of benzyl mercaptan nucleophile on the TMS protected nitrile adduct **168** to form **204a/b**.

Table 38: The approximate chemical shift values and integrations obtained from the ^1H NMR spectrum for both the major and minor diastereomer **204a/b**.

Major and Minor diastereomer combined (**204a/b**)			
Assignment	**Approximate chemical shift values (ppm)**	**Combining partial integrations**	**Overall integration**
Ar-H	7.74-7.10	0.39H + 1.52H + 0.45H + 7.17H	9H
H-7	5.4	0.55H + 0.40H	1H
H-11	3.8	0.78H + 1.07H	2H

H-8	3.2	0.49H + 0.34H	1H
H-9	2.8	0.69H + 0.48H + 0.54H	2H

Table 39: The ^{13}C NMR data for both the major and minor diastereomer **204a/b**.

Assignment	Major diastereomer	**Assignment**	Minor diastereomer
Ar-C	138.1	**Ar-C'**	139.1
Ar-C	137.3	**Ar-C'**	137.1
Ar-C	133.1	**Ar-C'**	132.7
Ar-C	130.2	**Ar-C'**	130.1
Ar-C	128.9	**Ar-C'**	129.1
Ar-C	128.7	**Ar-C'**	128.8
Ar-C	128.4	**Ar-C'**	128.17
Ar-C	127.9	**Ar-C'**	128.21
Ar-C	127.3	**Ar-C'**	127.5
Ar-C	121.2	**Ar-C'**	121.9
C-10	118.1	**C-10'**	119.6
C-7	71.9	**C-7'**	70.6
C-8	39.3	**C-8'**	39.2
C-11	36.3	**C-11'**	36.4
C-9	27.2	**C-9'**	30.6

The IR spectrum showed all the important signals, such as the nitrile signal around 2247 cm^{-1}. The NMR data also verified the formation of the product, showing all the expected signals. The aromatic signals were observed in the aromatic deshielded region between 7.10-7.74 ppm. All these aromatic signals showed coupling to each other. H-7 was found around 5.42 and 5.36 ppm, integrating for a single proton and appearing as doublets, coupling to the H-8 proton. Like the other diastereomers, the peaks were integrated using H-7 as the reference for integration. Peaks at 3.85 and 3.73 ppm belong to H-11, as the integrations combined to make up 2 protons, which was

also confirmed using the HSQC spectrum. This spectrum also showed the corresponding carbon peak around 36.4 and 36.3 ppm for both the major and minor diastereomer.

The next two peaks in the ^{1}H NMR spectrum were at 3.25 and 3.13 ppm and belong to the H-8 proton, as both proton peaks showed coupling to adjacent carbons in the HSQC spectrum, and they also integrate for 1 proton. The corresponding carbon peaks were found around 39 ppm. The last three peaks in the shielded region between 2.48-3.00 ppm belonged to H-9 protons, as they make up for 2 protons and show coupling to adjacent carbon peaks on the HSQC spectrum, implying that they belong to both major and the minor diastereomer. The peaks appeared as multiplets and doublets of doublets, showing coupling to each other, as well as the H-8 proton. The carbon peaks that this signal coupled to was found around 30.6 and 27.2 ppm in the HSQC spectrum. All the carbon assignments were confirmed using the DEPT spectra. The nitrile peak was also found in its typical region, around 119 ppm.

Table 40: Overall summary of the nucleophilic addition reaction using Benzyl mercaptan nucleophile.

Compound no.	**Type of adduct (Ester or nitrile)**	**Protecting group (TBDMS/TMS)**	**Allylic substitution or not**	**Both or single diastereomers and diastereomeric ratios**
203a/b	Ester	TMS	NO	Both (2:1)
204a/b	Nitrile			Both (1.4:1)

The addition of benzyl mercaptan nucleophile on both ester and nitrile adduct did not give the allylic substitution product, even though TMS is present, which is a good leaving group. Both diastereomers were observed for compounds **203a/b** and **204a/b** in a ratio of 2:1 and 1.4:1 (**Table 40**). The ratio shows less selectivity, this is due to the presence of the TMS group, which is not bulky enough to block the plane of the double bond and control the addition of the nucleophile and the incoming proton forming both diastereomers in almost equal ratios. TMS group was used, to compare the diastereomeric ratios obtained with that of the bulky TBDMS group.

3.1.3.2.2. 4-Methylbenzenethiol nucleophile

The next type of sulfur nucleophile that was added was 4-methylbenzenethiol on both ester and nitrile TMS protected adducts.

3.1.3.2.2.1.Addition of 4-methylbenzenethiol to the TMS protected ester adduct 166.

4-Methylbenzenethiol was added to the ester adduct **166** to form compound **205a/b** (**Figure 36**). The product was obtained as a mixture of diastereomers in a 2:1 ratio. The addition on ester adduct was successful and gave the desired product **205a/b** as confirmed by IR and NMR spectroscopy (**Table 41** and **42**).

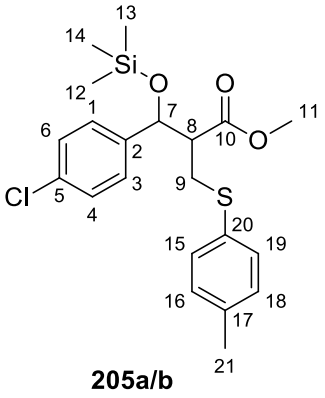

205a/b

Figure 36: Conjugate addition reaction of 4-methylbenzenethiol nucleophile to the TMS protected ester adduct **166** to form **205a/b**.

Table 41: The approximate chemical shift values and integrations obtained from the ^{1}H NMR spectrum for both the major and minor diastereomer **205a/b**.

Major and Minor diastereomer combined			
Assignment	**Approximate chemical shift values (ppm)**	**Combining partial integrations**	**Overall integration**
Ar-H	7.30-7.00	1.05H + 0.69H + 1.08H + 0.76H + 3.67H	8H
H-7	4.8	0.55H + 0.34H	1H
H-11	3.7	1.08H + 1.63H	3H

H-8	2.9	0.25H + 0.55H	1H
H-9	3.2	0.44H + 0.56H + 0.23H + 0.25H + 0.34H	2H
H-21	2.3	3H	3H
H-12,13,14	0.01	5.77H + 3.31H	9H

Table 42: The ^{13}C NMR data for both the major and minor diastereomer **205a/b**.

Assignment	**Major diastereomer**	**Assignment**	**Minor diastereomer**
C-10	172.3	**C-10'**	173.1
Ar-C	140.7	**Ar-C'**	140.1
Ar-C	136.2	**Ar-C'**	136.7
Ar-C	133.4	**Ar-C'**	133.8
Ar-C	131.7	**Ar-C'**	131.1
Ar-C	129.9	**Ar-C'**	130.7
Ar-C	129.6	**Ar-C'**	129.7
Ar-C	128.4	**Ar-C'**	128.6
Ar-C	127.6	**Ar-C'**	128.1
C-7	74.8	**C-7'**	75.3
C-8	55.3	**C-8'**	54.8
C-11	51.71	**C-11'**	51.74
C-9	31.6	**C-9'**	32.6
C-21	20.99	**C-21'**	21.02
C-12,13,14	-0.1	**C-12',13',14'**	-0.1

The diastereomer **205a/b** was obtained in a yield of 63%. The IR spectrum showed the carbonyl signal around 1730 cm^{-1}. The ^{1}H NMR spectrum also showed all the expected signals, such as the aromatic signals in the aromatic region between 7.00-7.30 ppm, where all the partially integrating signals appeared as multiplets coupling to each other. The next two ^{1}H NMR signals around 4.90 and 4.78 ppm belonged to the H-7 proton, with both appearing as doublets, coupling to the adjacent

H-8 proton, also shown in the COSY spectrum. The corresponding carbon peaks for the H-7 proton, were found around 75 ppm as shown from the HSQC spectrum. The next two peaks belonged to H-11, similar to the benzyl mercaptan proton assignments. This was confirmed by integration as well as the HSQC spectrum, which showed their coupling to adjacent carbon peaks, showing that they belong to the same proton on the major and the minor diastereomer. It was also confirmed from the HMBC spectrum as it showed coupling to the carbonyl carbon at around 172 ppm. The corresponding carbon peaks from the HSQC spectrum were around 52 ppm.

The peaks around 3.18, 3.16, 2.89, 2.84, and 2,65 ppm belong to H-9 protons, as combining all these peak integrations gives two protons, and all the signals also showed coupling to two neighbouring carbon peaks in the HSQC spectrum. The corresponding carbon peaks were found around 32 ppm. The H-8 peaks were found around 2.87 and 2.81 ppm, and these peaks together make up for 1 proton and show coupling to H-7 in the COSY spectrum. The corresponding carbon peaks were found around 50 ppm in the HSQC spectrum. The peak around 2.30 ppm integrated for 3 protons and belongs to the H-21 protons, as it showed coupling to the aromatic protons in the HMBC spectrum. The corresponding carbon peaks in the HSQC spectrum were found at around 21 ppm for both the major and the minor diastereomer. The rest of the peaks in the shielded region between -0.05-0.01 belong to the TBDMS protons and their corresponding carbon peaks were found using the HSQC spectrum.

3.1.3.2.2.2. Addition of 4-methylbenzenethiol to the TMS protected nitrile adduct 170.

The nucleophilic addition reaction using 4-methylbenzenethiol on the TMS protected nitrile adduct **170** gave the conjugate addition product **206a/b** (**Figure 37**). However, the TMS group was lost during the reaction or purification giving the deprotected product. The addition reaction was successful giving a mixture of two diastereomers, as confirmed using IR and NMR spectroscopy (**Table 43** and **44**). Product **206a/b** was obtained in a yield of 70%, which is a good yield.

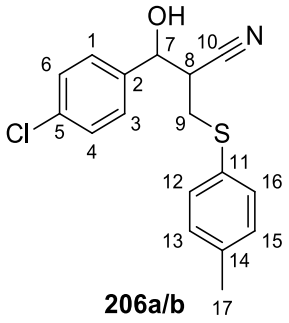

206a/b

Figure 37: Conjugate addition reaction of 4-methylbenzenethiol nucleophile on the nitrile adduct **170** to form **206a/b**.

Table 43: The approximate chemical shift values and integrations obtained from the ^{1}H NMR spectrum for both the major and minor diastereomer **206a/b**.

Major and Minor diastereomer combined (**206a/b**)			
Assignment	**The approximate chemical shift values (ppm)**	**Combining partial integrations**	**Overall integration**
Ar-H	7.34-7.02	6H + 2H	8H
H-7	5	0.29H + 0.64H	1H
H-8	3	0.80H + 0.31H	1H
H-9	2.9	2H	2H
H-17	2.27	2.93H	3H

Table 44: The ^{13}C NMR data for both the major and minor diastereomer **206a/b**.

Assignment	Major diastereomer	**Assignment**	Minor diastereomer
Ar-C	138.1	**Ar-C'**	138.1
Ar-C	137.7	**Ar-C'**	137.7
Ar-C	135.0	**Ar-C'**	135.0
Ar-C	131.9	**Ar-C'**	131.8
Ar-C	130.4	**Ar-C'**	130.3
Ar-C	129.9	**Ar-C'**	129.9

Ar-C	129.13	**Ar-C'**	129.10
Ar-C	127.9	**Ar-C'**	127.4
C-10	118.8	**C-10'**	118.8
C-7	72.2	**C-7'**	71.0
C-8	40.8	**C-8'**	41.2
C-9	33.2	**C-9'**	31.0
C-17	21.2	**C-17'**	21.2

The IR spectrum showed all the typical signals belonging to the functional groups present in the compound, such as the nitrile and the alcohol group at 2256 and 3388 cm^{-1}, respectively.

The ^{1}H NMR also verified the formation of the product, showing all the expected signals, such as the aromatic signals in the aromatic region between 7.02-7.34 ppm, integrating for 8 protons. Like the other diastereomers, the integration was referenced against H-7. The H-7 peaks were found at 5.03 and 4.95 ppm, belonging to both diastereomers. Both H-7 peaks appeared as doublets, coupling to the neighbouring H-8 protons, which was also shown in the COSY spectrum. The carbon peak coupling to the H-7 proton was found at around 72 ppm in the HSQC spectrum.

The H-8 proton was divided into two peaks at 3.08 and 2.77 ppm and combining the two peaks gave the integration of 1 proton. The corresponding carbon peaks were found at 41 ppm. The H-9 peak was found at 2.96 ppm, and its corresponding carbon peaks in the HSQC spectrum were found at 33 and 31 ppm. The last peak in the shielded region at 2.27 ppm belong to the methyl protons, H-17. The corresponding carbons peaks were found at 21 ppm. All these carbon assignments were confirmed using the DEPT spectrum, which showed the positive and negative signals. The C-9 signal belonged to a CH_2, hence appeared in the negative region; all the other peaks were in the positive region as they belonged to a CH or a CH_3.

Table 45: Overall summary of the nucleophilic addition reaction using 4-methylbenzenethiol nucleophile.

Compound no.	**Type of adduct (Ester or nitrile)**	**Protecting group (TBDMS/TMS)**	**Allylic substitution or not**	**Both or single diastereomers and**

				diastereomeric ratios
205a/b	Ester	TMS	NO	Both (2:1)
206a/b	Nitrile			Both (2:1)

Allylic substitution products are not obtained for conjugate addition reactions using 4-methylbenzenethiol to form compounds **205a/b** and **206a/b** (**Table 45**). Allylic substitution would normally be expected due to the presence of the TMS group, which is a good leaving group. Both compounds were obtained in a 2:1 ratio of major:minor diastereomer. The diastereoselectivity is not good, due to the presence of the TMS group, which is not bulky enough to control the addition of the nucleophile.

3.1.3.2.3. Benzenethiol nucleophile

The next addition was the addition of benzenethiol to the TBDMS protected nitrile adduct **165** to give product **207a/b** (**Figure 38**) as a mixture of diastereomers. The diastereomers were obtained in a yield of 67%. The identity of the diastereomers was confirmed using IR and NMR spectroscopy (**Table 46** and **47**).

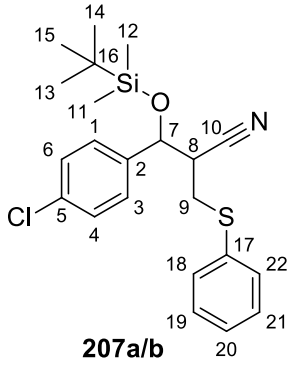

207a/b

Figure 38: Conjugate addition reaction of benzenethiol nucleophile on the TBDMS protected adduct **165** to form **207a/b**.

Table 46: The approximate chemical shift values and integrations obtained from the ^{1}H NMR spectrum for both the major and minor diastereomer **207a/b**

Major and Minor diastereomer combined (**207a/b**)

Assignment	**Approximate chemical shift values (ppm)**	**Combining partial integrations**	**Overall integration**
Ar-H	7.52-7.20	1H + 1H + 7H	9H
H-7	4.9	0.31H + 0.67H	1H
H-9	3.2	0.34H + 1.61H	2H
H-8	2.9	0.73H + 0.30H	1H
H-13,14,15	0.9	2.97H + 5.78H	9H
H-11	0.08	2.83H	3H
H-12	-0.15	1.80H + 1.07H	3H

Table 47: The ^{13}C NMR data for both the major and minor diastereomer **207a/b**

Assignment	Major diastereomer	**Assignment**	Minor diastereomer
Ar-C	137.0	**Ar-C'**	138.3
Ar-C	133.7	**Ar-C'**	134.5
Ar-C	130.5	**Ar-C'**	131.0
Ar-C	129.3	**Ar-C'**	129.4
Ar-C	129.1	**Ar-C'**	128.8
Ar-C	127.9	**Ar-C'**	127.7
Ar-C	127.5	**Ar-C'**	127.3
Ar-C	127.2	**Ar-C'**	127.2
C-10	118.9	**C-10'**	118.9
C-7	73.0	**C-7'**	72.0
C-8	41.9	**C-8'**	42.3
C-9	32.0	**C-9'**	33.3
C-13,14,15	25.7	**C-13',14',15'**	25.7
C-16	18.1	**C-16'**	18.1
C-12	-4.7	**C-12'**	-4.6
C-11	-5.2	**C-11'**	-5.1

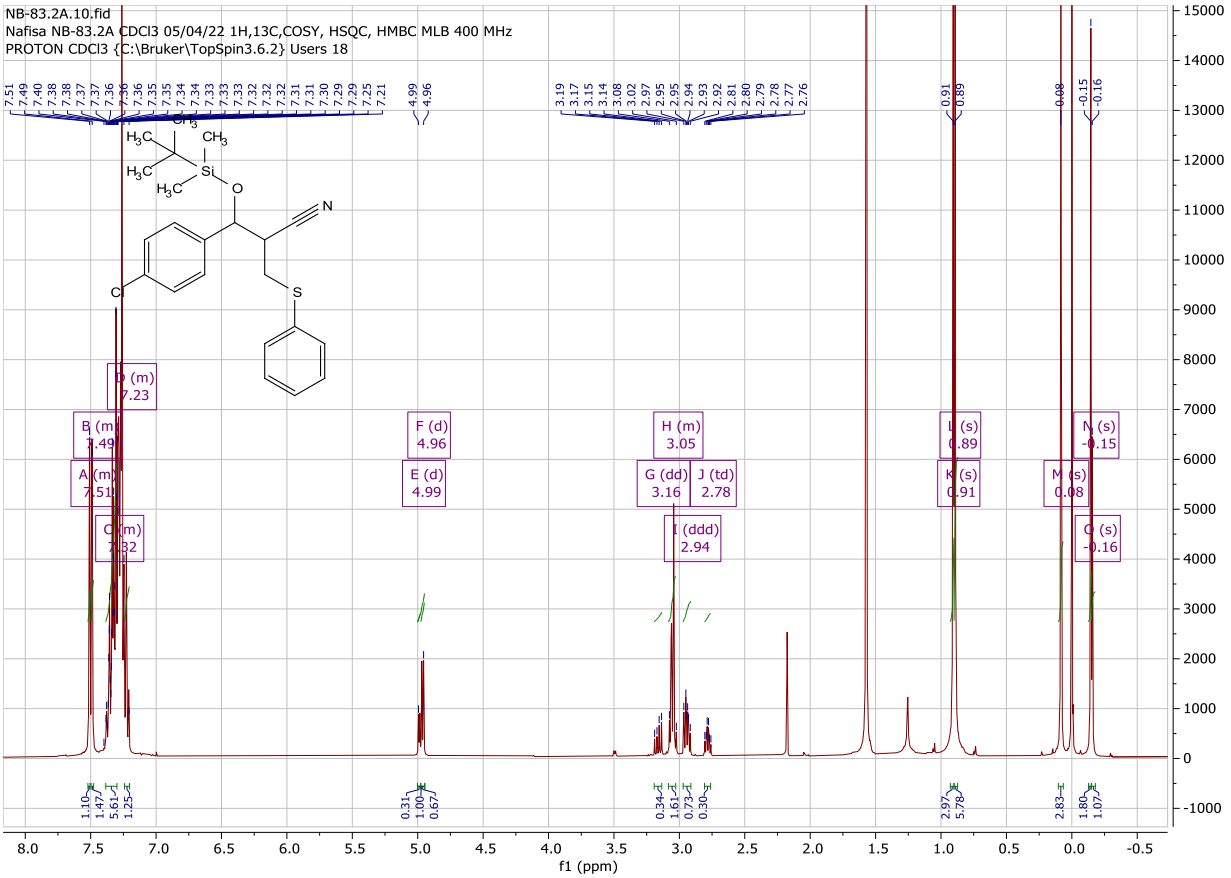

Figure 39: The ^{1}H NMR spectrum of compound **207a/b**.

The IR spectrum showed all the important stretches, such as the nitrile stretch at 2240 cm^{-1} and the Si-O stretch at 838 cm^{-1}. The NMR spectra also showed the formation of the product. The ^{1}H NMR spectrum shown in figure 39 showed all the expected aromatic signals in the aromatic region between 7.20-7.52 ppm. It also showed the H-7 signals integrating for 1 proton, with both H-7 signals for the major and minor diastereomer appearing as doublets, coupling to the H-8 proton as shown in the COSY spectrum. The next two peaks belong to the H-9 protons; they integrated for 2 protons and showed coupling to adjacent carbon peaks in the HSQC spectrum. These signals appeared as a doublet of doublets and a multiplet, coupling to each other and the adjacent H-8 proton. The corresponding C-9 peaks in the HSQC spectrum were found around 32 ppm, and they appeared as negative signals in the DEPT spectrum.

The next two peaks belong to H-8 proton, appearing as a doublet of doublet of doublets and a triplet of doublets, coupling to the neighbouring H-9 and H-7 protons. These peaks were attached to the carbon at 42 ppm in the HSQC, which appeared in the positive region in the DEPT spectrum,

confirming that these peaks belong to the H-8 proton. The rest of the peaks in the shielded region between -0.16-0.91 belong to the TBDMS protons. All the carbon peaks were assigned using the HSQC spectrum and confirmed using the DEPT spectrum.

Table 48: Overall summary of the nucleophilic addition reaction using benzenethiol nucleophile.

Compound no.	**Type of adduct (Ester or nitrile)**	**Protecting group (TBDMS/TMS)**	**Allylic substitution or not**	**Both or single diastereomers and diastereomeric ratios**
207a/b	Nitrile	TBDMS	NO	Both (2:1)

Allylic substitution product was not obtained, because the TBDMS is not a good leaving group, preventing the occurrence of the allylic substitution product by the elimination of the OTBDMS group. Both diastereomers were obtained in a 2:1 ratio. The TBDMS group controls the diastereoselectivity, by blocking one side of plane of the double bond due to its bulkiness. However, less selectivity was observed which was unexpected.

Overall summary of the conjugate addition reactions using different nucleophiles.

The conjugate addition reactions were successful, and the desired products were obtained. Some of the conjugate addition products were observed as a mixture of diastereomers, and some as single diastereomer. The formation of only a single diastereomer is due to the heavy dominance of one diastereomer over the other, making the other diastereomer undetectable, or the loss of the other diastereomer during the addition reaction or purification.

The heavy dominance of one diastereomer occurs as a result of the bulky protecting groups present. From the literature it has been proven that the use of bulky protecting groups has a great effect on the diastereoselectivity of the reaction, since it directs the addition of nucleophiles as well as the approach of the incoming proton by blocking one side of the plane of the double bond increasing the possibility of the formation of one diastereomer over the other.

The downside of the addition reaction was the side reaction occurring. Allylic substitution reaction occurred as a side reaction giving the allylic substitution product. These byproducts were obtained as minor products, usually in a 1:2 ratio of allylic substitution: addition product. The allylic substitution reaction occurs as a result of the presence of a good leaving group, which would normally be expected for the TMS group and not the TBDMS protecting group. The TMS group is a good leaving group, hence, it would be removed easily giving the allylic substitution product.

Table 49 shows the different nitrogen nucleophiles used in the conjugate addition reaction on different MBH adducts, the type of products obtained from the reaction, as well as the diastereomeric ratios obtained. The protecting group acts as a leaving group during the allylic substitution reaction, hence, the type of protecting group present affect whether the allylic substitution reaction occurs or not. We would expect the adducts with TMS protecting group to give the allylic substitution product, since the TMS group is a good leaving group, compared to the TBDMS protecting group. However, from the results presented in table 49, the formation of the allylic substitution product is shown to be independent of the type of protecting group present, since both groups (TBDMS and TMS) gave the allylic substitution product. Table 49 also shows that the unprotected adduct does not give the allylic substitution product, this is due to the presence of the hydroxyl group, which is a poor leaving group.

Piperidine nucleophile gave the allylic substitution product for both ester and nitrile adducts protected with either TBDMS or TMS protecting group. Benzylamine additions gave the allylic substitution products even though TBDMS is not a good leaving group. 4-methoxybenzylamine addition on the TBDMS protected adducts gave the allylic substitution product for the nitrile adduct and not for the ester adduct. No allylic substitution products were obtained for the aniline and the 4-methoxyaniline addition.

Whether single or both diastereomers are obtained and the ratio in which they were obtained is independent of the type of nucleophile used, since there is no specific trend observed from the table 49. As stated above, the presence of the protecting group controls the diastereoselectivity of the addition reaction, hence, the size of the protecting group (TBDMS or TMS) might also affect the diastereomeric ratio. TBDMS group would control the diastereoselectivity better than the TMS group, due to its bulkiness by directing the addition of the nucleophile. However, from the results obtained there is no such trend observed. As both TBDMS and TMS protecting group gave both

diastereomers as well as single diastereomer and there is no trend observed in the diastereomeric ratios.

All the ester piperidine adducts protected with three different groups gave a single diastereomer showing no relation to the protecting group present. All the other adducts protected with TBDMS group gave either both or single diastereomers with different diastereomeric ratios showing no relation to the TBDMS protecting group. Benzylamine nucleophile gave both diastereomers.

Table 49: Overall summary of the conjugate addition reaction using different nitrogen nucleophiles on different protected adducts and whether diastereomers and allylic substitution product were obtained or not and the diastereomeric ratios obtained from the reaction.

Comp-ound no.	**Nitrogen nucleophile**	**Type of adduct: ester/nitrile**	**Alcohol protection**	**Allylic substitution or not**	**Single or both diastereomers Observed**	**Diastereomer ratio (major :minor)**
186	Piperidine	Ester	TMS	YES	Single	-
189			TBDMS	NO	Single	-
190			-	NO	Single	-
191a/b		Nitrile	TMS	NO	Both	2:1
192a/b			TBDMS	YES	Both	3:1
194a/b	Benzylamine	Ester	TBDMS	YES	Both	2:1
196a/b		Nitrile		YES	Both	3:1
198	4-methoxy benzylamine	Ester		NO	Single	-
199		Nitrile		YES	Single	-
201	Aniline	Ester		NO	Single	-
202a/b	4-Methoxy Aniline	Ester	TBDMS	NO	Both	3:1

Table 50 shows the different types of sulfur nucleophiles used and the results obtained from the conjugate addition reaction. It shows that allylic substitution reaction does not occur at all when using sulfur nucleophiles as compared to nitrogen nucleophiles, which gave the allylic substitution products. Mixture of diastereomers were obtained for all the sulfur nucleophiles and most of them

in a 2:1 major: minor diastereomer ratio. It also shows that the type of protecting group whether bulky or not (TBDMS and TMS) has no direct effect on the diastereomeric ratio. The results show that the type of sulfur nucleophile used has no effect on the diastereoselectivity.

Table 50: Overall summary of the conjugate addition reaction using different sulfur nucleophiles on different protected adducts and whether diasteromers and allylic substitution product were obtained or not from these reactions and the diastereomeric ratios obtained.

Comp-ound no.	**Sulfur nucleophile**	**Type of adduct: ester/nitrile**	**Alcohol protection**	**Allylic substitution or not**	**Single or both diastereomers Observed**	**Diastereomer ratio (major :minor)**
203a/b	Benzyl mercaptan	Ester	TMS	NO	Both	2:1
204a/b		Nitrile		NO	Both	1.4:1
205a/b	4-methylbenzenethiol	Ester	TMS	NO	Both	2:1
206a/b		Nitrile		NO	Both	2:1
207a/b	Benzenethiol	Nitrile	TBDMS	NO	Both	2:1

The results from both the nitrogen and sulfur nucleophiles, show that better diastereoselectivity is obtained for the nitrogen nucleophiles compared to the sulfur nucleophiles. It also shows that the sulfur nucleophiles give both diastereomers independent of the type of sulfur nucleophile and the protecting group present. The results also show that the sulfur nucleophiles do not give the allylic substitution product from the conjugate addition reaction, whereas the nitrogen nucleophiles give the allylic substitution products. The type of the adduct (ester or nitrile) had no direct effect on the nucleophilic addition reaction.

3.1.4. Preparation and characterization of the deprotected conjugate addition products

The next step was performing a deprotection on some of the addition products to obtain the final product. The deprotection was done on two of the conjugate addition products **148**. It was performed using TBAF in THF as the solvent. The reaction was done at 0 ºC for 20 minutes and then at room temperature until the reaction was complete. The crude product was purified by column chromatography to obtain the final products **149** as diastereomers. The procedure was followed as previously performed in our laboratory,[69] with minor alterations such as using TBAF in THF not in toluene and leaving the reaction longer than 20 minutes.

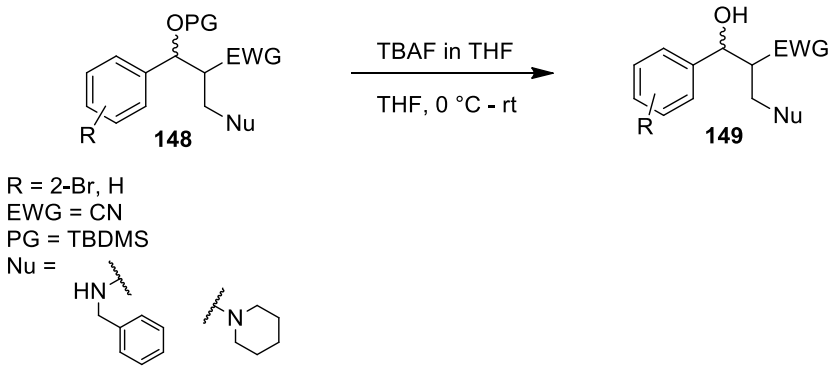

Scheme 58: the deprotection of the alcohol on the conjugate addition product **148** using TBAF in THF to form **149**.

3.1.4.1. Deprotection of TBDMS protected benzylamine nitrile adduct 196a/b.

Compound **196a/b**, a mixture of diastereomers was deprotected using the conditions described to obtain **208a/b** as a mixture of diastereomers, as expected. The desired product **208a/b** was obtained, as verified by IR and NMR spectroscopy (**Table 51** and **52**).

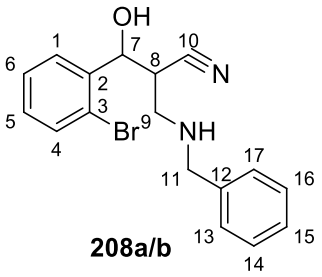

Figure 40: Deprotection of the TBDMS protected adduct to form **208a/b**.

Table 51: The approximate chemical shift values and integrations obtained from the ^{1}H NMR spectrum for both the major and minor diastereomer **208a/b**.

Major and Minor diastereomer combined (**208a/b**)			
Assignment	**Approximate chemical shift values (ppm)**	**Combining partial integrations**	**Overall integration**
Ar-H	7.85-7.12	0.20H + 0.89H + 8H	9H
H-7	5.4	0.72H + 0.21H	1H
H-11	3.9	0.46H + 0.81H + 0.75H	2H
H-9	3.4	0.29H + 0.33H + 0.84H + 0.84H	2H
H-8	3.2	0.26H + 0.75H	1H
N-H	2.2	1H	1H

Table 52: The ^{13}C NMR data for both the major and minor diastereomer **208a/b**.

Assignment	Major diastereomer	**Assignment**	Minor diastereomer
Ar-C	139.4	**Ar-C'**	138.9
Ar-C	137.9	**Ar-C'**	138.1
Ar-C	133.0	**Ar-C'**	132.4
Ar-C	129.7	**Ar-C'**	129.8
Ar-C	128.8	**Ar-C'**	128.9
Ar-C	128.7	**Ar-C'**	128.6
Ar-C	128.2	**Ar-C'**	128.3
Ar-C	127.9	**Ar-C'**	128.1
Ar-C	127.7	**Ar-C'**	127.8
Ar-C	121.6	**Ar-C'**	121.1
C-10	119.2	**C-10'**	119.2
C-7	74.3	**C-7'**	73.9
C-11	53.7	**C-11'**	53.9
C-9	46.2	**C-9'**	50.0

C-8	35.3	**C-8'**	37.8

The IR spectrum showed all the important stretches, such as the OH, NH and the CN stretch in their typical regions of 3307, 3290 and 2224 cm^{-1}. The absence of the O-Si signal and the presence of the broad signal around 3307 cm^{-1} belonging to the OH functional group, confirmed the deprotection of the adduct.

The ^{1}H NMR spectrum showed the formation of the desired product. The reaction was successful since the NMR spectrum showed the absence of the TBDMS protons in the shielded region. The rest of the peaks also showed the deprotected version. The aromatic protons were found in the aromatic region between 7 and 8 ppm, they appeared as doublets of doublets and multiplets showing coupling to each other. The H-7 signal was also found at around 5.46 and 5.30 ppm, belonging to both diastereomers and together integrating for 1 proton. Both H-7 signals appeared as doublets, coupling to the neighbouring H-8 proton as shown in the COSY spectrum.

The H-7 integration was used as the reference integration for the rest of the diastereomer peaks. The corresponding carbon peaks in the HSQC spectrum were found around 74 ppm. The next three peaks belong to H-11, the partial integrations combined make up for 2 protons belonging to both the major and the minor diastereomer. This was confirmed using the HMBC spectrum, which showed coupling of the proton peak to neighbouring aromatic carbons, as well as the C-9 peak. These H-11 peaks appeared as multiplets and doublets with a coupling constant of 13 Hz, showing coupling to each other. The corresponding carbon peaks were found around 54 ppm in the HSQC spectrum.

The H-9 peaks were found using HSQC, looking at the couplings to the major and minor carbon peaks, these were found around 3.41, 3.14, 3.04, and 2.81 ppm. All these peaks combined make up for 2 protons belonging to both the major and the minor diastereomer. All these peaks appeared as doublets of doublets, which showed coupling to each other as well as the neighbouring H-8 proton with a coupling constant value of around 12 and 4 Hz, respectively. The corresponding C-9 carbon was found around 50 and 46 ppm in the HSQC spectrum. The DEPT spectrum also confirmed this, as it is a CH_2 and appeared as a negative signal. The H-8 proton also appeared as a multiplet around 3.25 and 3.19 ppm, coupling to neighbouring H-9 and H-7 protons. C-8 was found at around 37 and 35 ppm in the HSQC spectrum, which was also confirmed using the DEPT experiment as it appeared as a positive signal.

3.1.4.2. **Deprotection of TBDMS protected nitrile adduct 192a/b.**

The next compound to be deprotected was the piperidine TBDMS adduct **192a/b**. This was done using the same method as previously described. The expected product **209a/b** (**Figure 41**) was obtained as a mixture of diastereomers, as confirmed using IR and NMR spectroscopy (**Table 53** and **54**).

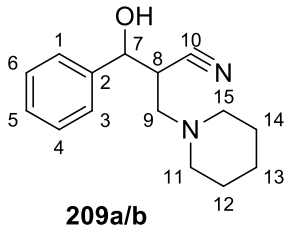

209a/b

Figure 41: deprotection of TBDMS protected adduct.

Table 53: The approximate chemical shift values and integrations obtained from the ^{1}H NMR spectrum for both the major and minor diastereomer **209a/b**

Major and Minor diastereomer combined (209a/b)			
Assignment	**Approximate chemical shift values (ppm)**	**Combining partial integrations**	**Overall integration**
Ar-H	7.50-7.29	5H	5H
H-7	5	0.28H + 0.62H	1H
H-9	2.9	0.30H + 0.36H + 0.17H + 0.66H + 0.25H	2H
H-8	3	0.27H + 0.58H	1H
H-11	2.7	0.22H + 1.9H	2H
H-15	2.7	0.22H + 1.9H	2H
H-12,13,14	1.7	4.43H + 2.43H	6H

Table 54: The ^{13}C NMR data for both the major and minor diastereomer **209a/b**

Assignment	Major diastereomer	**Assignment**	Minor diastereomer

Ar-C	140.7	**Ar-C'**	140.0
Ar-C	128.6	**Ar-C'**	128.5
Ar-C	128.2	**Ar-C'**	128.2
Ar-C	126.5	**Ar-C'**	126.1
C-10	118.5	**C-10'**	118.7
C-7	77.1	**C-7'**	74.3
C-9	60.5	**C-9'**	58.3
C-11,15	55.3	**C-11',15'**	54.7
C-8	35.9	**C-8'**	36.2
C-12,14	25.8	**C-12',14'**	26.0
C-13	23.7	**C-13'**	23.7

The IR spectrum showed the presence of all the significant signals, such as the OH and nitrile present at 2981 and 2220 cm^{-1}, respectively. The absence of the O-Si peak and the presence of the OH signal confirmed that the expected product was obtained.

The NMR spectra also confirmed the formation of the desired products as a mixture of two diastereomers. The ^{1}H NMR spectrum showed the presence of the aromatic signals integrating for 5 protons in the aromatic region between 7.29-7.50 ppm. The H-7 signals were also found around 5.12 and 4.96 ppm belonging to both diastereomers making up 1 proton. All the integrations of the other signals were referenced against the H-7 signals. The H-7 signals appeared as doublets, showing coupling to the neighbouring H-8 proton as shown in the COSY spectrum.

The corresponding C-7 peaks were found around 77.1 and 74.3 ppm in the HSQC spectrum for both major and the minor diastereomer. These were also confirmed using the DEPT spectrum which showed the signals in the positive region. H-8 peaks for both the major and the minor diastereomer were found around 3.18 and 2.97 ppm as deduced from the HSQC spectrum which showed connectivity to both major and the minor carbon peaks, which were found around 36.2 and 35.9 ppm. This was also confirmed using the DEPT spectrum as it was found in the positive region.

H-9 peaks were also found by combining all the partial integrations as shown from the couplings in the HSQC spectrum, to make up two protons. These H-9 peaks appeared as multiplets, doublets and singlets, showing coupling to each other as well as to the H-8 proton. The corresponding carbon peaks were found around 60.5 and 58.3 ppm from the HSQC spectrum. This was also confirmed from the DEPT spectrum as it was found as a negative signal. The piperidine peaks were found in the shielded region in the range of 1-2 ppm. The corresponding carbon peaks were found around 55 ppm, 26 ppm, and 23 ppm from the HSQC spectrum, also confirmed from the DEPT spectrum.

Assigning *syn* or *anti* configuration to the major and the minor diastereomers.

Interestingly, as soon as the deprotection was carried out, the NMR spectra of compounds **208a/b** and **209a/b** (**Figure 42** and **43**) were better defined. It is possible that the better definition in the NMR spectrum is a result of hydrogen bonding between the OH proton and the nitrogen of the nucleophile, giving a chair conformation (**Figure 44**).

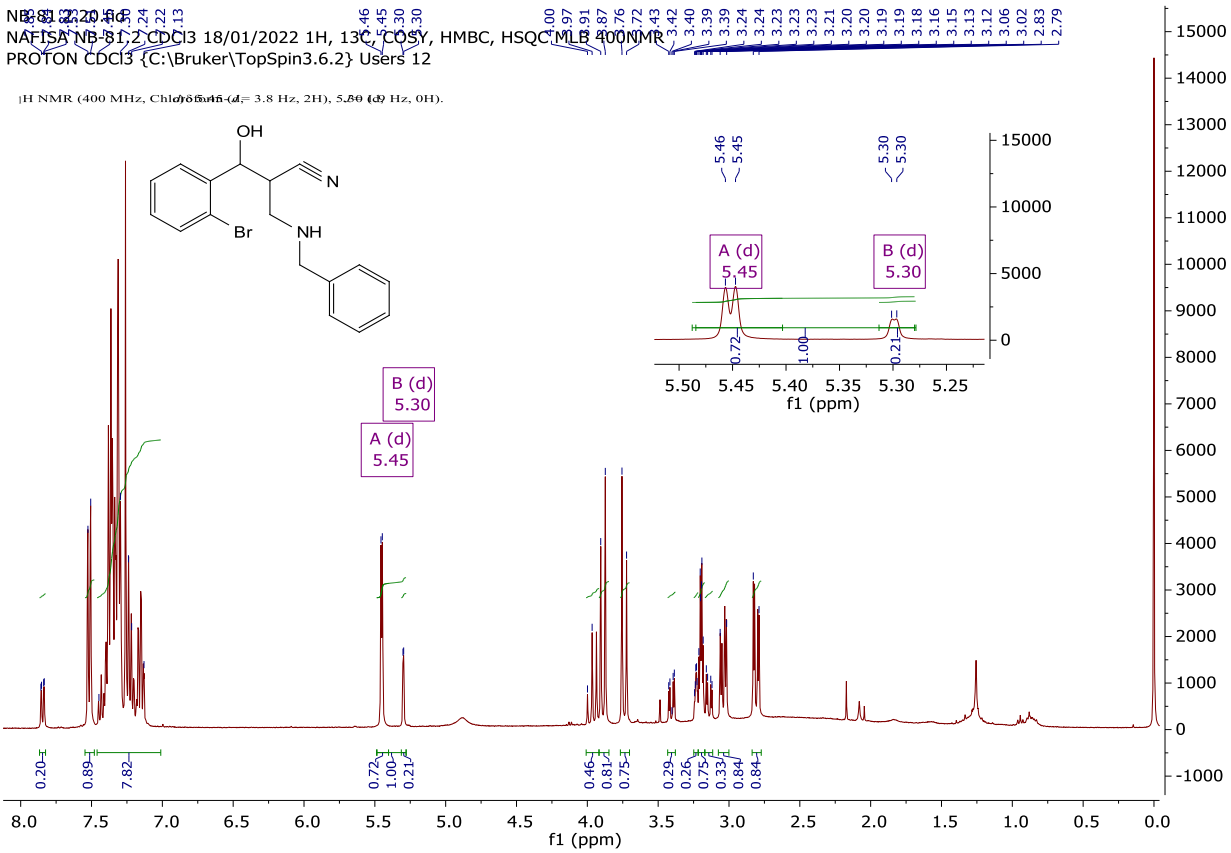

Figure 42: The ^{1}H NMR spectrum of compound **208a/b**.

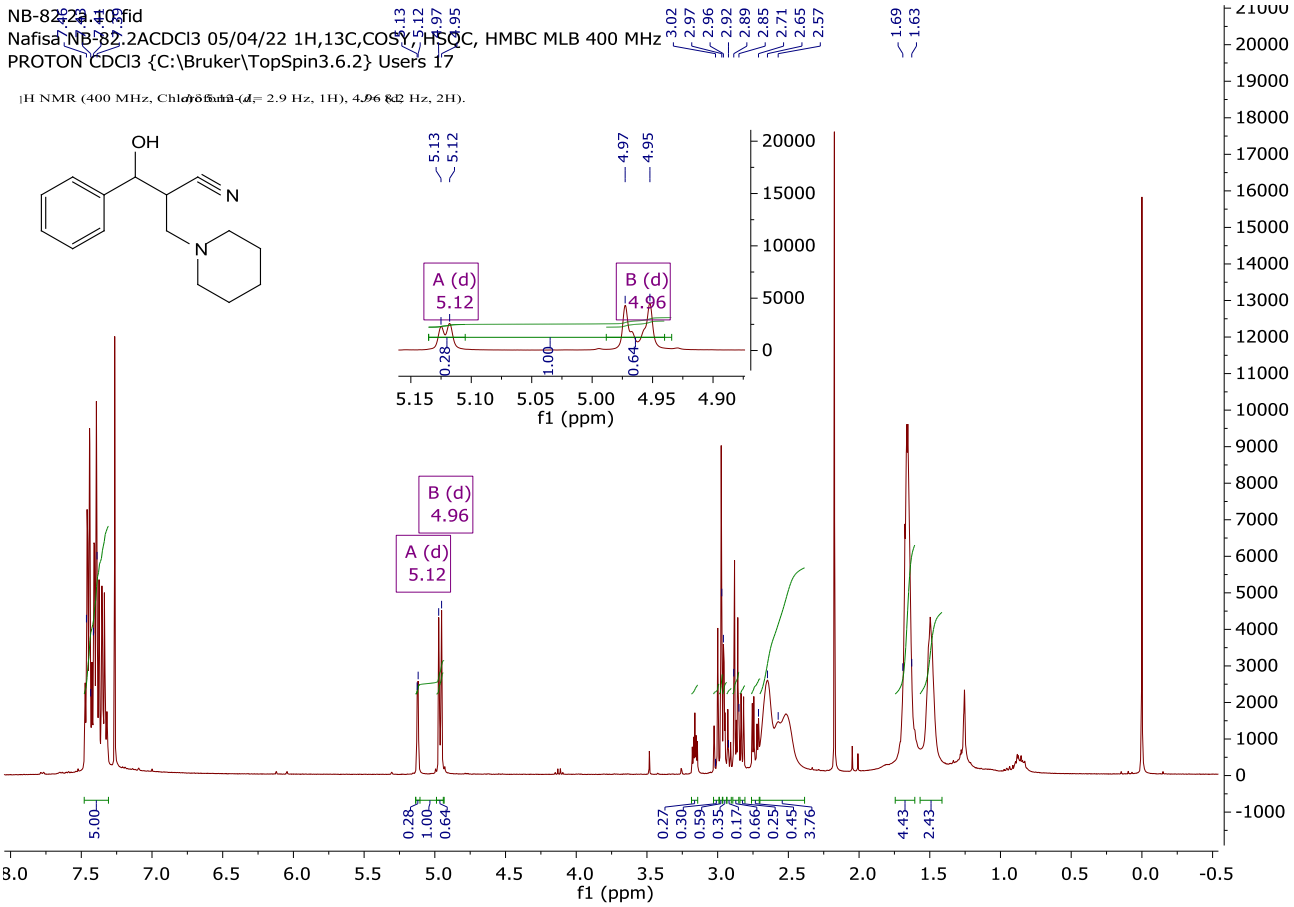

Figure 43: The ^{1}H NMR spectrum of compound **209a/b**.

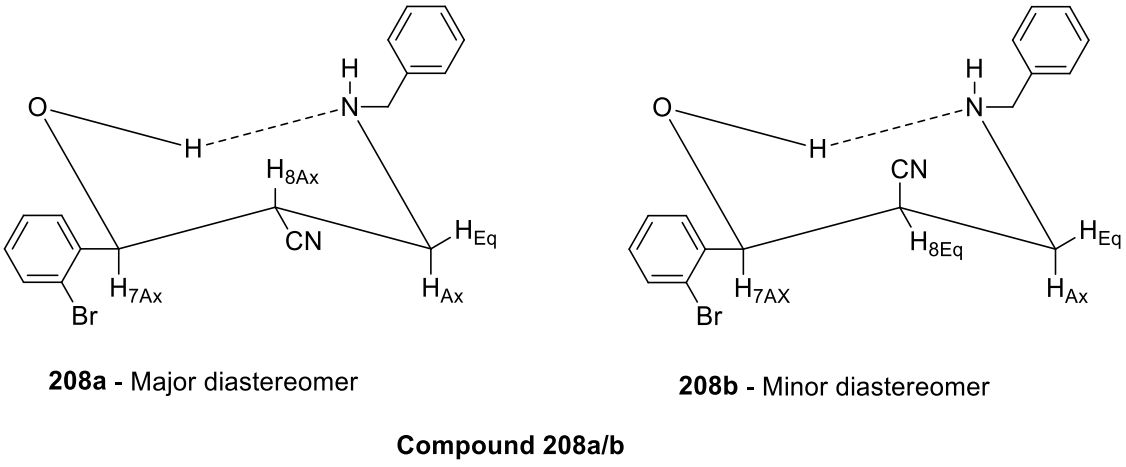

208a - Major diastereomer

208b - Minor diastereomer

Compound 208a/b

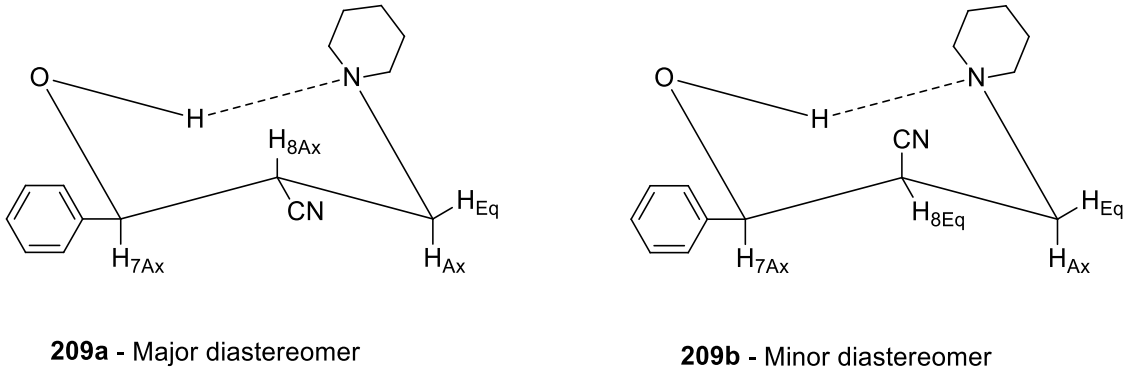

209a - Major diastereomer

209b - Minor diastereomer

Compound 209a/b

Figure 44: The major and minor diastereomer **208a/b** and **209a/b** in a chair conformation

In the chair conformation, the phenyl groups would be in the equatorial position, giving the most stable conformation (**Figure 44**). The only difference between the two diastereomers is the position of the nitrile group, which is either in the axial or the equatorial position. By calculating the coupling constants of various axial and equatorial interactions from the proton NMR and comparing it to the general coupling constants of the chair conformation of the 6-membered ring, it can be determined whether the *syn* diastereomer is the major or the minor product.[69]

For the minor diastereomer of compound **209b**, the H-7 proton signal appears as a doublet with a *J* coupling value of 2.9 Hz, and for the major diastereomer **209a**, the H-7 proton appears as a doublet which is a bit distorted with a *J* coupling value of 8.2 Hz. This shows the H-7 proton coupling to the neighbouring H-8 proton. If the *syn* product is the major diastereomer, then the *J*

coupling value of the H-7 coupling to H-8 has to be big because it is axial to axial coupling in the hydrogen bonded chair conformation, and a value of 7-12 Hz is expected. From **209a**, a value of 8.2 Hz is obtained, which falls within the range given. For the minor diastereomer, it is axial to equatorial coupling and a smaller value of 2-5 Hz is expected. From **209b**, a value of 2.9 Hz is obtained, which falls within the range given. Hence, the major diastereomer is the *syn* product.

For compound **208a/b**, the chair conformation is less well defined, and the two coupling values of the major and the minor diastereomer are much smaller. However, the major diastereomer does have a larger coupling constant than the minor one, implying that the major diastereomer is the *syn* product.

3.2. Preparation and characterization of MBH amide adducts and their conjugate addition products.

The next goal was to synthesize MBH adducts carrying amide as the electron withdrawing group and adding long alkyl chain nitrogen nucleophiles on it to synthesize compounds that mimic natural antibacterial peptides (**Figure 11**).[79] The MBH amides were prepared in alternative ways since the simple MBH reaction using acrylamides have been reported to give the desired products in very low yields and also lead to the formation of byproducts.[92]

3.2.1. Initially proposed route

The initial route was to prepare the MBH amide adducts **210** by reacting substituted benzaldehydes **211** with methyl and ethyl acrylate **212** giving MBH esters **213** which could be further transformed into amides **210**. The plan was to hydrolyze the protected MBH ester **213** to obtain a carboxylic acid **214** and then to convert this into an MBH amide **210**. Conjugate addition reactions using different nucleophiles would then be attempted on these amides **210**, which would be deprotected to obtain the final product **215**.

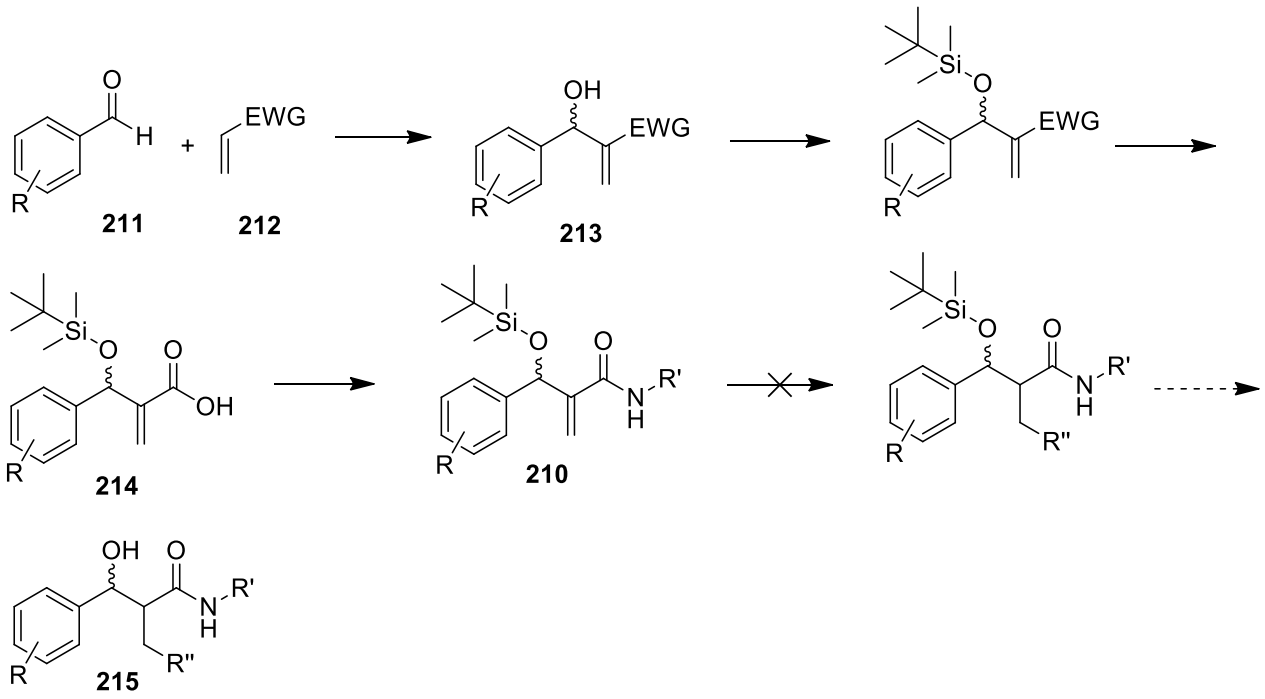

R = 4-Cl, 2-Cl
EWG = CO_2Me, CO_2Et
R' = Benzylamine, Propylamine
R'' = Nitrogen Nu

Scheme 59: The initially proposed route to obtaining the MBH amide **210** from MBH ester **213** and performing a conjugate addition reaction on them.

3.2.1.1. Synthesis of the MBH ester adducts.

The first step was the formation of the MBH ester adducts **213**. These adducts were synthesized using the exact method reported earlier, using methyl or the ethyl acrylate **211** and substituted benzaldehydes **212** in the presence of DABCO as a catalyst at room temperature (**Scheme 60**).[69] These products were obtained as racemic mixtures since the reaction leads to the formation of a stereogenic centre. The desired products **216**, **153** and **217** were obtained as confirmed using IR and NMR spectroscopy (**Table 56**).

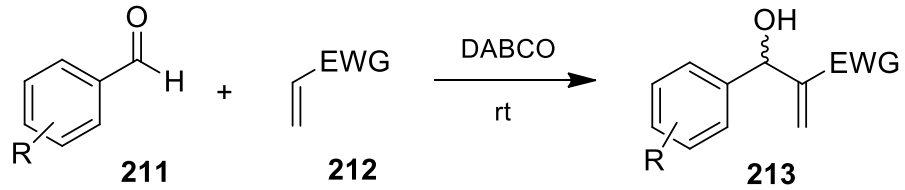

R = 4-Br, 4-Cl
EWG = CO_2Me, CO_2Et

Scheme 60: The Morita Baylis Hillman reaction on different substituted benzaldehydes **211** and activated alkenes **212** to form MBH adduct **213**.

Table 55 shows the yields obtained from the MBH reaction using activated alkenes with different electron withdrawing groups and differently substituted benzaldehydes. The best yield was obtained for the ethyl acrylate adduct, which was 89 %. Very good yields were obtained for all the products **216**, **153** and **217** (**Figure 45**).

Table 55: The yields obtained from the Morita Baylis Hillman reaction between different substituted benzaldehydes and methyl or ethyl acrylate.

Compound no.	**R**	**EWG**	**Yield (%)**
216	4-Br	CO_2CH_3	76
217	4-Cl	$CO_2CH_2CH_3$	89

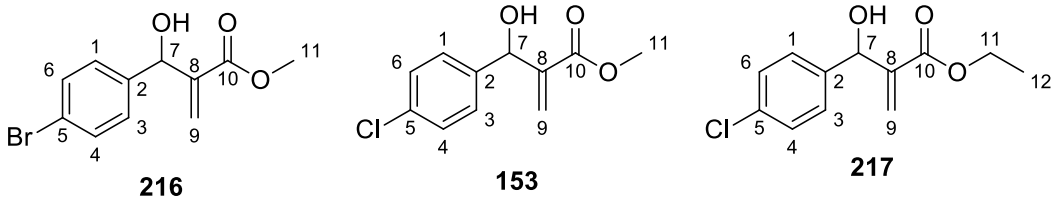

Figure 45: The Morita Baylis Hillman ester adducts synthesised.

Table 56: The IR and the NMR data obtained for the above adducts.

Compound No.	**IR** (neat, cm^{-1})	**NMR**

216	3330 (OH), 2942 (C-H), 1717 (C=O)	**^{1}H NMR (400 MHz, $CDCl_3$)** δ 6.63 – 6.58 (2H, m, H-4,6), 6.41 – 6.36 (2H, m, H-1,3), 5.48 (1H, s, H-9a), 4.96 (1H, s, H-9b), 4.64 (1H, d, *J*=5.7 Hz, H-7), 2.86 (3H, s, H-11), 2.22 (1H, d, *J*=5.8 Hz, OH).**^{13}C NMR (101 MHz, $CDCl_3$)** δ 166.6 (C-10), 141.6 (C-2), 140.3 (C-8), 131.6 (C-4,6), 128.3 (C-1,3), 126.4 (C-9), 121.8 (C-5), 72.8 (C-7), 52.1 (C-11).
217	2983 (C-H), 1703 (C=O)	**^{1}H NMR (400 MHz, $CDCl_3$)** δ 7.35 – 7.28 (4H, m, Ar-H), 6.34 (1H, s, H-9a), 5.81 (1H, s, H-9b), 5.52 (1H, s, H-7), 4.17 (2H, q, *J*=7.2 Hz, H-11), 3.21 (1H, s, OH), 1.25 (3H, t, H-12). **^{13}C NMR (101 MHz, $CDCl_3$)** δ 166.2 (C-10), 141.8 (C-8), 139.9 (C-2), 133.6 (C-5), 128.6 (C-4,6), 128.0 (C-1,3), 126.2 (C-9), 72.8 (C-7), 61.1 (C-11), 14.1 (C-12).

The IR spectrum showed all the important stretches. The presence of the OH stretch at 3330 cm^{-1} confirmed the formation of the product **216**. The IR spectra showed other stretches as well, such as the carbonyl stretch at around 1700 cm^{-1}.

The first adduct **216** was synthesized using 4-bromobenzaldehyde and methyl acrylate and was obtained in a very good yield of 76%. NMR spectroscopy confirmed the formation of the product. The ^{1}H NMR spectrum showed the aromatic peaks between 6.36-6.63 ppm, integrating for 4 protons, and also showed the terminal alkene protons as two separate peaks at 4.96 and 5.48 ppm. These peaks appeared as singlets and did not couple to any other protons. The corresponding carbon peak was found at 126.4 ppm from the HSQC spectrum. The next peak in the ^{1}H spectrum belongs to H-7, which showed connectivity to the carbon peak at 72.8 ppm in the HSQC spectrum. The peak at 2.86 ppm integrated for 3 protons, belonging to H-11, and the corresponding carbon peak was found at 52.1 ppm. The last signal which appeared as a doublet, belongs to the alcohol group, showing coupling to the neighbouring H-7 proton, hence appearing as a doublet. The second MBH adduct **153** has already been made before.

The other adduct **217** was synthesized using 4-chlorobenzaldehyde and the ethyl acrylate. The expected product was obtained, as confirmed by the presence of the OH peak in the ^{1}H NMR spectrum. All other expected signals were also present, for example, the aromatic signals at 7.28-7.35 ppm, the terminal alkene protons at 5.81 and 6.34 ppm and the H-7 signal at 5.52 ppm. It also showed the CH_2 signal appearing as a quartet coupling to the neighbouring CH_3. The OH signal was found at 3.21 ppm and the CH_3 signal at 1.25 ppm, appearing as a triplet coupling to the CH_2 protons. All the carbon peaks were assigned using the HSQC spectrum and confirmed using the DEPT spectrum.

3.2.1.2. Preparation and characterization of the alcohol protected ester adducts.

The next step was the protection of the alcohol group and the method reported earlier in section 3.1.2. was used. It involved using TBDMSCl with imidazole as a base in anhydrous DMF at room temperature, under nitrogen.[81] The expected products **219**, **162** and **220** (**Figure 46**) were obtained, and confirmed using IR and NMR spectroscopy (**Table 58**). TBDMS groups were used to protect the alcohol for all three adducts. As reported earlier, the protecting groups are important, since they can control the diastereoselectivity in the subsequent conjugate addition reaction by directing the addition of nucleophiles to the adducts.

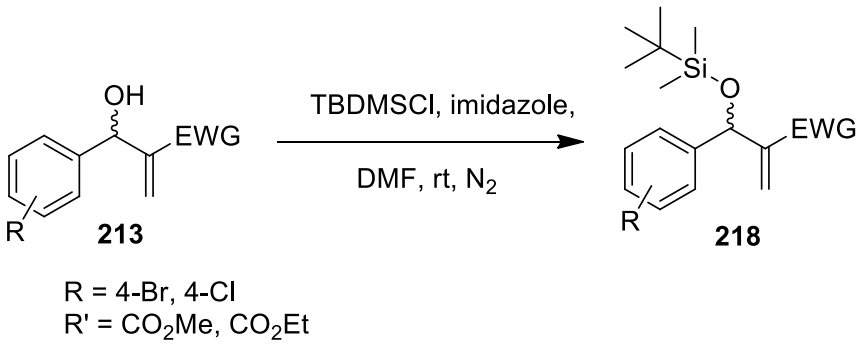

Scheme 61: The protection of the alcohol group on the MBH adducts **213** using TBDMSCl.

Table 57 shows the yield obtained for compound **219** and **220.** Compound **220** gave a very good yield. However, the yield for compound **219** was moderate. This might be due to the loss of the product during purification or incomplete reaction.

Table 57: The yields obtained from alcohol protection reaction of MBH ester adducts to form **219** and **220**.

Compound no.	**R**	**EWG**	**Yield (%)**
219	4-Br	CO_2CH_2	67
220	4-Cl	$CO_2CH_2CH_3$	80

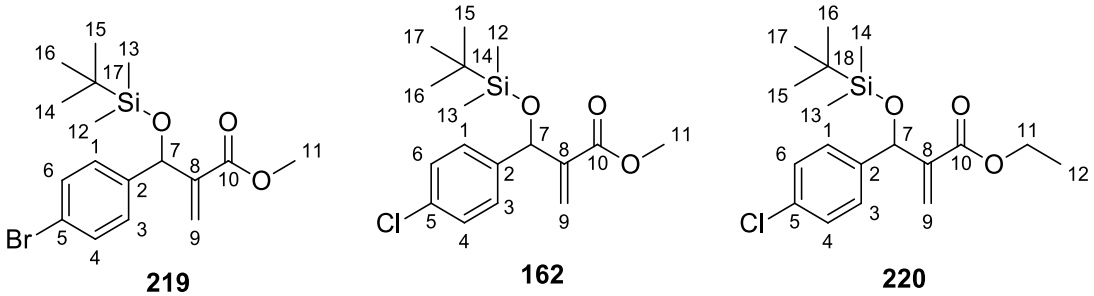

Figure 46: The alcohol protected Morita Baylis Hillman ester adducts **219**, **162** and **220**.

Table 58: The IR and the NMR data obtained for the above adducts.

Compound No.	**IR** (neat, cm^{-1})	**NMR**
219	2929 (C-H), 1719 (C=O), 835 (Si-O)	**^{1}H NMR (400 MHz, $CDCl_3$)** δ 7.54 – 7.49 (2H, m, H-4,6), 7.36 – 7.31 (2H, m, H-1,3), 6.36 (1H, s, H-9a), 6.20 (1H, s, H-9b), 5.65 (1H, s, H-7), 3.78 (3H, s, H-11), 0.97 (9H, s, H-14,15,16), 0.15 (3H, s, H-12), 0.00 (3H, s, H-13). **^{13}C NMR (101 MHz, $CDCl_3$)** δ 166.2 (C-10), 143.5 (C-2), 141.9 (C-8), 131.2 (C-4,6), 128.8 (C-1,3), 124.1 (C-9), 121.3 (C-5), 72.1 (C-7), 51.7 (C-11), 25.7 (C-14,15,16), 18.2 (C-17), -4.9 (C-13), -5.1 (C-12).
220	2930 (C-H), 1715 (C=O), 835 (Si-O);	**^{1}H NMR (400 MHz, $CDCl_3$)** δ 7.27 – 7.18 (4H, m, Ar-H), 6.21 (1H, s, H-9a), 6.03 (1H, s, H-9b), 5.51 (1H, s, H-7), 4.14 – 4.00 (2H, m, H-11), 1.23 – 1.14 (3H, m, H-12), 0.82 (9H, s, H-15, 16, 17), 0.01 (3H, s, H-13), -0.15 (3H, s, H-14).

		^{13}C NMR (101 MHz, $CDCl_3$) δ 165.8 (C-10), 143.8 (C-2), 141.4 (C-8), 133.0 (C-5), 128.5 and 128.2 (C-1,3 and C-4,6), 123.8 (C-9), 72.1 (C-7), 60.7 (C-11), 25.7 (C-15, 16 ,17), 18.2 (C-18), 14.1 (C-12), -4.9 (C-14), -5.0 (C-13).

Compound **162** has been prepared before and reported in earlier sections.

The IR spectrum showed all the important stretches for compounds **219** and **220**, such as the carbonyl stretch at around 1710 cm^{-1} and the O-Si stretch at around 835 cm^{-1} in their typical region and the absence of the OH stretch confirmed the protection of the alcohol group.

NMR spectroscopy also confirmed the formation of the two protected adducts **219** and **220**. The ^{1}H NMR spectrum showed the aromatic signals in the aromatic region between 7.18-7.54 ppm, integrating for 4 protons. The next peaks were the terminal alkene proton peaks (H-9), which appeared as two separate peaks at around 6 ppm. They appeared as singlets, showing no coupling to each other. The H-7 peaks appeared as singlets at 5.65 and 5.51 ppm for both compounds.

The C-7 and C-9 peaks were found around 72 and 74 ppm, for both protected adducts. The next peak in the methyl ester adduct belongs to the methyl protons, integrating for three protons. For the ethyl ester adduct, the ethyl CH_2 protons appeared around 4 ppm and the ethyl CH_3 was more shielded at around 1 ppm. The rest of the peaks in the shielded region belong to the TBDMS protons for both adducts. All the carbon signals were assigned using the HSQC spectrum and confirmed using the DEPT spectrum.

3.2.1.3. Preparation and characterization of the carboxylic acid product.

The third step was the hydrolysis of the ester adducts **218**. The alcohol protected ester adducts were hydrolyzed using LiOH in acetonitrile/water in a 1:1 ratio. The solution was stirred at 60 ºC, and upon completion, HCl was added to the crude product and extraction was done using ethyl acetate to obtain the final product **214** (**Scheme 62**). This method has been reported before on similar MBH adducts by Cocco *et al.*[93] The exact same method was followed without any alterations.

Other methods were also applied, which involved using sodium hydroxide in ethanol and the mixture stirring at room temperature. After dilution with $NaHCO_3$ solution, the reaction was extracted using ethyl acetate. The other method that was also used involved using KOH in water under reflux for 4 hours.[69] All these methods gave the products **214**, but in very low yields (**Scheme 62**). The other method tested involved using the enzyme lipozyme CALB L LCN 02106, in the presence of phosphate buffer to maintain the pH at 7, at 30 ˚C in acetone. This method did not work at all as no conversion occurred and the starting materials were recovered (**Scheme 63**).[69]

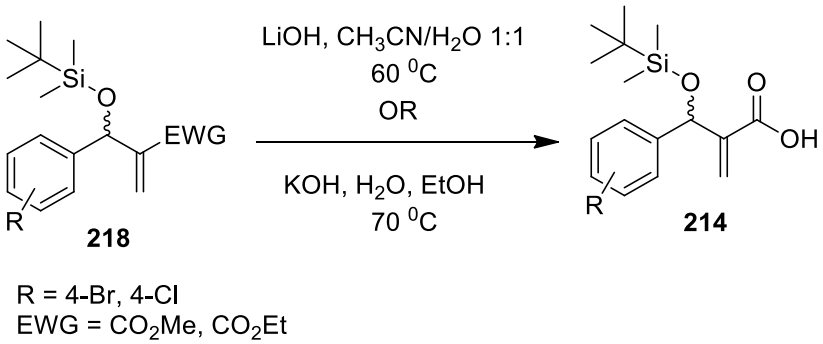

Scheme 62: The hydrolysis of the MBH ester adduct **218** to form carboxylic acid **214**.

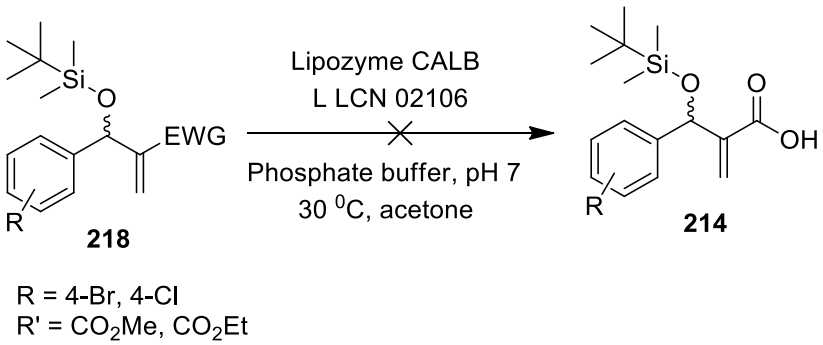

Scheme 63: An attempt to hydrolyze the MBH ester adduct **218** to form carboxylic acid **214** using enzyme lipozyme.

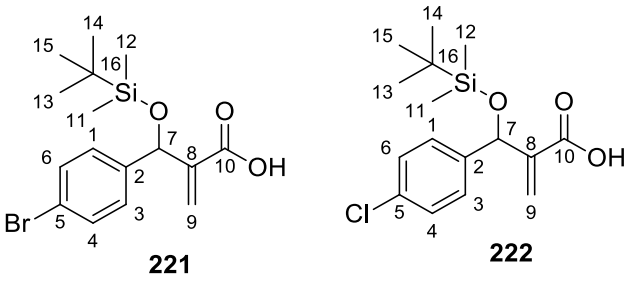

Figure 47: Carboxylic acids **221** and **222** obtained from the MBH ester adducts through the hydrolysis reaction.

Very poor yields (**Table 59**) were obtained from the hydrolysis reactions, even though different methods were used to try and improve the yields. The best method from all the methods reported above for the hydrolysis of esters into carboxylic acids **221** and **222** was using LiOH in acetonitrile and water reported by Cocco *et al.*[93]

Table 59: The yields of the carboxylic acids **221** and **222**.

Compound	**Yield (%)**
221	39
222	11

Table 60: The IR and NMR data obtained for the above adducts **221** and **222**.

Compound No.	**IR** (neat, cm^{-1})	**NMR**
221	2951 (OH), 2929 (C-H), 1688 (C=O), 825 (Si-O)	**^{1}H NMR (400 MHz, $CDCl_3$)** δ 7.52 – 7.48 (2H, m, H-4,6), 7.33 – 7.30 (2H, m, H-1,3), 6.48 (1H, t, *J*=1.3 Hz, H-9a), 6.26 (1H, t, *J*=1.5 Hz, H-9b), 5.60 (1H, s, H-7), 0.96 (9H, s, H-13,14,15), 0.14 (3H, s, H-11), 0.00 (3H, s, H-12). **^{13}C NMR (101 MHz, $CDCl_3$)** δ 169.7 (C-10), 142.7 (C-2), 141.4 (C-8), 131.3 (C-4,6), 128.7 (C-1,3), 126.6 (C-9), 121.5 (C-5), 72.1 (C-7), 25.7 (C-13,14,15), 18.2 (C-16), -4.9 (C-12), -5.1 (C-11).

222	2952 (OH), 1695 (C=O), 834 (Si-O)	**^{1}H NMR (300 MHz, $CDCl_3$)** δ 7.19 – 7.15 (4H, m, Ar-H), 6.29 (1H, t, *J*=1.3 Hz, H-9a), 6.07 (1H, t, *J*=1.3 Hz, H-9b), 5.43 (1H, s, H-7), 0.77 (9H, s, H-13,14,15), -0.04 (3H, s, H-11), -0.19 (3H, s, H-12). **^{13}C NMR (101 MHz, $CDCl_3$)** δ 169.3 (C-10), 142.7 (C-2), 140.8 (C-8), 133.3 (C-5), 128.4 (C-4,6), 128.3 (C-1,3), 126.4 (C-9), 72.1 (C-7), 25.6 (C-13, 14, 15), 18.2 (C-16), -4.9 (C-12), -5.1 (C-11).

The identity of products **221** and **222** were confirmed using IR and NMR spectroscopy (**Table 60**). The IR spectra showed the expected stretches, such as the carboxylic acid OH and the carbonyl stretch around 2951 and 1688 cm^{-1}, respectively. The presence of the OH signal in the IR spectrum confirmed that ester hydrolysis had occured

NMR spectroscopy also confirmed the synthesis of the expected products showing the absence of the ester protons. Both compounds showed remarkably similar shift values. The ^{1}H NMR spectra showed the aromatic protons in the aromatic region between 7.15-7.52 ppm. For compound **221**, aromatic protons, H-4,6 appeared deshielded, at 7.50 ppm, due to the bromine atom which pulls electron density away. This aromatic peak and the aromatic peak at 7.31 ppm appeared as multiplets and showed coupling to each other. For compound **222**, the aromatic made up a single signal. The next two peaks in both compounds appeared as triplets around 6 ppm, these peaks belong to the H-9 protons, and they couple to each other and to H-7. The corresponding carbon peaks in the HSQC spectrum were found around 126 ppm for both compounds, which appeared as negative signals in the DEPT spectrum.

The H-7 peak was found around 5 ppm for both compounds, appearing as singlets and not coupling to any other protons. The corresponding carbon peak was found around 72.1 ppm. The rest of the signals belong to the TBDMS protons. The most deshielded carbon peak belongs to the C-10 carbon at 169 ppm, the next most deshielded peak belongs to the C-2 aromatic carbon as it shows coupling to aromatic protons in the HMBC spectrum and it is absent from the DEPT spectrum.

The next peak belongs to the C-8 carbon. All the carbon peaks were assigned using the HSQC spectrum and confirmed using the DEPT spectrum.

Similar MBH acids have been synthesized before reported by Giovanni W. *et al.*[94]

3.2.1.4. Preparation and characterization of the amide product

The next step was the synthesis of the amide **210** from the carboxylic acid **214** by reacting it with an amine (**Scheme 64**). Two different methods were applied, the first method involved using *N,N*'-Dicyclohexylcarbodiimide (DCC) as the dehydrating agent to form the amide, whereas the second method involved using Carbonyldiimidazole (CDI).

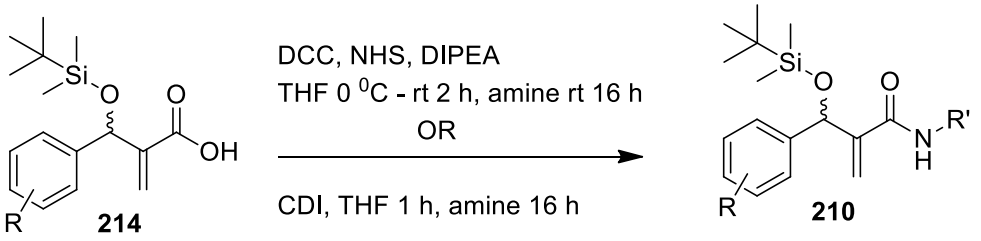

R = 4-Br, 4-Cl
R' = Benzylamine, propylamine

Scheme 64: Converting the carboxylic acids **214** into amides **210** using different methods.

3.2.1.4.1. Amide synthesis using DCC.

The first method was applied on the bromo substituted carboxylic acid **221**. The reaction was done in THF using DCC, DIPEA and NHS at 0 ºC for the first 15 minutes, and then kept at room temperature for another 2 hours, after which benzylamine was added and the mixture was stirred at room temperature until the reaction was complete. The mixture was then filtered and extracted using ethyl acetate. This method has been reported on similar compounds by Cocco *et al.* and was followed exactly as reported.[93]

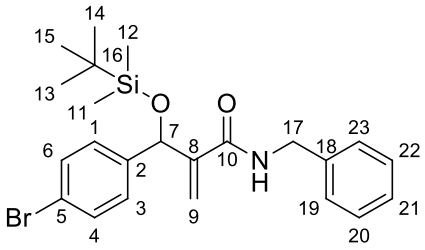

223

Figure 48: Compound **223** obtained from compound **221**.

Table 61: The IR and the NMR data obtained for adduct **223**.

Compound No.	**IR** (neat, cm^{-1})	**NMR**
223	3295 (NH), 2927 (C-H), 1621 (C=O), 825 (Si-O)	**^{1}H NMR (400 MHz, $CDCl_3$)** δ 7.43 – 7.39 (2H, m, Ar-H), 7.25 – 7.22 (3H, m, Ar-H, N-H), 7.19 – 7.15 (2H, m, Ar-H), 6.94 – 6.87 (3H, m, Ar-H), 6.12 (1H, s, H-7), 5.63 (1H, s, H-9), 5.54 (1H, s, H-9), 4.47 (1H, dd, *J*=14.7, 6.3 Hz, H-17a), 4.23 (1H, dd, *J*=15.0, 5.1 Hz, H-17b), 0.85 (9H, s, H-13,14,15), 0.07 (3H, s, H-11), 0.04 (3H, s, H-12)

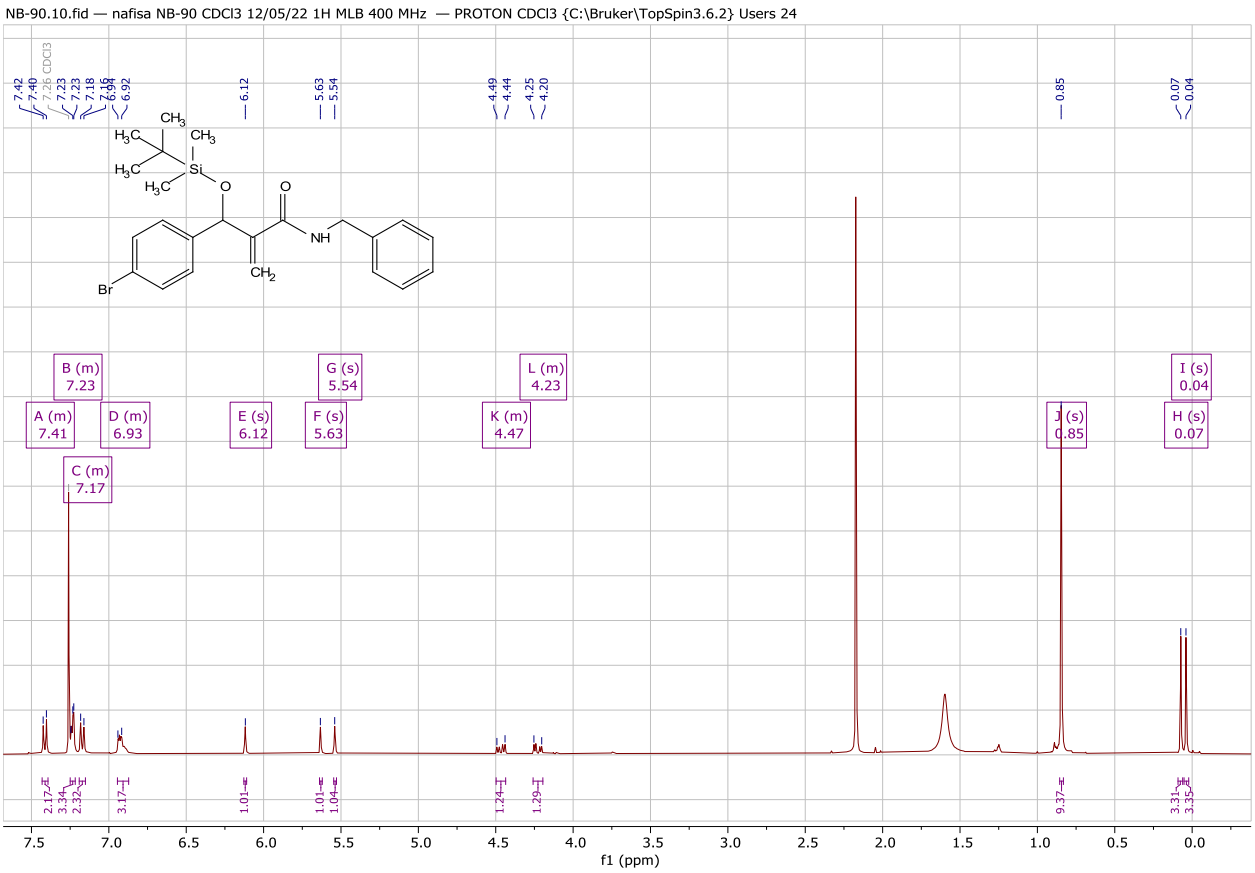

Figure 49: The ^{1}H NMR spectrum of compound **223**.

The product **223** was successfully obtained as a brown oil. However, in low yield of 39%. The product identity was confirmed using IR and NMR spectroscopy (**Figure 49**,**Table 61**). The IR spectrum showed all the important peaks such as the carbonyl at 1621 cm^{-1}, which is typical for the amide carbonyl. The alkene (C=C) signal was found at 1496 cm^{-1} as well as the NH signal at 3295 cm^{-1}, which shows the successful synthesis of amide **223** from the carboxylic acid **221**. The ^{1}H NMR spectrum confirmed the synthesis of the amide, as it showed all the aromatic peaks in the aromatic region, as well as the NH peak at 7.23 ppm. These aromatic peaks appeared as multiplets, showing coupling to one another.

The H-7 peak was found at 6.12 ppm, appearing as a singlet as there was no coupling to any other protons. The next signals belonged to H-9, they appeared as singlets at 5.63 ppm and showed no coupling. The next two peaks belong to H-17 protons, which appeared as doublets of doublets, showing coupling to each other and probably the NH proton. The rest of the peaks belong to the

TBDMS protons. Product **223** was obtained in a low yield and in order to improve the yield, a different method was applied.

3.2.1.4.2. Amide synthesis using CDI.

For this alternative method, CDI was added to the carboxylic acid **214** in anhydrous THF (**Scheme 64**). The mixture was stirred at room temperature for an hour, after which the amine was added and stirred overnight. The product **210** was obtained and purified using column chromatography.[94] This method was successful, it improved the yields and used less reagents compared to the above method. This method was applied to compound **222** using benzylamine and propylamine. Both reactions were successful and gave the desired product.

3.2.1.4.2.1. Using benzylamine.

The reaction in which benzylamine was used as the amine gave the product **224** as a white solid, and a byproduct **225** (**Figure 50**) was also obtained. The byproduct formed as a result of two reactions occurring, the amide synthesis reaction which was desired, and the nucleophilic addition reaction which was unexpected. The identity of both products was confirmed using NMR spectroscopy (**Table 62**).

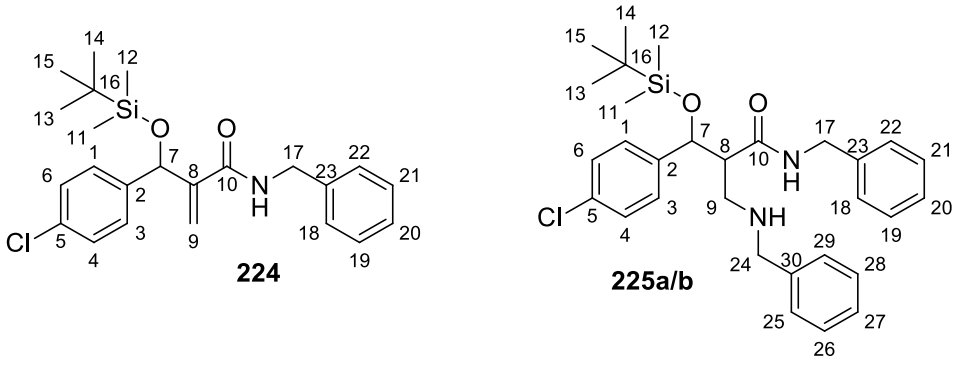

Figure 50: Product **224** and byproduct **225a/b** obtained from the reaction of benzylamine and compound **222**.

Table 62: The IR and the NMR data obtained for adduct **224**.

Compound No.	**NMR**

224	**^{1}H NMR (300 MHz, $CDCl_3$)** δ 7.23 (1H, s, NH), 7.22 – 7.06 (9H, m, Ar-H), 6.02 (1H, s, H-9a), 5.53 (1H, s, H-7), 5.46 (1H, s, H-9b), 4.41 – 4.32 (1H, m, H-17a), 4.18 – 4.09 (1H, m, H-17b), 0.78 – 0.72 (9H, m, H-13,14,15), -0.04 (6H, d, *J*=10.4 Hz, H-11,12)

Product **224** and byproduct **225a/b** were obtained in a yield of 30% and 18%, respectively. The yield of the desired product **224** is very low, this might be due to incomplete reaction and also due to the side reaction occurring giving the byproduct **225a/b**.

The expected product **224** was obtained as confirmed by the NMR data (**Table 62**). The ^{1}H NMR spectrum showed the NH peak, which was the most deshielded peak at 7.23 ppm. The presence of the NH peak confirmed the formation of the product. The aromatic peak was also found between 7.06-7.22 ppm which integrated for 9 protons and appeared as a multiplet. H-9 terminal alkene protons appeared as two separate peaks, where one was found around 6.02 ppm and the other appeared more shielded around 5.46 ppm. H-7 also appeared at 5.53 ppm. H-17 protons were observed as two separate peaks at 4.35 and 4.15 ppm. The other peaks were in the shielded region below 0.78 ppm and belonged to the TBDMS protecting group.

The byproduct **225a/b**, where the nucleophilic addition reaction occured along with the amide synthesis was obtained as a mixture of diastereomers. This product was characterized using IR and NMR spectroscopy (**Table 63** and **64**). The IR spectrum showed all the important signals such as the carbonyl signal at 1665 cm^{-1}.

Table 63: The approximate chemical shift values and integrations obtained from the ^{1}H NMR spectrum for both the major and minor diastereomer of the byproduct **225a/b**.

Major and Minor diastereomer combined (**225a/b**)			
Assignment	**Approximate chemical shift values (ppm)**	**Combining partial integrations**	**Overall integration**
NH	7.77	1H	1H
Ar-H	7.65-6.88	9.89H + 2.61H + 0.42H + 1.16H	14H

H-7	5	0.31H + 0.73H	1H
H-17	4.7	0.71H + 1.32H + 0.33H	2H
H-24	4.4	0.33H + 0.49H + 0.34H + 0.64H	2H
H-9	4.3	0.78H + 0.37H + 0.74H	2H
H-8	3.8	0.83H + 0.09H + 0.18H	1H
H-13,14,15	1.0	9H	9H
H-11	0.3	3H	3H
H-12	0.01	3H	3H

Table 64: The ^{13}C NMR data for both the major and minor diastereomer obtained of byproduct **225a/b**

Assignment	Major diastereomer	**Assignment**	Minor diastereomer
C-10	169.6	**C-10'**	-
Ar-C	140.4	**Ar-C'**	-
Ar-C	137.1	**Ar-C'**	-
Ar-C	134.0	**Ar-C'**	-
Ar-C	129.0	**Ar-C'**	-
Ar-C	128.9	**Ar-C'**	-
Ar-C	128.7	**Ar-C'**	-
Ar-C	128.6	**Ar-C'**	-
Ar-C	128.5	**Ar-C'**	-
Ar-C	128.1	**Ar-C'**	-
Ar-C	127.8	**Ar-C'**	-
Ar-C	127.5	**Ar-C'**	-
Ar-C	127.4	**Ar-C'**	-
C-7	74.4	**C-7'**	74.1
C-8	52.2	**C-8'**	46.9
C-9	59.9	**C-9'**	60.4

C-17	47.4	**C-17'**	45.0
C-24	44.9	**C-24'**	43.2
C-13,14,15	25.8	**C-13',14',15'**	25.5
C-16	18.1	**C-16'**	18.0
C-12	-4.4	**C-12'**	-4.7
C-11	-5.1	**C-11'**	-5.7

The ^{1}H NMR spectrum showed the peaks for both diastereomers **225 a/b**, and by combining the partial integrations of the peaks from both the major and the minor diastereomers, the full integration values were obtained (**Table 63**). The aromatic protons integrated for 14 protons found in the aromatic region belonging to all the three aromatic rings. The most deshielded peak at 7.77 ppm belongs to NH of the amide, as it does not show coupling to any peaks in any 2D spectrum. All the integration values were referenced against the H-7 peaks, where the two partial integrations combined from the two peaks were assigned an integration value of one proton. H-17 protons belonging to both the major and the minor diastereomers were found at 4.82, 4.67 amd 3.96 ppm, and the partial integrations for the three peaks combined to make up for two protons. These were found using the HSQC spectrum, as they showed coupling to C-17 carbon peaks belonging to both the major and minor diastereomer.

H-24 also integrated for 2 protons and the integrations were found by combining all the partial integrations from the peaks belonging to H-24 found from the HSQC spectrum through coupling with the same carbon peaks. H-9 peaks also integrated for 2 protons and were found using HSQC spectrum through their corresponding carbon peaks. They appeared as multiplets coupling to each other as well as to neighbouring H-8 protons. H-8 peaks were also found using the HSQC spectrum. The rest of the peaks in the shielded region belong to the TBDMS protons. The ^{13}C NMR spectrum did not show the peaks belonging to the aromatic carbons from the minor diastereomer, this was due to the poor intensity of the NMR spectrum as a result of a small amount of product being available for the NMR spectra.

3.2.1.4.2.2. Using propylamine.

The next reaction was the addition of propylamine to carboxylic acid **222** to obtain an amide product **226** (**Figure 51**). The product was successfully obtained, as verified using NMR spectroscopy (**Table 65**).

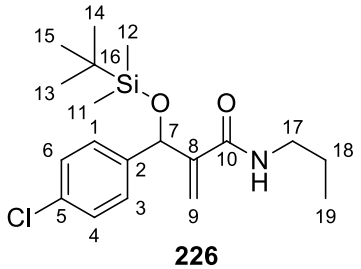

226

Figure 51: Amide product **226** prepared using propylamine.

Table 65: The IR and the NMR data obtained for product **226**.

Compound No.	**NMR**
226	**^{1}H NMR (400 MHz, $CDCl_3$)** δ 7.22 – 7.14 (4H, m, Ar-H), 6.53 (1H, br s, N-H), 5.99 (1H, s, H-9a), 5.49 (1H, s, H-9b), 5.46 (1H, s, H-7), 3.11 – 2.97 (2H, m, H-17), 1.35 – 1.23 (2H, m, H-18), 0.86 (9H, s, H-13,14,15), 0.73 – 0.65 (3H, m, H-19), 0.03 (3H, s, H-11), 0.01 (3H, s, H-12). **^{13}C NMR (101 MHz, $CDCl_3$)** δ 165.7 (C-10), 144.5 (C-8), 140.2 (Ar-C), 133.2 (Ar-C), 128.4 (Ar-C), 127.0 (Ar-C), 122.0 (C-9), 75.1 (C-7), 40.9 (C-17), 25.8 (C-13,14,15), 22.6 (C-18), 18.2 (C-16), 11.3 (C-19), -4.9 (C-12), -5.1 (C-11).

The NMR spectrum showed all the important signals, such as the aromatic signals integrating for 4 protons. The amide NH peak appeared as a broad singlet at 6.53 ppm. The terminal alkene H-9 peaks appeared as singlets, and their corresponding C-9 peak was found at 122.0 ppm, as seen from the HSQC spectrum. The H-7 peak appeared as a singlet around 5.46 ppm and its corresponding carbon peak was found at 75.1 ppm. H-17 and H-18 were also seen, both integrating for 2 protons, with H-17 being more deshielded at 2.97 ppm compared to H-18 at 1.30 ppm. The

other three peaks in the shielded region belong to TBDMS protons. All the carbon peaks were assigned using the HSQC spectrum following the coupling pattern and confirmed using the DEPT spectrum.

3.2.1.5. Attempted conjugate addition reaction on amide adduct.

The last step attempted was the conjugate addition reaction on the amide **224** (**Scheme 65**) to give compound **227**. This reaction was done using different amines in the presence of triethylamine as a catalyst in THF and refluxed overnight.[95] The reaction was unsuccessful and did not give the desired product, the starting material was recovered.

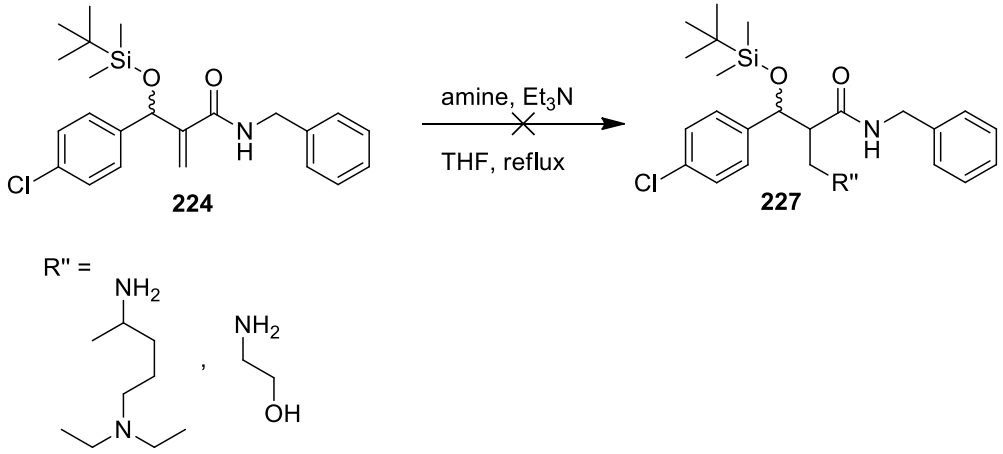

Scheme 65: An attempted conjugate addition reaction on the amide product **224**.

The first four steps were successfully performed however, the conjugate addition reaction on the amide product **224** did not give the desired product. Very low yields were obtained for the steps involving hydrolyzing the ester and conversion into an amide. Alternative routes were attempted to improve the yields of the amide adducts, as well as obtaining the conjugate addition product.

3.2.2. Alternative routes to obtaining MBH amide and its conjugate addition product.

A few methods were applied to try and improve the overall yields of the amide product and the conjugate addition amide product. The hydrolysis of the protected ester gave very poor yield, as seen in the previous section and therefore, alternative routes were considered.

3.2.2.1. The first approach

The first approach involved synthesizing an MBH ester **228** and protecting it and then performing a conjugate addition reaction on the protected MBH ester **229** since this has been proven to work really well. The conjugate addition product **230** could then be converted into a carboxylic acid **231** through a hydrolysis reaction, followed by synthesizing an amide **232** by conversion of the carboxylic acid (**Scheme 66**).

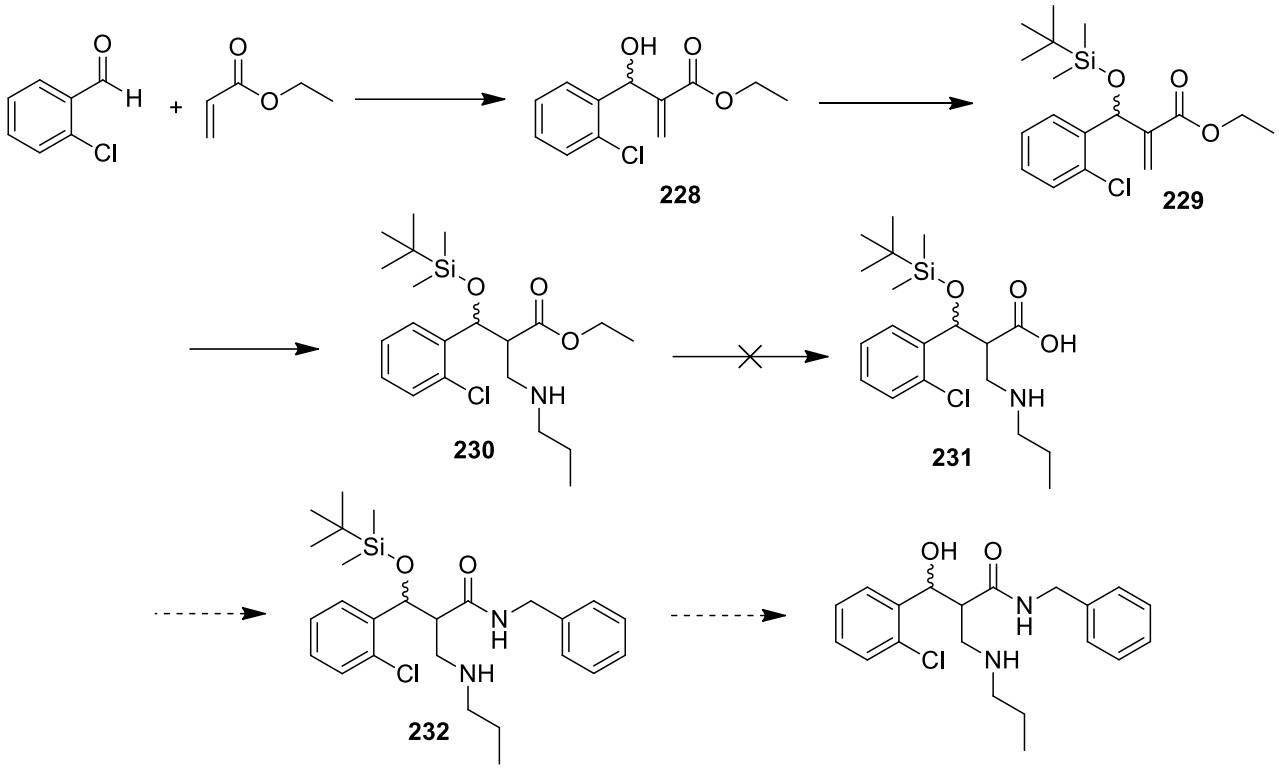

Scheme 66: The first alternative route.

3.2.2.1.1. Synthesis of the MBH ester adducts.

The first step involved synthesizing an MBH adduct **228** and this was done using the same method previously reported (**Scheme 67**), using 2-chlorobenzaldehyde **233** and ethyl acrylate **234** in the presence of DABCO at room temperature [69] The reaction was successful and gave **228** (**Figure 52**) in a very good yield of 87%. The product identity was confirmed using IR and NMR spectroscopy (**Table 66**).

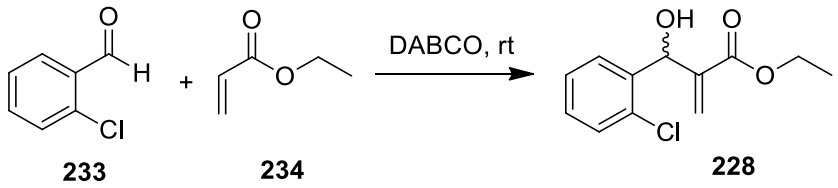

Scheme 67: The MBH reaction on 2-chlorobenzaldehyde **233** and the ethyl acrylate **234** in the presence of DABCO, at room temperature.

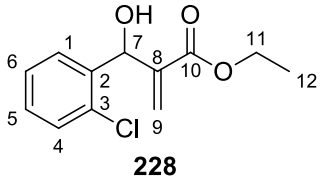

Figure 52: Compound **228** obtained from compound **233** and **234**.

Table 66: The IR and the NMR data obtained for compound **228**.

Compound No.	**IR** (neat, cm^{-1})	**NMR**
228	3440 (OH), 2982 (C-H), 1703 (C=O)	**^{1}H NMR (300 MHz, $CDCl_3$)** δ 7.56 (1H, dd, *J*=7.7,1.9 Hz, Ar-H), 7.39 – 7.32 (1H, m, Ar-H), 7.32 – 7.21 (2H, m, Ar-H), 6.35 (1H, s, H-9a), 5.98 (1H, d, *J*=4.9 Hz, H-7), 5.58 (1H, s, H-9b), 4.23 (2H, q, *J* = 7.2 Hz, H-11), 3.28 (1H, d, *J*=4.8 Hz, OH), 1.28 (3H, t, *J* = 7.2 Hz, H-12) **^{13}C NMR (75 MHz, $CDCl_3$)** δ 166.6 (C-10), 140.8 (C-2), 138.3 (C-8), 132.9 (Ar-C), 129.5 (Ar-C), 129.0 (Ar-C), 128.2 (Ar-C), 127.1 (C-1), 126.7 (C-9), 69.5 (C-7), 61.1 (C-11), 14.1 (C-12).

The IR spectrum showed the presence of all the important signals, such as the alcohol signal at 3440 cm^{-1} and the carbonyl signal at 1703 cm^{-1}. The NMR spectra also confirmed the formation of the expected product, as it showed the presence of the hydroxyl signal at 3.28 ppm. The aromatic signals were present between 7.21-7.56 ppm. All the other signals were present such as the terminal

alkene protons around 6.35 and 5.58 ppm, appearing as singlets. Their corresponding C-9 signal was found at 126.7 ppm. The other signal at 5.98 ppm belongs to H-7, integrating for 1 proton and appearing as a doublet. It shows coupling to the OH proton from the COSY spectrum and to the neighbouring aromatic protons from the HMBC spectrum. The corresponding C-7 signal was found at 69.5 ppm.

The next signal belongs to H-11, integrating for 2 protons, and gives a quartet coupling pattern, as it would couple to its neighbouring H-12 protons. The next signal was the OH signal, appearing as a doublet and coupling to the neighbouring H-7 proton. The most shielded peak integrates for 3 protons and belongs to the methyl group, appearing as a triplet and coupling to the neighbouring CH_2 protons. The C-12 carbon peak was found at 14.1 ppm, as determined from the HMBC spectrum. The most deshielded peak in the ^{13}C NMR spectrum belongs to the carbonyl carbon at 166.6 ppm. All the carbon peaks were assigned using the HSQC spectrum and confirmed using the DEPT spectrum.

3.2.2.1.2. Protection of the alcohol group on the MBH ester adduct.

The second step was the protection of the alcohol group on the ester adduct **228**. The method used was the same as previously described, using TBDMSCl in the presence of imidazole as the base in anhydrous DMF at room temperature under nitrogen (**Scheme 68**).[81] The protected ester **229** (**Figure 53**) was obtained with a very good yield of 83% and the product identity was verified using NMR spectroscopy (**Table 67**).

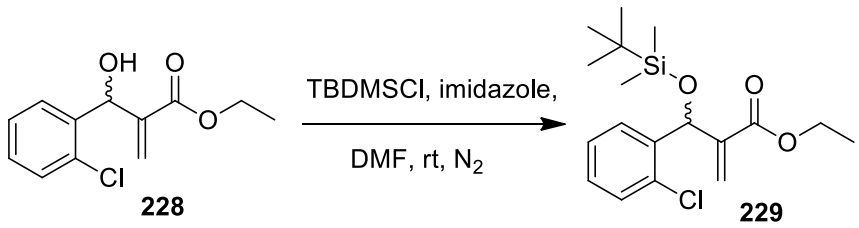

Scheme 68: Protection of the alcohol group on the MBH ester adduct **228**.

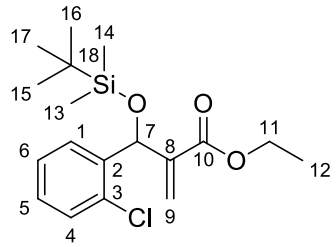

229

Figure 53: Protection of alcohol on the MBH ester adduct **228**.

Table 67: The IR and the NMR data obtained for the adduct **229**.

Compound No.	**NMR**
229	**^{1}H NMR (400 MHz, $CDCl_3$)** δ 7.45 – 7.40 (1H, m, Ar-H), 7.32 – 7.27 (1H, m, Ar-H), 7.24 – 7.13 (2H, m, Ar-H), 6.30 (1H, s, H-9a), 6.03 (1H, s, H-7), 5.85 (1H, s, H-9b), 4.21 – 4.06 (2H, m, H-11), 1.21 (3H, t, *J* = 7.1 Hz, H-12), 0.85 (9H, s, H-15,16,17), 0.09 (3H, s, H-13), -0.11 (3H, s, H-14). **^{13}C NMR (101 MHz, $CDCl_3$)** δ 165.9 (C-10), 143.2 (C-8), 140.0 (Ar-C), 132.7 (Ar-C), 129.23 (Ar-C), 129.18 (Ar-C), 128.6 (Ar-C), 126.7 (Ar-C), 125.1 (C-9), 69.0 (C-7), 60.7 (C-11), 25.8 (C-15,16,17), 18.1 (C-18), 14.1 (C-12), -4.9 (C-14), -5.0 (C-13).

The ^{1}H NMR spectrum showed the presence of all the expected signals such as the aromatic signals in the 7.13-7.45 ppm, integrating for 4 protons. The H-9 proton, as for other adducts, appeared as two separate peaks and as singlets, not coupling to any protons. H-7 also appeared as a singlet around 6.03 ppm and its corresponding carbon peak was found at 69.0 from the HSQC spectrum. The next two peaks belonged to the ethyl group, where CH_2 is more deshielded compared to the CH_3 group.

The CH_2 proton peak integrated for 2 protons and appeared as a multiplet, coupling to the neighbouring CH_3 protons. The other peak integrated for 3 protons and belonged to the methyl group; it appeared as a triplet, coupling to the neighbour CH_2 protons. The corresponding C-11 and C-12 peaks were found using the HSQC spectrum around 60.7 and 14.1 ppm, respectively.

The rest of the peaks in the shielded region belong to the TBDMS protons. The most deshielded peak in the carbon NMR belongs to the carbonyl carbon at 165.9 ppm; all the other carbon peaks were assigned using the 2D spectrum.

3.2.2.1.3. Conjugate addition reaction on the protected MBH ester adduct 229.

The next step was the nucleophilic addition reaction using propylamine, which was done using a very simple method. The propylamine and the alcohol protected ester adduct **229** were stirred at room temperature in methanol (**Scheme 69**).[69] The product **230** was successfully obtained as a mixture of diastereomers (**Figure 54**).

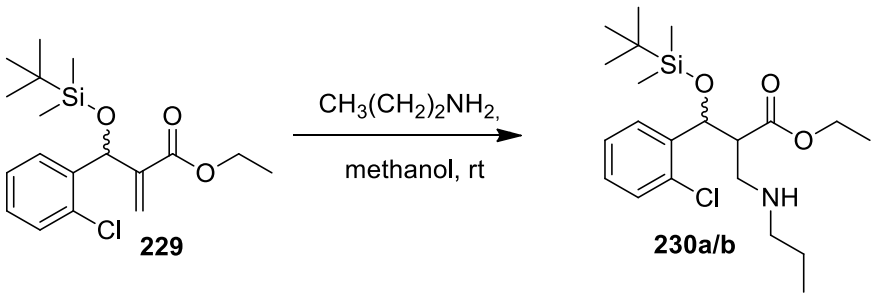

Scheme 69: Conjugate addition reaction on the alcohol protected MBH ester adduct **299** to form **230a/b**.

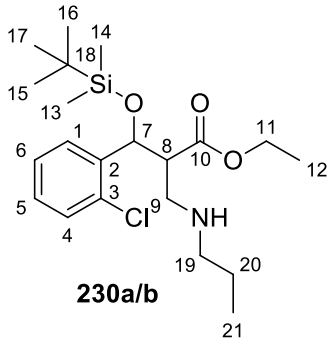

Figure 54: The diastereomer **230a/b** obtained from the addition reaction on **229**.

Table 68: The integrations obtained from the ^{1}H NMR spectrum for both the major and minor diastereomer **230a/b.**

Major and Minor diastereomer combined (**230a/b**)

Assignment	**Combining partial integrations**	**Overall integration**
Ar-H	1H + 1H + 2H	4H
H-7	0.72H + 0.22H	1H
H-11	2H	2H
H-9	1H + 1H	2H
H-8	1H	1H
H-19	1.71H + 0.54H	2H
NH	1H	1H
H-20	2H	2H
H-12	1H + 2H	3H
H-15,16,17	7H + 2H	9H
H-21	3H	3H
H-13	3H	3H
H-14	3H	3H

Table 69: The chemical shift values from the ^{13}C NMR of the conjugate addition product **230a/b**.

Assignment	Major diastereomer	**Assignment**	Minor diastereomer
C-10	172.7	**C-10'**	173.3
Ar-C	140.0	**Ar-C'**	140.4
Ar-C	131.6	**Ar-C'**	132.2
Ar-C	129.3	**Ar-C'**	129.2
Ar-C	129.0	**Ar-C'**	129.1
Ar-C	128.7	**Ar-C'**	128.8
Ar-C	126.5	**Ar-C'**	127.0
C-7	71.2	**C-7'**	71.2
C-11	60.6	**C-11'**	60.4
C-8	48.1	**C-8'**	48.1
C-19	51.8	**C-19'**	51.4

C-9	46.3	**C-9'**	46.3
C-15,16,17	25.7	**C-15',16',17'**	25.6
C-20	23.1	**C-20'**	23.0
C-18	18.0	**C-18'**	17.9
C-12	14.0	**C-12'**	14.2
C-21	11.7	**C-21'**	11.6
C-14	-4.8	**C-14'**	-4.9
C-13	-5.5	**C-13'**	-5.5

The partial integrations of the two diastereomers were combined to give full integration values (**Table 68**). H-7 peaks were used as the reference peaks, as the two H-7 peaks combined were assigned an integration value of 1 proton. The most deshielded peaks between 7.15-7.60 ppm integrated for 4 protons and belong to the aromatic protons. All the aromatic peaks appeared as multiplets coupling to each other. The next two peaks belong to H-7, the two peaks combined integrated for 1 proton. These peaks appeared as doublets coupling to the neighbouring H-8 protons. The corresponding C-7 peaks were found at 71.2 ppm. The next peak belongs to H-11 and integrated for 2 protons; appearing as a multiplet coupling to the neighbouring CH_3 protons. The corresponding C-11 peaks were found at 60.6 and 60.4 ppm using the HSQC spectrum.

H-9 peaks were found at 3.12 and 2.69 ppm for both the major and the minor diastereomer, appearing as doublets of doublets coupling to each other and to the neighbouring H-8 proton. The C-9 carbon peaks were found at 46.3 ppm. The H-8 proton peak was found at 2.97 ppm, appearing as a multiplet coupling to the neighbouring H-7 and H-9 protons. The C-8 peaks were found around 52.2 ppm and 48.1 ppm. The H-19 proton peaks were found between 2.47 and 2.31 ppm, integrating for 2 protons. They appeared as a triplet and a multiplet coupling to the neighbouring H-20 protons. The corresponding carbon peaks were found using HSQC.

The next peak integrated for 3 protons and belongs to the NH group and H-20. The corresponding C-20 peaks were found at 23.1 and 23.0 ppm. The next two peaks belong to H-12, integrating for 3 protons and appearing as a multiplet coupling to the neighbouring H-11 protons. H-21 was found at 0.84 ppm integrating for 3 protons, coupling to the neighbouring H-20 protons. The C-21 peaks

were found at 11.7 and 11.6 ppm. The rest of the proton peaks belong to the TBDMS protons. All the carbon peaks were assigned using the HSQC spectrum.

3.2.2.1.4. Hydrolysis of the ester on the conjugate addition product 230.

The next step involved converting the ester **230** to a carboxylic acid **231** through a hydrolysis reaction using KOH in water. The reaction was performed in ethanol at 70 ˚C (**Scheme 70**). This reaction did not work well as it did not give the expected product and the starting material was recovered.[69]

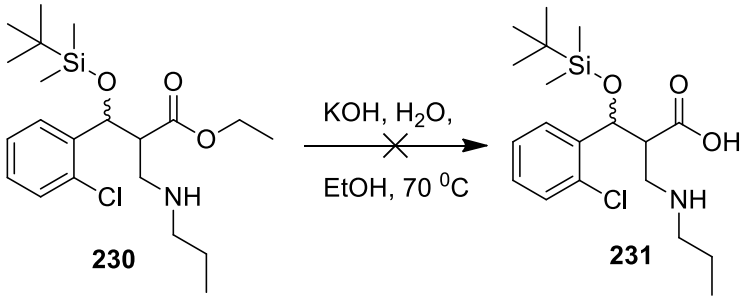

Scheme 70: Attempted hydrolysis of ester **230** to form compound **231**.

The first approach did not work well, since it was able to do a conjugate addition reaction on the protected ester **229**, however, could not go any further to convert the conjugate addition product **230** into a carboxylic acid **231** and then to an amide **232**.

3.2.2.2. The second approach

As a result of the problems encountered with the first approach, another route was tested. The second approach involved synthesizing the carboxylic acid **235** first from the MBH ester **228** through ester hydrolysis and then protecting the carboxylic acid to form **236** and further reacting it with an amine, and deprotecting it to obtain amide **237**. The protection step is very important for the nucleophilic addition reaction since it controls the diastereoselectivity during the conjugate addition reaction. The second approach was tested based on the fact that the hydrolysis of an unprotected MBH ester, which was similar to compound **228,** was previously performed in our laboratory and was reported to work very well.[40]

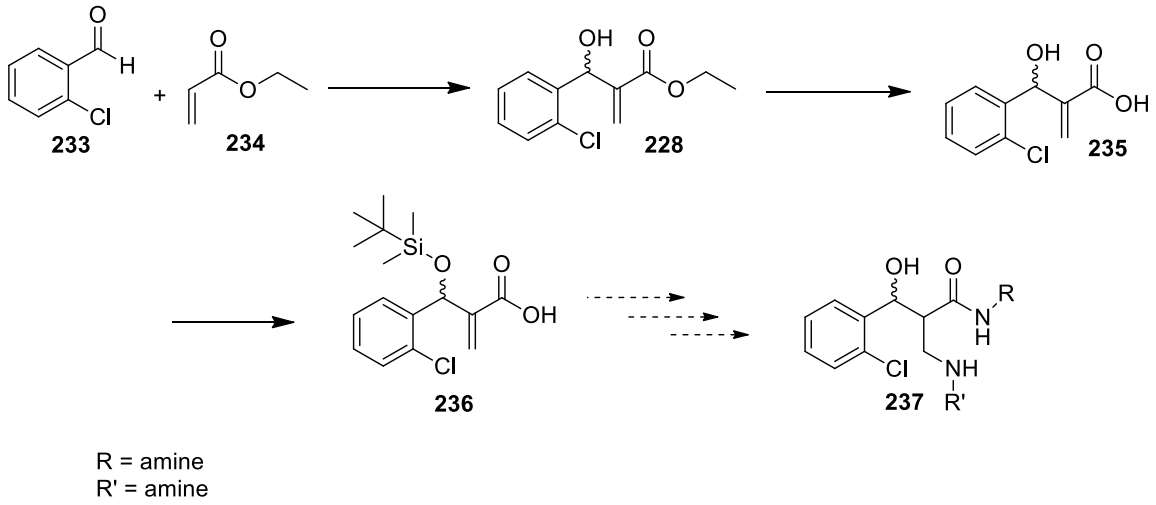

Scheme 71: The second alternative route to obtaining amide containing conjugate addition product **237**

3.2.2.2.1. Hydrolysis of the unprotected MBH ester adduct 228.

The first step was the synthesis of the MBH adduct **228**, which has been synthesized before and reported in section 3.2.2.1.[69] The second step was the hydrolysis of this adduct **228**, using the method shown above, which has previously been used in our laboratory on a similar compound. The method involved using potassium hydroxide in ethanol and refluxing the MBH adduct containing mixture for 4 hours.[69] After the reaction was complete, starting material was extracted using ethyl acetate. The aqueous layer obtained, acidified and again extracted with ethyl acetate (**Scheme 72**). The expected product **235** (**Figure 55**) was obtained and the identity confirmed using IR and NMR spectroscopy (**Table 70**).

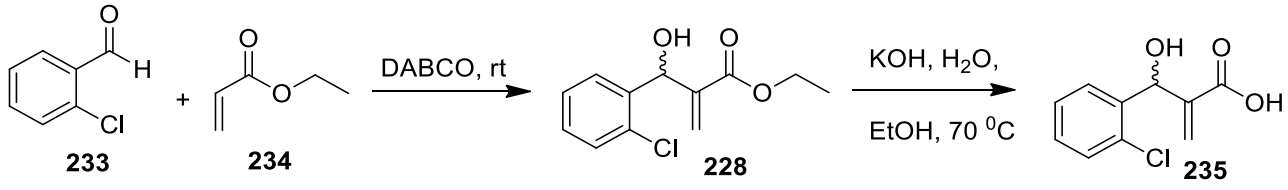

Scheme 72: The formation of the MBH ester adduct **228** and its conversion into a carboxylic acid **235** through ester hydrolysis.

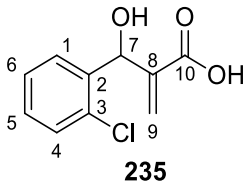

235

Figure 55: Carboxylic acid **235** obtained by the hydrolysis of ester **228**.

Table 70: The IR and the NMR data obtained for compound **235**.

Compound No.	**IR** (neat, cm^{-1})	**NMR**
235	3359 (OH), 1683 (C=O)	**^{1}H NMR (400 MHz, $CDCl_3$)** δ 7.58 – 7.53 (1H, m, Ar-H), 7.39 – 7.23 (3H, m, Ar-H), 6.49 (1H, s, H-9a), 5.99 (1H, s, H-7), 5.68 (1H, s, H-9b), 5.27 (2H, br s, OH). **^{13}C NMR (101 MHz, $CDCl_3$)** δ 171.2 (C-10), 140.0 (C-8), 138.0 (Ar-C), 132.8 (Ar-C), 129.6 (Ar-C), 129.5 (C-9), 129.2 (Ar-C), 128.1 (Ar-C), 127.1 (Ar-C), 69.0 (C-7).

The IR spectrum showed the OH and the carbonyl stretches at 3359 and 1683 cm^{-1} (**Table 70**), respectively. The absence of the ethyl group and the presence of an OH signal confirmed the formation of a carboxylic acid. The ^{1}H NMR showed the aromatic signals integrating for 4 protons as expected. It also showed the terminal alkene protons, H-9 appearing as two separate peaks at 6.49 and 5.68 ppm. The H-9 peaks appeared as singlets, showing no coupling to any other protons. The C-9 peak was found at 129.5 ppm from the HSQC spectrum. The H-7 peak was found between the two H-9 peaks, around 5.99 ppm, appearing as a singlet, showing no coupling. The corresponding C-7 peak was found at 69 ppm from the HSQC spectrum. The next peak was broad and belonged to the 2 OH protons. It appeared as a broad singlet, coupling to no other protons. The HMBC spectrum showed coupling of the H-9 protons to the C-7, C-8, and the carbonyl carbon signal. The H-7 signal showed coupling to the C-8, the carbonyl and the aromatic carbon peaks.

3.2.2.2.2. Protection of the alcohol group on the carboxylic acid 235.

The next step was the protection of OH group on compound **235**, which was done using the same method shown above using TBDMSCl in anhydrous DMF under nitrogen at room temperature (**Scheme 73**).[81] The reaction gave the expected product **236** in a low yield of 17%, along with a byproduct. The byproduct was suspected to be the compound where both OH groups were protected instead of only the desired OH group but there wasn't enough material to confirm this. The identity of the product **236** (**Figure 56**) was confirmed using IR and NMR spectroscopy (**Table 71**).

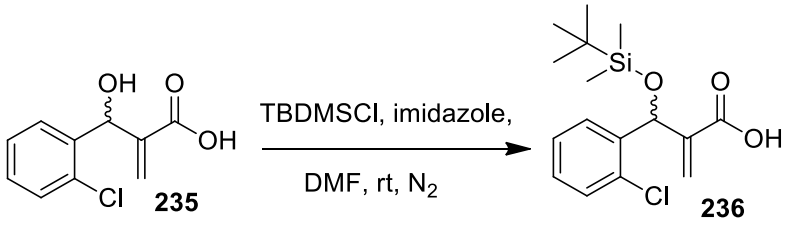

Scheme 73: Protection of the alcohol group on compound **235** to form compound **236**.

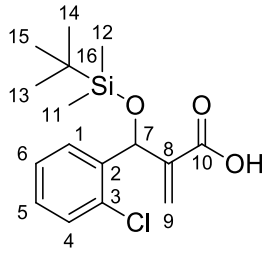

236

Figure 56: Compound **236** obtained from the protection of OH on **235**.

Table 71: The IR and the NMR data obtained for compound **236**.

Compound No.	**IR** (neat, cm^{-1})	**NMR**
103	2949 (C-H), 1687 (C=O), 835 (Si-O)	**^{1}H NMR (400 MHz, $CDCl_3$)** δ 7.52 – 7.47 (1H, m, Ar-H), 7.34 – 7.28 (1H, m, Ar-H), 7.26 – 7.17 (2H, m, Ar-H), 6.39 (1H, s, H-9a), 6.03 (1H, s, H-7), 5.87 (1H, s, H-9b), 0.88 (9H, s, H-13,14,15), 0.11 (3H, s, H-11), -0.07 (3H, s, H-12)

		^{13}C NMR (101 MHz, $CDCl_3$) δ 169.0 (C-10), 141.5 (C-8), 139.3 (Ar-C), 132.5 (Ar-C), 129.4 (Ar-C), 128.9 (Ar-C), 128.8 (Ar-C), 127.6 (C-9), 126.8 (Ar-C), 69.4 (C-7), 25.7 (C-13,14,15), 18.1 (C-16), -4.9 (C-11), -5.1 (C-12).

The IR spectrum showed a carbonyl stretch at 1687 cm^{-1}. The NMR spectra showed the presence of all the expected signals. The absence of the OH signal and the presence of the TBDMS group confirmed the formation of the product. The ^{1}H NMR spectrum showed the presence of the aromatic proton signals integrating for 4 protons. H-9 appeared as two separate signals around 6.39 and 5.87 ppm, and their corresponding carbon peak was at 127.6 ppm. H-9 showed coupling to the neighbour C-7 as well as carbonyl carbon peaks in the HMBC spectrum. The H-7 peak appeared around 6.03 ppm, integrating for 1 proton, and showing a cross-peak to a carbon peak at 69.4 ppm in the HSQC spectrum. The rest of the peaks in the shielded region belong to the TBDMS protons as they are typically found in that region. All the carbon peaks were assigned using the HSQC spectrum and the DEPT spectrum.

The second approach was successful until the protection of hydroxyl group on compound **235** to form compound **236**. However, compound **236** was obtained in low yield and a byproduct was also formed. The second approach did not work since there was not enough product **236** present to perform the next step on it.

3.2.2.3. The third approach

As a result of the problems encountered with the second approach, a third approach was tested. This approach involved performing a conjugate addition reaction on the alcohol protected carboxylic acid adduct **238** first to form compound **239**, before converting it into an amide **240**. This method was tested because the originally proposed route gave the undesired byproduct **225a/b** for the amide synthesis step, where the amine would also add on to the alkene doing an unplanned conjugate addition reaction giving the desired product **224** in a lower yield. Hence, an attempt was made to improve the yield by doing the conjugate addition reaction first using the desired amine and then synthesizing an amide **240** using a different amine (**Scheme 74**).

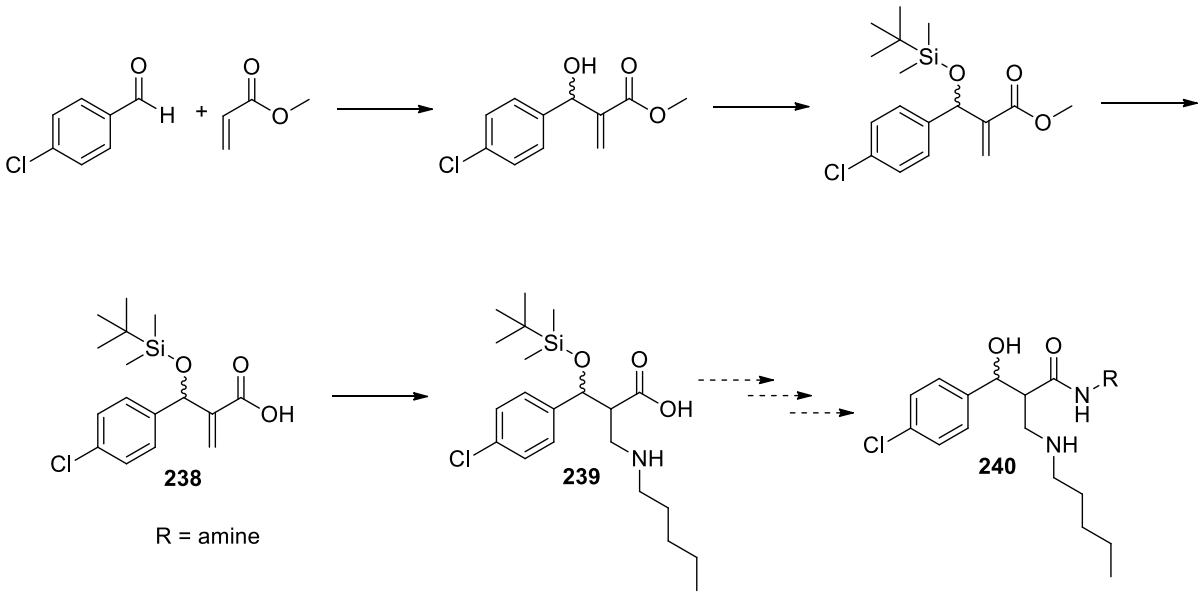

Scheme 74: The third alternative route to obtaining an amide and performing a conjugate addition reaction.

The first step was synthesizing an ester adduct, followed by protecting it and then converting it into a carboxylic through ester hydrolysis. All these steps have been performed before in the originally proposed route using the same starting materials, the only difference from the original route was to perform the nucleophilic addition first on the protected carboxylic acid **238** before converting it into an amide **240**.

3.2.2.3.1. Performing a conjugate addition reaction on compound 238 to form compound 239.

The conjugate addition reaction was done using the same method shown in section 3.2.1.5, using the amine, 1-aminopentane and triethylamine in THF under reflux, until the reaction was complete to give compound **239** (**Scheme 75**).[95]

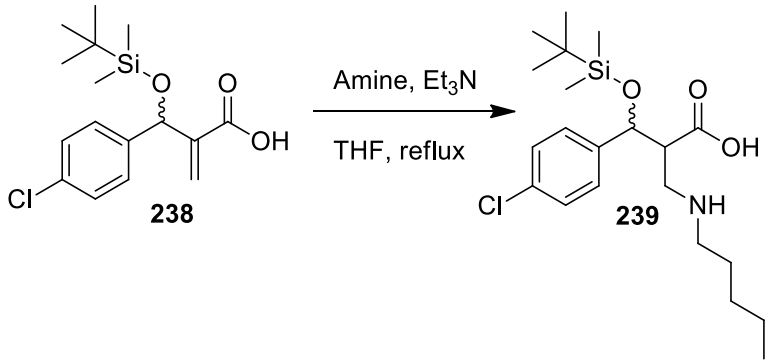

Scheme 75: The conjugate addition reaction on the protected carboxylic acid **238**.

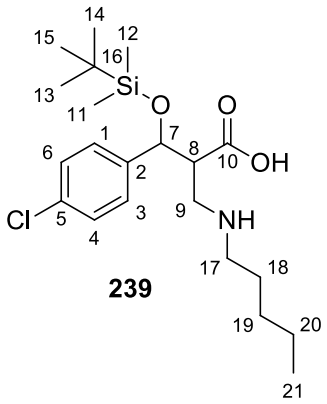

Figure 57: Product **239** obtained from the conjugate addition reaction on the protected carboxylic acid **238**.

Table 72: NMR data obtained for compound **239.**

Compound No.	**NMR**
239	**^{1}H NMR (300 MHz, $CDCl_3$)** δ 7.43 – 7.37 (2.80H, m, Ar-H), 7.35 – 7.25 (0.66H, m, Ar-H), 7.21 – 7.13 (0.49H, m, Ar-H), 5.21 (0.30H, d, *J*=6.2 Hz, H-7), 5.05 (0.71H, d, *J*=7.4 Hz, H-7), 4.34 – 4.23 (0.32H, m, H-8), 3.96 (0.20H, s), 3.94 – 3.87 (0.31H, m, H-9), 3.87 – 3.81 (0.08H, m, H-17), 3.64 – 3.50 (1.17H, m, H-17), 3.50 – 3.45 (0.70H, m, H-17), 3.47 – 3.40 (1.88H, m, H-9), 3.05 – 2.95 (1.05H, m, H-8), 1.44 – 1.35 (0.88H, m, H-18), 1.34 – 1.28 (1.73H, m, H-19), 1.30 – 1.24 (1.28H, m, H-18), 1.25 – 1.15 (2.33H, m, H-

	20), 1.02 – 0.85 (12.28H, m, H-13,14,15,21), 0.14 (1H, s, H-11) , 0.11 (2H, S, H-11), -0.09 (1H, s, H-12), -0.14 (2H, s, H-12)

From the NMR data it looked as if the expected product had been made. However, it was not confirmed as the data was very difficult to interpret as the product was obtained as a mixture of diastereomers and due to its complex structure, it was difficult to confirm that the desired product had been obtained.

None of the approaches tested could give the desired conjugate addition product on the MBH adduct carrying amide as the electron withdrawing group, and due to time constraints, the last step could not be achieved. The yields of the ester hydrolysis and the amide synthesis step did not improve; hence, the conjugate addition product could not be obtained.

CHAPTER FOUR

4. CONCLUSION AND FUTURE WORK

4.1. Conclusion

MBH adducts **152-159** were successfully synthesized using the Morita-Baylis-Hillman reaction. These MBH adducts were successfully protected using TBDMS and TMS protecting groups. The conjugate addition reactions using different nitrogen and sulfur nucleophiles were successfully performed and the final step, which was the deprotection, gave the desired compounds (**Scheme 76**). The identity of the products was verified by different characterization methods: the melting point, IR, 1D and 2D NMR spectroscopy. All the characterization data showed the successful formation of the products.

All the MBH adducts belonging to a specific activated alkene had very similar IR, ^{1}H and ^{13}C NMR spectra, due to minor differences in their structure such as the substituent on the aromatic ring. High yields were obtained for all the adducts in a range of 70-80%, except for compound **152** and **159** which gave yields below 61%. The alcohol protection step also gave very good yields for both TBDMS and TMS protecting groups. The conjugate addition reactions with different nucleophiles were successful. However, the yields were low, and the byproducts, the allylic substitution products, were also obtained.

The effect of the protecting group on the conjugate addition reactions was determined. From the results obtained it was clear that the protecting group did not have much of an effect on the formation of the diastereomers and the diastereomeric ratios. The diastereomers were mostly obtained in a ratio of 1:2, which would normally be obtained in an unprotected version of the adducts. It is also clear that the occurrence of the side reaction, the allylic substitution reaction is independent of the type of protecting group used, as well as the type of adduct present (ester/nitrile). However, the type of nucleophile used, does influence the occurrence of the allylic substitution reaction as well as the diastereoselectivity of the conjugate addition reaction. The results also showed that the type of adduct, whether nitrile or ester did not have any effect on the nucleophilic addition reaction.

The deprotection of the conjugate addition products was carried out in very good yields. It allowed for better definition of the NMR spectra of the conjugate addition products, allowing the determination of the structures of the major and minor diastereomers. The major diastereomer was obtained with a *syn*-configuration, while the minor diastereomer was obtained with an *anti*-configuration.

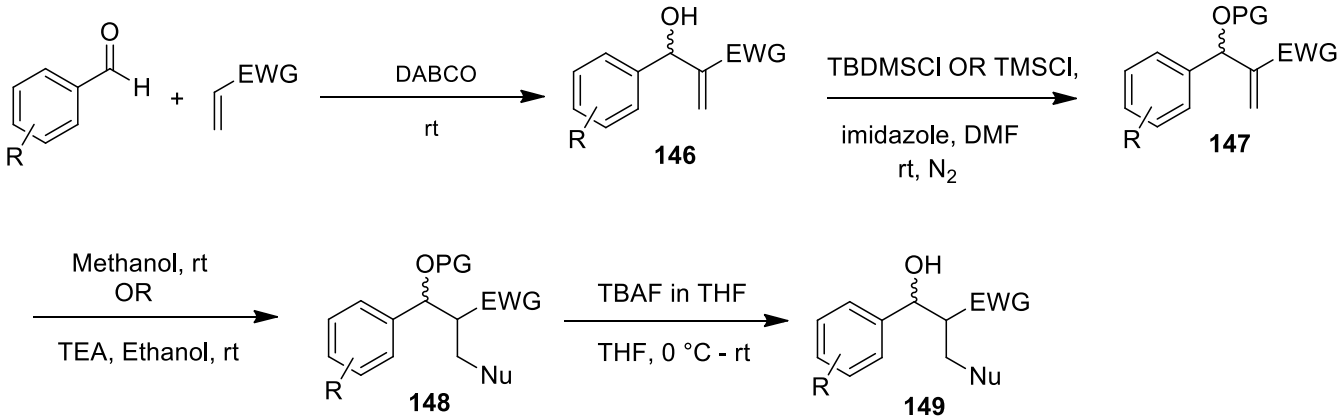

R = H, 4-Cl, 4-NO_2, 2-Br, 2-Cl
EWG = CO_2Me, CN, COMe
PG = TBDMS, TMS
Nu = amine and sulfur Nu

Scheme 76: Diastereomeric compounds obtained from the MBH adducts using different nucleophiles.

The MBH adducts carrying amide as the electron withdrawing groups were successfully obtained. However, the conjugate addition reactions on these compounds were not successfully performed. Alternative routes were attempted, however, none of them led to the desired conjugate addition product on the amide adduct. MBH amide adducts were also characterized using the melting point, IR, 1D and 2D NMR spectroscopy. These characterizations showed the successful formation of the amide adducts. From all the alternative routes the most successful route was the originally proposed route, involving the hydrolysis of the MBH ester adduct to obtain the carboxylic acid and its conversion into an amide. Due to time constraints the last step, which was the formation of the conjugate addition product on the amide adducts could not be achieved.

4.2. Future work

Future work should involve synthesizing a variety of MBH adducts with differently substituted benzaldehydes and methyl vinyl ketone as the activated alkene using the MBH reaction. A better method for the synthesis of these methyl vinyl ketone adducts is needed since the normal conditions using benzaldehyde and methyl vinyl ketone in DABCO did not give a clean reaction. Future work should also involve applying different methods for the MBH reaction to improve the reaction duration. Different catalysts also need to be applied instead of DABCO, to determine their effect on the MBH reaction.

Other protecting groups need to be tested in the protection of the hydroxyl group, which are bulkier than the TBDMS group and also smaller than the TMS group. The effect of these different groups on the subsequent conjugate addition reaction needs to be investigated. More unprotected adducts need to be synthesized to compare diastereomeric ratios obtained from the subsequent conjugate addition reaction with those of the different protected adducts. Conjugate addition reactions using different nucleophiles need to be investigated, such as the phosphorus and oxygen nucleophiles. Future work should also focus on other ways to determine the confirmation of the major and minor diastereomers obtained from the conjugate addition reaction.

Future work should also focus on new methods to obtain the MBH adducts carrying amide as the electron withdrawing group with better yields and also methods need to be investigated for performing successful conjugate addition reactions on these compounds. Different amine nucleophiles with long alkyl chains need to be added to the amide MBH adducts so that the biological properties of these compounds can be investigated. Work should also focus on generating more structures that would mimic the antibacterial peptides.

CHAPTER FIVE

5. EXPERIMENTAL PROCEDURES

5.1. Purification of solvents and reagents

All the solvents that were required for the reactions and purification using column chromatography were dried, distilled, and stored under nitrogen atmosphere before use. Solvents like toluene and THF were distilled and dried over sodium wires and benzophenone was used as an indicator. Calcium hydride was used to distill dichloromethane and dimethylformamide.

5.2. Chromatography

Thin layer chromatography (TLC) was used to monitor the reaction; Merck silica gel 60 F_{254} plates with aluminium backings were used. Column chromatography to purify compounds was done using normal silica gel with particle size 0.063-0.200 mm or flash silica gel with particle size 0.040-0.063 mm, purchased from Merck.

5.3. Spectroscopy and physical data

Melting points were determined using open capillary tubes on a Stuart SMP 10 apparatus for all the compounds and are uncorrected. All the infrared spectra were acquired using Bruker tensor 27 single channel infrared spectrometer by directly loading the sample on the instrument. All the NMR spectra were obtained using either a Bruker AVANCE 300 MHz, Bruker AVANCE 400 MHz or Bruker AVANCE III 500 MHz instrument. All the spectra were recorded using deuterated chloroform. All the chemical shift values for both ^{1}H and ^{13}C NMR spectra are reported in parts per million (ppm) and all the spectra are referenced against the internal standard, tetramethyl silane (TMS), which is found at zero parts per million. All the coupling constants are reported in Hertz (Hz). HRMS data were recorded using an ESI positive source.

5.4. Preparation and characterization of ester, nitrile, and ketone MBH adducts and their conjugate addition products.

5.4.1. General procedure for the synthesis of MBH adducts.

To a mixture of the appropriate benzaldehyde (0.098 mol) and activated alkene (0.608 mol) was added DABCO (0.098 mol). The reaction mixture was stirred at room temperature until the

reaction was complete. Upon completion of the reaction, water was added, and the solution was extracted with ethyl acetate. The organic layer obtained was dried over anhydrous Na_2SO_4, filtered and concentrated *in vacuo*. The product was then purified by column chromatography using 40% ethyl acetate in hexane.

5.4.1.1. Synthesis of methyl 2-(hydroxy(phenyl)methyl)acrylate (152)

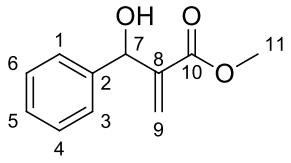

152

Benzaldehyde (2 g) and methyl acrylate (10.53 ml) were used, and the mixture was stirred for 2 days affording the desired product **152** as white solid (2.15 g, 59%). M.P: 38-40 ˚C, R_f = 0.70 (40% ethyl acetate:hexane). IR ν_{max} (neat,cm^{-1}) 3318 (OH), 2958 (=C-H), 1714 (C=O), 1456 (C=C); ^{1}H NMR (400 MHz, $CDCl_3$) δ 7.40-7.25 (5H, m, Ar-H), 6.34 (1H, s, H-9a), 5.84 (1H, s, H-9b), 5.57 (1H, d, *J* = 5.6 Hz, H-7), 3.73 (3H, s, H-11), 3.05 (1H, d, *J* = 5.6 Hz, OH); ^{13}C NMR (101 MHz, $CDCl_3$) δ 166.8 (C-10), 141.9 (C-2), 141.2 (C-8), 128.4 (C-1,3), 127.8 (C-5), 126.5 (C-4,6), 126.2 (C-9), 73.3 (C-7), 52.0 (C-11).

5.4.1.2. Synthesis of methyl 2-((4-chlorophenyl)(hydroxy)methyl)acrylate (153)

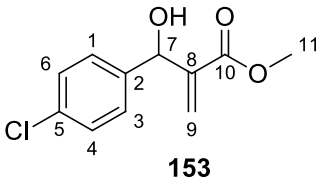

153

4-Chlorobenzaldehyde (2 ml) and methyl acrylate (9.51 ml) were used, and the reaction mixture was stirred for 1 day, the product **153** was isolated as a white solid (3.22, 84%). M.P: 61-63 ˚C, R_f = 0.62 (40% ethyl acetate:hexane). IR ν_{max} (neat,cm^{-1}) 3331 (OH), 2942 (=C-H), 1721 (C=O), 1456 (C=C); ^{1}H NMR (400 MHz, $CDCl_3$) δ 7.34-7.31 (4H, m, Ar-H), 6.35 (1H, s, H-9a), 5.83 (1H, s, H-9b), 5.53 (1H, d, *J* = 5.7 Hz, H-7), 3.74 (3H, s, H-11), 3.08 (1H, d, *J* = 4.0 Hz, OH); ^{13}C NMR (101 MHz, $CDCl_3$) δ 166.7 (C-10), 141.6 (C-2), 139.8 (C-8), 133.6 (C-5), 128.6 (C-1,3), 128.0 (C-4,6), 126.5 (C-9), 72.8 (C-7), 52.1 (C-11).

5.4.1.3. Synthesis of methyl 2-(hydroxy(4-nitrophenyl)methyl)acrylate (154)

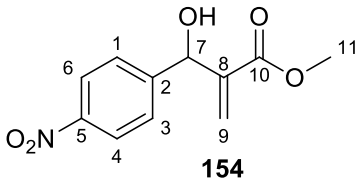

154

4-Nitrobenzaldehyde (1 ml) and methyl acrylate (5.72 ml) were used, and the mixture was stirred for 1 day, affording the product **154** as an off white solid (1.72 g, 71%). M.P: 99-101 ˚C, R_f = 0.42 (40% ethyl acetate:hexane). IR ν_{max} (neat,cm^{-1}) 3508 (OH), 2981 (=C-H), 1695 (C=O), 1440 (C=C); ^{1}H NMR (400 MHz, $CDCl_3$) δ 8.21 (2H, d, *J* = 6.7 Hz, H-4,6), 7.58 (2H, d, *J* = 6.8 Hz, H-1,3), 6.39 (1H, s, H-9a), 5.87 (1H, s, H-9b), 5.63 (1H, d, *J* = 6.2 Hz, H-7), 3.75 (3H, s, H-11), 3.29 (1H, d, *J* = 6.1 Hz, OH); ^{13}C NMR (101 MHz, $CDCl_3$) δ 166.4 (C-10), 148.6 (C-5), 147.5 (C-8), 141.0 (C-2), 127.33 (C-1,3), 127.26 (C-9), 123.6 (C-4,6), 72.8 (C-7), 52.2 (C-11).

5.4.1.4. Synthesis of methyl 2-((2-bromophenyl)(hydroxy)methyl)acrylate (155)

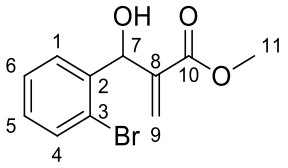

155

2-Bromobenzaldehyde (1 ml) and methyl acrylate (4.8 ml) were used, and the reaction mixture was stirred for 1 day, affording the product **155** as a pale-yellow oil (1.79, 78%). R_f = 0.60 (40% ethyl acetate:hexane). IR ν_{max} (neat,cm^{-1}) 2951 (=C-H), 1708 (C=O), 1437 (C=C); ^{1}H NMR (400 MHz, $CDCl_3$) δ 7.55 (2H, d, *J* = 7.7 Hz, H-1,4), 7.36 (1H, t, *J* = 7.6 Hz, H-5), 7.17 (1H, t, *J* = 7.6 Hz, H-6), 6.35 (1H, s, H-9a), 5.95 (1H, s, H-7), 5.56 (1H, s, H-9b), 3.79 (3H, s, H-11), 3.33 (1H, m, OH). ^{13}C NMR (101 MHz, $CDCl_3$) δ 167.0 (C-10), 140.6 (C-8), 139.8 (C-3), 132.8 (C-4), 129.4 (C-6), 128.4 (C-1), 127.7 (C-5), 127.2 (C-9), 123.1 (C-2), 71.5 (C-7), 52.2 (C-11).

5.4.1.5. Synthesis of 2-(hydroxy(phenyl)methyl)acrylonitrile (156)

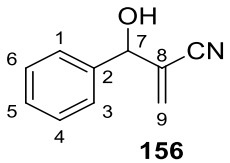

156

Benzaldehyde (1 ml) and acrylonitrile (3.98 ml) were used, and the mixture was stirred for 1 day affording the desired product **156** as a colourless oil (1.35, 87%). R_f = 0.47 (40% ethyl acetate:hexane). IR ν_{max} (neat,cm^{-1}) 3450 (OH), 2981 (=C-H), 2229 (CN), 1454 (C=C); ^{1}H NMR (400 MHz, $CDCl_3$) δ 7.43-7.35 (5H, m, Ar-H), 6.12 (1H, s, H-9a), 6.04 (1H, s, H-9b), 5.32-5.30 (1H, m, H-7), 2.42-2.36 (1H, m, OH). ^{13}C NMR (101 MHz, $CDCl_3$) δ 139.2 (C-2), 129.8 (C-9), 129.1 (C-4,6), 129.0 (C-1,3), 126.6 (C-5), 126.3 (C-8), 116.9 (CN), 74.3 (C-7).

5.4.1.6. Synthesis of 2-((2-chlorophenyl)(hydroxy)methyl)acrylonitrile (157)

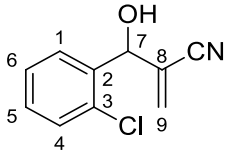

157

2-Chlorobenzaldehyde (1 ml) and acrylonitrile (3.6 ml) were used, and the reaction time was changed to 15 hr. Product was purified by column chromatography affording the desired product **157** as an off white solid (1.32, 77%). M.P: 83-85 ˚C, R_f = 0.57 (40% ethyl acetate:hexane). IR ν_{max} (neat,cm^{-1}) 3450 (OH), 2949 (=C-H), 2229 (CN), 1437 (C=C); ^{1}H NMR (400 MHz, $CDCl_3$) δ 7.61 (1H, d, *J* = 7.7 Hz, H-4), 7.41-7.28 (3H, m, H-1,5,6), 6.07 (2H, s, H-9), 5.77 (1H, d, *J* = 4.6 Hz, H-7), 2.59-2.56 (1H, m, OH). ^{13}C NMR (101 MHz, $CDCl_3$) δ 136.4 (C-2), 132.6 (C-3), 131.3 (C-9), 130.1 (C-5), 129.8 (C-6), 128.0 (C-4), 127.6 (C-1), 124.6 (C-8), 116.7 (CN), 70.6 (C-7).

5.4.1.7. Synthesis of 2-((2-bromophenyl)(hydroxy)methyl)acrylonitrile (158)

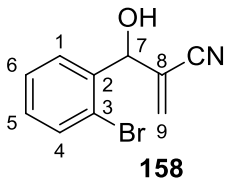

158

2-Bromobenzaldehyde (1 ml) and acrylonitrile (3.5 ml) were used, and the reaction time was changed to 1 day. Product **158** was purified by column chromatography affording the desired product as a pale-yellow solid (1.68, 83%). M.P: 52-55 ˚C, R_f = 0.70 (40% ethyl acetate:hexane). IR ν_{max} (neat,cm^{-1}) 3420 (OH), 2238 (CN), 1439 (C=C); ^{1}H NMR (400 MHz, $CDCl_3$) δ 7.64-7.56 (2H, m, H-1,4), 7.41 (1H, t, *J* = 7.6 Hz, H-5), 7.27-7.21 (1H, m, H-6), 6.09 (2H, s, H-9), 5.76 (1H, s, H-7), 2.53-2.51 (1H, m, OH). ^{13}C NMR (101 MHz, $CDCl_3$) δ 138.0 (C-2), 133.1 (C-4), 131.5 (C-9), 130.4 (C-6), 128.3 (C-1), 128.2 (C-5), 124.6 (C-3), 122.8 (C-8), 116.6 (CN), 72.8 (C-7).

5.4.1.8. Synthesis of 3-(hydroxy(phenyl)methyl)but-3-en-2-one (159)

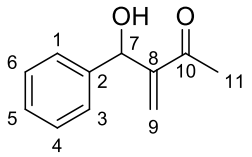

159

Benzaldehyde (1 ml) and methyl vinyl ketone (1.63 ml) were used, and the reaction mixture was stirred for 3 days. The product **159** was purified by column chromatography affording the desired product as a yellow oil (1.1 g, 61%). R_f = 0.40 (40% ethyl acetate:hexane). ^{1}H NMR (400 MHz, $CDCl_3$) δ 7.39 -7.21 (5H, m, Ar-H), 6.19 (1H, s, H-9a), 5.97 (1H, s, H-9b), 5.66-5.59 (1H, m. H-7), 3.12-3.06 (1H, m, OH), 2.34 (3H, s, H-12). ^{13}C NMR (101 MHz, $CDCl_3$) δ 200.3 (C-10), 150.0 (C-8), 141.5 (C-2), 128.4 (C-4,6), 127.7 (C-5), 126.7 (C-9), 126.5 (C-1,3), 72.9 (C-7), 26.5 (C-11).

5.4.1.9. Synthesis of methyl 2-(hydroxy(phenyl)methyl)acrylate (216)

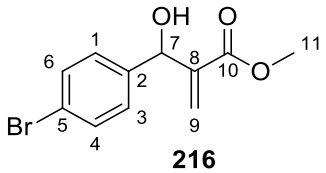

216

4-bromobenzaldehyde (4 g) and methyl acrylate (12.08 ml) were used, and the mixture was stirred for 1 day affording the product **216** as a white solid (4.12 g, 76%). M.P: 70-72 ˚C, R_f = 0.6 (40% ethyl acetate: hexane). IR ν_{max} (neat, cm^{-1}) 3330 (OH), 2942 (=C-H), 1717 (C=O), 1433 (C=C); ^{1}H NMR (400 MHz, $CDCl_3$) δ 6.63 – 6.58 (2H, m, H-4,6), 6.41 – 6.36 (2H, m, H-1,3), 5.48 (1H, s, H-9a), 4.96 (1H, s, H-9b), 4.64 (1H, d, *J*=5.7 Hz, H-7), 2.86 (3H, s, H-11), 2.22 (1H, d, *J*=5.8 Hz, OH). ^{13}C NMR (101 MHz, $CDCl_3$) δ 166.6 (C-10), 141.6 (C-2), 140.3 (C-8), 131.6 (C-4,6), 128.3 (C-1,3), 126.4 (C-9), 121.8 (C-5), 72.8 (C-7), 52.1 (C-11).

5.4.1.10. Synthesis of ethyl 2-((4-chlorophenyl)(hydroxy)methyl)acrylate (217)

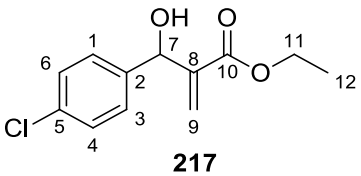

217

4-chlorobenzaldehyde (4 g) and ethyl acrylate (19.81 ml) were used, and the mixture was stirred for 1 day affording the desired product **217** as a colourless oil (6.08 g, 89%). R_f = 0.3 (20% ethyl acetate: hexane). IR ν_{max} (neat, cm^{-1}) 2983 (=C-H), 1703 (C=O), 1489 (C=C); ^{1}H NMR (400 MHz, $CDCl_3$) δ 7.35 – 7.28 (4H, m, Ar-H), 6.34 (1H, s, H-9a), 5.81 (1H, s, H-9b), 5.52 (1H, s, H-7), 4.17 (2H, q, J=7.2 Hz, H-11), 3.21 (1H, s, OH), 1.25 (3H, t, H-12). ^{13}C NMR (101 MHz, $CDCl_3$) δ 166.2 (C-10), 141.8 (C-8), 139.9 (C-2), 133.6 (C-5), 128.6 (C-4,6), 128.0 (C-1,3), 126.2 (C-9), 72.8 (C-7), 61.1 (C-11), 14.1 (C-12).

5.4.2. General procedure for the protection of alcohols using TBDMSCl

To a solution of MBH adduct (1 mmol) in anhydrous *N*,*N*-dimethylformamide (DMF) (0.3 ml) was added *tert*-butyl dimethyl silyl chloride (TBDMSCl) (1.3 mmol) and imidazole (2.5 mmol). The reaction mixture was stirred at room temperature under nitrogen, until all the starting material was consumed as indicated by TLC analysis (8-18 h). After reaction completion, hexane (10 ml) was added to the mixture to quench the reaction, which was washed sequentially with brine solution (3 x 5 ml). The organic layer was dried over anhydrous sodium sulphate and concentrated under reduced pressure. The product was purified by column chromatography using 20% ethyl acetate in hexane.

5.4.2.1. Synthesis of methyl 2-(((*tert*-butyldimethylsilyl)oxy)(phenyl)methyl) acrylate (160)

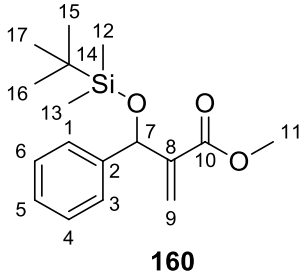

160

The product **160** was isolated as a colourless oil (0.55 g, 69%). R_f = 0.75 (20% ethyl acetate:hexane). IR ν_{max} (neat,cm^{-1}) 2953 (=C-H), 1720 (C=O), 1462 (C=C); 840 (Si-O); ^{1}H NMR (400 MHz, $CDCl_3$) δ 7.37 – 7.32 (2H, m, H-1,3), 7.31 – 7.27 (2H, m, H-4,6), 7.24 – 7.19 (1H, m, H-5), 6.24 (1H, s, H-9a), 6.06 (1H, s, H-9b), 5.60 (1H, s, H-7), 3.67 (3H, s, H-11), 0.87 (9H, s, H-15,16,17), 0.05 (3H, s, H-12), -0.12 (3H, s, H-13); ^{13}C NMR (101 MHz, $CDCl_3$) δ 166.4 (C-10),

144.0 (C-8), 142.6 (C-2), 128.0 (C-4,6), 127.4 (C-5), 127.0 (C-1,3), 123.8 (C-9), 72.7 (C-7), 51.6 (C-11), 25.8 (C-15,16,17), 18.2 (C-14), -4.9 (C-12), -5.1 (C-13).

5.4.2.2. Synthesis of methyl 2-((2-bromophenyl)((*tert*-butyldimethylsilyl)oxy) methyl) acrylate (161)

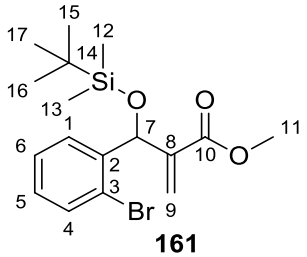

161

The product **161** was isolated as colourless oil (0.76, 53%). R_f = 0.72 (20% ethyl acetate:hexane). IR ν_{max} (neat,cm^{-1}) 2937 (=C-H), 1726 (C=O), 1470 (C=C); 840 (Si-O), ^{1}H NMR (400 MHz, $CDCl_3$) δ 7.52 – 7.43 (2H, m, H-1,4), 7.32 – 7.26 (1H, m, H-5), 7.14 – 7.08 (1H, m, H-6), 6.28 (1H, s, H-9a), 6.00 (1H, s, H-7), 5.75 (1H, s, H-9b), 3.71 (3H, s, H-11), 0.86 (9H, s, H-15,16,17), 0.11 (3H, s, H-12), -0.10 (3H, s, H-13); ^{13}C NMR (101 MHz, $CDCl_3$) δ 166.4 (C-10), 143.0 (C-8), 141.4 (C-2), 132.6 (C-4), 129.5 (C-1), 128.9 (C-6), 127.3 (C-5), 125.5 (C-9), 122.9 (C-3), 71.5 (C-7), 51.7 (C-11), 25.8 (C-15,16,17), 18.1 (C-14), -4.8 (C-12), -5.0 (C-13).

5.4.2.3. Synthesis of methyl 2-(((*tert*-butyldimethylsilyl)oxy)(4-chlorophenyl)methyl) acrylate (162)

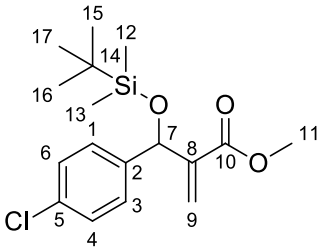

162

The product **162** was isolated as a colourless oil (1.39, 93%). R_f = 0.74 (20% ethyl acetate:hexane). IR ν_{max} (neat,cm^{-1}) 2930 (=C-H), 1719 (C=O), 1472 (C=C); 835 (Si-O); ^{1}H NMR (400 MHz, $CDCl_3$) δ 7.31 – 7.23 (4H, m, Ar-H), 6.25 (1H, s, H-9a), 6.08 (1H, s, H-9b), 5.56 (1H, s, H-7), 3.67 (3H, s, H-11), 0.87 (9H, s, H-15,16,17), 0.05 (3H, s, H-12), -0.10 (3H, s, H-13); ^{13}C NMR (101

MHz, $CDCl_3$) δ 166.2 (C-10), 143.6 (C-5), 141.3 (C-8), 133.1 (C-2), 128.4 (C-4,6), 128.2 (C-1,3), 124.0 (C-9), 72.1 (C-7), 51.7 (C-11), 25.7 (C-15,16,17), 18.2 (C-14), -4.9 (C-12), -5.1 (C-13).

5.4.2.4. Synthesis of 2-((2-bromophenyl)((*tert*-butyldimethylsilyl)oxy)methyl) acrylonitrile (163)

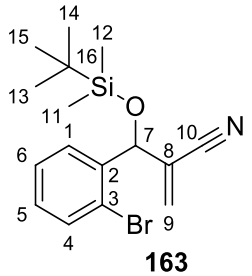

163

The product **163** was isolated as a white solid (0.79 g, 75%). M.P: 45-49˚C, R_f = 0.76 (20% ethyl acetate:hexane). IR ν_{max} (neat,cm^{-1}) 3007 (=C-H), 1464 (C=C), 2223 (CN), 845 (Si-O); ^{1}H NMR (400 MHz, $CDCl_3$) δ 7.65 – 7.61 (1H, d, H-4), 7.55 – 7.52 (1H, d, H-1), 7.41 – 7.36 (1H, t, H-5), 7.22 – 7.17 (1H, t, H-6), 5.98 (1H, d, *J* = 1.3 Hz, H-9a), 5.95 (1H, d, *J* = 1.0 Hz, H-9b), 5.68 (1H, br s, H-7), 0.91 (9H, s, H-13,14,15), 0.13 (3H, s, H-11), -0.03 (3H, s, H-12); ^{13}C NMR (101 MHz, $CDCl_3$) δ 139.1 (C-3), 132.6 (C-1), 129.9 (C-9), 129.8 (C-4), 128.9 (C-5), 128.0 (C-6), 126.2 (C-8), 122.0 (C-2), 116.8 (C-10), 73.3 (C-7), 25.6 (C-13,14,15), 18.2 (C-16), -5.0 (C-11), -5.1 (C-12). HRMS *m/z* calcd for $C_{16}H_{22}BrNOSi$ [$M+H^+$]: 352.0727, found: 352.0655.

5.4.2.5. Synthesis of 2-(((*tert*-butyldimethylsilyl)oxy)(phenyl)methyl)acrylonitrile (164)

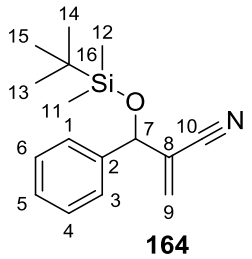

164

The product **164** was isolated as a white solid (0.19 g, 17.7%). M.P: 45-48 ˚C, R_f = 0.68 (20% ethyl acetate:hexane). IR ν_{max} (neat,cm^{-1}) 2957 (=C-H), 2225 (CN), 1472 (C=C); 860 (Si-O); ^{1}H NMR (400 MHz, $CDCl_3$) δ 7.37 – 7.29 (5H, m, Ar-H), 6.03 (1H, d, *J* = 1.6 Hz, H-9a), 5.93 (1H, br s, H-9b), 5.23 (1H, t, H-7), 0.91 (9H, s, H-13,14,15), 0.10 (3H, s, H-11), -0.05 (3H, s, H-12); ^{13}C NMR (101 MHz, $CDCl_3$) δ 140.1 (C-2), 128.6 (C-4,6), 128.42 (C-8), 128.35 (C-9), 127.9 (C-5), 126.4

(C-1,3), 117.1 (C-10), 75.0 (C-7), 25.7 (C-13,14,15), 18.2 (C-16), -4.9 (C-11), -5.1 (C-12). HRMS *m/z* calcd for $C_{16}H_{23}NOSi$ [M+H$^+$]: 274.1622, found: 274.1574.

5.4.2.6. Synthesis of 2-(((*tert*-butyldimethylsilyl)oxy)(4-chlorophenyl)methyl) acrylonitrile (165)

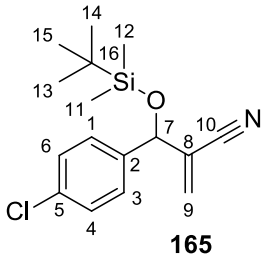

165

The product **165** was isolated as a white solid (0.99 g, 64%). M.P: 66-69˚C, R_f = 0.56 (20% ethyl acetate:hexane). IR ν_{max} (neat,cm^{-1}) 2981 (=C-H), 2229 (CN), 1471 (C=C); 834 (Si-O); ^{1}H NMR (400 MHz, $CDCl_3$) δ 7.37 – 7.35 (1H, m, H-4), 7.35 – 7.33 (1H, m, H-6), 7.32 – 7.30 (1H, m, H-1), 7.30 – 7.27 (1H, m, H-3), 6.04 (1H, d, H-9a), 5.96 – 5.94 (1H, m, H-9b), 5.20 (1H, t, H-7), 0.91 (9H, s, H-13,14,15), 0.10 (3H, s, H-11), -0.04 (3H, s, H-12). ^{13}C NMR (101 MHz, $CDCl_3$) δ 138.7 (C-5), 134.3 (C-2), 128.9 (C-4,6), 128.6 (C-9), 127.7 (C-1,3), 127.5 (C-8), 116.9 (C-10), 74.3 (C-7), 25.6 (C-13,14,15), 18.2 (C-16), -4.9 (C-11), -5.1 (C-12).

5.4.2.7. Synthesis of methyl 2-((4-bromophenyl)((*tert*-butyldimethylsilyl)oxy) methyl)acrylate (219)

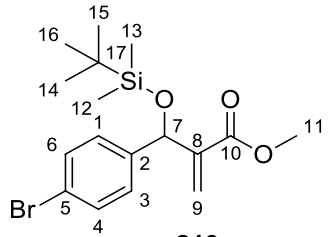

219

The product **219** was isolated as a colourless oil (3.35 g, 67%). R_f = 0.7 (20% ethyl acetate: hexane). IR ν_{max} (neat, cm^{-1}) 2929 (=C-H), 1719 (C=O), 1437 (C=C), 835 (Si-O); ^{1}H NMR (400 MHz, $CDCl_3$) δ 7.54 – 7.49 (2H, m, H-4,6), 7.36 – 7.31 (2H, m, H-1,3), 6.36 (1H, s, H-9a), 6.20 (1H, s, H-9b), 5.65 (1H, s, H-7), 3.78 (3H, s, H-11), 0.97 (9H, s, H-14,15,16), 0.15 (3H, s, H-12), 0.00 (3H, s, H-13).^{13}C NMR (101 MHz, $CDCl_3$) δ 166.2 (C-10), 143.5 (C-2), 141.9 (C-8), 131.2 (C-4,6),

128.8 (C-1,3), 124.1 (C-9), 121.3 (C-5), 72.1 (C-7), 51.7 (C-11), 25.7 (C-14,15,16), 18.2 (C-17), -4.9 (C-13), -5.1 (C-12).

5.4.2.8. Synthesis of ethyl 2-(((*tert*-butyldimethylsilyl)oxy)(4-chlorophenyl)methyl) acrylate (220)

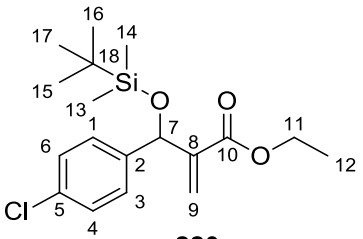

220

The product **220** was isolated as a colourless oil (6.5 g, 80%). R_f = 0.7 (40% ethyl acetate: hexane). IR ν_{max} (neat, cm^{-1}) 2930 (=C-H), 1715 (C=O), 1490 (C=C), 835 (Si-O); ^{1}H NMR (400 MHz, $CDCl_3$) δ 7.27 – 7.18 (4H, m, Ar-H), 6.21 (1H, s, H-9a), 6.03 (1H, s, H-9b), 5.51 (1H, s, H-7), 4.14 – 4.00 (2H, m, H-11), 1.23 – 1.14 (3H, m, H-12), 0.82 (9H, s, H-15, 16, 17), 0.01 (3H, s, H-13), -0.15 (3H, s, H-14). ^{13}C NMR (101 MHz, $CDCl_3$) δ 165.8 (C-10), 143.8 (C-2), 141.4 (C-8), 133.0 (C-5), 128.5 and 128.2 (C-1,3 and C-4,6), 123.8 (C-9), 72.1 (C-7), 60.7 (C-11), 25.7 (C-15, 16 ,17), 18.2 (C-18), 14.1 (C-12), -4.9 (C-14), -5.0 (C-13). HRMS *m/z* calcd for $C_{18}H_{27}ClO_3Si$ [$M+H^+$]: 355.1491, found: 355.1420.

5.4.3. General procedure for the protection of alcohols using TMSCl

To a solution of the MBH adduct (1 mmol) in anhydrous *N*,*N*-dimethylformamide (DMF) (0.3 ml) was added trimethyl silyl chloride (TMSCl) (1.3 mmol) and imidazole (2.5 mmol). The reaction mixture was stirred at room temperature under nitrogen, until all the starting material was consumed as indicated by TLC analysis (8-18 h). After reaction completion, hexane (10 ml) was added to the mixture to quench the reaction, which was washed sequentially with brine solution (3 x 5 ml). The organic layer was dried over anhydrous sodium sulphate and concentrated under reduced pressure. The product was purified by column chromatography.

5.4.3.1. Synthesis of methyl 2-((4-chlorophenyl)((trimethylsilyl)oxy)methyl)acrylate (166)

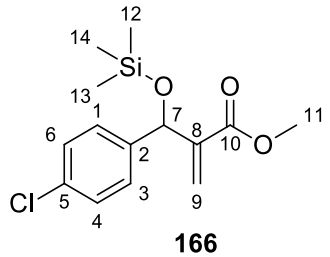

166

The crude product was purified by column chromatography to afford the desired product **166** as a colourless oil (0.53 g, 41%). R_f = 0.60 (10% ethyl acetate:hexane). IR ν_{max} (neat,cm^{-1}) 2922 (=C-H), 1719 (C=O), 1490 (C=C); 840 (Si-O); ^{1}H NMR (400 MHz, $CDCl_3$) δ 7.31 – 7.23 (4H, m, Ar-H), 6.28 (1H, s, H-9a), 6.01 (1H, s, H-9b), 5.57 (1H, s, H-7), 3.68 (3H, s, H-11), 0.06 (9H, br s, H-12,13,14); ^{13}C NMR (101 MHz, $CDCl_3$) δ 166.2 (C-10), 143.3 (C-8), 141.1 (C-2), 133.2 (C-5), 128.5 (C-4,6), 128.4 (C-1,3), 124.6 (C-9), 71.9 (C-7), 51.7 (C-11), 0.0 (C-12,13,14).

5.4.3.2. Synthesis of methyl 2-((2-bromophenyl)((trimethylsilyl)oxy)methyl)acrylate (167)

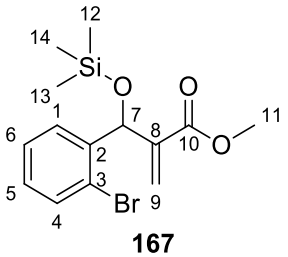

167

The crude product was purified by column chromatography to afford the desired product **167** as a colourless oil (0.22 g, 79%). R_f = 0.69 (20% ethyl acetate:hexane). IR ν_{max} (neat,cm^{-1}) 2966 (=C-H), 1724 (C=O), 1469 (C=C); 840 (Si-O); ^{1}H NMR (400 MHz, $CDCl_3$) δ 7.51 (1H, d, *J* = 8.0 Hz, H-4), 7.46 (1H, d, *J* = 8.8 Hz, H-1), 7.30 (1H, t, *J* = 7.5 Hz, H-5), 7.13 (1H, t, *J* = 8.4 Hz, H-6), 6.30 (1H, s, H-9a), 6.01 (1H, s, H-7), 5.65 (1H, s, H-9b), 3.73 (3H, s, H-11), 0.10 (9H, s, H-12,13,14); ^{13}C NMR (101 MHz, $CDCl_3$) δ 166.3 (C-10), 142.7 (C-8), 141.2 (C-2), 132.6 (C-1), 129.2 (C-4), 129.0 (C-5), 127.4 (C-6), 125.9 (C-9), 123.0 (C-3), 71.5 (C-7), 51.8 (C-11), 0.1 (C-12,13,14).

5.4.3.3. Synthesis of 2-((2-bromophenyl)((trimethylsilyl)oxy)methyl)acrylonitrile (168)

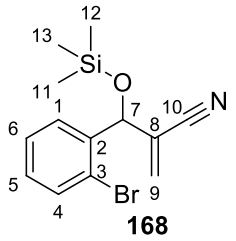

168

The product **168** was isolated as a colourless oil (0.19 g, 31%). R_f = 0.50 (20% ethyl acetate:hexane). ^{1}H NMR (400 MHz, $CDCl_3$) δ 7.64 – 7.60 (1H, d, H-4), 7.55 – 7.52 (1H, d, H-1), 7.41 – 7.35 (1H, m, H-5), 7.23 – 7.17 (1H, m, H-6), 5.96 (2H, dd, *J* = 4.6 Hz, H-9), 5.67 (1H, br s, H-7), 0.13 (9H, s, H-11, 12, 13); ^{13}C NMR (101 MHz, $CDCl_3$) δ 138.9 (C-3), 132.7 (C-1), 130.02 (C-9), 129.95 (C-4), 128.9 (C-5), 128.0 (C-6), 126.1 (C-8), 122.1 (C-2), 116.9 (C-10), 73.1 (C-7), -0.1 (C-11, 12, 13).

5.4.3.4. Synthesis of 2-(phenyl((trimethylsilyl)oxy)methyl)acrylonitrile (169)

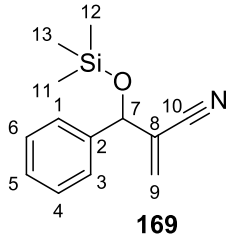

169

The product **169** was isolated as a light-yellow oil (0.49 g, 70%). R_f = 0.55 (20% ethyl acetate:hexane). IR ν_{max} (neat,cm^{-1}) 2229 (CN), 1454 (C=C); 847 (Si-O); ^{1}H NMR (400 MHz, $CDCl_3$) δ 7.38 – 7.31 (5H, m, Ar-H), 6.03 – 6.01 (1H, m, H-9a), 5.96 – 5.94 (1H, m, H-9b), 5.25 – 5.20 (1H, m, H-7) , 0.11 (9H, s, H-11 ,12, 13); ^{13}C NMR (101 MHz, $CDCl_3$) δ 139.9 (C-2), 128.7 (C-9), 128.6 (C-4,6), 128.5 (C-5), 127.6 (C-8), 126.5 (C-1,3), 117.2 (C-10), 74.7 (C-7), -0.1 (C-11, 12, 13).

5.4.3.5. Synthesis of 2-((4-chlorophenyl)((trimethylsilyl)oxy)methyl)acrylonitrile (170)

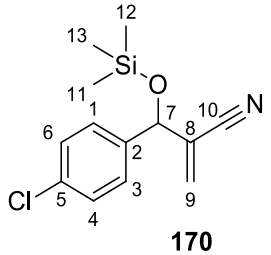

170

The product **170** was isolated as a colourless oil (0.59 g, 72%). R_f = 0.60 (20% ethyl acetate:hexane). IR ν_{max} (neat,cm^{-1}) 2981 (=C-H), 2229 (CN), 1471 (C=C); 834 (Si-O); ^{1}H NMR (400 MHz, $CDCl_3$) δ 7.37 – 7.35 (1H, m, H-4), 7.35 – 7.33 (1H, m, H-6), 7.32 – 7.30 (1H, m, H-1), 7.29 – 7.28 (1H, m, H-3), 6.05 – 6.02 (1H, m, H-9a), 5.98 – 5.95 (1H, m, H-9b), 5.20 (1H, t, *J*=1.5 Hz, H-7), 0.13 (9H, s, H-11,12,13). ^{13}C NMR (101 MHz, $CDCl_3$) δ 138.6 (C-5), 134.5 (C-2), 129.0 (C-4,6), 129.0 (C-1,3), 128.0 (C-9), 127.4 (C-8), 117.0 (C-10), 74.2 (C-7), 0.00 (C-11,12,13).

5.4.4. Conjugate addition reaction of TMS protected adduct 166 with piperidine.

To the protected MBH adduct **166** (0.25 g, 1.12 mmol) in methanol (5 ml) was added piperidine (0.13 ml, 2.25 mmol). The stoppered reaction mixture was stirred at room temperature for 2 days until the reaction was complete. Upon reaction completion, the mixture was concentrated in vacuo, and purification by column chromatography (40% ethyl acetate:hexane) led to the isolation of three products, methyl 3-(4-chlorophenyl)-2-(piperidin-1-ylmethyl)-3-((trimethyl silyl)oxy) propanoate (**186**), methyl 3-(4-chlorophenyl)-3-hydroxy-2-(piperidin-1-ylmethyl)propanoate (**187**), (*E*)-methyl 3-(4-chlorophenyl)-2-(piperidin-1-ylmethyl)acrylate (**188**).

5.4.4.1. Synthesis of methyl 3-(4-chlorophenyl)-2-(piperidin-1-ylmethyl)-3-((trimethyl silyl)oxy)propanoate (186)

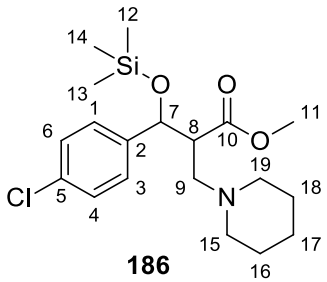

186

The product **186** was isolated as a white solid (0.25 g, 31%). M.P: 88-89˚C, R_f = 0.50 (40% ethyl acetate: hexane). IR ν_{max} (neat, cm^{-1}) 2949 (=C-H), 1731 (C=O), 1455 (C=C), 820 (Si-O); ^1H NMR (400 MHz, $CDCl_3$) δ 7.30 – 7.27 (4H, m, Ar-H), 4.96 (1H, d, *J* = 12.0 Hz, H-7), 3.41 (3H, s, H-11), 3.10 – 2.99 (1H, m , H-9a), 2.92 – 2.83 (1H, m, H-8), 2.78 – 2.63 (3H, m, H-9b,15a,19a), 2.43 – 2.41 (2H, m, H-15b,19b), 1.65 – 1.63 (4H, m, H-16,18) , 1.53 (2H, s, H-17), 0.00 (9H, s, H-12,13,14). ^{13}C NMR (400 MHz, $CDCl_3$) δ 171.8 (C-10), 140.8 (Ar-C), 133.4 (Ar-C), 128.3 (Ar-C), 128.0 (Ar-C), 77.2 (C-7), 61.2 (C-9), 54.9 (C-15,19), 51.6 (C-11), 49.8 (C-8), 25.9 (C-16,18), 23.9 (C-17), 0.0 (C-12,13,14).

5.4.4.2. Synthesis of methyl 3-(4-chlorophenyl)-3-hydroxy-2-(piperidin-1-ylmethyl) propanoate (187)

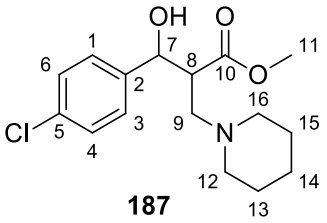

187

The product **187** was isolated as a white solid (0.08 g, 31%). M.P: 87-89 ˚C, R_f = 0.80 (40% ethyl acetate: hexane). IR ν_{max} (neat, cm^{-1}) 3665 (OH), 1731 (C=O); ^1H NMR (400 MHz, $CDCl_3$) δ 7.31 – 7.26 (4H, m, Ar-H), 4.96 (1H, d, *J* = 9.0 Hz, H-7), 3.41 (3H, s, H-11), 3.09 – 2.98 (1H, m, H-9a), 2.92 – 2.81 (1H, m, H-8), 2.76 – 2.63 (3H, m, H-9b,12a,16a), 2.43 – 2.41 (2H, m, H-12b,16b), 1.70 – 1.55 (4H, m, H-13,15), 1.53 – 1.43 (2H, m, H-14). ^{13}C NMR (101 MHz, $CDCl_3$) δ 171.8 (C-10), 140.8 (Ar-C), 133.4 (Ar-C), 128.3 (Ar-C), 128.0 (Ar-C), 77.5 (C-7), 61.3 (C-9), 54.9 (C-12,16), 51.6 (C-11), 49.8 (C-8), 25.9 (C-13,15), 23.9 (C-14). HRMS *m/z* calcd for $C_{16}H_{22}ClNO_3$ $[M+H^+]$: 312.1303, found: 312.1303.

5.4.4.3. Synthesis of (E)-methyl 3-(4-chlorophenyl)-2-(piperidin-1-ylmethyl)acrylate (188)

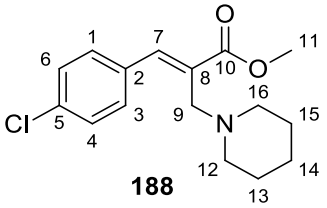

188

The product **188** was isolated as a yellow oil (0.035, 14%). R_f = 0.67 (40% ethyl acetate: hexane). IR ν_{max} (neat, cm^{-1}) 2933 (=C-H), 1710 (C=O), 1434 (C=C); ^{1}H NMR (400 MHz, $CDCl_3$) δ 7.76 (1H, s, H-7), 7.69 (2H, d, *J* = 7.7 Hz, Ar-H), 7.36 (2H, d, *J* = 7.9 Hz, Ar-H), 3.82 (3H, s, H-11), 3.25 (2H, s, H-9), 2.40 – 2.38 (4H, m, H-12,16), 1.55 – 1.53 (4H, m, H-13,15), 1.27 – 1.25 (2H, m, H-14). ^{13}C NMR (101 MHz, $CDCl_3$) δ 169.1 (C-10), 141.8 (C-7), 134.9 (Ar-C), 134.0 (Ar-C), 132.1 (Ar-C), 130.8 (C-8), 128.5 (Ar-C), 54.0 (C-9), 53.9 (C-12,16), 52.1 (C-11), 26.2 (C-13,15), 24.4 (C-14).

5.4.5. Synthesis of methyl 3-((*tert*-butyldimethylsilyl)oxy)-3-phenyl-2-(piperidin-1-ylmethyl)propanoate (189)

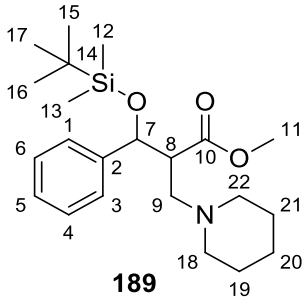

189

To the protected MBH adduct **160** (0.15 g, 1.12 mmol) in methanol (5 ml) was added piperidine (0.011 ml, 2.25 mmol). The stoppered reaction mixture was stirred at room temperature for 2 days until the reaction was complete. Upon reaction completion, the mixture was concentrated in vacuo, and purification by column chromatography (40% ethyl acetate:hexane) led to the isolation of the product **189** as a brown oil (0.10 g, 53%). R_f = 0.50 (40% ethyl acetate: hexane). IR ν_{max} (neat, cm^{-1}) 2936 (C-H), 1736 (C=O), 1455 (C=C), 840 (Si-O); ^{1}H NMR (400 MHz, $CDCl_3$) δ 7.34 – 7.24 (5H, m, Ar-H), 4.75 (1H, d, *J* = 7.7 Hz, H-7), 3.41 (3H, s, H-11), 2.98 – 2.90 (1H, m, H-8), 2.87 – 2.79 (1H, m, H-9a), 2.71 (1H, dd, *J*=12.4, 3.6 Hz, H-9b), 2.46-2.36 (2H, m, H-18,22), 2.27-2.19 (2H, m, H-18,22), 1.54 – 1.45 (4H, m, H-19,21), 1.42 – 1.32 (2H, m, H-20), 0.86 (9H, s, H-15,16,17), 0.01 (3H, s, H-12), -0.26 (3H, s, H-13). ^{13}C NMR (101 MHz, $CDCl_3$) δ 173.8 (C-10), 142.7 (Ar-C), 127.9 (Ar-C), 127.5 (Ar-C), 126.5 (Ar-C), 75.4 (C-7), 58.2 (C-9), 54.4 (C-18,22), 53.7 (C-8), 51.2 (C-11), 30.9 (C-19,21), 26.1 (C-20), 25.8 (C-15,16,17), 18.1 (C-14), -4.6 (C-12), -5.2 (C-13).

5.4.6. Synthesis of methyl 3-hydroxy-3-phenyl-2-(piperidin-1-ylmethyl)propanoate (190)

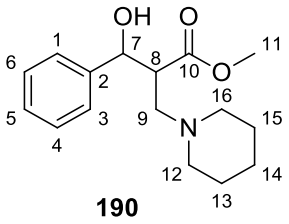

190

To the unprotected MBH adduct **152** (0.4 g, 2.60 mmol) in methanol (5 ml) was added piperidine (0.31 ml, 3.90 mmol). The stoppered reaction mixture was stirred at room temperature for 2 days until the reaction was complete. Upon reaction completion, the mixture was concentrated in vacuo, and purification by column chromatography (40% ethyl acetate:hexane) led to the isolation of the product **190** as a yellow oil (0.34 g, 59%). R_f = 0.30 (40% ethyl acetate: hexane). IR ν_{max} (neat, cm^{-1}) 3708 (OH), 2952 (C-H), 1731 (C=O), 1455 (C=C); ^{1}H NMR (400 MHz, $CDCl_3$) δ 7.37 – 7.28 (4H, m, Ar-H), 7.25 – 7.21 (1H, m, Ar-H), 4.98 (1H, d, *J*=9.1 Hz, H-7), 3.38 (3H, s, H-11), 3.10 – 3.01 (1H, m, H-9a), 2.98 – 2.88 (1H, m, H-8), 2.79 – 2.62 (3H, m, H-9b,12a,16a), 2.49 – 2.36 (2H, m, H-12b,16b), 1.70 – 1.62 (4H, m, H-13,15), 1.52 – 1.45 (2H, m, H-14). ^{13}C NMR (101 MHz, $CDCl_3$) δ 172.0 (C-10), 142.2 (C-2), 128.2 (C-4,6), 127.8 (C-5), 126.6 (C-1,3), 78.2 (C-7), 61.3 (C-9), 54.9 (C-12,16), 51.5 (C-11), 49.9 (C-8), 25.9 (C-13,15), 24.0 (C-14).

5.4.7. Synthesis of 3-(4-chlorophenyl)-3-hydroxy-2-(piperidin-1-ylmethyl) propane nitrile (191a/b)

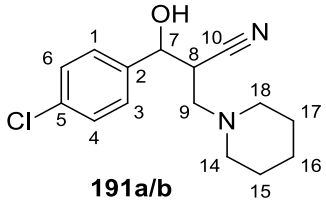

191a/b

To the protected MBH adduct **170** (0.25 g, 1 mmol) in methanol (5 ml) was added piperidine (0.33 ml, 3.5 mmol). The stoppered reaction mixture was stirred at room temperature for 2 days until the reaction was complete. Upon reaction completion, the mixture was concentrated in vacuo, and purification by column chromatography (30% ethyl acetate:hexane) led to the isolation of the product **191a/b** as a brown solid (0.26 g, 80%). M.P: 85-82 ˚C, R_f = 0.4 (30% ethyl acetate: hexane). IR ν_{max} (neat, cm^{-1}) 3416 (OH), 2940 (=C-H), 2255 (CN), 1493 (C=C); ^{1}H NMR (400

MHz, $CDCl_3$) δ 7.44 – 7.33 (4H, m, Ar-H), 5.10 (0.58H, d, *J*=2.8 Hz, H-7), 4.93 (0.24H, d, *J*=8.3 Hz, H-7), 3.15 – 3.09 (0.60H, m, H-8), 3.04 (0.04H, s, H-9), 3.01 (0.13H, d, *J*=1.7 Hz, H-9), 2.97 (0.10H, s, H-9), 2.93 – 2.91 (0.13H, m, H-9), 2.90 – 2.89 (0.24H, m, H-8), 2.89-2.86 (0.39H, m, H-9), 2.83 (0.50H, d, *J*=6.8 Hz, H-9), 2.76 (0.88H, dd, *J*=13.4, 4.2 Hz, H-9), 2.72 – 2.43 (4H, m, H-14,18), 1.72 – 1.56 (4H, m, H-15,17), 1.55 – 1.43 (2H, m, H-16). ^{13}C NMR (101 MHz, $CDCl_3$) δ 139.2 (Ar-C'), 138.6 (Ar-C), 134.3 (Ar-C'), 134.0 (Ar-C), 128.7 (Ar-C'), 128.7 (Ar-C), 127.9 (Ar-C'), 127.5 (Ar-C), 118.6 (C-10), 118.1 (C-10'), 76.6 (C-7'), 73.9 (C-7), 60.6 (C-9'), 58.3 (C-9), 55.4 (C-14,18), 54.7 (C-14',18'), 36.1 (C-8), 35.8 (C-8'), 26.0 (C-15,17), 25.9 (C-16'), 25.8 (C-15',17'), 23.7 (C-16). HRMS *m/z* calcd for $C_{15}H_{19}ClN_2O$ [M+H$^+$]: 279.1259, found: 279.1199.

5.4.8. Conjugate addition reaction of TBDMS protected adduct 164 with piperidine.

To the protected MBH adduct **164** (0.4 g, 1 mmol) in methanol (5 ml) was added piperidine (0.51 ml, 3.5 mmol). The stoppered reaction mixture was stirred at room temperature for 2 days until the reaction was complete. Upon reaction completion, the mixture was concentrated in vacuo, and purification by column chromatography (30% ethyl acetate:hexane) led to the isolation of two products, 3-((*tert*-butyldimethylsilyl)oxy)-3-phenyl-2-(piperidin-1-ylmethyl)propanenitrile (**192 a/b**), (*E*)-3-phenyl-2-(piperidin-1-ylmethyl)acrylonitrile (**193**).

5.4.8.1. Synthesis of 3-((*tert*-butyldimethylsilyl)oxy)-3-phenyl-2-(piperidin-1-ylmethyl) propanenitrile (192a/b)

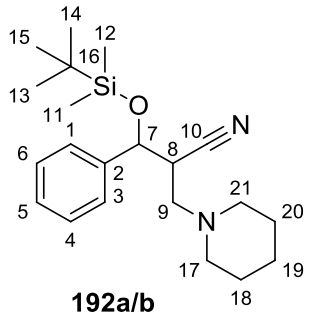

192a/b

The product **192a/b** was isolated as a yellow oil (0.44 g, 80%). R_f = 0.74 (30 % ethyl acetate: hexane). IR ν_{max} (neat, cm^{-1}) 2934 (=C-H), 1455 (C=C), 2230 (CN), 836 (Si-O); ^{1}H NMR (400 MHz, $CDCl_3$) δ 7.33 – 7.18 (5H, m, Ar-H), 4.86 – 4.83 (0.72H, m, H-7), 4.83 – 4.82 (0.27H, m,

H-7), 3.00 (0.73H, td, *J*=7.3, 5.5 Hz, H-8), 2.81 – 2.75 (0.28H, m, H-8), 2.56 – 2.50 (0.29H, m, H-9), 2.47 – 2.43 (0.32H, m, H-9), 2.43 – 2.39 (0.74H, m, H-9), 2.36 – 2.31 (1.08H, m, H-9), 2.32 – 2.19 (4H, m, H-17,21), 1.53 – 1.43 (4H, m, H-18,20), 1.37 – 1.28 (2H, m, H-19), 0.82 (2H, s, H-13,14,15), 0.80 (7H, s, H-13,14,15), -0.03 (2.93H, s, H-11), -0.10 (0.33H, s, H-11), -0.25 (2.18H, s, H-12), -0.30 (0.70H, s, H-12). ^{13}C NMR (101 MHz, $CDCl_3$) δ 141.7 (Ar-C'), 140.2 (Ar-C), 128.4 (Ar-C'), 128.3 (Ar-C), 128.21 (Ar-C), 128.17 (Ar-C'), 126.8 (Ar-C), 126.3 (Ar-C'), 120.1 (C-10), 119.6 (C-10'), 72.8 (C-7), 72.1 (C-7'), 57.4 (C-9'), 56.6 (C-9), 54.5 (C-17,21), 40.8 (C-8'), 39.9 (C-8), 26.0 (C-18,20), 25.9 (C-18',20'), 25.7 (C-13,14,15), 24.22 (C-19'), 24.19 (C-19), 18.13 (C-16'), 18.11 (C-16), -4.5 (C-12'), -4.7 (C-12), -5.2 (C-11'), -5.3 (C-11). HRMS *m/z* calcd for $C_{21}H_{34}N_2OSi$ [M+H$^+$]: 359.2513, found: 359.2438.

5.4.8.2. Synthesis of (*E*)-3-phenyl-2-(piperidin-1-ylmethyl)acrylonitrile (193)

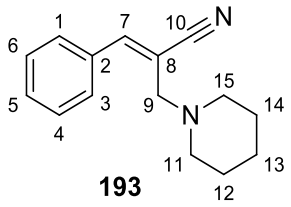

193

The product **193** was isolated as a brown oil (0.07 g, 19%). R_f = 0.10 (% ethyl acetate: hexane). IR ν_{max} (neat, cm^{-1}) 2936 (=C-H), 1450 (C=C), 2220 (CN); ^{1}H NMR (400 MHz, $CDCl_3$) δ 7.81 – 7.73 (2H, m, Ar-H), 7.46 – 7.36 (3H, m, Ar-H), 7.09 (1H, s, H-7), 3.26 (2H, s, H-9), 2.54 – 2.43 (4H, m, H-11,15), 1.67 – 1.56 (4H, m, H-12,14), 1.50 – 1.40 (2H, m, H-13). ^{13}C NMR (101 MHz, $CDCl_3$) δ 145.0 (C-7), 133.4 (Ar-C), 130.2 (Ar-C), 128.9 (Ar-C), 128.8 (Ar-C), 118.9 (C-10), 108.8 (C-8), 63.2 (C-9), 54.1 (C-11,15), 25.9 (C-12,14), 24.2 (C-13).

5.4.9. Conjugate addition reaction of TBDMS protected adduct 161 with benzylamine.

To the protected MBH adduct **161** (0.25 g, 1 mmol) in methanol (5 ml) was added benzylamine (0.25 ml, 3.5 mmol). The stoppered reaction mixture was stirred at room temperature for 2 days until the reaction was complete. Upon reaction completion, the mixture was concentrated in vacuo, and purification by column chromatography (30% ethyl acetate:hexane) led to the isolation of

three products, methyl 2-((benzylamino)methyl)-3-(2-bromophenyl)-3-((*tert*-butyl dimethylsilyl) oxy)propanoate (**(*rac*)-194a**), methyl 2-((benzylamino)methyl)-3-(2-bromophenyl)-3-((*tert*-butyl dimethylsilyl)oxy)propanoate (**(*rac*)-194b**), and (E)-methyl 2-((benzylamino)methyl)-3-phenylacrylate (**195**).

5.4.9.1. Synthesis of methyl 2-((benzylamino)methyl)-3-(2-bromophenyl)-3-((*tert*-butyl dimethylsilyl)oxy)propanoate ((*rac*)-194a)

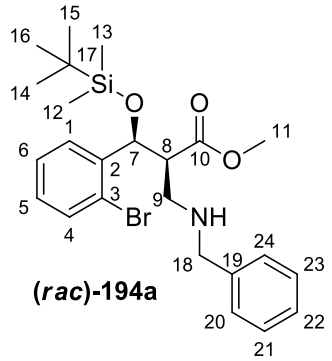

(*rac*)-194a

The product **194a** was isolated as a yellow oil (0.21 g, 60%). R_f = 0.8 (30% ethyl acetate: hexane). IR (neat, cm^{-1}) ν_{max} 3665 (N-H), 2950 (=C-H), 1734 (C=O), 1455 (C=C), 820 (Si-O); ^{1}H NMR (400 MHz, $CDCl_3$) δ 7.53 – 7.45 (2H, m, Ar-H), 7.34 – 7.27 (1H, m, Ar-H), 7.26 – 7.21 (2H, m, Ar-H), 7.22 – 7.16 (3H, m, Ar-H), 7.12 – 7.10 (1H, m, Ar-H), 5.31 (1H, d, *J*=7.5 Hz, H-7), 3.70 (3H, s, H-11), 3.68 (1H, m, H-18a), 3.59 (1H, m, H-18b), 2.99 (2H, m, H-8,9a), 2.44 (1H, s, H-9b), 1.53 (1H, s, NH), 0.81 (9H, s, H-14,15,16), 0.02 (3H, s, H-12), -0.28 (3H, s, H-13). ^{13}C NMR (101 MHz, $CDCl_3$) δ 173.5 (C-10), 142.0 (C-2), 140.8 (C-19), 140.0 (C-22), 132.4 (C-4), 129.2 (C-5), 128.3 (C-21,23), 128.0 (C-20,24), 127.6 (C-1), 126.8 (C-6), 122.5 (C-3), 73.1 (C-7), 56.0 (C-8) 53.4 (C-18), 51.5 (C-11), 47.5 (C-9), 25.6 (C-14,15,16), 17.9 (C-17), -4.8 (C-12), -5.4 (C-13). HRMS *m/z* calcd for $C_{24}H_{34}BrNO_3Si$ [M+H^+]:492.1564, found:492.1597.

5.4.9.2. Synthesis of methyl 2-((benzylamino)methyl)-3-(2-bromophenyl)-3-((*tert*-butyl dimethylsilyl)oxy)propanoate ((*rac*)-194b)

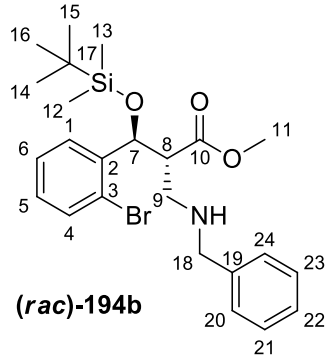

(*rac*)-194b

The product **194b** was isolated as a yellow oil (0.13 g, 36%). R_f = 0.8 (30% ethyl acetate: hexane). IR ν_{max} (neat, cm^{-1}) 3665 (N-H), 2950 (=C-H), 1734 (C=O), 1455 (C=C), 820 (Si-O); ^{1}H NMR (400 MHz, $CDCl_3$) δ 7.52 – 7.44 (2H, m, Ar-H), 7.31 – 7.26 (2H, m, Ar-H), 7.25 – 7.16 (4H, m, Ar-H), 7.15 – 7.08 (1H, m, Ar-H), 5.50 (1H, s, H-7), 3.71 – 3.62 (5H, m, H-11,18), 3.19 – 3.12 (1H, m, H-9a), 3.07 – 2.99 (1H, m, H-8), 2.73 – 2.64 (1H, m, H-9b), 0.85 (9H, s, H-14,15,16), 0.01 (3H, s, H-12), -0.24 (3H, s, H-13). ^{13}C NMR (101 MHz, $CDCl_3$) δ 173.0 (C-10), 141.3 (C-2), 140.2 (C-19), 132.7 (C-22), 129.2 (C-4), 129.0 (C-5), 128.3 (C-21,23), 128.1 (C-20,24), 127.1 (C-1), 126.8 (C-6), 121.6 (C-3), 73.5 (C-7), 53.8 (C-18), 51.72 (C-8), 51.70 (C-11), 45.3 (C-9), 25.7 (C-14,15,16), 18.0 (C-17), -4.8 (C-12), -5.5 (C-13). HRMS *m/z* calcd for $C_{24}H_{34}BrNO_3Si$ [$M+H^+$]: 492.1564, found: 492.1600.

5.4.9.3. Synthesis of (*E*)-methyl 2-((benzylamino)methyl)-3-phenylacrylate (195)

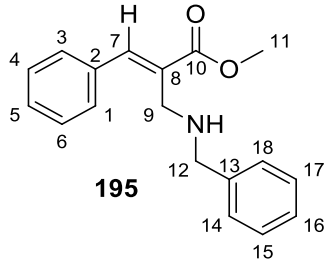

195

The product **195** was isolated as a brown oil (0.003 g, 3%). R_f = 0.2 (30% ethyl acetate: hexane). IR ν_{max} (neat, cm^{-1}) 2950 (=C-H), 1714 (C=O), 1454 (C=C); ^{1}H NMR (400 MHz, $CDCl_3$) δ 7.84 (1H, s, H-7), 7.59 (2H, m, Ar-H), 7.50 – 7.42 (2H, m, Ar-H), 7.29 – 7.27 (1H, m, Ar-H), 7.24 – 7.13 (4H, m, Ar-H), 3.85 (3H, s, H-11), 3.73 (2H, s, H-12), 3.48 (2H, s, H-9). ^{13}C NMR (101 MHz,

$CDCl_3$) δ 142.0 (Ar-C), 140.9 (Ar-C), 132.6 (Ar-C), 130.9 (Ar-C), 130.0 (Ar-C), 128.3 (Ar-C), 127.2 (Ar-C), 126.9 (Ar-C), 77.2 (C-7), 53.3 (C-12), 52.2 (C-11), 45.0 (C-9).

5.4.10. Conjugate addition reaction of TBDMS protected adduct 163 with benzylamine.

To the protected MBH adduct **163** (0.3 g, 1 mmol) in methanol (5 ml) was added benzylamine (0.33 ml, 3.5 mmol). The stoppered reaction mixture was stirred at room temperature for 2 days until the reaction was complete. Upon reaction completion, the mixture was concentrated in vacuo, and purification by column chromatography (20% ethyl acetate:hexane) led to the isolation of two products, 2-((benzylamino)methyl)-3-(2-bromophenyl)-3-((*tert*-butyldimethylsilyl)oxy)propane nitrile (**196a/b**), (E)-2-((benzylamino)methyl)-3-(2-bromophenyl)acrylonitrile (**197**).

5.4.10.1. Synthesis of 2-((benzylamino)methyl)-3-(2-bromophenyl)-3-((*tert*-butyl dimethylsilyl)oxy)propanenitrile (196a/b)

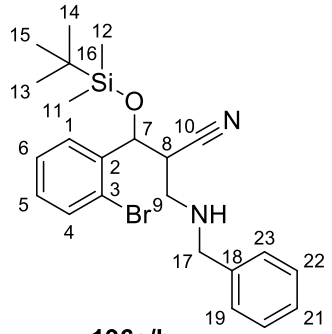

196a/b

The product **196a/b** was isolated as a white solid (0.31 g, 76%). M.P: 70-72˚C, R_f = 0.6 (20% ethyl acetate: hexane). IR ν_{max} (neat, cm^{-1}) 3347 (NH), 2926 (=C-H), 2240 (CN) 1468 (C=C), 830 (Si-O); ^{1}H NMR (400 MHz, $CDCl_3$) δ 7.72 (0.27H, d, *J*=7.8 Hz, Ar-H), 7.57 – 7.47 (1.81H, m, Ar-H), 7.42 – 7.27 (3.85H, m, Ar-H), 7.26 – 7.14 (3.05H, m, Ar-H), 5.44 – 5.28 (0.72H, m, H-7), 5.31 – 5.29 (0.22H, m, H-7), 3.84 (0.49H, s, H-17), 3.82 – 3.69 (1.58H, m, H-17), 3.22 – 3.04 (1.31H, m, H-8), 2.96 (1H, dd, *J*=12.2, 8.6 Hz, H-9), 2.80 (0.75H, dd, *J*=12.3, 4.6 Hz, H-9), 2.18 (1H, s, N-H), 0.91 (2H, s, H-13,14,15), 0.88 (7H, s, H-13,14,15), 0.14 (2H, s, H-11), 0.07 (1H, s, H-11), -0.15 (2H, s, H-12), -0.18 (1H, s, H-12). ^{13}C NMR (101 MHz, $CDCl_3$) δ 140.2 (Ar-C'), 139.5 (Ar-C), 132.8 (Ar-C), 132.5 (Ar-C'), 129.82 (Ar-C), 129.76 (Ar-C'), 129.1 (Ar-C'), 128.9 (Ar-C'), 128.9 (Ar-C), 128.52 (Ar-C'), 128.45 (Ar-C), 128.13 (Ar-C'), 128.10 (Ar-C), 127.8 (Ar-C'), 127.6

(Ar-C), 127.2 (Ar-C'), 127.1 (Ar-C), 121.8 (Ar-C), 121.1 (Ar-C'), 119.8 (C-10), 71.9 (C-7), 70.6 (C-7'), 53.5 (C-17), 53.3 (C-17'), 48.2 (C-9'), 45.7 (C-9), 41.4 (C-8'), 40.2 (C-8), 25.7 (C-13',14',15'), 25.7 (C-13,14,15), 18.08 (C-16'), 18.05 (C-16), -4.7 (C-12'), -4.9 (C-12), -5.2 (C-11'), -5.3 (C-11).

5.4.10.2. Synthesis of (*E*)-2-((benzylamino)methyl)-3-(2-bromophenyl)acrylonitrile (197)

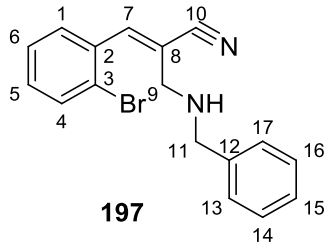

197

The product **197** was isolated as a brown oil (0.05 g, 13%). R_f = 0.3 (20% ethyl acetate: hexane). IR ν_{max} (neat, cm^{-1}) 2927 (=C-H), 2215 (CN), 1454 (C=C); ^{1}H NMR (400 MHz, $CDCl_3$) δ 7.91 (1H, dd, *J*=8.0, 1.7 Hz, H-7), 7.64 (1H, dd, *J*=8.1, 1.2 Hz, Ar-H), 7.46 – 7.33 (5H, m, Ar-H), 7.32 – 7.27 (1H, m, Ar-H), 7.26 – 7.17 (2H, m, Ar-H), 3.88 (2H, s, H-11), 3.62 (2H, d, *J*=1.4 Hz, H-9), 1.25 (1H, s, N-H). ^{13}C NMR (101 MHz, $CDCl_3$) δ 143.2 (Ar-C), 139.4 (Ar-C), 133.7 (Ar-C), 133.0 (Ar-C), 131.3 (Ar-C), 129.6 (C-7), 128.6 (Ar-C), 128.3 (Ar-C), 127.8 (Ar-C), 127.3 (Ar-C), 124.3 (Ar-C), 117.7 (C-10), 114.0 (C-8), 52.2 (C-9), 52.1 (C-11). HRMS *m/z* calcd for $C_{17}H_{15}BrN_2$ [$M+H^+$]: 327.0491, found: 327.0508.

5.4.11. Synthesis of methyl 3-((*tert*-butyldimethylsilyl)oxy)-3-(4-chlorophenyl)-2-(((4-methoxybenzyl)amino)methyl)propanoate (198)

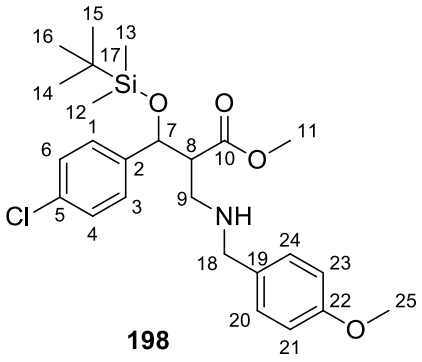

198

To the protected MBH adduct **162** (0.25 g, 1 mmol) in methanol (5 ml) was added 4-methoxybenzylamine (0.11 ml, 1.1 mmol). The stoppered reaction mixture was stirred at room

temperature for 2 days until the reaction was complete. Upon reaction completion, the mixture was concentrated in vacuo, and purification by column chromatography (10% ethyl acetate:hexane) led to the isolation of the product **198** as a yellow oil (0.25 g, 69%). R_f = 0.3 (10% ethyl acetate: hexane). IR ν_{max} (neat, cm^{-1}) 3187 (N-H), 2952 (=C-H), 1727 (C=O), 1614 (C=C), 820 (Si-O); ^{1}H NMR (400 MHz, $CDCl_3$) δ 7.31 – 7.26 (2H, m, H-4,6), 7.26 – 7.17 (4H, m, H-1,3,20,24), 6.85 (2H, d, *J*=8.5 Hz, H-21,23), 5.12 (1H, d, *J*=3.7 Hz, H-7), 3.93 – 3.87 (1H, m, H-18a), 3.80 (3H, s, H-25), 3.77 – 3.72 (1H, m, H-18b), 3.64 (3H, s, H-11), 3.20 – 3.08 (2H, m, H-9a,8), 2.85 – 2.78 (1H, m, H-9b), 0.82 (9H, s, H-14,15,16), -0.04 (3H, s, H-12), -0.23 (3H, s, H-13). ^{13}C NMR (101 MHz, $CDCl_3$) δ 172.4 (C-10), 159.6 (C-22), 140.0 (C-2), 133.6 (C-19), 130.4 (C-20,24), 128.6 (C-4,6), 128.5 (C-5), 127.4 (C-1,3), 114.2 (C-21,23), 73.8 (C-7), 55.3 (C-25), 52.6 (C-8), 52.3 (C-11), 51.9 (C-18), 44.2 (C-9), 25.6 (C-14,15,16), 18.0 (C-17), -4.6 (C-13), -5.5 (C-12).

5.4.12. Conjugate addition reaction of TBDMS protected adduct 165 with 4-methoxybenzylamine.

To the protected MBH adduct **165** (0.3 g, 1 mmol) in methanol (5 ml) was added 4-methoxybenzylamine (0.45 ml, 3.5 mmol). The stoppered reaction mixture was stirred at room temperature for 2 days until the reaction was complete. Upon reaction completion, the mixture was concentrated in vacuo, and purification by column chromatography (10% ethyl acetate:hexane) led to the isolation of two products, 3-((*tert*-butyldimethylsilyl)oxy)-3-(4-chlorophenyl)-2-(((4-methoxybenzyl)amino)methyl)propanenitrile (**199**), Synthesis of (E)-3-(4-chlorophenyl)-2-(((4-methoxybenzyl)amino)methyl) acrylonitrile (**200**).

5.4.12.1. Synthesis of 3-((*tert*-butyldimethylsilyl)oxy)-3-(4-chlorophenyl)-2-(((4-methoxybenzyl)amino)methyl)propanenitrile (199)

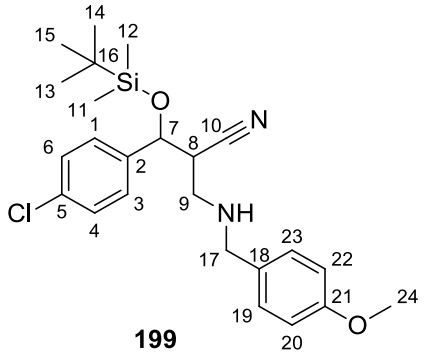

199

The product **199** was isolated as a yellow oil (0.39 g, 91%). R_f = 0.35 (10% ethyl acetate: hexane). IR ν_{max} (neat, cm^{-1}) 2925 (=C-H), 2225 (CN), 1491 (C=C), 835 (Si-O); ^{1}H NMR (400 MHz, $CDCl_3$) δ 7.34 – 7.24 (4H, m, Ar-H), 7.21-7.16 (2H, m, Ar-H), 6.90 – 6.80 (2H, m, Ar-H), 4.88 (1H, d, *J*=6.5 Hz, H-7), 3.81 (3H, s, H-24), 3.72 (2H, s, H-17), 3.01 – 2.71 (3H, m, H-8,9), 2.21 (1H, s, N-H), 0.89 (3H, s, H-13,14,15), 0.86 (6H, s, H-13,14,15), 0.06 (3H, s, H-11), -0.18 (3H, s, H-12). ^{13}C NMR (101 MHz, $CDCl_3$) δ 158.9 (Ar-C), 139.2 (Ar-C), 134.2 (Ar-C), 131.6 (Ar-C), 129.3 (Ar-C), 128.7 (Ar-C), 127.9 (Ar-C), 119.4 (C-10), 113.9 (Ar-C), 72.6 (C-7), 55.3 (C-24), 53.0 (C-17), 46.6 (C-9), 42.6 (C-8), 25.7 (C-13,14,15), 18.0 (C-16), -4.7 (C-12), -5.2 (C-11). HRMS *m/z* calcd for $C_{24}H_{33}ClN_2O_2Si$ [M+H^+]: 445.2126, found: 445.2101.

5.4.12.2. Synthesis of (E)-3-(4-chlorophenyl)-2-(((4-methoxybenzyl)amino)methyl) acrylonitrile (200)

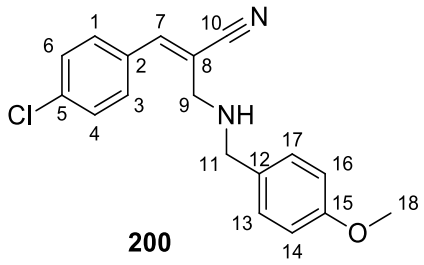

200

The product **200** was isolated as a brown oil (0.03 g, 6%). R_f = 0.10 (10% ethyl acetate: hexane). IR ν_{max} (neat, cm^{-1}) 2924 (=C-H), 2213 (CN), 1491 (C=C); ^{1}H NMR (400 MHz, $CDCl_3$) δ 7.69 (2H, d, *J*=8.7 Hz, Ar-H), 7.40 (2H, d, *J*=8.6 Hz, Ar-H), 7.25 – 7.19 (2H, m, Ar-H), 7.03 (1H, s, H-7), 6.90 – 6.87 (2H, m, Ar-H), 3.80 (3H, s, H-18), 3.78 (2H, s, H-11), 3.56 (2H, s, H-9), 2.02 (1H, s, N-H). ^{13}C NMR (101 MHz, $CDCl_3$) δ 158.9 (Ar-C), 142.6 (C-7), 136.2 (Ar-C), 131.4 (Ar-C), 130.0 (Ar-C), 129.4 (Ar-C), 129.3 (Ar-C), 129.2 (Ar-C), 114.1 (C-10), 113.9 (Ar-C), 111.1 (C-8), 55.3 (C-18), 52.5 (C-9), 51.7 (C-11). HRMS *m/z* calcd for $C_{18}H_{17}ClN_2O$ [M+H^+]: 313.1102, found: 313.1118.

5.4.13. Synthesis of methyl 3-((*tert*-butyldimethylsilyl)oxy)-3-phenyl-2-((phenylamino) methyl)propanoate (201)

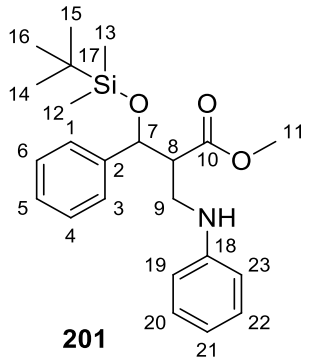

201

To the protected MBH adduct **160** (0.25 g, 1 mmol) in methanol (5 ml) was added aniline (0.08 ml, 1.1 mmol). The stoppered reaction mixture was stirred at room temperature for 2 days until the reaction was complete. Upon reaction completion, the mixture was concentrated in vacuo, and purification by column chromatography (20% ethyl acetate:hexane) led to the isolation of the product **201** as a brown oil (0.1 g, 11%). R_f = 0.60 (20% ethyl acetate: hexane). IR ν_{max} (neat, cm^{-1}) 2955 (=C-H), 1735 (C=O), 1462 (C=C), 835 (Si-O); ^{1}H NMR (400 MHz, $CDCl_3$) δ 7.38 – 7.29 (5H, m, H-1,3,4,5,6), 7.10 – 7.03 (2H, m, H-20,22), 6.67 – 6.61 (1H, m, H-21), 6.34 (2H, d, *J* = 8.0 Hz, H-19,23), 5.15 (1H, d, *J* = 5.7 Hz, H-7), 3.99 (1H, s, N-H), 3.73 – 3.66 (1H, m, H-9a), 3.56 (3H, s, H-11), 3.48 – 3.41 (1H, m, H-9b), 2.93 (1H, s, H-8), 0.91 (9H, s, H-14,15,16), 0.03 (3H, s, H-12), -0.19 (3H, s, H-13). ^{13}C NMR (101 MHz, $CDCl_3$) δ 173.1 (C-10), 147.6 (C-18), 142.4 (C-2), 129.2 (20,22), 128.2 (C-4,6), 127.7 (C-5), 126.2 (C-1,3), 117.2 (C-21), 112.7 (C-19,23), 74.7 (C-7), 53.8 (C-8), 51.7 (C-11), 41.0 (C-9), 25.8 (C-14,15,16), 18.1 (C-17), -4.6 (C-12), -5.4 (C-13). HRMS *m/z* calcd for $C_{23}H_{33}NO_3Si$ $[M+H^+]$:400.2302, found:400.2238.

5.4.14. Synthesis of methyl 3-((*tert*-butyldimethylsilyl)oxy)-3-(4-chlorophenyl)-2-(((4-methoxyphenyl)amino)methyl)propanoate (202)

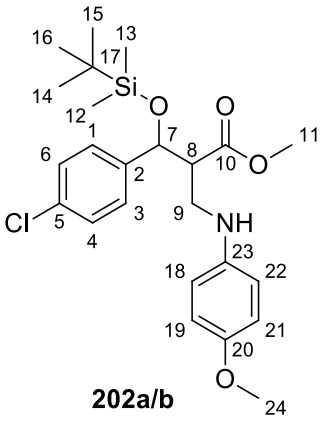

202a/b

To a solution of MBH adduct **162** (0.25 g, 1 mmol) in dichloromethane (2 ml) was added *p*-anisidine (0.2 g, 2 mmol), triethylamine (0.7 ml) and $ZnCl_2$ (0.02 g). The mixture was stirred at room temperature for 2 days. The solvent was evaporated under reduced pressure and the residue was purified by column chromatography to afford the product **202a/b** as a brown oil (0.1 g, 15%). R_f = 0.50 (20% ethyl acetate: hexane). IR ν_{max} (neat, cm^{-1}) 3665 (N-H), 2967 (=C-H), 1732 (C=O), 1455 (C=C), 1235 (C-O), 820 (Si-O); ^{1}H NMR (400 MHz, $CDCl_3$) δ 7.34 – 7.29 (2H, m, Ar-H), 7.29 – 7.24 (2H, m, Ar-H), 6.74 – 6.69 (2H, m, Ar-H), 6.41 – 6.34 (2H, m, Ar-H), 5.08 (0.67H, d, *J*=6.2 Hz, H-7), 4.98 (0.27H, d, *J*=8.5 Hz, H-7), 3.90 – 3.89 (0.05H, m, H-9), 3.82 – 3.79 (0.11H, m, H-9), 3.73 (3H, s, H-24), 3.72 (1H, s, H-11), 3.68 – 3.62 (0.30H, m, H-9), 3.55 (2H, s, H-11), 3.53 – 3.50 (0.66H, m, H-9), 3.39 (0.7H, dd, *J*=13.3, 3.7 Hz, H-9), 3.11 – 3.06 (0.20H, m, H-9), 3.02 – 2.96 (0.21H, m, H-8), 2.93 – 2.87 (0.88H, m, H-8,9), 0.89 (6H, s, H-14,15,16), 0.83 (3H, s, H-14,15,16), 0.03 (2H, s, H-12), 0.01 (1H, s, H-12), -0.20 (2H, s, H-13), -0.25 (1H, s, H-13). ^{13}C NMR (101 MHz, $CDCl_3$) δ 173.8 (C-10'), 173.0 (C-10), 152.3 (Ar-C'), 152.1 (Ar-C), 141.70 (Ar-C), 141.67 (Ar-C'), 141.1 (Ar-C), 140.4 (Ar-C'), 133.8 (Ar-C'), 133.4 (Ar-C), 128.6 (Ar-C'), 128.4 (Ar-C), 128.1 (Ar-C'), 127.7 (Ar-C), 114.9 (Ar-C), 114.8 (Ar-C'), 114.3 (Ar-C'), 114.1 (Ar-C), 74.3 (C-7'), 74.1 (C-7), 55.8 (C-24, 24'), 54.2 (C-8'), 53.9 (C-8), 51.9 (C-11'), 51.7 (C-11), 43.2 (C-9'), 42.3 (C-9), 25.7 (C-14,15,16), 25.6 (C-14',15',16'), 18.1 (C-17), 17.9 (C-17'), -4.59 (C-12), -4.63 (C-12'), -5.3 (C-13), -5.4 (C-13'). HRMS *m/z* calcd for $C_{24}H_{34}ClNO_4Si$ [$M+H^+$]: 464.2018, found: 464.2055.

5.4.15. General procedure for the conjugate addition of sulfur nucleophiles.

To a stirred solution of the MBH adduct (1.84 mmol) in ethanol (7 ml) was added the appropriate thiol (3.67 mmol) and triethylamine (0.7 ml) at room temperature. The reaction was stirred for 1-2 days. The solvent was evaporated under high pressure and the product purified by column chromatography.

5.4.15.1. Synthesis of methyl 2-((benzylthio)methyl)-3-(2-bromophenyl)-3-((trimethylsilyl) oxy)propanoate (203a/b)

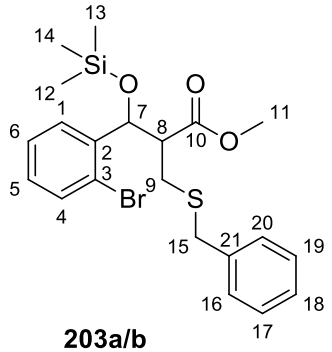

203a/b

Benzylmercaptan was used, affording a mixture of diastereomers **203a/b** as pale yellow oil (0.04 g, 81%). R_f = 0.71 (20% ethyl acetate: hexane). IR ν_{max} (neat, cm^{-1}) 2952 (=C-H), 1739 (C=O), 1435 (C=C), 820 (Si-O); ^{1}H NMR (400 MHz, $CDCl_3$) δ 7.53 (0.56H, dd, *J*=8.1, 1.1 Hz, Ar-H), 7.49 – 7.41 (1.30H, m, Ar-H), 7.37 – 7.25 (1.25H, m, Ar-H), 7.21 – 7.12 (3.79H, m, Ar-H), 7.08 – 7.06 (0.73H, m, Ar-H), 6.99 – 6.96 (1.18H, m, Ar-H), 5.37 (0.54H, d, *J*=4.3 Hz, H-7), 5.28 (0.36H, d, *J*=8.3 Hz, H-7), 3.71 (0.95H, s, H-11), 3.70 (1.74H, s, H-11), 3.58 (0.70H, d, *J*=4.2 Hz, H-15), 3.53 (0.70H, d, *J*=13.6 Hz, H-15), 3.43 (0.70H, d, *J*=13.6 Hz, H-15), 3.10 – 3.05 (0.59H, m, H-8), 3.02 – 2.96 (0.42H, m, H-8), 2.88 (0.63H, dd, *J*=13.8, 11.1 Hz, H-9), 2.73 (0.42H, dd, *J*=13.4, 11.4 Hz, H-9), 2.38 (0.61H, dd, *J*=13.9, 2.9 Hz, H-9), 2.16 (0.38H, dd, *J*=13.5, 4.4 Hz, H-9), -0.03 (4.61H, s, H-12,13,14), -0.04 (4.02H, s, H-12,13,14). ^{13}C NMR (101 MHz, $CDCl_3$) δ 172.8 (C-10'), 172.2 (C-10), 141.3 (Ar-C'), 140.8 (Ar-C), 138.3 (Ar-C), 137.7 (Ar-C'), 132.8 (Ar-C), 132.4 (Ar-C'), 129.3 (Ar-C), 129.18 (Ar-C'), 129.15 (Ar-C), 128.9 (Ar-C'), 128.8 (Ar-C'), 128.7 (Ar-C), 128.42 (Ar-C'), 128.37 (Ar-C), 127.8 (Ar-C'), 127.3 (Ar-C), 126.9 (Ar-C'), 126.7 (Ar-C), 122.5 (Ar-C'), 121.4 (Ar-C), 73.9 (C-7,7'), 55.1 (C-8'), 52.1 (C-11'), 51.9 (C-11), 51.7 (C-8), 36.1 (C-15), 35.7 (C-15'), 28.7 (C-9'), 26.5 (C-9), -0.2 (C-12',13',14'), -0.3 (C-12,13,14). HRMS *m/z* calcd for $C_{21}H_{27}BrO_3SSi$ [$M+H^+$]:387.1445, found: 387.1372.

5.4.15.2. Synthesis of 2-((benzylthio)methyl)-3-(4-chlorophenyl)-3-hydroxypropanenitrile (204a/b)

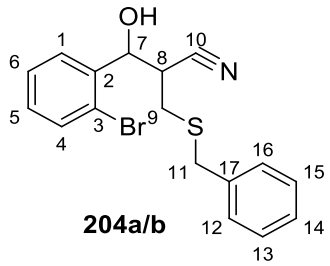

204a/b

Benzylmercaptan was used affording the product **204a/b** as a yellow oil (0.13 g, 95%). R_f = 0.85 (10% ethyl acetate: hexane). IR ν_{max} (neat, cm^{-1}) 3425 (OH), 2923 (=C-H), 2247 (CN), 1454 (C=C); ^{1}H NMR (400 MHz, $CDCl_3$) δ 7.74 (0.39H, dd, *J*=7.7, 1.7 Hz, Ar-H), 7.60 – 7.48 (1.52H, m, Ar-H), 7.42 (0.45H, td, *J*=7.6, 1.2 Hz, Ar-H), 7.38 – 7.10 (7.17H, m, Ar-H), 5.42 (0.55H, d, *J*=4.5 Hz, H-7), 5.36 (0.40H, d, *J*=2.9 Hz, H-7), 3.85 (0.78H, s, H-11), 3.80 – 3.65 (1.07H, m, H-11), 3.29 – 3.20 (0.49H, m, H-8), 3.18 – 3.09 (0.34H, m, H-8), 3.00 – 2.83 (0.69H, m, H-9), 2.73 (0.48H, dd, *J*=14.1, 10.1 Hz, H-9), 2.48 (0.54H, dd, *J*=14.2, 4.3 Hz, H-9). ^{13}C NMR (101 MHz, $CDCl_3$) δ 139.1 (Ar-C'), 138.1 (Ar-C), 137.3 (Ar-C), 137.1 (Ar-C'), 133.1 (Ar-C), 132.7 (Ar-C'), 130.2 (Ar-C), 130.1 (Ar-C'), 129.1 (Ar-C'), 128.9 (Ar-C), 128.8 (Ar-C'), 128.7 (Ar-C), 128.4 (Ar-C), 128.2 (Ar-C'), 128.2 (Ar-C'), 127.9 (Ar-C), 127.5 (Ar-C'), 127.3 (Ar-C), 121.9 (Ar-C'), 121.2 (Ar-C), 119.6 (C-10'), 118.1 (C-10), 71.9 (C-7), 70.6 (C-7'), 39.3 (C-8), 39.2 (C-8'), 36.4 (C-11'), 36.3 (C-11), 30.6 (C-9'), 27.2 (C-9). HRMS *m/z* calcd for $C_{17}H_{16}BrNOS$ [$M+H^+$]: 362.0209, found: 362.0193.

5.4.15.3. Synthesis of methyl 3-(4-chlorophenyl)-2-((p-tolylthio)methyl)-3-((trimethylsilyl) oxy)propanoate (205a/b)

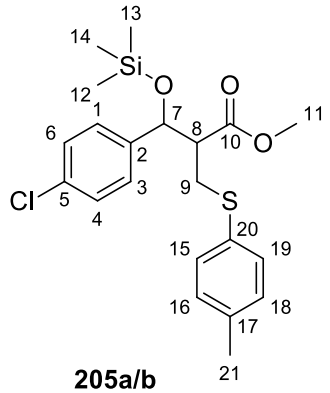

205a/b

4-methylbenzenethiol was used, affording a mixture of diastereomers **205a/b** as a white oil (0.1 g, 63%). R_f = 0.40 (30% ethyl acetate: hexane). IR ν_{max} (neat, cm^{-1}) 2952 (=C-H), 1730 (C=O), 1434 (C=C), 830 (Si-O); ^{1}H NMR (400 MHz, $CDCl_3$) δ 7.30 – 7.27 (1.05H, m, Ar-H), 7.25 – 7.24 (0.69H, m, Ar-H), 7.19 – 7.17 (1.08H, m, Ar-H), 7.17-7.15 (0.76H, m, Ar-H) , 7.09 – 7.00 (3.67H, m, Ar-H), 4.90 (0.55H, d, *J*=6.5 Hz, H-7), 4.78 (0.34H, d, H-7), 3.68 (1.08H, s, H-11), 3.50 (1.63H, s, H-11), 3.18 (0.44H, d, *J*=2.9 Hz, H-9), 3.16 (0.56H, s, H-9), 2.90 – 2.87 (0.23H, m, H-9), 2.87–2.86 (0.25H, m, H-8), 2.85-2.83 (0.25H, m, H-9), 2.83 – 2.78 (0.55H, m, H-8), 2.66 – 2.63 (0.34H, m, H-9), 2.30 (3H, s, H-21), 0.01 (5.77H, s, H-12,13,14), -0.05 (3.31H, s, H-12,13,14). ^{13}C NMR (101 MHz, $CDCl_3$) δ 173.1 (C-10'), 172.3 (C-10), 140.7 (Ar-C), 140.1 (Ar-C'), 136.7 (Ar-C'), 136.2 (Ar-C), 133.8 (Ar-C'), 133.4 (Ar-C), 131.7 (Ar-C), 131.1 (Ar-C'), 130.7 (Ar-C'), 129.9 (Ar-C), 129.7 (Ar-C'), 129.6 (Ar-C), 128.6 (Ar-C'), 128.4 (Ar-C), 128.1 (Ar-C'), 127.6 (Ar-C), 75.3 (C-7'), 74.8 (C-7), 55.3 (C-8), 54.8 (C-8'), 51.74 (C-11'), 51.71 (C-11), 32.6 (C-9'), 31.6 (C-9), 21.02 (C-21'), 20.99 (C-21), -0.1 (C-12,13,14), -0.1 (C-12',13',14').

5.4.15.4. Synthesis of 3-(4-chlorophenyl)-3-hydroxy-2-((p-tolylthio)methyl)propanenitrile (206a/b)

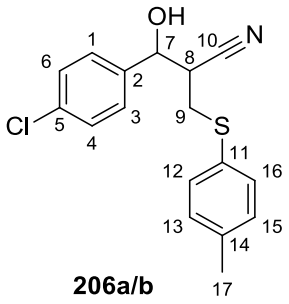

206a/b

4-methylbenzenethiol was used, affording the product **206a/b** as a mixture of diastereomers as an off white solid (0.25 g, 70%). M.P: 91-95 ˚C, R_f = 0.1 (10% ethyl acetate: hexane). IR ν_{max} (neat, cm^{-1}) 3388 (OH), 2924 (=C-H), 2256 (CN), 1491 (C=C); ^{1}H NMR (400 MHz, $CDCl_3$) δ 7.34 – 7.17 (6H, m, Ar-H), 7.11 – 7.02 (2H, m, Ar-H), 5.03 (0.29H, d, *J*=4.1 Hz, H-7), 4.95 (0.64H, d, *J*=5.3 Hz, H-7), 3.20 – 2.98 (0.80H, m, H-8), 3.02 – 2.89 (2H, m, H-9), 2.81 – 2.74 (0.31H, m, H-8), 2.27 (2.93H, s, H-17). ^{13}C NMR (75 MHz, $CDCl_3$) δ 138.1 (Ar-C, Ar-C'), 137.7 (Ar-C, Ar-C'), 135.0 (Ar-C, Ar-C'), 131.9 (Ar-C), 131.8 (Ar-C'), 130.4 (Ar-C'), 130.3 (Ar-C), 129.9 (Ar-C, Ar-C'), 129.13 (Ar-C'), 129.10 (Ar-C), 127.9 (Ar-C), 127.4 (Ar-C'), 118.8 (C-10), 72.2 (C-7), 71.0 (C-7'), 41.2 (C-8'), 40.8 (C-8), 33.2 (C-9), 31.0 (C-9'), 21.2 (C-17).

5.4.15.5. Synthesis of 3-((*tert*-butyldimethylsilyl)oxy)-3-(4-chlorophenyl)-2-((phenylthio) methyl)propanenitrile (207a/b)

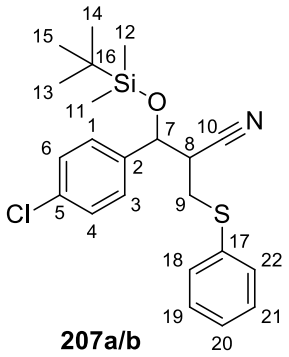

207a/b

Benzenethiol was used, affording the product **207a/b** as a yellow oil (0.77 g, 67%). R_f = 0.1 (10% ethyl acetate: hexane). IR ν_{max} (neat, cm^{-1}) 2928 (=C-H), 2240 (CN), 1473 (C=C), 838 (Si-O); ^1H NMR (400 MHz, $CDCl_3$) δ 7.52 – 7.50 (1H, m, Ar-H), 7.50 – 7.47 (1H, m, Ar-H), 7.39 – 7.20 (7H, m, Ar-H), 4.99 (0.31H, d, *J*=4.1 Hz, H-7), 4.96 (0.67H, d, *J*=5.4 Hz, H-7), 3.16 (0.34H, dd, *J*=13.9, 7.2 Hz, H-9), 3.08 – 3.02 (1.61H, m, H-9), 2.94 (0.73H, ddd, H-8), 2.78 (0.30H, td, *J*=7.3, 4.1 Hz, H-8), 0.91 (2.97H, s, H-13,14,15), 0.89 (5.78H, s, H-13,14,15), 0.08 (2.83H, s, H-11), -0.15 (1.80H, s, H-12), -0.16 (1.07H, s, H-12). ^{13}C NMR (101 MHz, $CDCl_3$) δ 138.3 (Ar-C'), 137.0 (Ar-C), 134.5 (Ar-C'), 133.7 (Ar-C), 131.0 (Ar-C'), 130.5 (Ar-C), 129.4 (Ar-C'), 129.3 (Ar-C), 129.1 (Ar-C), 128.8 (Ar-C'), 127.9 (Ar-C), 127.7 (Ar-C'), 127.5 (Ar-C), 127.3 (Ar-C'), 127.2 (Ar-C), 118.9 (C-10), 73.0 (C-7), 72.0 (C-7'), 42.3 (C-8'), 41.9 (C-8), 33.3 (C-9'), 32.0 (C-9), 25.7 (C-13,14,15), 18.1 (C-16'), 18.1 (C-16), -4.6 (C-12'), -4.7 (C-12), -5.1 (C-11'), -5.2 (C-11).

5.4.16. General procedure for the deprotection of MBH adducts.

To a mixture of MBH adduct (3 mmol) in THF (20 ml) at 0 ˚C was added TBAF in THF (3.6 mmol). The mixture was stirred for 20 minutes at 0 ˚C and then warmed to room temperature for 2 hours. The mixture was concentrated *in vacuo* and the residue purified by column chromatography.

5.4.16.1. Synthesis of 2-((benzylamino)methyl)-3-(2-bromophenyl)-3-hydroxypropane nitrile (208a/b)

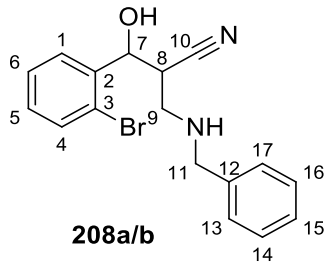

208a/b

The product **208a/b** was isolated as a brown solid (0.18 g, 71%). M.P: 68-70˚C, R_f = 0.3 (5% ethyl acetate: hexane). IR ν_{max} (neat, cm^{-1}) 3307 (OH), 3290 (NH), 2922 (=C-H), 2224 (CN), 1433 (C=C); ^{1}H NMR (400 MHz, $CDCl_3$) δ 7.85 (0.20H, dd, *J*=7.8, 1.8 Hz, Ar-H), 7.52 (0.89H, dd, *J*=7.9, 1.3 Hz, Ar-H), 7.46 – 7.12 (8H, m, Ar-H), 5.46 (0.72H, d, *J*=3.8 Hz, H-7), 5.30 (0.21H, d, *J*=1.9 Hz, H-7), 4.03 – 3.94 (0.46H, m, H-11), 3.89 (0.81H, d, *J*=13.0 Hz, H-11), 3.74 (0.75H, d, *J*=13.0 Hz, H-11), 3.41 (0.29H, dd, *J*=12.5, 3.3 Hz, H-9), 3.27 – 3.22 (0.26H, m, H-8), 3.22 – 3.16 (0.75H, m, H-8), 3.14 (0.33H, dd, *J*=12.5, 3.5 Hz, H-9), 3.04 (0.84H, dd, *J*=12.6, 4.6 Hz, H-9), 2.81 (0.84H, dd, *J*=12.6, 3.5 Hz, H-9), 2.20 (1H, s, NH). ^{13}C NMR (101 MHz, $CDCl_3$) δ 139.4 (Ar-C), 138.9 (Ar-C'), 138.1 (Ar-C'), 137.9 (Ar-C), 133.0 (Ar-C), 132.4 (Ar-C'), 129.8 (Ar-C'), 129.7 (Ar-C), 128.9 (Ar-C'), 128.8 (Ar-C), 128.7 (Ar-C), 128.6 (Ar-C'), 128.3 (Ar-C'), 128.2 (Ar-C), 128.1 (Ar-C'), 127.9 (Ar-C), 127.8 (Ar-C'), 127.7 (Ar-C), 121.6 (Ar-C), 121.1 (Ar-C'), 119.2 (C-10), 74.3 (C-7), 73.9 (C-7'), 53.9 (C-11'), 53.7 (C-11), 50.0 (C-9'), 46.2 (C-9), 37.8 (C-8'), 35.3 (C-8). HRMS *m/z* calcd for $C_{17}H_{17}BrN_2O$ [$M+H^+$]: 345.0597, found: 345.0530.

5.4.16.2. Synthesis of 3-hydroxy-3-phenyl-2-(piperidin-1-ylmethyl)propanenitrile (209a/b)

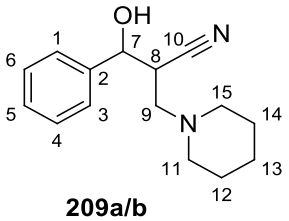

209a/b

The product **209a/b** was isolated as a brown solid (0.05 g, 52%). M.P: 60-62 ˚C, R_f = 0.37 (30% ethyl acetate: hexane). IR ν_{max} (neat, cm^{-1}) 2981(OH), 2922 (=C-H), 2220 (CN), 1454 (C=C); ^{1}H NMR (400 MHz, $CDCl_3$) δ 7.50 – 7.29 (5H, m, Ar-H), 5.12 (0.28H, d, *J*=2.8 Hz, H-7), 4.96 (0.62H, d, *J*=8.2 Hz, H-7), 3.18-3.14 (0.27H, m, H-8), 3.20 – 3.12 (0.30H, m, H-9), 2.97 (0.58H, s, H-8),

2.96 (0.36H, s, H-9), 2.92 (0.17H, s, H-9), 2.87 (0.66H, d, *J*=14.5 Hz, H-9), 2.83 (0.25H, d, *J*=7.2 Hz, H-9), 2.73 (0.44H, dd, *J*=13.3, 4.2 Hz, H-11,15), 2.71 – 2.35 (3.75H, m, H-11,15), 1.73 – 1.57 (4.43H, m, H-12,13,14), 1.53 – 1.46 (2.43H, m, H-12,13,14). ^{13}C NMR (101 MHz, $CDCl_3$) δ 140.7 (Ar-C), 140.0 (Ar-C'), 128.6 (Ar-C), 128.5 (Ar-C'), 128.2 (Ar-C'), 126.5 (Ar-C), 126.1 (Ar-C'), 118.7 (C-10'), 118.5 (C-10), 77.1 (C-7), 74.3 (C-7'), 60.5 (C-9), 58.3 (C-9'), 55.3 (C-11,15), 54.7 (C-11',15'), 36.2 (C-8'), 35.9 (C-8), 26.0 (C-12',14'), 25.8 (C-12,14), 23.7 (C-13).

5.5. Preparation and characterization of amide MBH adducts and their conjugate addition products.

5.5.1. Preparation and characterization of carboxylic acids

5.5.1.1. Synthesis of 2-((4-bromophenyl)((*tert*-butyldimethylsilyl)oxy)methyl)acrylic acid (221)

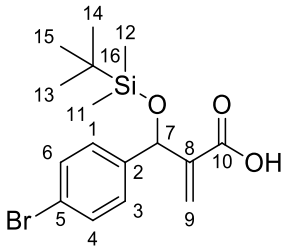

221

LiOH (1.99 g, 10 mmol) was added to a mixture of MBH adduct (3.2 g, 1 mmol) in CH_3CN/H_2O (1:1, 20 ml). The solution was stirred overnight at 60 ˚C. Upon completion, the mixture was concentrated in vacuo. 1 M HCl (10 ml) was added to the residue and the mixture was extracted with ethyl acetate (4 x 25 ml). The organic phases were combined, washed with brine solution (30 ml), dried over anhydrous sodium sulphate, filtered, and concentrated under vacuum. The residue was purified by column chromatography, affording the product **221** as a white solid (1.2 g, 39%). M.P: 73-75˚C, R_f = 0.3 (10% ethyl acetate: hexane). IR ν_{max} (neat, cm^{-1}) 2951 (OH), 2929 (=C-H), 1688 (C=O), 1440 (C=C), 825 (Si-O); ^{1}H NMR (400 MHz, $CDCl_3$) δ 7.52 – 7.48 (2H, m, H-4,6), 7.33 – 7.30 (2H, m, H-1,3), 6.48 (1H, t, *J*=1.3 Hz, H-9a), 6.26 (1H, t, *J*=1.5 Hz, H-9b), 5.60 (1H, s, H-7), 0.96 (9H, s, H-13,14,15), 0.14 (3H, s, H-11), 0.00 (3H, s, H-12). ^{13}C NMR (101 MHz, $CDCl_3$) δ 169.7 (C-10), 142.7 (C-2), 141.4 (C-8), 131.3 (C-4,6), 128.7 (C-1,3), 126.6 (C-9), 121.5 (C-5), 72.1 (C-7), 25.7 (C-13,14,15), 18.2 (C-16), -4.9 (C-12), -5.1 (C-11).

5.5.1.2. Synthesis of 2-(((*tert*-butyldimethylsilyl)oxy)(4-chlorophenyl)methyl)acrylic acid (222)

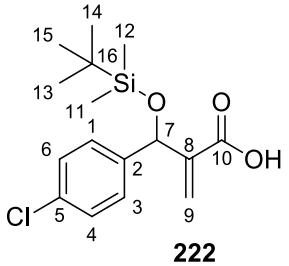

222

To a mixture of MBH adduct (2 g, 1 equiv) in ethanol (2 ml) was added KOH (0.3 g, 1.2 equiv) in water (10 ml). The mixture was refluxed for 4 h. Upon reaction completion, ethanol was evaporated under reduced pressure and any unreacted starting material was extracted using ethyl acetate (20 ml). The aqueous layer obtained was acidified using HCl and extracted using ethyl acetate (4 x 20 ml). Affording the product **222** as a colourless oil (0.2 g, 11%). R_f = 0.7 (40% ethyl acetate: hexane). IR ν_{max} (neat, cm^{-1}) 2952 (OH), 1695 (C=O), 1490 (C=C), 834 (Si-O); ^{1}H NMR (300 MHz, $CDCl_3$) δ 7.19 – 7.15 (4H, m, Ar-H), 6.29 (1H, t, *J*=1.3 Hz, H-9a), 6.07 (1H, t, *J*=1.3 Hz, H-9b), 5.43 (1H, s, H-7), 0.77 (9H, s, H-13,14,15), -0.04 (3H, s, H-11), -0.19 (3H, s, H-12). ^{13}C NMR (101 MHz, $CDCl_3$) δ 169.3 (C-10), 142.7 (C-2), 140.8 (C-8), 133.3 (C-5), 128.4 (C-4,6), 128.3 (C-1,3), 126.4 (C-9), 72.1 (C-7), 25.6 (C-13, 14, 15), 18.2 (C-16), -4.9 (C-12), -5.1 (C-11).

5.5.2. Preparation and characterization of amides.

5.5.2.1. Synthesis of N-benzyl-2-((4-bromophenyl)((*tert*-butyldimethylsilyl)oxy)methyl) acrylamide (223)

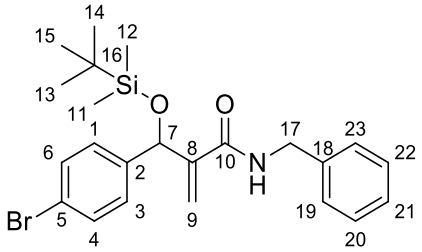

223

To a solution of the carboxylic acid **221** (1.2 g, 1.39 mmol) in THF (10 ml) was added DCC (0.67 g, 1.39 mmol, 1 equiv), DIPEA (0.84 ml, 2.10 mmol, 1.5 equiv) and NHS (0.37 g, 1 equiv). The mixture was kept at 0 ˚C for 15 mins, warmed to room temperature and kept for another 2 h.

Benzylamine (24 ml, 2 equiv) was then added to the solution and stirred at room temperature overnight. The reaction mixture was filtered and extracted with ethyl acetate (4 x 30 ml). Saturated NH_4Cl (20 ml) was then used to wash the organic phase. Which was then dried using anhydrous sodium sulphate, filtered, and concentrated. The residue was purified by column chromatography affording the product **223** as a brown oil (0.27 g, 20%). R_f = 0.4 (10% ethyl acetate: hexane). IR ν_{max} (neat, cm^{-1}) 3295 (NH), 2927 (=C-H), 1621 (C=O), 1496 (C=C), 825 (Si-O); ^1H NMR (400 MHz, $CDCl_3$) δ 7.43 – 7.39 (2H, m, Ar-H), 7.25 – 7.22 (3H, m, Ar-H, N-H), 7.19 – 7.15 (2H, m, Ar-H), 6.94 – 6.87 (3H, m, Ar-H), 6.12 (1H, s, H-7), 5.63 (1H, s, H-9), 5.54 (1H, s, H-9), 4.47 (1H, dd, *J*=14.7, 6.3 Hz, H-17a), 4.23 (1H, dd, *J*=15.0, 5.1 Hz, H-17b), 0.85 (9H, s, H-13,14,15), 0.07 (3H, s, H-11), 0.04 (3H, s, H-12).

The product **223** deprotected on standing in the NMR tube, the ^{13}C NMR data is for the deprotected version:

^{13}C NMR (126 MHz, $CDCl_3$) δ 167.6 (C-10), 154.8 (C-8), 145.2 (Ar-C), 137.5 (Ar-C), 133.9 (Ar-C), 131.6 (Ar-C), 128.7 (Ar-C), 127.7 (Ar-C), 127.6 (Ar-C), 127.5 (Ar-C), 120.5 (C-9), 74.6 (C-7), 43.4 (C-17).

5.5.2.2. Alternative approach for the synthesis of amide adducts.

To a solution of carboxylic acid **222** (0.2 g, 3 mmol) in anhydrous THF (5 ml) was added CDI (0.2 g, 4.5 mmol, 1.5 equiv). The mixture was stirred for 1 h at room temperature. Benzylamine (0.13 ml, 6 mmol) was added to the mixture and stirred overnight. The solvent was evaporated under reduced pressure and the product was purified by column chromatography, which led to the isolation of two products, *N*-benzyl-2-(((*tert*-butyldimethylsilyl)oxy)(4-chlorophenyl)methyl) acrylamide (**224**), *N*-benzyl-2-((benzylamino)methyl)-3-((*tert*-butyldimethylsilyl)oxy)-3-(4-chlorophenyl)propenamide (**225a/b**).

5.5.2.2.1. Synthesis of *N*-benzyl-2-(((*tert*-butyldimethylsilyl)oxy)(4-chlorophenyl) methyl) acrylamide (224)

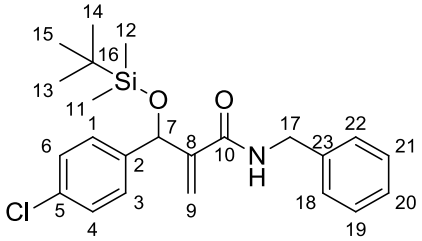

224

The product **224** was isolated as a white solid (0.08 g, 30%). R_f = 0.6 (20% ethyl acetate: hexane); ^{1}H NMR (300 MHz, $CDCl_3$) δ 7.23 (1H, s, NH), 7.22 – 7.06 (9H, m, Ar-H), 6.02 (1H, s, H-9a), 5.53 (1H, s, H-7), 5.46 (1H, s, H-9b), 4.41 – 4.32 (1H, m, H-17a), 4.18 – 4.09 (1H, m, H-17b), 0.78 – 0.72 (9H, m, H-13,14,15), -0.04 (6H, d, *J*=10.4 Hz, H-11,12).

The product **224** deprotected on standing in the NMR tube, the ^{13}C NMR data is for the deprotected version:

^{13}C NMR (126 MHz, $CDCl_3$) δ 167.6 (C-10), 145.3 (C-8), 139.5 (Ar-C), 137.5 (Ar-C), 133.5 (Ar-C), 128.7 (Ar-C), 128.6 (Ar-C), 127.6 (Ar-C), 127.6 (Ar-C), 127.5 (Ar-C), 120.5 (C-9), 74.5 (C-7), 43.4 (C-17). HRMS *m/z* calcd for $C_{23}H_{30}ClNO_2Si$ [M+H$^+$]: 416.1807, found: 416.1838.

5.5.2.2.2. Synthesis of *N*-benzyl-2-((benzylamino)methyl)-3-((*tert*-butyldimethylsilyl) oxy)-3-(4-chlorophenyl)propenamide (225a/b)

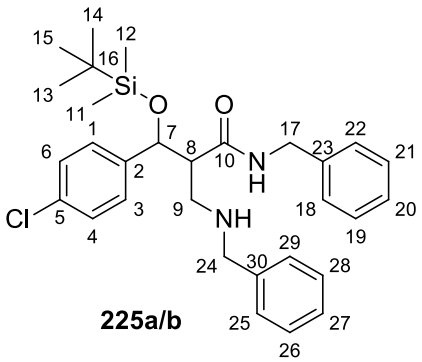

225a/b

The product **225a/b** was isolated as a yellow oil (0.04, 18%). R_f = 0.8 (30% ethyl acetate: hexane). IR ν_{max} (neat, cm^{-1}) 2954 (C-H), 1665 (C=O), 1567 (C=C), 820 (Si-O); ^{1}H NMR (400 MHz,

$CDCl_3$) δ 7.77 (1H, s, NH), 7.65 – 7.40 (9.89H, m, Ar-H), 7.31 – 7.10 (2.61H, m, Ar-H), 7.01 – 6.94 (0.42H, m, Ar-H), 6.88 (1.16H, m, Ar-H), 5.12 (0.31H, d, *J* = 7.5 Hz, H-7), 5.05 (0.73H, d, *J* = 9.2 Hz, H-7), 4.86 – 4.80 (0.71H, m, H-17), 4.71 – 4.60 (1.32H, m, H-17), 4.46 – 4.40 (0.33H, m, H-24), 4.41 – 4.36 (0.49H, m, H-24), 4.37 – 4.31 (0.78H, m, H-9), 4.32 – 4.22 (0.34H, m, H-24), 4.15 – 4.08 (0.64H, m, H-24), 3.99 – 3.87 (0.33H, m, H-17), 3.85 (0.83H, s, H-8), 3.72 (0.09H, s, H-8), 3.68 – 3.61 (0.18H, m, H-8), 3.42 – 3.28 (0.37H, m, H-9), 3.03 – 2.94 (0.74H, m, H-9), 1.04 (9H, s, H-13,14,15), 0.33 – 0.22 (3H, m, H-11), 0.01 (3H, m, H-12). ^{13}C NMR (101 MHz, $CDCl_3$) δ 169.6 (C-10), 140.4 (Ar-C), 137.1 (Ar-C), 134.0 (Ar-C), 129.0 (Ar-C), 128.9 (Ar-C), 128.7 (Ar-C), 128.6 (Ar-C), 128.5 (Ar-C), 128.1 (Ar-C), 127.8 (Ar-C), 127.5 (Ar-C), 127.4 (Ar-C), 74.4 (C-7), 74.1 (C-7'), 60.4 (C-9'), 59.9 (C-9), 56.9 (C-8'), 52.2 (C-8), 47.4 (C-17), 45.0 (C-17'), 44.9 (C-24), 43.2 (C-24'), 25.8 (C-13',14',15'), 25.5 (C-13,14,15), 18.1 (C-16), 18.0 (C-16'), -4.4 (C-12), -4.7 (C-12'), -5.1 (C-11), -5.4 (C-11').

5.5.2.3. Synthesis of 2-(((*tert*-butyldimethylsilyl)oxy)(4-chlorophenyl)methyl)-N-propylacrylamide (226)

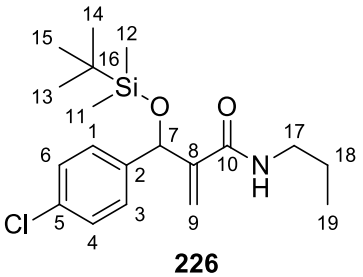

226

To a solution of carboxylic acid **222** (0.15 g, 3 mmol) in anhydrous THF (5 ml) was added CDI (0.15 g, 4.5 mmol, 1.5 equiv). The mixture was stirred for 1 h at room temperature. Propylamine (0.04 ml, 6 mmol) was added to the mixture and stirred overnight. The solvent was evaporated under reduced pressure and the product was purified by column chromatography to afford the product **226** as a yellow oil (0.03 g, 18%). R_f = 0.4 (20% ethyl acetate: hexane). ^{1}H NMR (400 MHz, $CDCl_3$) δ 7.22 – 7.14 (4H, m, Ar-H), 6.53 (1H, br s, N-H), 5.99 (1H, s, H-9a), 5.49 (1H, s, H-9b), 5.46 (1H, s, H-7), 3.11 – 2.97 (2H, m, H-17), 1.35 – 1.23 (2H, m, H-18), 0.86 (9H, s, H-13,14,15), 0.73 – 0.65 (3H, m, H-19), 0.03 (3H, s, H-11), 0.01 (3H, s, H-12). ^{13}C NMR (101 MHz, $CDCl_3$) δ 165.7 (C-10), 144.5 (C-8), 140.2 (Ar-C), 133.2 (Ar-C), 128.4 (Ar-C), 127.0 (Ar-C),

122.0 (C-9), 75.1 (C-7), 40.9 (C-17), 25.8 (C-13,14,15), 22.6 (C-18), 18.2 (C-16), 11.3 (C-19), -4.9 (C-12), -5.1 (C-11). HRMS *m/z* calcd for $C_{19}H_{30}ClNO_2Si$ [M+H$^+$]: 368.1807, found: 368.1735.

5.6. Preparation and characterization of amide MBH adducts, and their conjugate addition products obtained using alternative routes-First approach.

5.6.1. Synthesis of ethyl 2-((2-chlorophenyl)(hydroxy)methyl)acrylate (228)

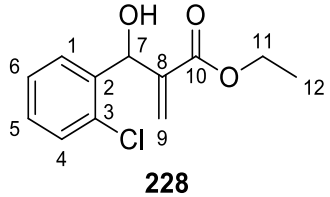

228

To a mixture of 4-chlorobenzaldehyde (4 g, 0.098 mol) and ethyl acrylate (19.81 ml, 0.608 mol) was added DABCO (3.4 g, 0.098 mol). The reaction mixture was stirred at room temperature until the reaction was complete. Upon completion of the reaction, water was added, and the solution was extracted with ethyl acetate. The organic layer obtained was dried over anhydrous Na_2SO_4, filtered and concentrated *in vacuo*. The product was then purified by column chromatography using 40% ethyl acetate in hexane affording the product **228** as a colourless oil (5.9 g, 87%). R_f = 0.3 (20% ethyl acetate: hexane). IR ν_{max} (neat, cm^{-1}) 3440 (OH), 2982 (=C-H), 1703 (C=O), 1631 (C=C); ^{1}H NMR (300 MHz, $CDCl_3$) δ 7.56 (1H, dd, *J*=7.7,1.9 Hz, Ar-H), 7.39 – 7.32 (1H, m, Ar-H), 7.32 – 7.21 (2H, m, Ar-H), 6.35 (1H, s, H-9a), 5.98 (1H, d, *J*=4.9 Hz, H-7), 5.58 (1H, s, H-9b), 4.23 (2H, q, *J* = 7.2 Hz, H-11), 3.28 (1H, d, *J*=4.8 Hz, OH), 1.28 (3H, t, *J* = 7.2 Hz, H-12). ^{13}C NMR (75 MHz, $CDCl_3$) δ 166.6 (C-10), 140.8 (C-2), 138.3 (C-8), 132.9 (Ar-C), 129.5 (Ar-C), 129.0 (Ar-C), 128.2 (Ar-C), 127.1 (C-1), 126.7 (C-9), 69.5 (C-7), 61.1 (C-11), 14.1 (C-12).

5.6.2. Synthesis of ethyl 2-(((*tert*-butyldimethylsilyl)oxy)(2-chlorophenyl)methyl) acrylate (229)

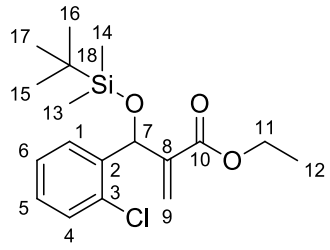

229

To a solution of MBH adduct **228** (3 g, 1 mmol) in anhydrous *N*,*N*-dimethylformamide (DMF) (0.3 ml) was added *tert*-butyl dimethyl silyl chloride (TBDMSCl) (2.44 g, 1.3 mmol) and imidazole (2.12 g, 2.5 mmol). The reaction mixture was stirred at room temperature under nitrogen, until all the starting material was consumed as indicated by TLC analysis (8-18 h). After reaction completion, hexane (10 ml) was added to the mixture to quench the reaction, which was washed sequentially with brine solution (3 x 5 ml). The organic layer was dried over anhydrous sodium sulphate and concentrated under reduced pressure. The product was purified by column chromatography using 20% ethyl acetate in hexane to afford the product **229** as a colourless oil (2.9 g, 83%). R_f = 0.7 (40% ethyl acetate: hexane); ^{1}H NMR (400 MHz, $CDCl_3$) δ 7.45 – 7.40 (1H, m, Ar-H), 7.32 – 7.27 (1H, m, Ar-H), 7.24 – 7.13 (2H, m, Ar-H), 6.30 (1H, s, H-9a), 6.03 (1H, s, H-7), 5.85 (1H, s, H-9b), 4.21 – 4.06 (2H, m, H-11), 1.21 (3H, t, *J* = 7.1 Hz, H-12), 0.85 (9H, s, H-15,16,17), 0.09 (3H, s, H-13), -0.11 (3H, s, H-14). ^{13}C NMR (101 MHz, $CDCl_3$) δ 165.9 (C-10), 143.2 (C-8), 140.0 (Ar-C), 132.7 (Ar-C), 129.23 (Ar-C), 129.18 (Ar-C), 128.6 (Ar-C), 126.7 (Ar-C), 125.1 (C-9), 69.0 (C-7), 60.7 (C-11), 25.8 (C-15,16,17), 18.1 (C-18), 14.1 (C-12), -4.9 (C-14), -5.0 (C-13).

5.6.3. Synthesis of ethyl 3-((*tert*-butyldimethylsilyl)oxy)-3-(2-chlorophenyl)-2-((propyl amino)methyl)propanoate (230a/b)

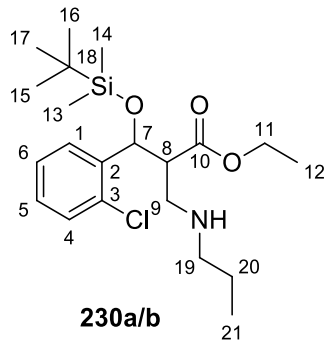

230a/b

To the protected MBH adduct **229** (0.78 g, 1 mmol) in methanol (5 ml) was added propylamine (0.4 ml, 3.5 mmol). The stoppered reaction mixture was stirred at room temperature until the reaction was complete. Upon reaction completion, the mixture was concentrated in vacuo, and the product purified by column chromatography to afford the product **230a/b** as a yellow oil (0.1 g, 4%). R_f = 0.55 (40% ethyl acetate: hexane); ^{1}H NMR (300 MHz, $CDCl_3$) δ 7.60 – 7.47 (1H, m, Ar-H), 7.34 – 7.28 (1H, m, Ar-H), 7.26 – 7.15 (2H, m, Ar-H), 5.51 (0.72H, d, *J*=5.0 Hz, H-7), 5.35

(0.22H, d, *J*=7.9 Hz, H-7), 4.24 – 3.97 (2H, m, H-11), 3.12 (1H, dd, *J* = 11.7, 9.5 Hz, H-9a), 3.05 – 2.87 (1H, m, H-8), 2.69 (1H, dd, *J* = 11.8, 3.4 Hz, H-9b), 2.47 (1.71H, t, *J* =7.3 Hz, H-19), 2.45 – 2.31 (0.54H, m, H-19), 1.52 – 1.33 (3H, m, N-H, H-20), 1.31 – 1.20 (1H, m, H-12), 1.21 – 1.09 (2H, m, H-12), 0.88 (7H, s, H-15,16,17), 0.88 – 0.82 (3H, m, H-21), 0.82 (2H, s, H-15,16,17), 0.03 (3H, s, H-13), -0.25 (3H, s, H-14). ^{13}C NMR (101 MHz, $CDCl_3$) δ 173.3 (C-10'), 172.7 (C-10), 140.4 (Ar-C'), 140.0 (Ar-C), 132.2 (Ar-C'), 131.6 (Ar-C), 129.3 (Ar-C), 129.2 (Ar-C'), 129.1 (Ar-C'), 129.0 (Ar-C), 128.8 (Ar-C'), 128.7 (Ar-C), 127.0 (Ar-C'), 126.5 (Ar-C), 71.2 (C-7), 60.6 (C-11), 60.4 (C-11'), 52.2 (C-8), 51.8 (C-19), 51.4 (C-19'), 48.1 (C-8'), 46.3 (C-9), 25.7 (C-15,16,17), 25.6 (C-15',16',17'), 23.1 (C-20), 23.0 (C-20'), 18.0 (C-18), 17.9 (C-18'), 14.2 (C-12'), 14.0 (C-12), 11.7 (C-21), 11.6 (C-21'), -4.8 (C-14), -4.9 (C-14'), -5.5 (C-13).

5.7. Second approach

5.7.1. Synthesis of 2-((2-chlorophenyl)(hydroxy)methyl)acrylic acid (235)

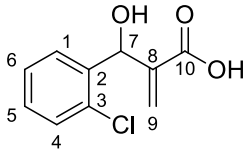

235

To a mixture of MBH adduct **228** (3 g, 1 equiv) in ethanol (2 ml) was added KOH (0.84 g, 1.2 equiv) in water (10 ml). The mixture was refluxed for 4 h. Upon reaction completion, ethanol was evaporated under reduced pressure and any unreacted starting material was extracted using ethyl acetate (20 ml). The aqueous layer obtained was acidified using HCl and extracted using ethyl acetate (4 x 20 ml) to afford the product **235** as a pale yellow oil (2.35 g, 90%). R_f = 0.10 (20% ethyl acetate: hexane). IR ν_{max} (neat, cm^{-1}) 3359 (OH), 1683 (C=O), 1632 (C=C); ^{1}H NMR (400 MHz, $CDCl_3$) δ 7.58 – 7.53 (1H, m, Ar-H), 7.39 – 7.23 (3H, m, Ar-H), 6.49 (1H, s, H-9a), 5.99 (1H, s, H-7), 5.68 (1H, s, H-9b), 5.27 (2H, br s, OH). ^{13}C NMR (101 MHz, $CDCl_3$) δ 171.2 (C-10), 140.0 (C-8), 138.0 (Ar-C), 132.8 (Ar-C), 129.6 (Ar-C), 129.5 (C-9), 129.2 (Ar-C), 128.1 (Ar-C), 127.1 (Ar-C), 69.0 (C-7).

5.7.2. Synthesis of 2-(((*tert*-butyldimethylsilyl)oxy)(2-chlorophenyl)methyl)acrylic acid (236)

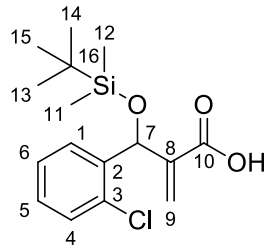

236

To a solution of carboxylic acid **235** (2 g, 1 mmol) in anhydrous *N*,*N*-dimethylformamide (DMF) (0.3 ml) was added *tert*-butyl dimethyl silyl chloride (1.84 g, TBDMSCl) (1.3 mmol) and imidazole (1.5 g, 2.5 mmol). The reaction mixture was stirred at room temperature under nitrogen, until all the starting material was consumed as indicated by the TLC (8-18 h). After reaction completion, 10 ml of hexane was added to the mixture to quench the reaction and washed sequentially with brine solution (3 x 5 ml). The organic layer was dried over anhydrous sodium sulphate and concentrated under reduced pressure. The product was purified by column chromatography using 20% ethyl acetate in hexane to afford the product **236** as a yellow solid (0.49 g, 32%). M.P: 60-63 ˚C, R_f = 0.7 (40% ethyl acetate: hexane). IR ν_{max} (neat, cm^{-1}) 2949 (C-H), 1687 (C=O), 1625 (C=C), 835 (Si-O); ^{1}H NMR (400 MHz, $CDCl_3$) δ 7.52 – 7.47 (1H, m, Ar-H), 7.34 – 7.28 (1H, m, Ar-H), 7.26 – 7.17 (2H, m, Ar-H), 6.39 (1H, s, H-9a), 6.03 (1H, s, H-7), 5.87 (1H, s, H-9b), 0.88 (9H, s, H-13,14,15), 0.11 (3H, s, H-11), -0.07 (3H, s, H-12). ^{13}C NMR (101 MHz, $CDCl_3$) δ 169.0 (C-10), 141.5 (C-8), 139.3 (Ar-C), 132.5 (Ar-C), 129.4 (Ar-C), 128.9 (Ar-C), 128.8 (Ar-C), 127.6 (C-9), 126.8 (Ar-C), 69.4 (C-7), 25.7 (C-13,14,15), 18.1 (C-16), -4.9 (C-11), -5.1 (C-12).

5.8. Third approach

5.8.1. Synthesis of 3-((*tert*-butyldimethylsilyl)oxy)-3-(4-chlorophenyl)-2-((pentylamino) methyl)propanoic acid (239)

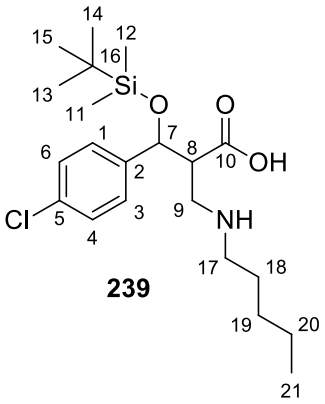

239

To a mixture of the protected carboxylic acid **236** (1.2 g, 1 mmol) and 1-aminopentane (0.32 g, 1 mmol) in anhydrous THF (2 ml) was added triethylamine (0.7 ml). The mixture was stirred for 2 days in a stoppered flask. The excess solvent was evaporated under reduced pressure and the residue was purified by column chromatography 40% ethyl acetate: hexane to afford the product **239** as a white solid (0.4 g, 26%). R_f = 0.5 (40% ethyl acetate: hexane); ^{1}H NMR (300 MHz, $CDCl_3$) δ 7.43 – 7.37 (2.80H, m, Ar-H), 7.35 – 7.25 (0.66H, m, Ar-H), 7.21 – 7.13 (0.49H, m, Ar-H), 5.21 (0.30H, d, *J*=6.2 Hz, H-7), 5.05 (0.71H, d, *J*=7.4 Hz, H-7), 4.34 – 4.23 (0.32H, m, H-8), 3.96 (0.20H, s), 3.94 – 3.87 (0.31H, m, H-9), 3.87 – 3.81 (0.08H, m, H-17), 3.64 – 3.50 (1.17H, m, H-17), 3.50 – 3.45 (0.70H, m, H-17), 3.47 – 3.40 (1.88H, m, H-9), 3.05 – 2.95 (1.05H, m, H-8), 1.44 – 1.35 (0.88H, m, H-18), 1.34 – 1.28 (1.73H, m, H-19), 1.30 – 1.24 (1.28H, m, H-18), 1.25 – 1.15 (2.33H, m, H-20), 1.02 – 0.85 (12.28H, m, H-13,14,15,21), 0.14 (1H, s, H-11) , 0.11 (2H, S, H-11), -0.09 (1H, s, H-12), -0.14 (2H, s, H-12).

CHAPTER 6

6. REFERENCES

1. Declerck V, Martinez J, Lamaty F. Aza-Baylis - Hillman reaction. Chem Rev. 2009 Jan 14;109(1):1–48.
2. Basavaiah D, Rao KV, Reddy RJ. The Baylis–Hillman reaction: A novel source of attraction, opportunities, and challenges in synthetic chemistry. Chem Soc Rev. 2007 Aug 24;36(10):1581–8.
3. Kataoka T, Kinoshita H, Kinoshita S, Iwamura T. The chalcogeno-Baylis–Hillman reaction of ketones and α-dicarbonyl compounds. J Chem Soc Perkin 1. 2002 Aug 5;2(18):2043–5.
4. Ma GN, Jiang JJ, Shi M, Wei Y. Recent extensions of the Morita-Baylis-Hillman reaction. Chemical Communications. Royal Society of Chemistry; 2009. p. 5496–514.
5. Krafft ME, Seibert KA, Haxell TFN, Hirosawa C. Unprecedented reactivity in the Morita-Baylis-Hillman reaction; intramolecular α-alkylation of enones using saturated alkyl halides. Chemical Communications. 2005 Dec 14;(46):5772–4.
6. Williams MTJ, Morrill LC, Browne DL. Expedient Organocatalytic Aza-Morita–Baylis–Hillman Reaction through Ball-Milling. ACS Sustain Chem Eng. 2020 Dec 7;8(48):17876–81.
7. Matsui K, Takizawa S, Sasai H. Bifunctional Organocatalysts for Enantioselective aza-Morita−Baylis−Hillman Reaction. J Am Chem Soc. 2005 Mar 1;127(11):3680–1.
8. Lindner C, Tandon R, Liu Y, Maryasin B, Zipse H. The aza-Morita–Baylis–Hillman reaction of electronically and sterically deactivated substrates. Org Biomol Chem. 2012;10(16):3210.
9. Benjamin W. Lam, A. Mitchel Owens, John W. Sheffield, Paul H. Mueller. Synthesis of Various Catalysts for the Morita-Baylis-Hillman Reaction. H-SC J of Sciences. 2016;v.
10. Williams MTJ, Morrill LC, Browne DL, Browne DL. Expedient Organocatalytic Aza-Morita-Baylis-Hillman Reaction through Ball-Milling. ACS Sustain Chem Eng. 2020 Dec 7;8(48):17876–81.
11. Singh V, Batra S. Advances in the Baylis-Hillman reaction-assisted synthesis of cyclic frameworks. Tetrahedron. 2008 Feb 29;64:4511–74.
12. Verdier RAT, Mikkelsen JH, Lindhardt AT. Studying the Morita-Baylis-Hillman Reaction in Continuous Flow Using Packed Bed Reactors. Org Process Res Dev. 2018 Nov 16;22(11):1524–33.

13. Bharadwaj KC. Intramolecular Morita-Baylis-Hillman and Rauhut-Currier reactions. A catalytic and atom economic route for carbocycles and heterocycles. Vol. 5, RSC Advances. Royal Society of Chemistry; 2015. p. 75923–46.
14. Zhao S, He M, Guo Z, Zhou N, Wang D, Li J, et al. Cl-H2O: An efficient and versatile solvent system for the DABCO-catalyzed Morita-Baylis-Hillman reaction. RSC Adv. 2015;5(41):32839–45.
15. Lima–Junior CG, Vasconcellos MLAA. Morita–Baylis–Hillman adducts: Biological activities and potentialities to the discovery of new cheaper drugs. Bioorg Med Chem. 2012 Jul;20(13):3954–71.
16. Amarante GW, Milagre HMS, Vaz BG, Vilachã Ferreira BR, Eberlin MN, Coelho F. Dualistic Nature of the Mechanism of the Morita−Baylis−Hillman Reaction Probed by Electrospray Ionization Mass Spectrometry. J Org Chem. 2009 Apr 17;74(8):3031–7.
17. Narendar Reddy T, Jayathirtha Rao V. Importance of Baylis-Hillman adducts in modern drug discovery. Tetrahedron Lett. 2018 Jul;59(30):2859–75.
18. Masson G, Housseman C, Zhu J. The Enantioselective Morita–Baylis–Hillman Reaction and Its Aza Counterpart. Angewandte Chemie International Edition. 2007 Jun 18;46(25):4614–28.
19. Carrasco-Sanchez V, Simirgiotis MJ, Santos LS. The morita-baylis-hillman reaction: Insights into asymmetry and reaction mechanisms by electrospray ionization mass spectrometry. Molecules. 2009 Oct 12;14(10):3989–4021.
20. Pellissier H. Recent developments in the asymmetric organocatalytic Morita−Baylis−Hillman reaction. Tetrahedron. 2017 May;73(20):2831–61.
21. Robiette R, Aggarwal VK, Harvey JN. Mechanism of the Morita−Baylis−Hillman Reaction: A Computational Investigation. J Am Chem Soc. 2007 Dec 1;129(50):15513–25.
22. Cantillo D, Kappe CO. A unified mechanistic view on the Morita-Baylis-Hillman reaction: Computational and experimental investigations. Journal of Organic Chemistry. 2010 Dec 17;75(24):8615–26.
23. Santos H, Zeoly LA, Rodrigues MT, Fernandes FS, Gomes RC, Almeida WP, et al. Recent Advances in Catalytic Systems for the Mechanistically Complex Morita–Baylis–Hillman Reaction. ACS Catal. 2023 Mar 17;13(6):3864–95.

24. Mansilla J, Saá JM. Enantioselective, Organocatalytic Morita-Baylis-Hillman and Aza-Morita-Baylis-Hillman Reactions: Stereochemical Issues. Molecules. 2010 Feb 1;15(2):709–34.
25. Plata RE, Singleton DA. A case study of the mechanism of alcohol-mediated morita baylis-hillman reactions. the importance of experimental observations. J Am Chem Soc. 2015 Mar 25;137(11):3811–26.
26. Kumar K, Rawal RK. CuI/DBU-Mediated MBH Reaction of Isatins: A Convenient Synthesis of 3-Substituted-3-hydroxy-2-oxindole. ChemistrySelect. 2020 Mar 13;5(10):3048–51.
27. Basavaiah D, Venkateswara Rao K, Jannapu Reddy R. The Baylis–Hillman reaction: a novel source of attraction, opportunities, and challenges in synthetic chemistry. Chem Soc Rev. 2007;36(10):1581.
28. Strauss CR, Galbraith MN, Faux AF. 2-(Hydroxymethyl) Acrylate derivatives and process for their preparations. United states patent WO1991018861A1. 1991 Dec 12.
29. Kataoka T, Iwama T, Tsujiyama S ichiro. The chalcogeno-Baylis–Hillman reaction: the first examples catalysed by chalcogenides in the presence of Lewis acids. Chemical Communications. 1998;(2):197–8.
30. Basavaiah D, Dharma Rao P, Suguna Hyma R. The Baylis-Hillman reaction: A novel carbon-carbon bond forming reaction. Tetrahedron. 1996 Jun;52(24):8001–62.
31. Kim KH, Lee HS, Kim YM, Kim JN. Remarkable Rate Acceleration of Baylis-Hillman Reaction of Notorious α,β-Unsaturated Aldehydes Catalyzed by Proton Donor. Bull Korean Chem Soc. 2011 Mar 20;32(3):1087–90.
32. Aggarwal VK, Dean DK, Mereu A, Williams R. Rate Acceleration of the Baylis−Hillman Reaction in Polar Solvents (Water and Formamide). Dominant Role of Hydrogen Bonding, Not Hydrophobic Effects, Is Implicated. J Org Chem. 2002 Jan 1;67(2):510–4.
33. Liu Y. Organocatalyzed Morita-Baylis-Hillman Reaction: Mechanism and Catalysis. [MRes dissertation]. China: Ludwig-Maximilians-Universitat Munchen; 2011
34. Xu YM, Shi M. Highly Efficient aza-Baylis−Hillman Reaction of N -Tosylated Imines with MVK, Acrolein, and Phenyl Acrylate or α-Naphthyl Acrylate: Lewis Base Effects and A Convenient Method to Synthesize α,β-Unsaturated β-Amino Carbonyl Compounds. J Org Chem. 2004 Jan 1;69(2):417–25.

35. Aggarwal VK, Mereu A, Tarver GJ, McCague R. Metal- and Ligand-Accelerated Catalysis of the Baylis−Hillman Reaction. J Org Chem. 1998 Oct 1;63(21):7183–9.
36. Patra A, Batra S, Joshi BS, Roy R, Kundu B, Bhaduri AP. TiCl 4 -Promoted Baylis−Hillman Reactions of Substituted 5-Isoxazolecarboxaldehydes with Cycloalkenones 1. J Org Chem. 2002 Aug 1;67(16):5783–8.
37. Baylis-Hillman Reaction and Chemical Transformations of Baylis-Hillman Adducts. Bull Korean Chem Soc. 2005 Oct 20;26(10):1481–90.
38. Drewes SE, Emslie ND. Necic acid synthons. Part 1. Total synthesis of integerrinecic acid. J Chem Soc Perkin 1. 1982;2079.
39. Hoffmann HMR, Rabe J. DABCO-catalyzed coupling of aldehydes with activated double bonds. 4. Stereoselective synthesis of trisubstituted olefins and terpenoid building blocks via 2-(hydroxyalkyl)-2-propenoic esters. J Org Chem. 1985 Oct 1;50(20):3849–59.
40. Dai S, Gu X, Wang Z, Yao W. Transition-Metal-Free Synthesis of 3-Ethynylcoumarins by a DBU-Promoted Intramolecular Morita–Baylis–Hillman-Type Reaction/Dehydration/Isomerization Cascade. Synlett. 2022 Dec 7;33(20):2009–12.
41. Aggarwal VK, Emme I, Fulford SY. Correlation between p K a and Reactivity of Quinuclidine-Based Catalysts in the Baylis−Hillman Reaction: Discovery of Quinuclidine as Optimum Catalyst Leading to Substantial Enhancement of Scope. J Org Chem. 2003 Feb 1;68(3):692–700.
42. Drewes SE, Freese SD, Emslie ND, Roos GHP. Synthesis of 3-Hydroxy-2-Methylene Carbonyl Compounds - Effect of Catalyst and Substrate on Reaction Rate. Synth Commun. 1988 Sep;18(13):1565–72.
43. Ameer F, Drewes SE, Freese S, Kaye PT. Rate Enhancement Effects in the Dabco Catalysed Synthesis of Hydroxyalkenoate Esters. Synth Commun. 1988 Apr;18(5):495–500.
44. Höfle G, Steglich W, Vorbrüggen H. 4-Dialkylaminopyridines as Highly Active Acylation Catalysts. [New synthetic method (25)]. Angewandte Chemie International Edition in English. 1978 Aug;17(8):569–83.
45. Patel C, Sunoj RB. TiCl 4 -Promoted Baylis−Hillman Reaction: Mechanistic Rationale toward Product Distribution and Stereoselectivity. J Org Chem. 2010 Jan 15;75(2):359–67.
46. Basavaiah D, Reddy GC. Intramolecular Baylis-Hillman reaction: synthesis of heterocyclic molecules. Arkivoc. 2015 Nov 19;2016(2):172–205.

47. Morita KI, Suzuki Z, Hirose H. A Tertiary Phosphine-catalyzed Reaction of Acrylic Compounds with Aldehydes. Bull Chem Soc Jpn. 1968 Nov;41(11):2815–2815.
48. Rafel S, Leahy JW. An Unexpected Rate AccelerationPractical Improvements in the Baylis−Hillman Reaction. J Org Chem. 1997 Mar 1;62(5):1521–2.
49. Shi M, Jiang JK, Feng YS. Titanium(IV) Chloride and the Amine-Promoted Baylis−Hillman Reaction. Org Lett. 2000 Aug 1;2(16):2397–400.
50. Basavaiah D, Naganaboina RT. The Baylis–Hillman reaction: a new continent in organic chemistry – our philosophy, vision and over three decades of research. New Journal of Chemistry. 2018;42(17):14036–66.
51. Pellissier H. Recent developments in the asymmetric organocatalytic Morita−Baylis−Hillman reaction. Tetrahedron. 2017 May;73(20):2831–61.
52. Dandamudi V. Lenin. Baylis-Hillman Reaction: A Novel Opportunity to the Synthetic Organic Chemistry. International Journal of Creative Research Thoughts. 2018;6(1).
53. Luna-Freire KR, Scaramal JPS, Resende JALC, Tormena CF, Oliveira FL, Aparicio R, et al. ChemInform Abstract: An Asymmetric Substrate-Controlled Morita-Baylis-Hillman Reaction as Approach for the Synthesis of Pyrrolizidinones and Pyrrolizidines. ChemInform. 2014 Sep 18;45(40):3319-26.
54. Ali Khan A, Stereochemical aspects of the baylis-hillman reaction [MRes dissertation]. Pietermaritzburg: University of Natal; 1992.
55. Gilbert A, Heritage TW, Isaacs NS. Asymmetric induction in the Baylis-Hillman reaction. Tetrahedron Asymmetry. 1991 Jan;2(10):969–72.
56. Bailey M, Markó IE, Ollis WD, Rasmussen PR. Stereoselective epoxidation of hydroxyenones. The synthesis of the sidechain of clerocidin. Tetrahedron Lett. 1990 Jan;31(31):4509–12.
57. Marko IE, Giles PR, Hindley NJ. Catalytic enantioselective Baylis-Hillman reactions. Correlation between pressure and enantiomeric excess. Tetrahedron. 1997 Jan;53(3):1015–24.
58. Yeo JE, Yang X, Kim HJ, Koo S. The intramolecular Baylis–Hillman reaction: easy preparation of versatile substrates, facile reactions, and synthetic applications. Chem Commun. 2004;(2):236–7.
59. Hayase T, Shibata T, Soai K, Wakatsuki Y. An enantioselective Baylis–Hillman reaction catalyzed by chiral phosphines under atmospheric pressure. Chemical Communications. 1998;(12):1271–2.

60. Oishi T, Oguri H, Hirama M. Asymmetric Baylis-Hillman reactions using chiral 2,3-disubstituted 1,4-diazabicyclo[2.2.2]octanes catalysts under high pressure conditions. Tetrahedron Asymmetry. 1995 Jun;6(6):1241–4.
61. Bhowmik S, Batra S. Applications of Morita-Baylis-Hillman Reaction to the Synthesis of Natural Products and Drug Molecules. Curr Org Chem. 2015 Jan 19;18(24):3078–119.
62. Yagyesh K, Kapil K. Morita-Baylis-Hillman reaction: scope and significance. J Pharm Chem Chem Sci. 2018 Jul 23;2(1):11-20.
63. Liu TY, Xie M, Chen YC. Organocatalytic asymmetric transformations of modified Morita–Baylis–Hillman adducts. Chem Soc Rev. 2012;41(11):4101.
64. Min S, Fei-Jun W, Mei-Xin Z, Yin W. The Chemistry of the Morita-Baylis-Hillman Reaction. Royal society of chemistry books; 2011.
65. Yadav L, Srivastava V, Patel R. The First One-Pot Synthesis of Morita-Baylis-Hillman Adducts Starting Directly from Alcohols. Synlett. 2010 Apr 10;2010(07):1047–50.
66. Lawrence NJ, Crump JP, McGown AT, Hadfield JA. Reaction of Baylis–Hillman products with Swern and Dess–Martin oxidants. Tetrahedron Lett. 2001 Jun;42(23):3939–41.
67. Bhuniya D, Gujjary S, Sengupta S. Synthesis of Novel Oxime Functionalized Aldol Products via Michael Addition of Oximes Onto Baylis–Hillman Adducts. Synth Commun. 2006 Feb 1;36(2):151–64.
68. Kamimura A, Morita R, Matsuura K, Omata Y, Shirai M. Simple preparation of β-hydroxy-α-thiomethyl carbonyl compounds via stereoselective conjugate addition of thiol to Baylis–Hillman adducts. Tetrahedron Lett. 2002 Aug;43(35):6189–91.
69. Juma WP. An investigation of the enzymatic kinetic resolution of Morita-Baylis-Hillman adducts and their further functionalisation. [Johannesburg]: University of the Witwatersrand ; 2019.
70. Wang W, Yu M. One pot sequential Baylis-Hillman and Michael reactions. Tetrahedron Lett. 2004 Aug;45:7141-43
71. Rios R. Organocatalytic enantioselective methodologies using Morita–Baylis–Hillman carbonates and acetates. Catal Sci Technol. 2012;2(2):267–78.
72. Talma M, Mucha A. P-C bond formation in reactions of Morita-Baylis-Hillman adducts with phosphorus nucleophiles. Arkivoc. 2016 Oct 11;2017(2):324–44.

73. Drewes SE, Horn MM, Ramesar N. Reaction of 2-Formyl Imidazole with Intermediates From the Baylis-Hillman Reaction. Synth Commun. 2000 Mar;30(6):1045–55.
74. Guo W, Wu W, Fan N, Wu Z, Xia C. Synthesis of α-Substituted N -Aryl Acrylamide Derivatives Through Baylis–Hillman Reaction. Synth Commun. 2005 May;35(9):1239–51.
75. Basavaiah D, Rao AJ, Satyanarayana T. Recent Advances in the Baylis−Hillman Reaction and Applications. Chem Rev. 2003 Mar 1;103(3):811–92.
76. Fernando C, Rodrigo C. An approach to oxazolidin-2-ones from the Baylis–Hillman adducts. Formal synthesis of a chloramphenicol derivative. Tetrahedron Lett. 2002 Feb 19;43:2797-800.
77. Franck X, Figadère B. Synthesis of acaterin via a new application of the Baylis–Hillman reaction. Tetrahedron Lett. 2002 Feb;43(8):1449–51.
78. Souza DM, Machado LL, Machado AHL. First total synthesis of (±)-floribundane B: An approach based on Johnson-Claisen rearrangement of a Morita-Baylis-Hillman adduct. Tetrahedron Lett. 2019 Jul;60(28):1811–3.
79. Teng P, Huo D, Nimmagadda A, Wu J, She F, Su M, et al. Small Antimicrobial Agents Based on Acylated Reduced Amide Scaffold. J Med Chem. 2016 Sep 8;59(17):7877–87.
80. Vieira ACS, da Silva Santos M, Leite AB, da Silva AE, Cavalcante-Silva LHA, de Souza Augusto Pereira G, et al. Leishmanicidal activity of Morita-Baylis–Hillman adducts. Parasitol Res. 2022 Feb 6;121(2):751–62.
81. Kohn LK, Pavam CH, Veronese D, Coelho F, De Carvalho JE, Almeida WP. Antiproliferative effect of Baylis–Hillman adducts and a new phthalide derivative on human tumor cell lines. Eur J Med Chem. 2006 Jun;41(6):738–44.
82. Coelho F, Wanda, Almeida P, Mateus CR, Furtado LD, Gouveia JCF. The influence of protecting groups on the diastereoselectivity of catalytic heterogeneous hydrogenation of Baylis-Hillman adducts. Arkivoc. 2003 Oct 22;2003(10):443–67.
83. Ghosh S, Dey R, Chattopadhyay K, Ranu BC. Water-promoted highly regio- and stereoselective synthesis of α-dehydro-β-amino esters and nitriles from Baylis–Hillman acetates. Tetrahedron Lett. 2009 Aug;50(34):4892–5.
84. Srihari P, Dutta P, Rao RS, Yadav JS, Chandrasekhar S, Thombare P, et al. Solvent free synthesis of 1,5-disubstituted tetrazoles derived from Baylis Hillman acetates as potential TNF-α inhibitors. Bioorg Med Chem Lett. 2009 Oct;19(19):5569–72.

85. Kalyva M, Zografos AL, Kapourani E, Giambazolias E, Devel L, Papakyriakou A, et al. Probing the Mechanism of Allylic Substitution of Morita–Baylis–Hillman Acetates (MBHAs) by using the Silyl Phosphonite Paradigm: Scope and Applications of a Versatile Transformation. Chemistry – A European Journal. 2015 Feb 16;21(8):3278–89.
86. Kundu MK, Bhat S V. A Convenient Route to β-Amino Propionic Acid Derivatives. Synth Commun. 1999 Jan 1;29(1):93–101.
87. Ian H. Nucleophilic Substitution Answers. University of Calgary. Available from: https://www.chem.ucalgary.ca/courses/350/Carey5th/Ch08/ch8-12-ans.html.
88. p-Anisidine is more basic than aniline - Justify with appropriate drawings. Available from: https://homework.study.com/explanation/p-anisidine-is-more-basic-than-aniline-justify-with-appropriate-drawings.html
89. Yamazaki S, Yamamoto M, Sumi A. Conjugate addition of aromatic amines to ethenetricarboxylates. Tetrahedron. 2007 Mar;63(10):2320–7.
90. William R, Emeritus. Nucleophilicity of Sulfur Compounds. Michigan state U: 2022. Available from: https://chem.libretexts.org/bookshelves/Organic_Chemistry/Supplemental_Modules_(Organic_Chemistry)/Thiols_and_sulfides/Nucleophilicity_of_Sulfur_Compounds
91. Kita Y, Shibata N, Miki T, Takemura Y, Tamura O. Chemistry of O-Silylated Ketene Acetals: A Stereoselective Synthesis of Optically Active Carbapenem Antibiotics, (+)-Thienamycin and (+)-PS-5. Chem Pharm Bull (Tokyo). 1992;40(1):12–20.
92. Xiaoyang Y, Charlie V, Mohammed A, Yves Q. Reactivity of secondary *N*-alkyl acrylamides in Morita-Baylis-Hillman reactions. C.R. Chimie. 2021 Aug; 24: 319-30
93. Cocco M, Miglio G, Giorgis M, Garella D, Marini E, Costale A, et al. Design, Synthesis, and Evaluation of Acrylamide Derivatives as Direct NLRP3 Inflammasome Inhibitors. ChemMedChem. 2016 Aug 19;11(16):1790–803.
94. Amarante GW, Rezende P, Cavallaro M, Coelho F. Acyloins from Morita–Baylis–Hillman adducts: an alternative approach to the racemic total synthesis of bupropion. Tetrahedron Lett. 2008 Jun;49(23):3744–8.
95. Idahosa KC, Davies-Coleman MT, Kaye PT. Exploratory applications of 2-nitrobenzaldehyde-derived Morita-Baylis-Hillman adducts as synthons in the construction of drug-like scaffolds. Synth Commun. 2019 Feb 1;49(3):417–30.

APPENDIX - NMR SPECTRA OF SELECTED COMPOUNDS

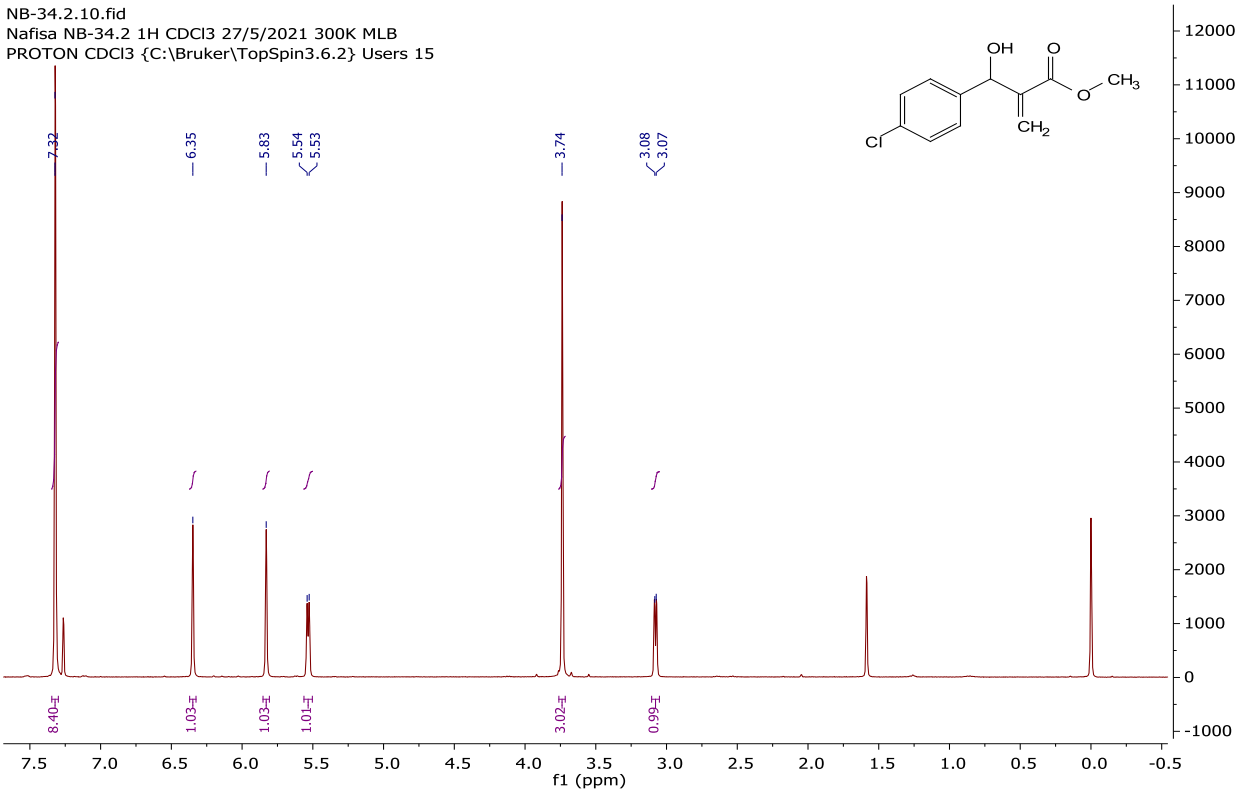

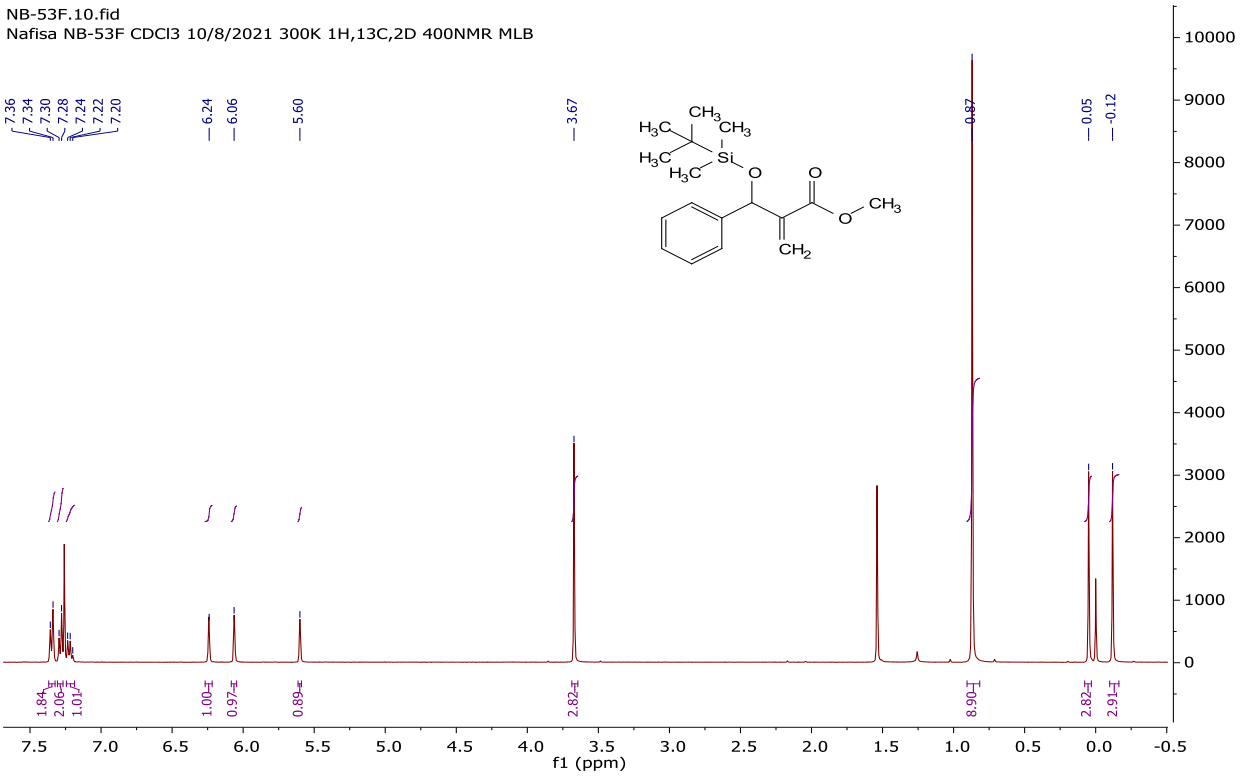
NB-53F.10.fid
Nafisa NB-53F CDCl3 10/8/2021 300K 1H,13C,2D 400NMR MLB
7.36
7.34
7.30
7.28
7.24
7.22
7.20
6.24
6.06
5.60
3.67
0.87
0.05
-0.12
1.84
2.06
1.01
1.00
0.97
0.89
2.82
8.90
2.82
2.91
f1 (ppm)

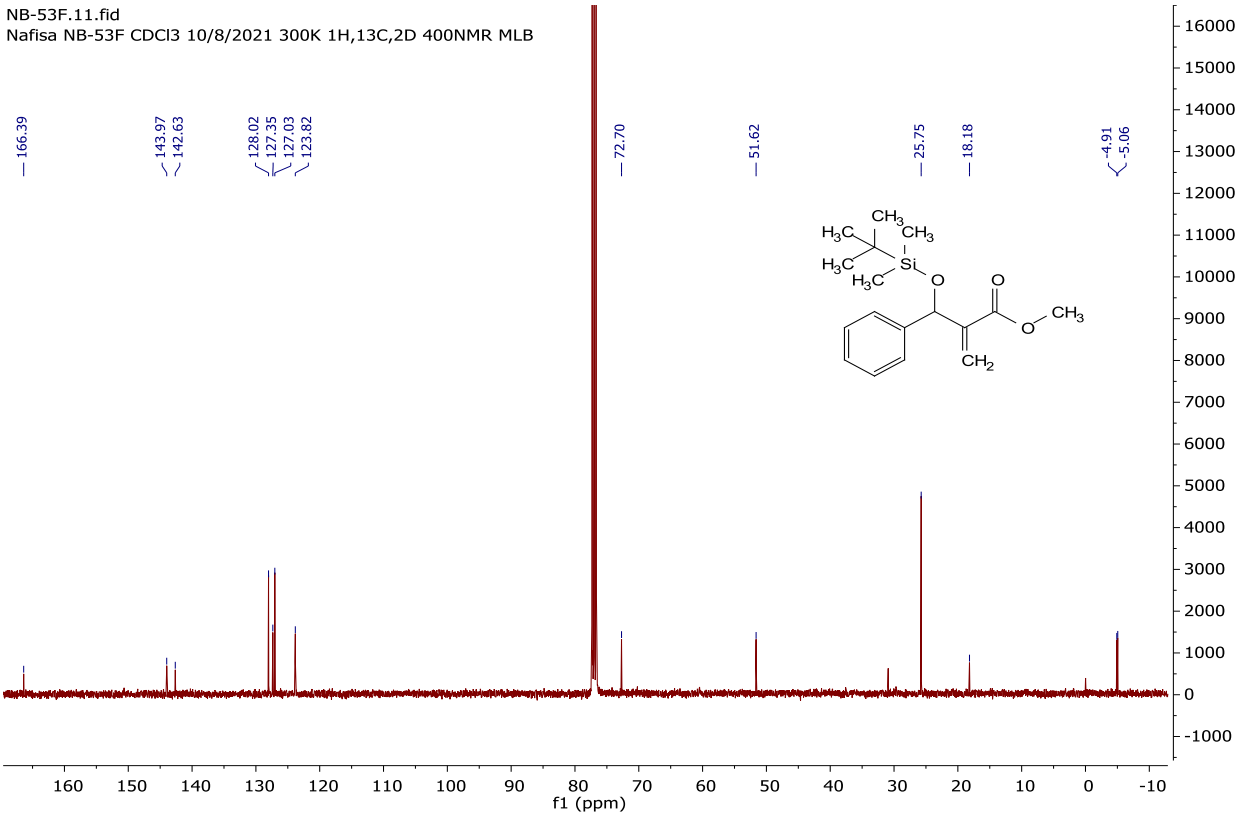
NB-53F.11.fid
Nafisa NB-53F CDCl3 10/8/2021 300K 1H,13C,2D 400NMR MLB
166.39
143.97
142.63
128.02
127.35
127.03
123.82
72.70
51.62
25.75
18.18
-4.91
-5.06
f1 (ppm)

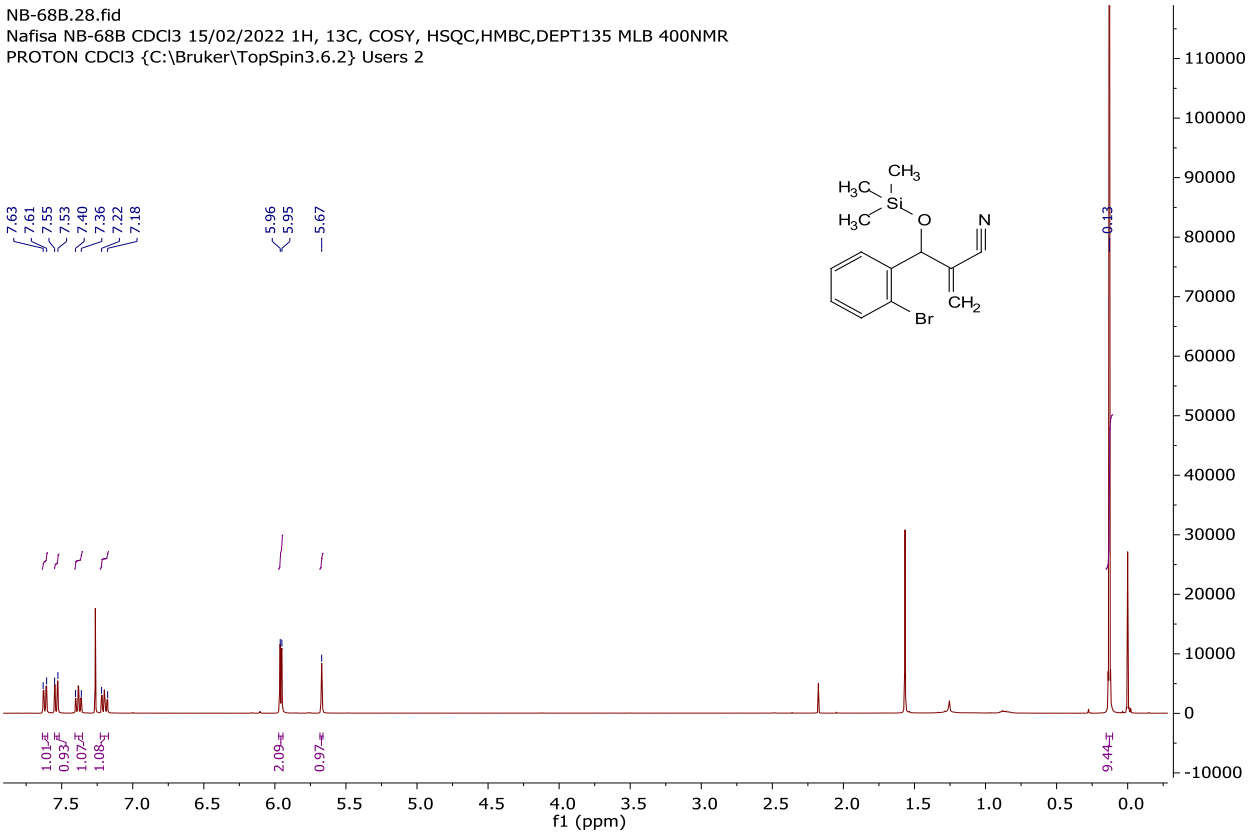
NB-68B.28.fid
Nafisa NB-68B CDCl3 15/02/2022 1H, 13C, COSY, HSQC,HMBC,DEPT135 MLB 400NMR
PROTON CDCl3 {C:\Bruker\TopSpin3.6.2} Users 2
7.63
7.61
7.55
7.53
7.40
7.36
7.22
7.18
5.96
5.95
5.67
0.13
1.01
0.93
1.07
1.08
2.09
0.97
9.44
f1 (ppm)

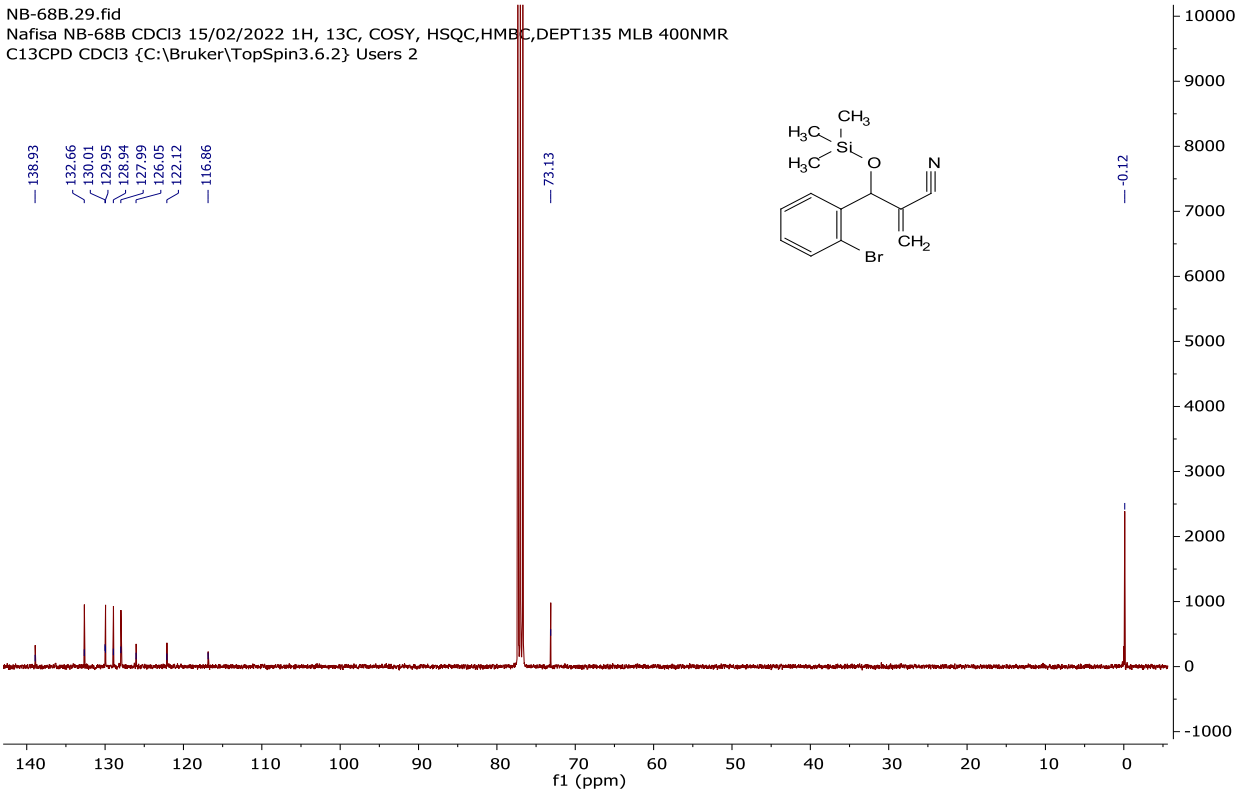
NB-68B.29.fid
Nafisa NB-68B CDCl3 15/02/2022 1H, 13C, COSY, HSQC,HMBC,DEPT135 MLB 400NMR
C13CPD CDCl3 {C:\Bruker\TopSpin3.6.2} Users 2
138.93
132.66
130.01
129.95
128.94
127.99
126.05
122.12
116.86
73.13
-0.12
f1 (ppm)

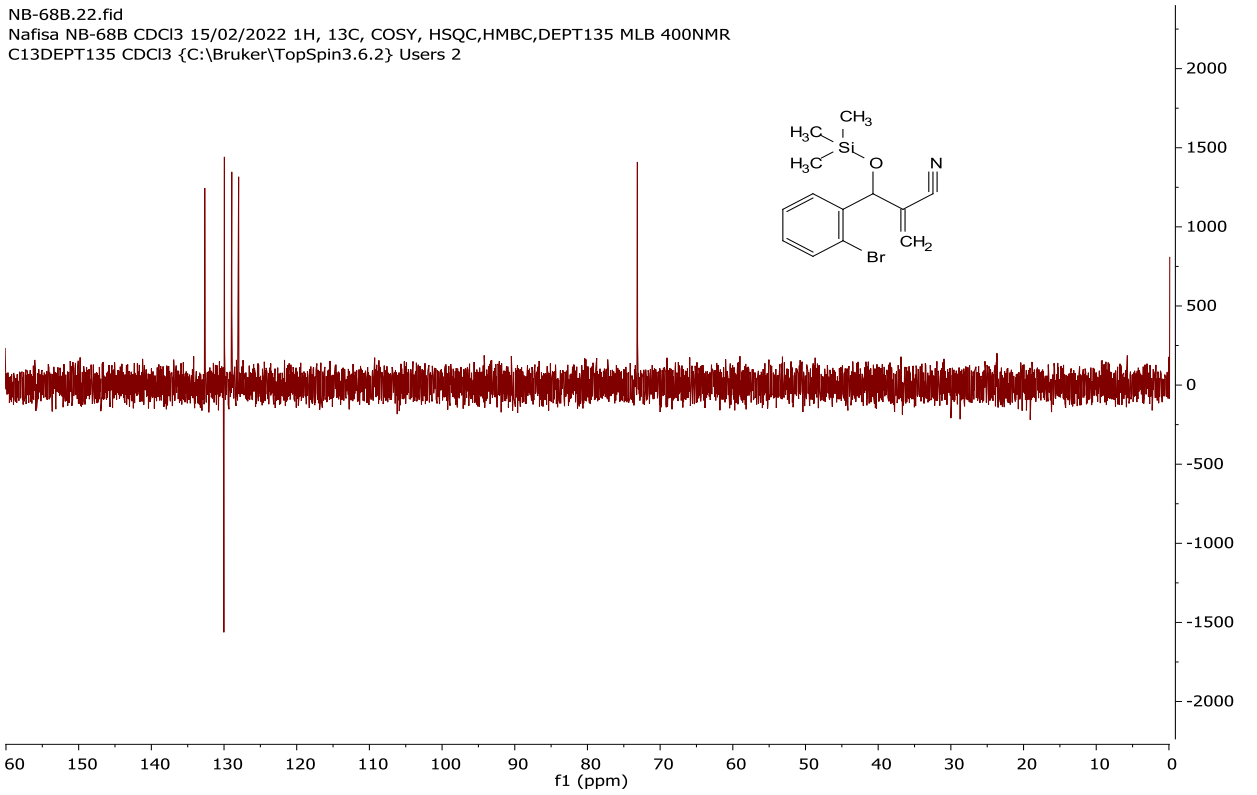
NB-68B.22.fid
Nafisa NB-68B CDCl3 15/02/2022 1H, 13C, COSY, HSQC,HMBC,DEPT135 MLB 400NMR
C13DEPT135 CDCl3 {C:\Bruker\TopSpin3.6.2} Users 2
f1 (ppm)

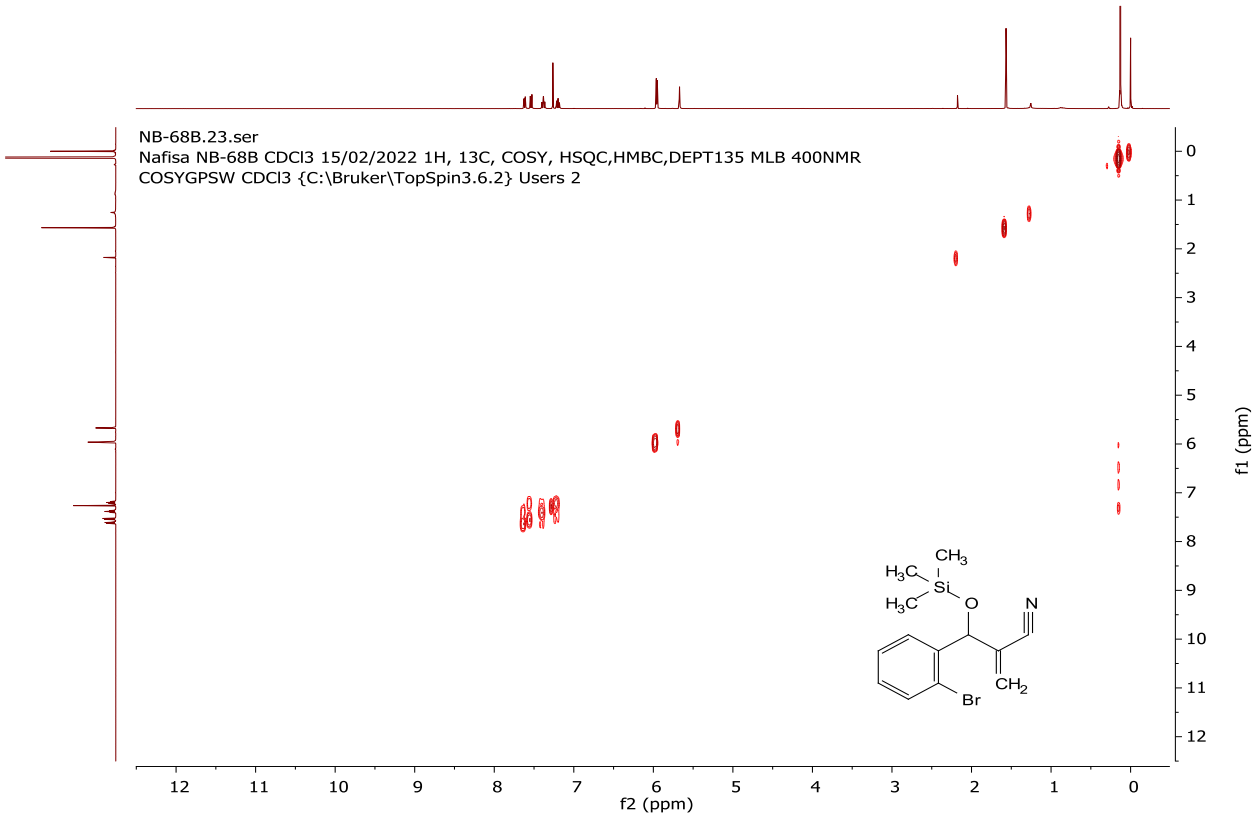
NB-68B.23.ser
Nafisa NB-68B CDCl3 15/02/2022 1H, 13C, COSY, HSQC,HMBC,DEPT135 MLB 400NMR
COSYGPSW CDCl3 {C:\Bruker\TopSpin3.6.2} Users 2
f2 (ppm)
f1 (ppm)

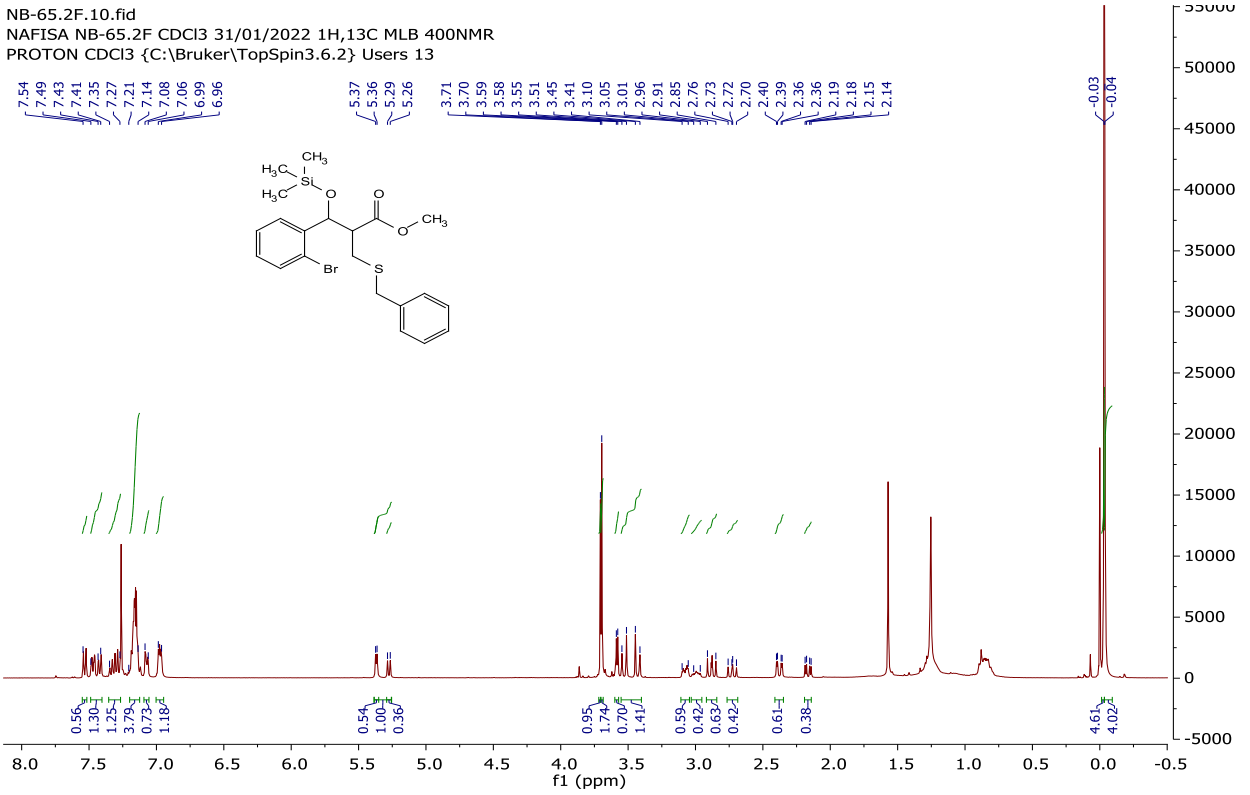
NB-65.2F.10.fid
NAFISA NB-65.2F CDCl3 31/01/2022 1H,13C MLB 400NMR
PROTON CDCl3 {C:\Bruker\TopSpin3.6.2} Users 13
f1 (ppm)

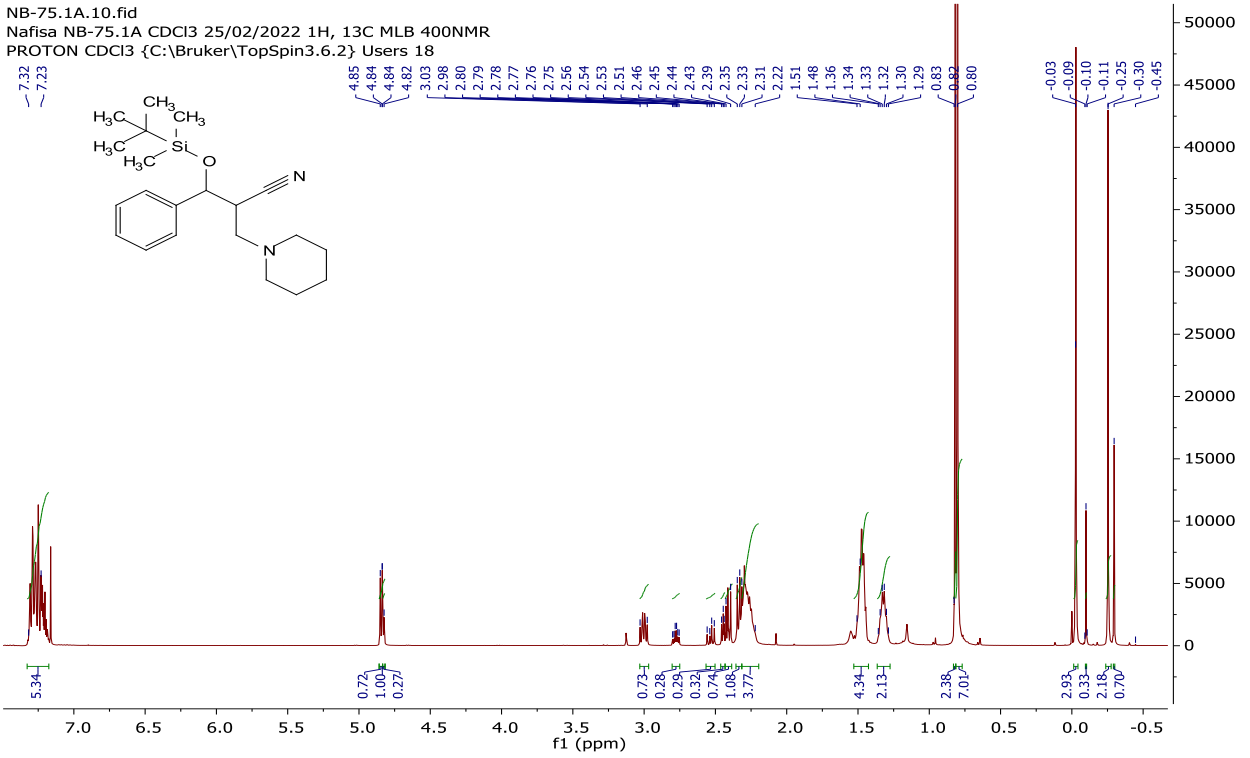
NB-75.1A.10.fid
Nafisa NB-75.1A CDCl3 25/02/2022 1H, 13C MLB 400NMR
PROTON CDCl3 {C:\Bruker\TopSpin3.6.2} Users 18
f1 (ppm)

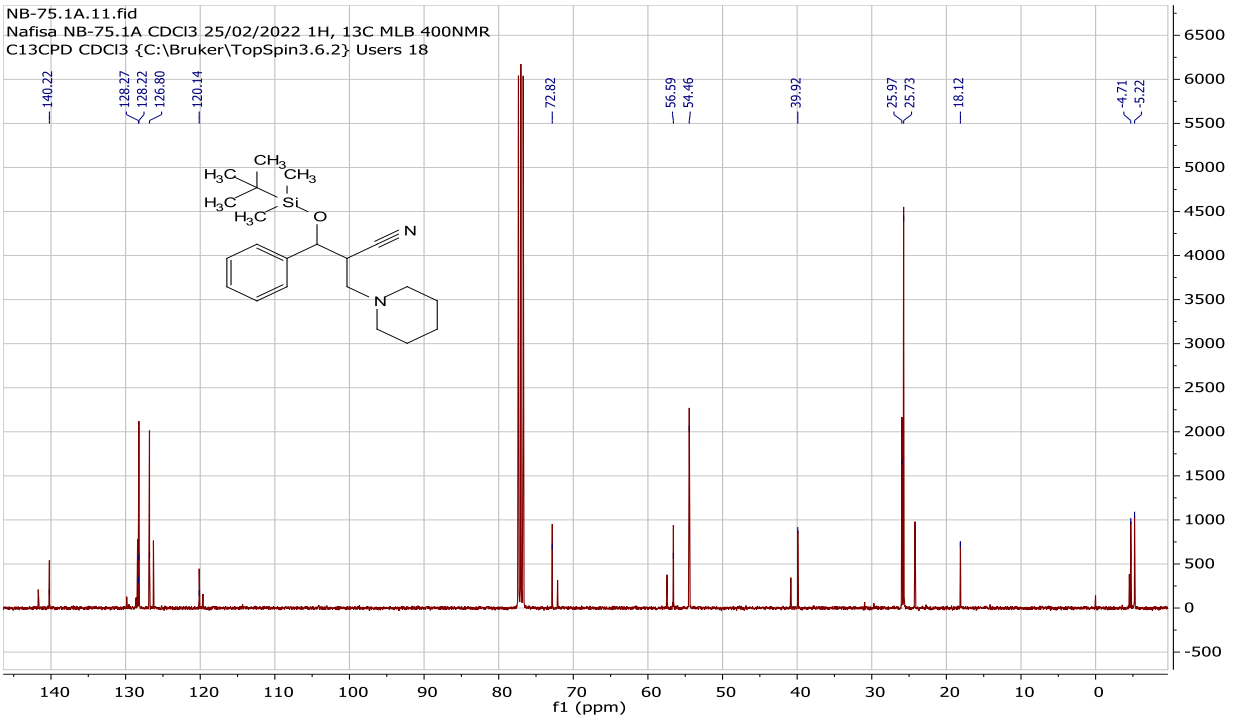
NB-75.1A.11.fid
Nafisa NB-75.1A CDCl3 25/02/2022 1H, 13C MLB 400NMR
C13CPD CDCl3 {C:\Bruker\TopSpin3.6.2} Users 18
140.22
128.27
128.22
126.80
120.14
72.82
56.59
54.46
39.92
25.97
25.73
18.12
-4.71
-5.22
f1 (ppm)

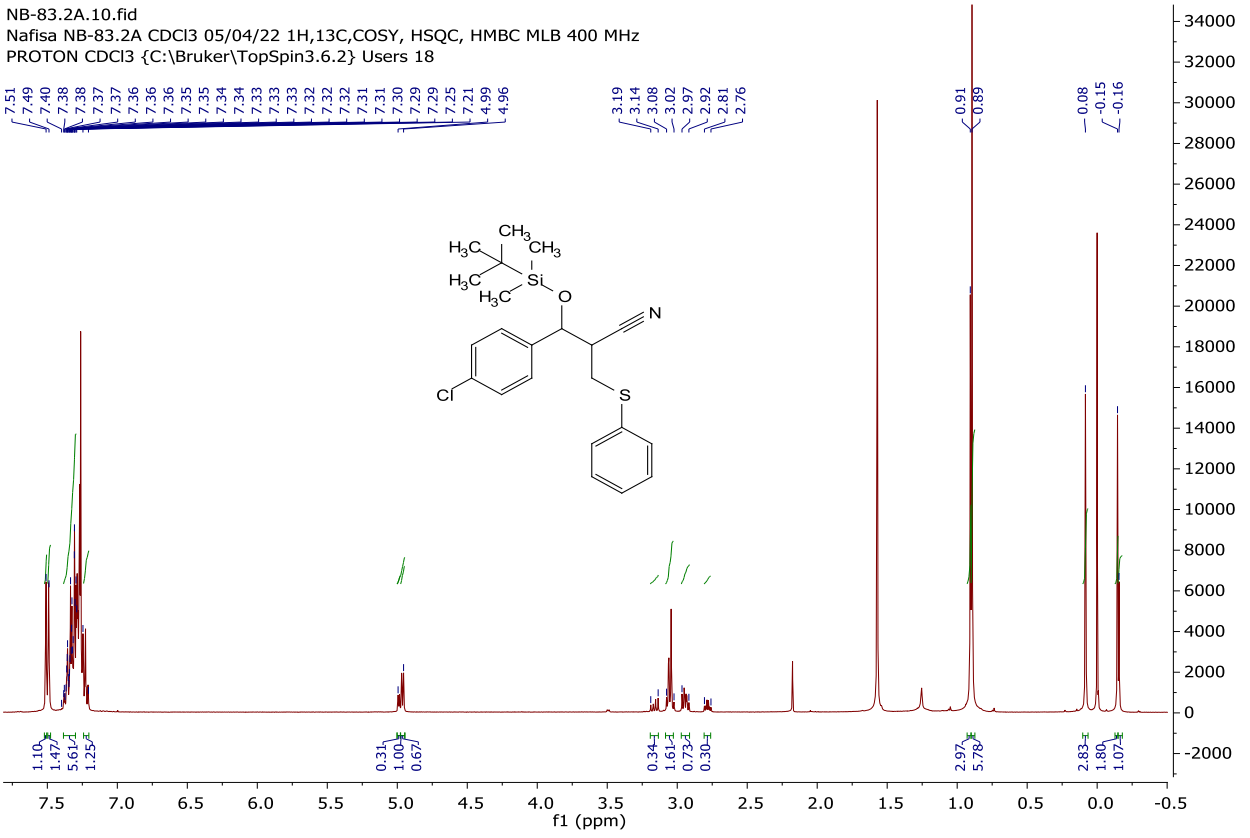
NB-83.2A.10.fid
Nafisa NB-83.2A CDCl3 05/04/22 1H,13C,COSY, HSQC, HMBC MLB 400 MHz
PROTON CDCl3 {C:\Bruker\TopSpin3.6.2} Users 18
7.51
7.49
7.40
7.38
7.38
7.37
7.37
7.36
7.36
7.36
7.35
7.35
7.34
7.34
7.33
7.33
7.33
7.32
7.32
7.32
7.31
7.31
7.30
7.29
7.29
7.25
7.21
4.99
4.96
3.19
3.14
3.08
3.02
2.97
2.92
2.81
2.76
0.91
0.89
0.08
-0.15
-0.16
1.10
1.47
5.61
1.25
0.31
1.00
0.67
0.34
1.61
0.73
0.30
2.97
5.78
2.83
1.80
1.07
f1 (ppm)

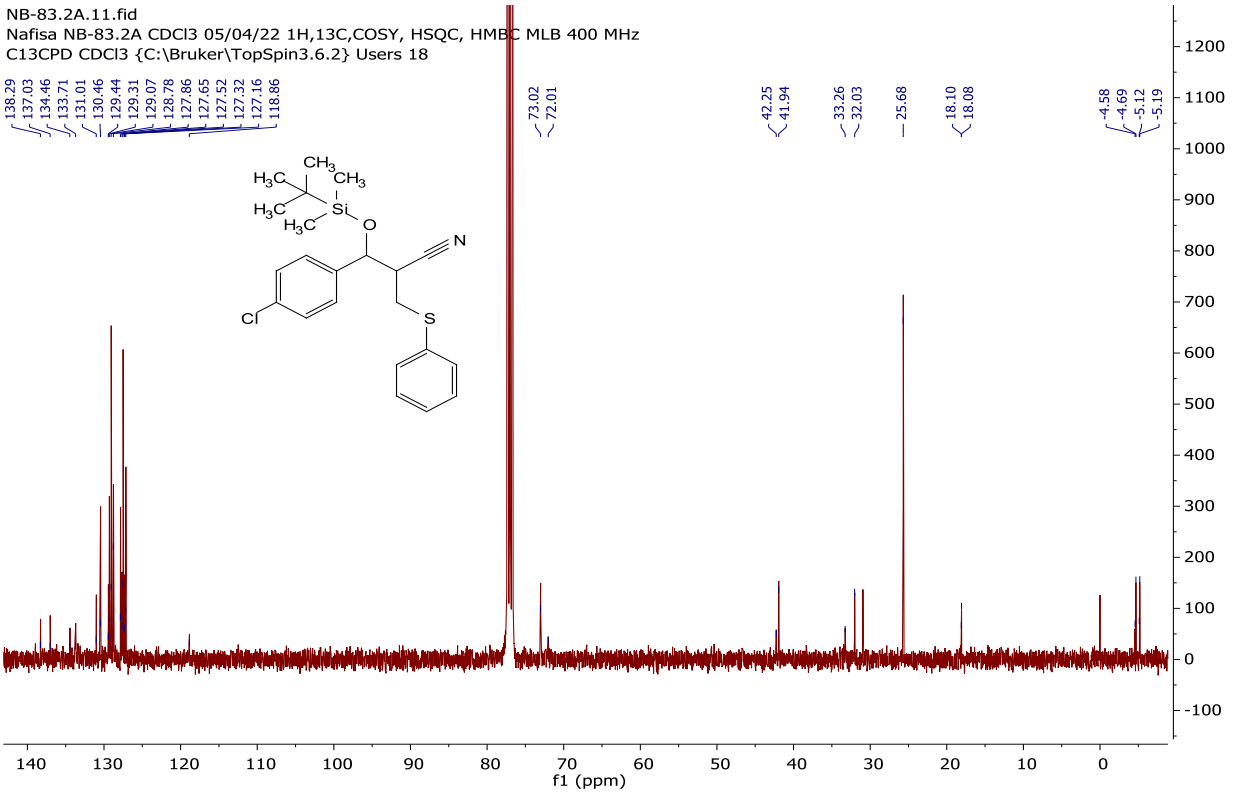
NB-83.2A.11.fid
Nafisa NB-83.2A CDCl3 05/04/22 1H,13C,COSY, HSQC, HMBC MLB 400 MHz
C13CPD CDCl3 {C:\Bruker\TopSpin3.6.2} Users 18
138.29
137.03
134.46
133.71
131.01
130.46
129.44
129.31
129.07
128.78
127.86
127.65
127.52
127.32
127.16
118.86
73.02
72.01
42.25
41.94
33.26
32.03
25.68
18.10
18.08
-4.58
-4.69
-5.12
-5.19
f1 (ppm)

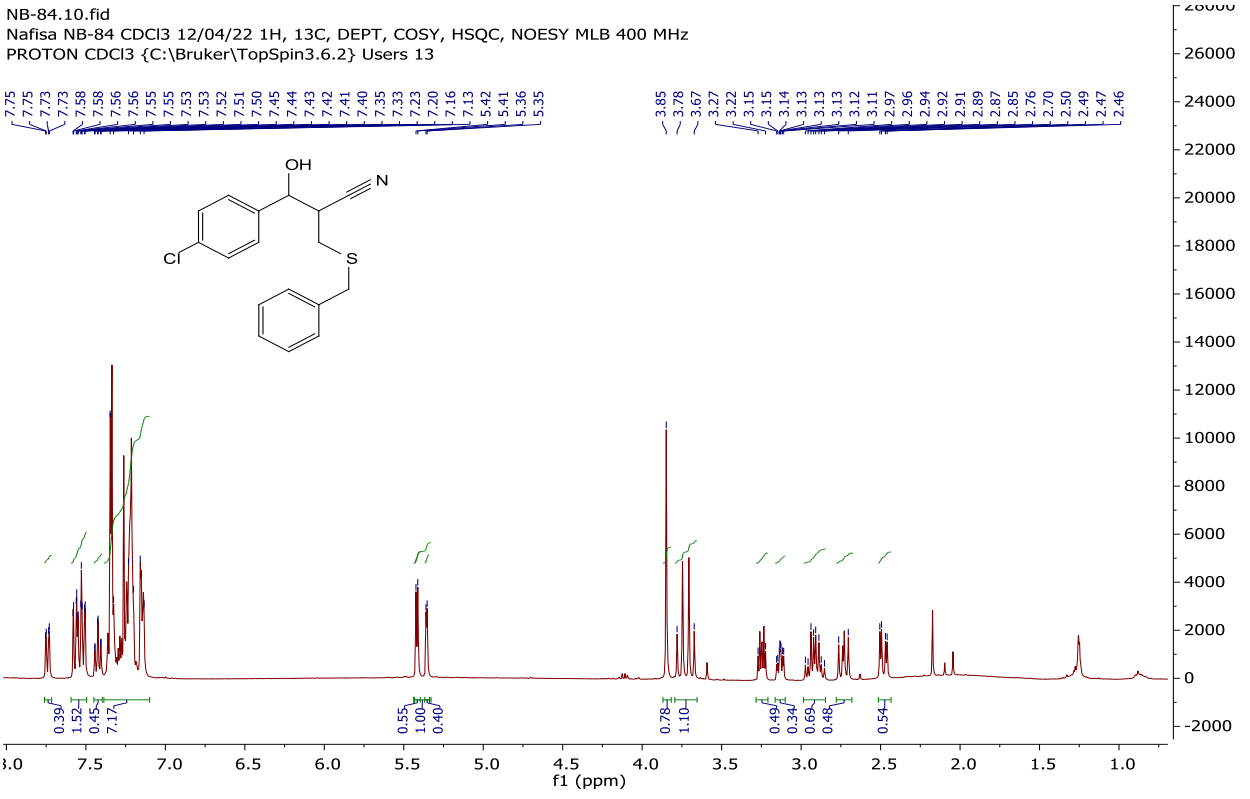
NB-84.10.fid
Nafisa NB-84 CDCl3 12/04/22 1H, 13C, DEPT, COSY, HSQC, NOESY MLB 400 MHz
PROTON CDCl3 {C:\Bruker\TopSpin3.6.2} Users 13
7.75
7.75
7.73
7.73
7.58
7.58
7.56
7.56
7.55
7.55
7.53
7.53
7.52
7.51
7.50
7.45
7.44
7.43
7.42
7.41
7.40
7.35
7.33
7.23
7.20
7.16
7.13
5.42
5.41
5.36
5.35
3.85
3.78
3.67
3.27
3.22
3.15
3.15
3.14
3.13
3.13
3.13
3.12
3.11
2.97
2.96
2.94
2.92
2.91
2.89
2.87
2.85
2.76
2.70
2.50
2.49
2.47
2.46
0.39
1.52
0.45
7.17
0.55
1.00
0.40
0.78
1.10
0.49
0.34
0.69
0.48
0.54
f1 (ppm)

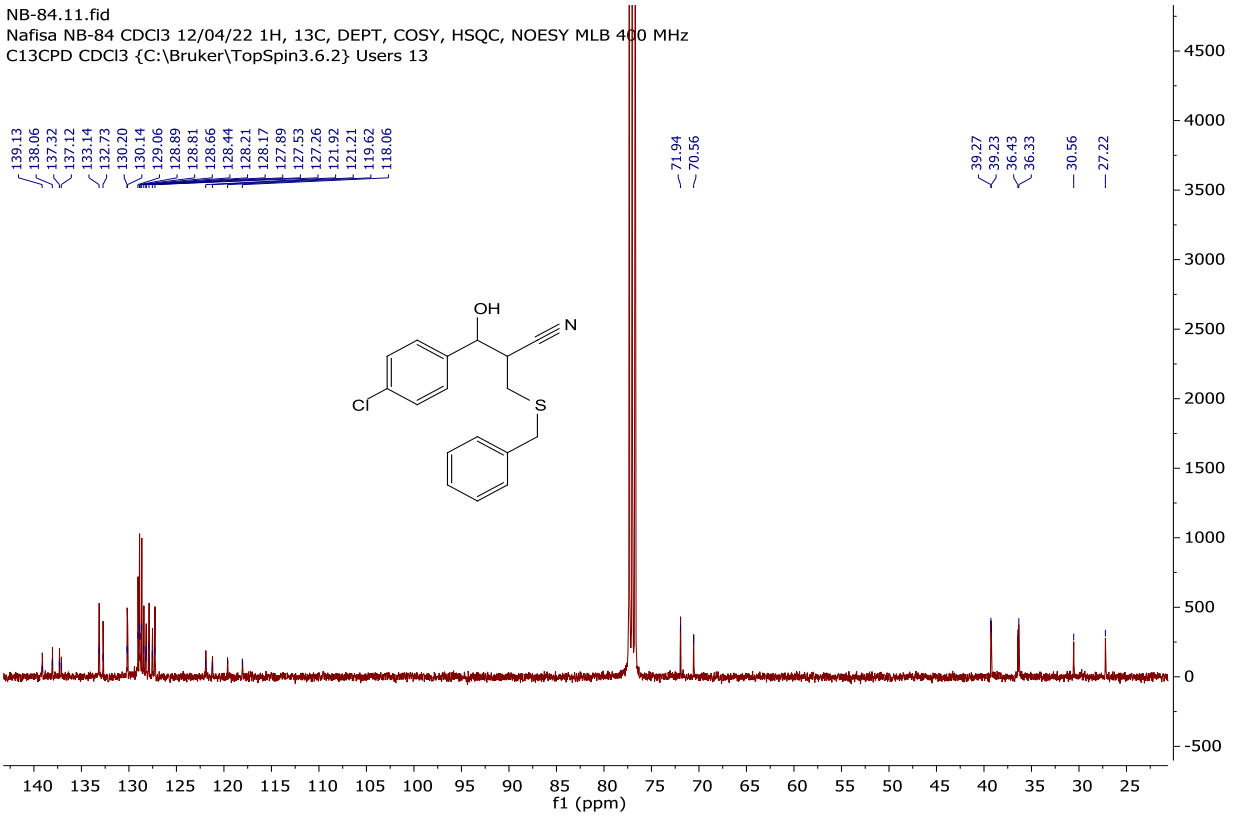
NB-84.11.fid
Nafisa NB-84 CDCl3 12/04/22 1H, 13C, DEPT, COSY, HSQC, NOESY MLB 400 MHz
C13CPD CDCl3 {C:\Bruker\TopSpin3.6.2} Users 13
139.13
138.06
137.32
137.12
133.14
132.73
130.20
130.14
129.06
128.89
128.81
128.66
128.44
128.21
128.17
127.89
127.53
127.26
121.92
121.21
119.62
118.06
71.94
70.56
39.27
39.23
36.43
36.33
30.56
27.22
OH
N
Cl
S
f1 (ppm)

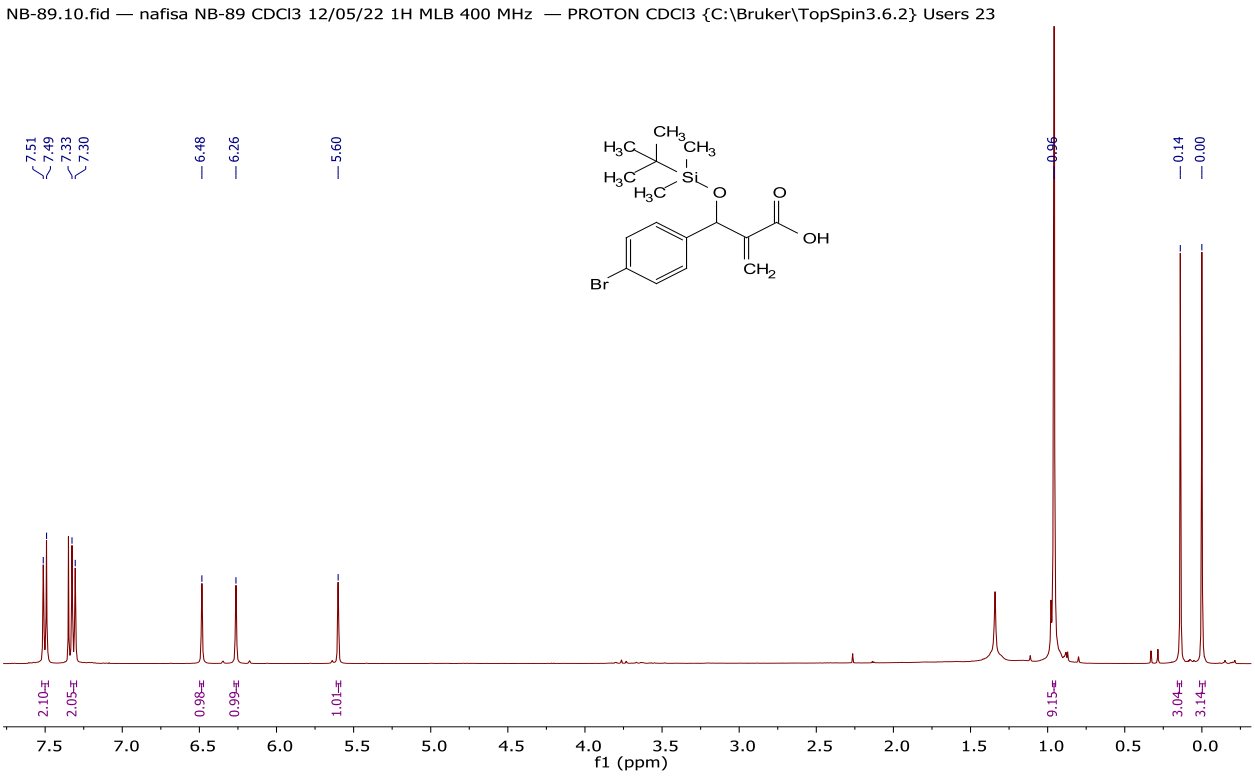
NB-89.10.fid — nafisa NB-89 CDCl3 12/05/22 1H MLB 400 MHz — PROTON CDCl3 {C:\Bruker\TopSpin3.6.2} Users 23
7.51
7.49
7.33
7.30
6.48
6.26
5.60
0.96
0.14
0.00
CH3
H3C
CH3
H3C
Si
H3C
O
O
OH
CH2
Br
2.10
2.05
0.98
0.99
1.01
9.15
3.04
3.14
f1 (ppm)

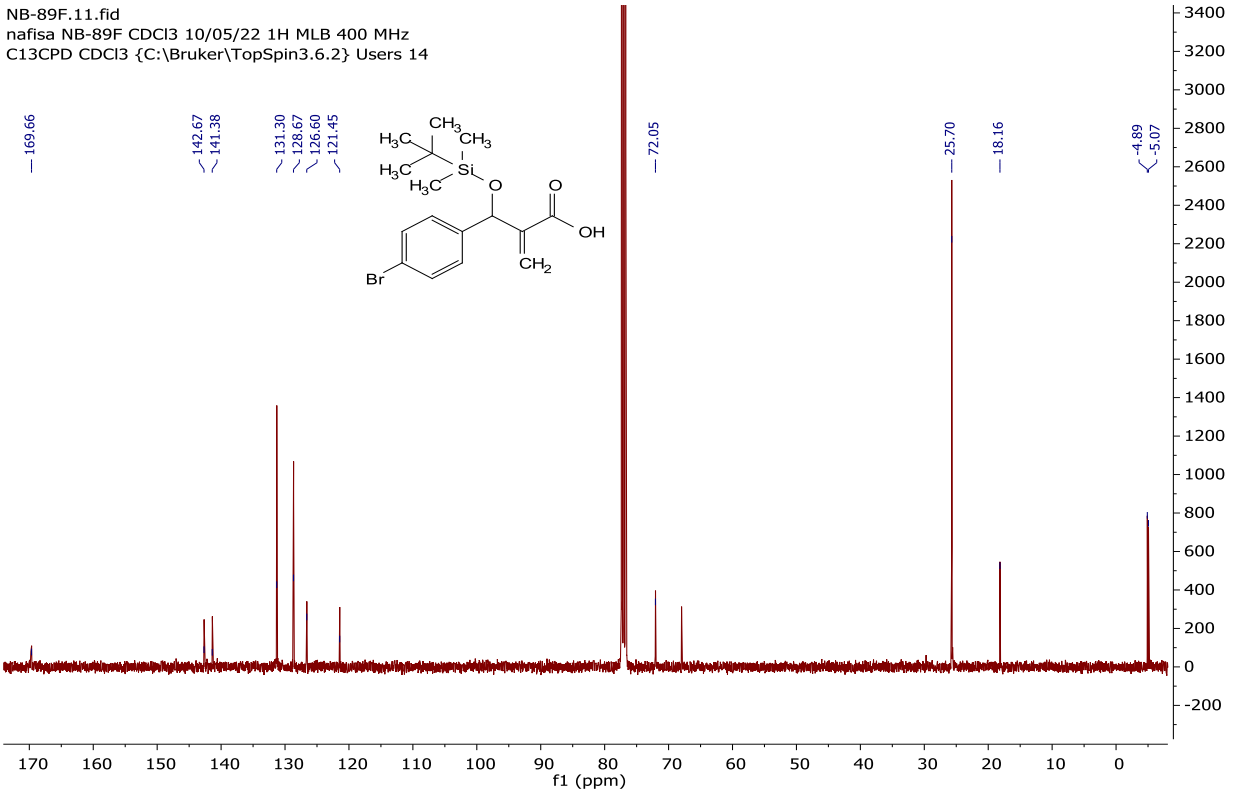
NB-89F.11.fid
nafisa NB-89F CDCl3 10/05/22 1H MLB 400 MHz
C13CPD CDCl3 {C:\Bruker\TopSpin3.6.2} Users 14
169.66
142.67
141.38
131.30
128.67
126.60
121.45
72.05
25.70
18.16
-4.89
-5.07
f1 (ppm)

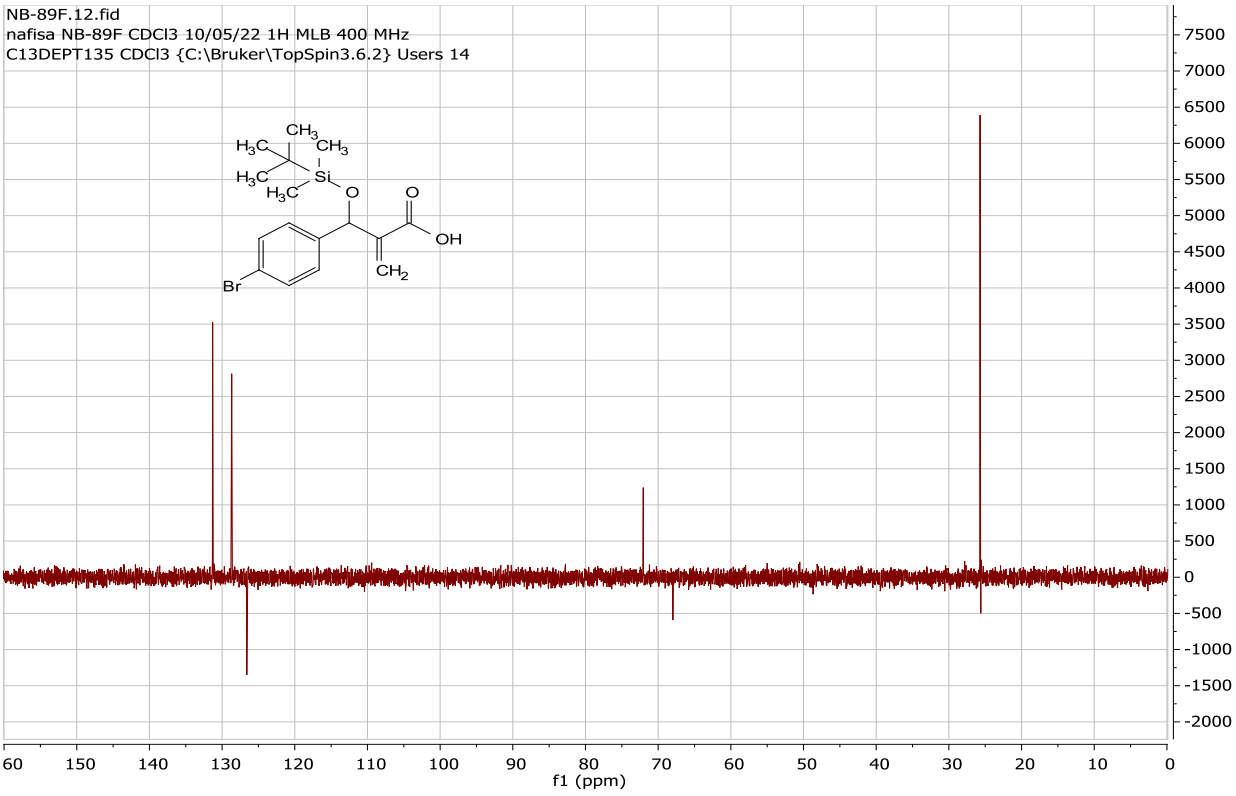
NB-89F.12.fid
nafisa NB-89F CDCl3 10/05/22 1H MLB 400 MHz
C13DEPT135 CDCl3 {C:\Bruker\TopSpin3.6.2} Users 14
f1 (ppm)

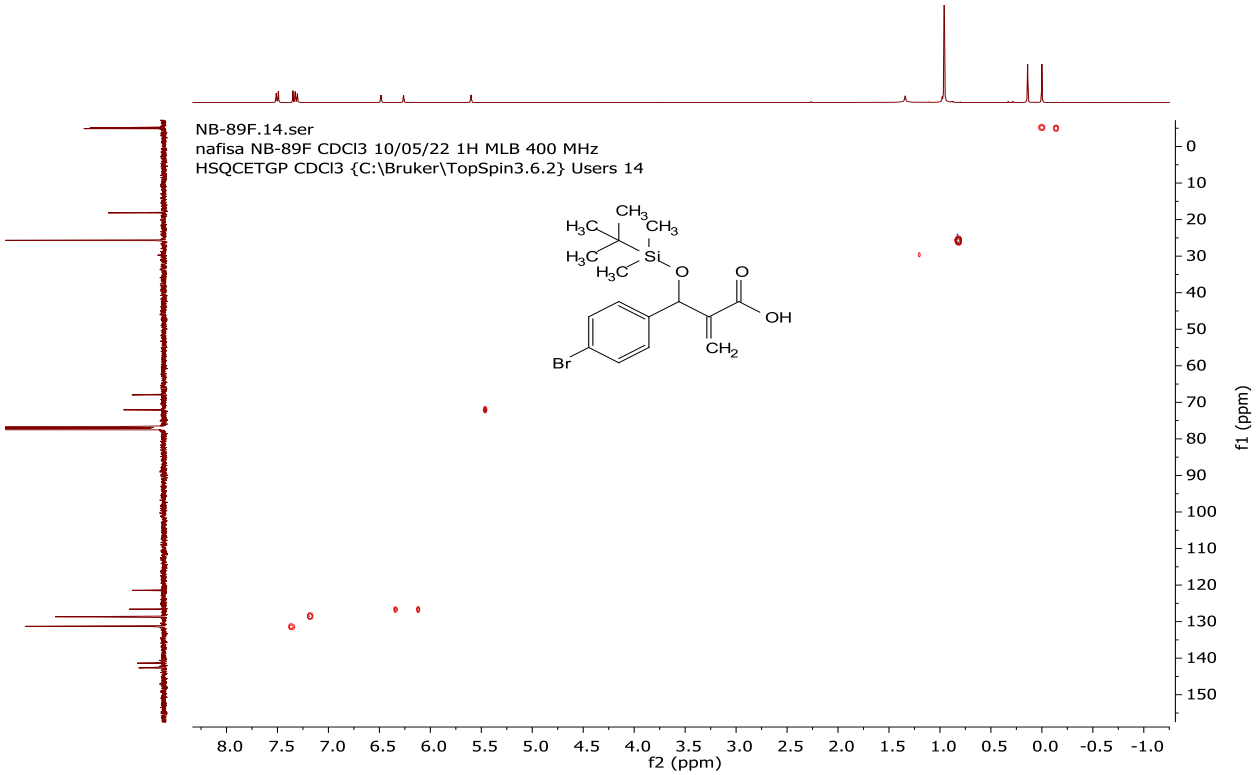
NB-89F.14.ser
nafisa NB-89F CDCl3 10/05/22 1H MLB 400 MHz
HSQCETGP CDCl3 {C:\Bruker\TopSpin3.6.2} Users 14
f2 (ppm)
f1 (ppm)

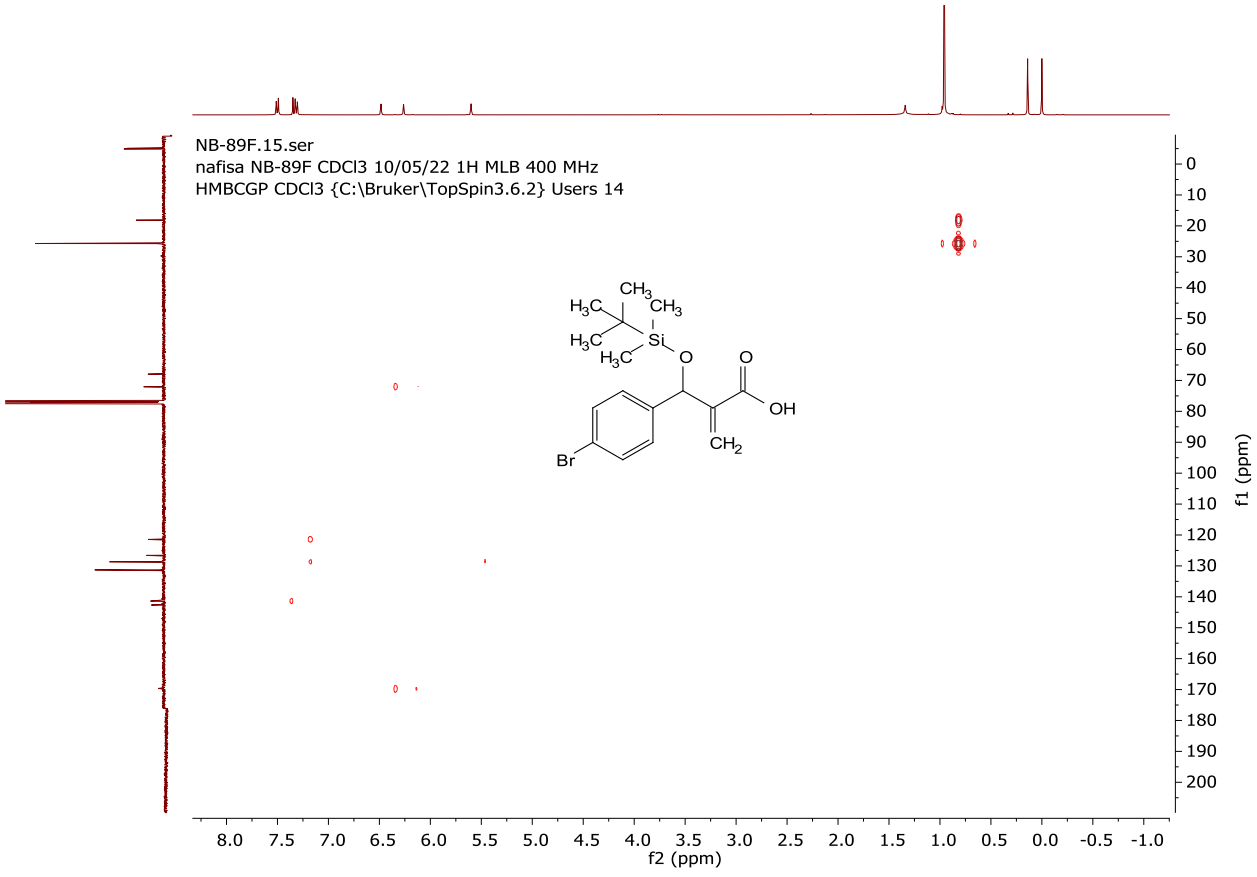
NB-89F.15.ser
nafisa NB-89F CDCl3 10/05/22 1H MLB 400 MHz
HMBCGP CDCl3 {C:\Bruker\TopSpin3.6.2} Users 14
f2 (ppm)
f1 (ppm)

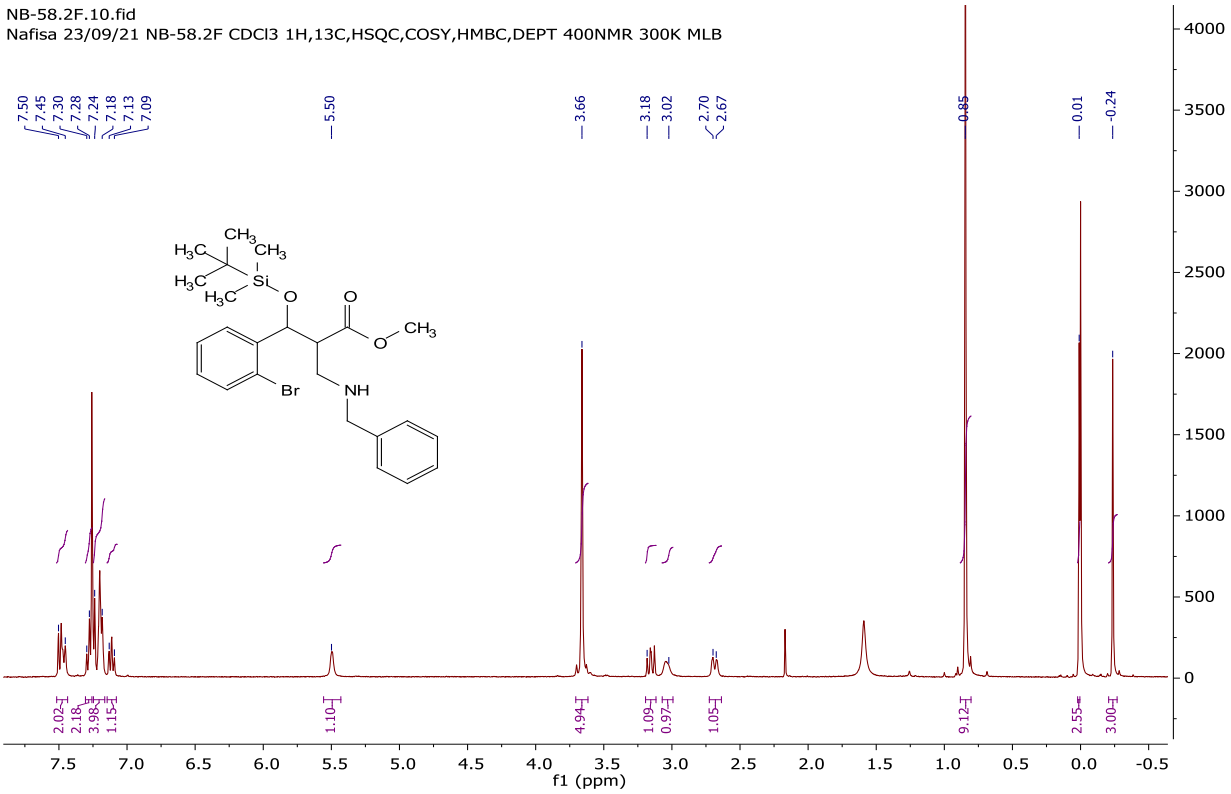
NB-58.2F.10.fid
Nafisa 23/09/21 NB-58.2F CDCl3 1H,13C,HSQC,COSY,HMBC,DEPT 400NMR 300K MLB
7.50
7.45
7.30
7.28
7.24
7.18
7.13
7.09
5.50
3.66
3.18
3.02
2.70
2.67
0.85
0.01
-0.24
CH3
H3C
CH3
H3C
Si
H3C
O
O
O
CH3
Br
NH
2.02
2.18
3.98
1.15
1.10
4.94
1.09
0.97
1.05
9.12
2.55
3.00
f1 (ppm)

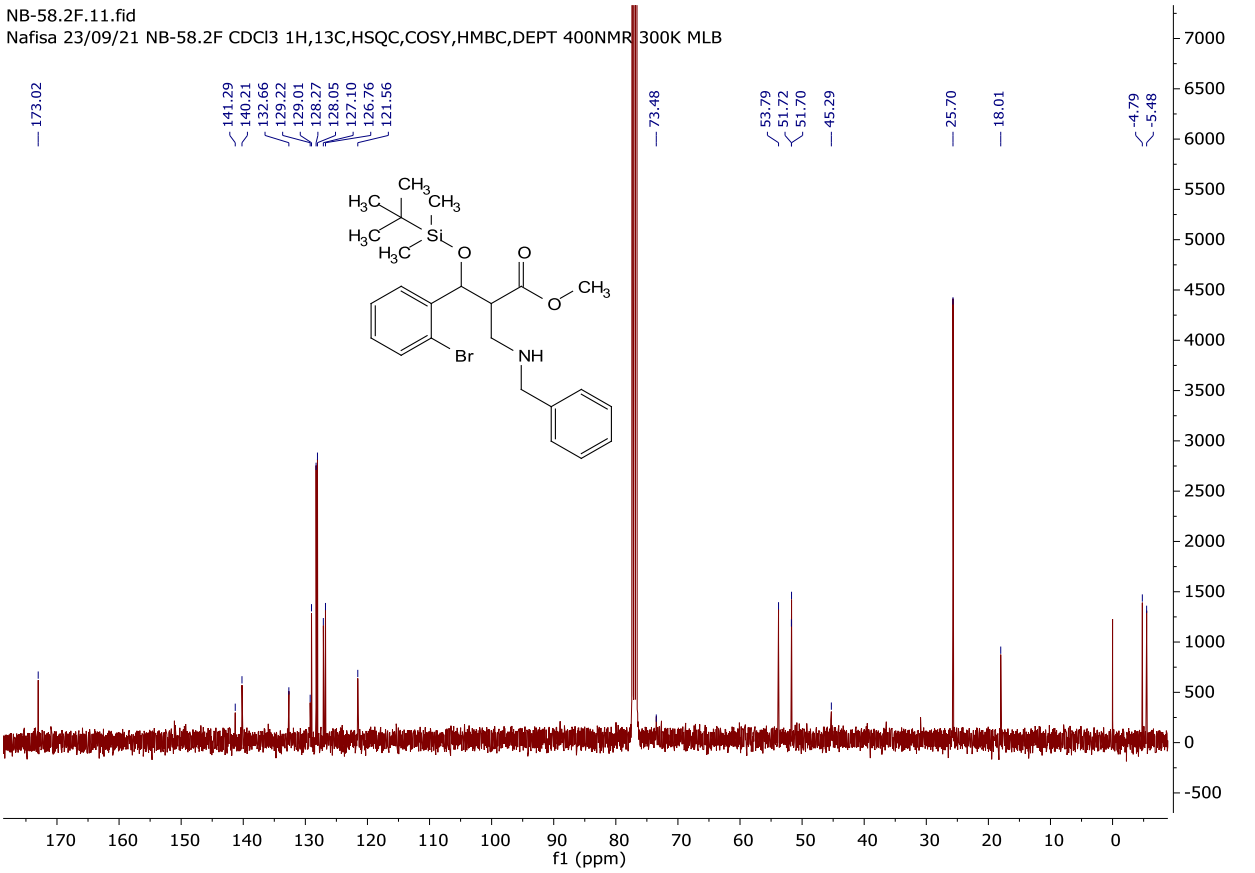
NB-58.2F.11.fid
Nafisa 23/09/21 NB-58.2F CDCl3 1H,13C,HSQC,COSY,HMBC,DEPT 400NMR 300K MLB
173.02
141.29
140.21
132.66
129.22
129.01
128.27
128.05
127.10
126.76
121.56
73.48
53.79
51.72
51.70
45.29
25.70
18.01
-4.79
-5.48
f1 (ppm)

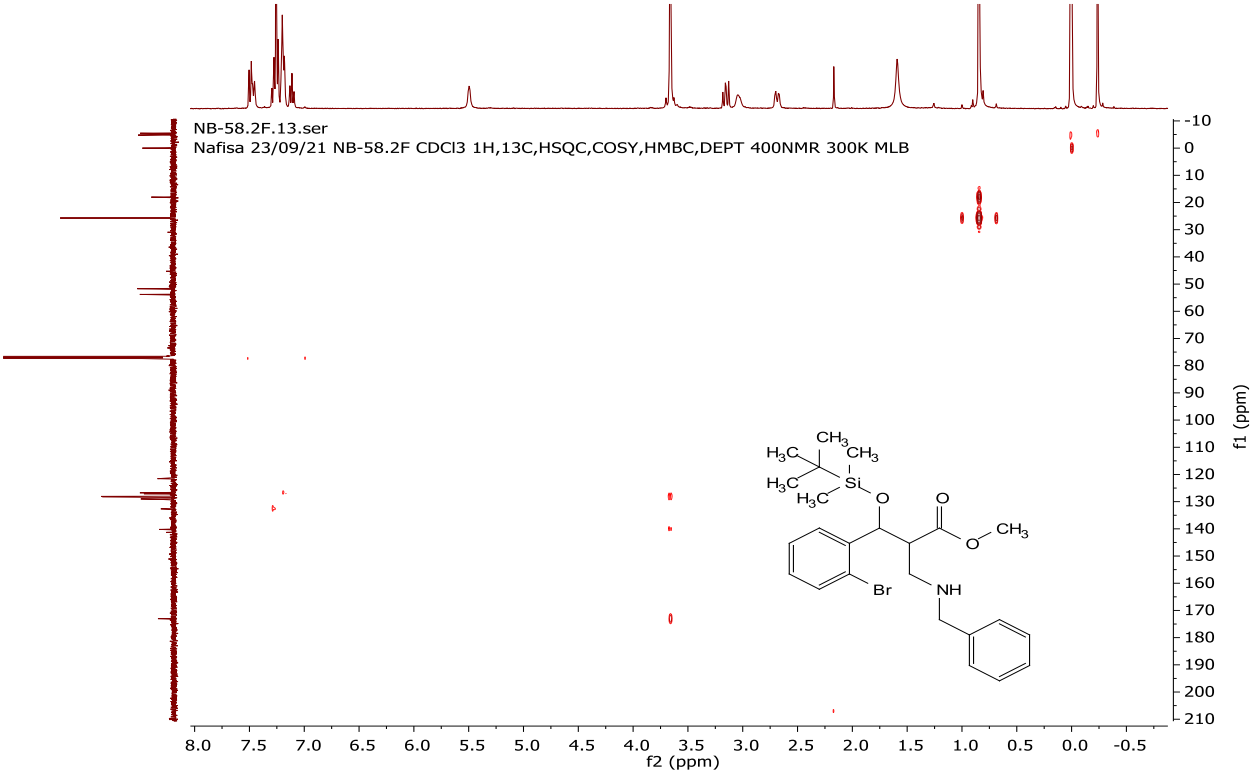
NB-58.2F.13.ser
Nafisa 23/09/21 NB-58.2F CDCl3 1H,13C,HSQC,COSY,HMBC,DEPT 400NMR 300K MLB
f2 (ppm)
f1 (ppm)

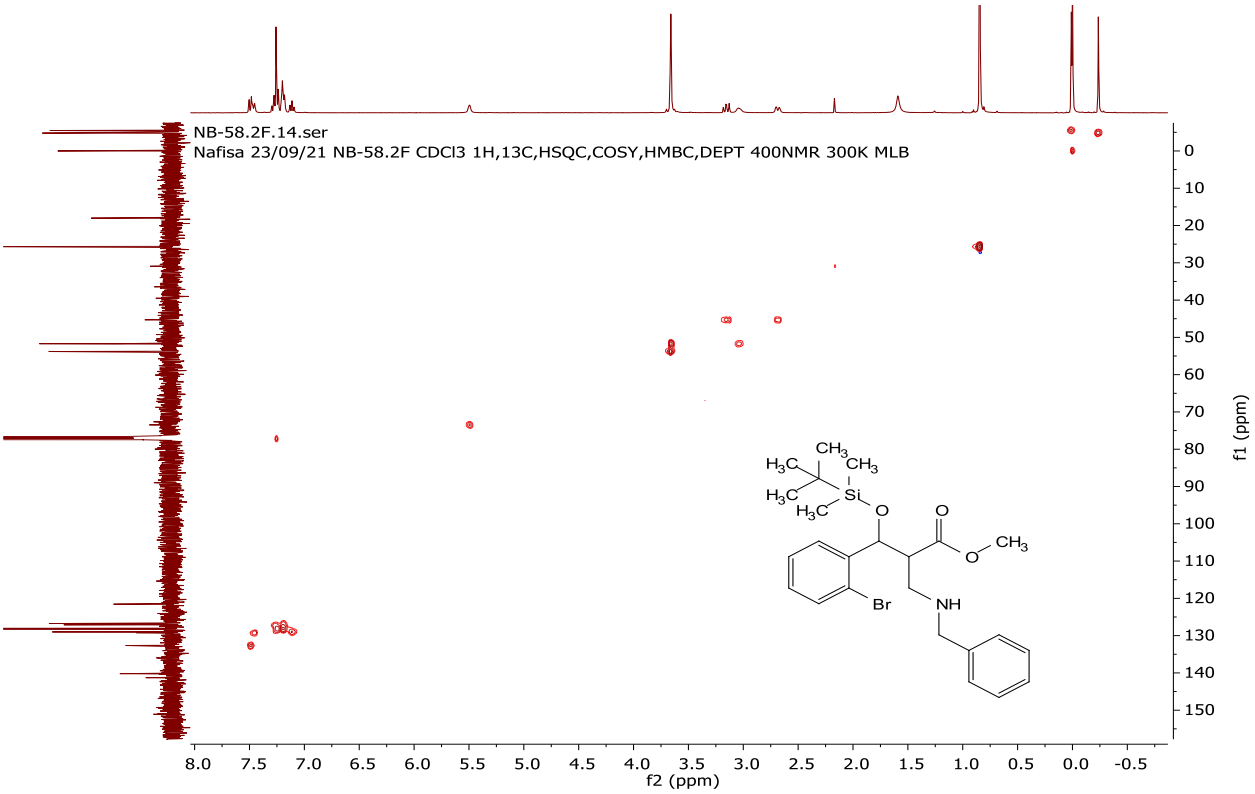
NB-58.2F.14.ser
Nafisa 23/09/21 NB-58.2F CDCl3 1H,13C,HSQC,COSY,HMBC,DEPT 400NMR 300K MLB
f2 (ppm)
f1 (ppm)
Br
NH
Si
O
CH3

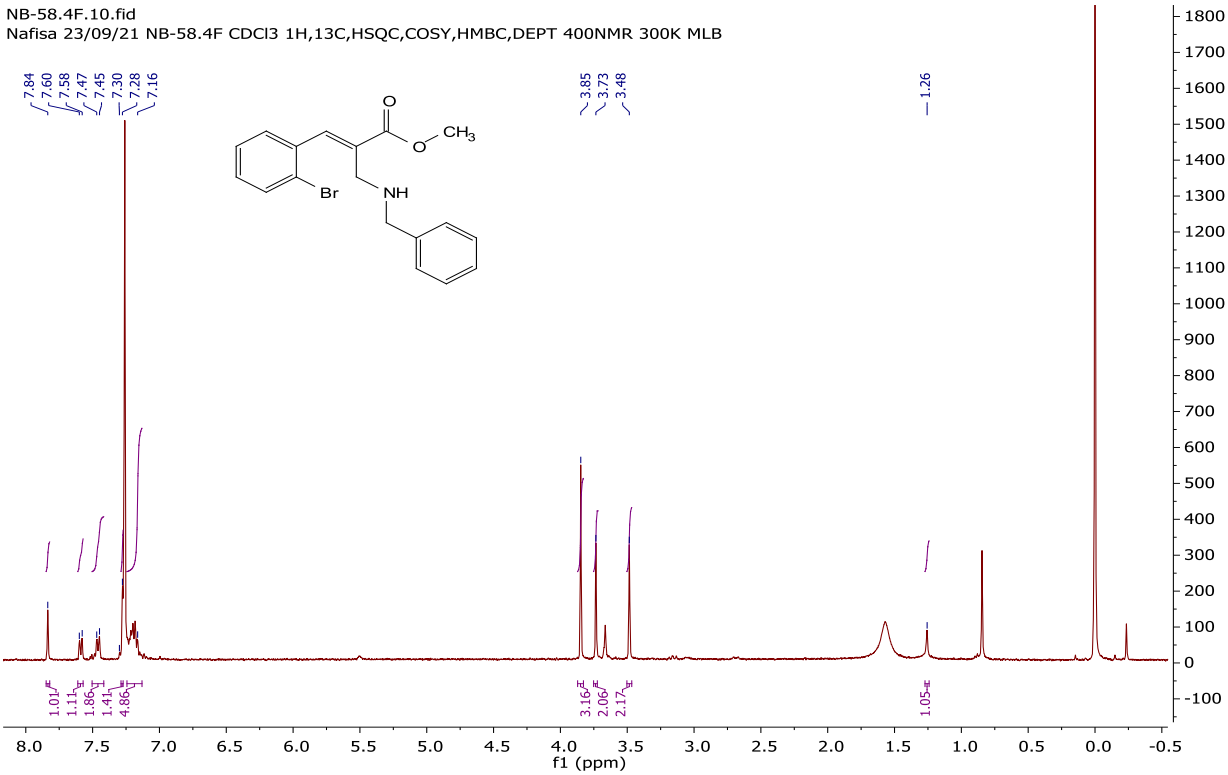
NB-58.4F.10.fid
Nafisa 23/09/21 NB-58.4F CDCl3 1H,13C,HSQC,COSY,HMBC,DEPT 400NMR 300K MLB
7.84
7.60
7.58
7.47
7.45
7.30
7.28
7.16
3.85
3.73
3.48
1.26
1.01
1.11
1.86
1.41
4.86
3.16
2.06
2.17
1.05
Br
NH
O
CH3
f1 (ppm)

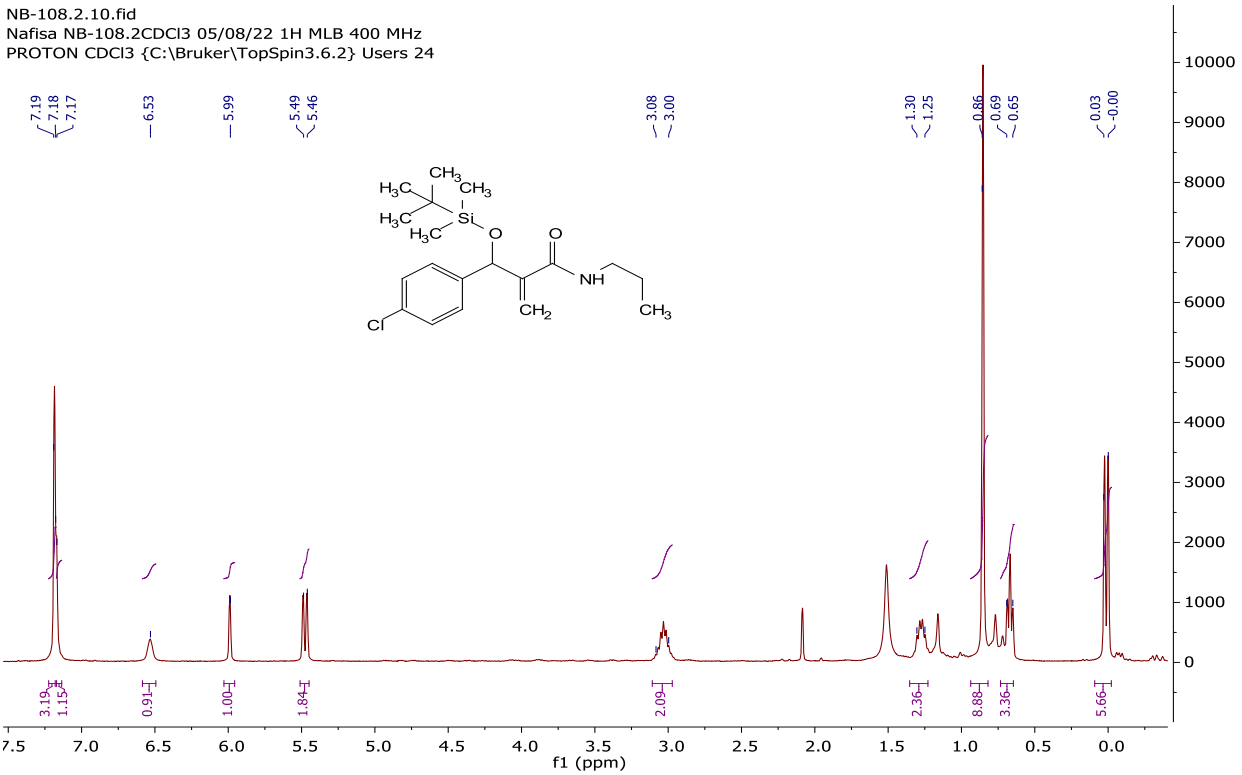
NB-108.2.10.fid
Nafisa NB-108.2CDCl3 05/08/22 1H MLB 400 MHz
PROTON CDCl3 {C:\Bruker\TopSpin3.6.2} Users 24
7.19
7.18
7.17
6.53
5.99
5.49
5.46
3.08
3.00
1.30
1.25
0.86
0.69
0.65
0.03
-0.00
3.19
1.15
0.91
1.00
1.84
2.09
2.36
8.88
3.36
5.66
f1 (ppm)

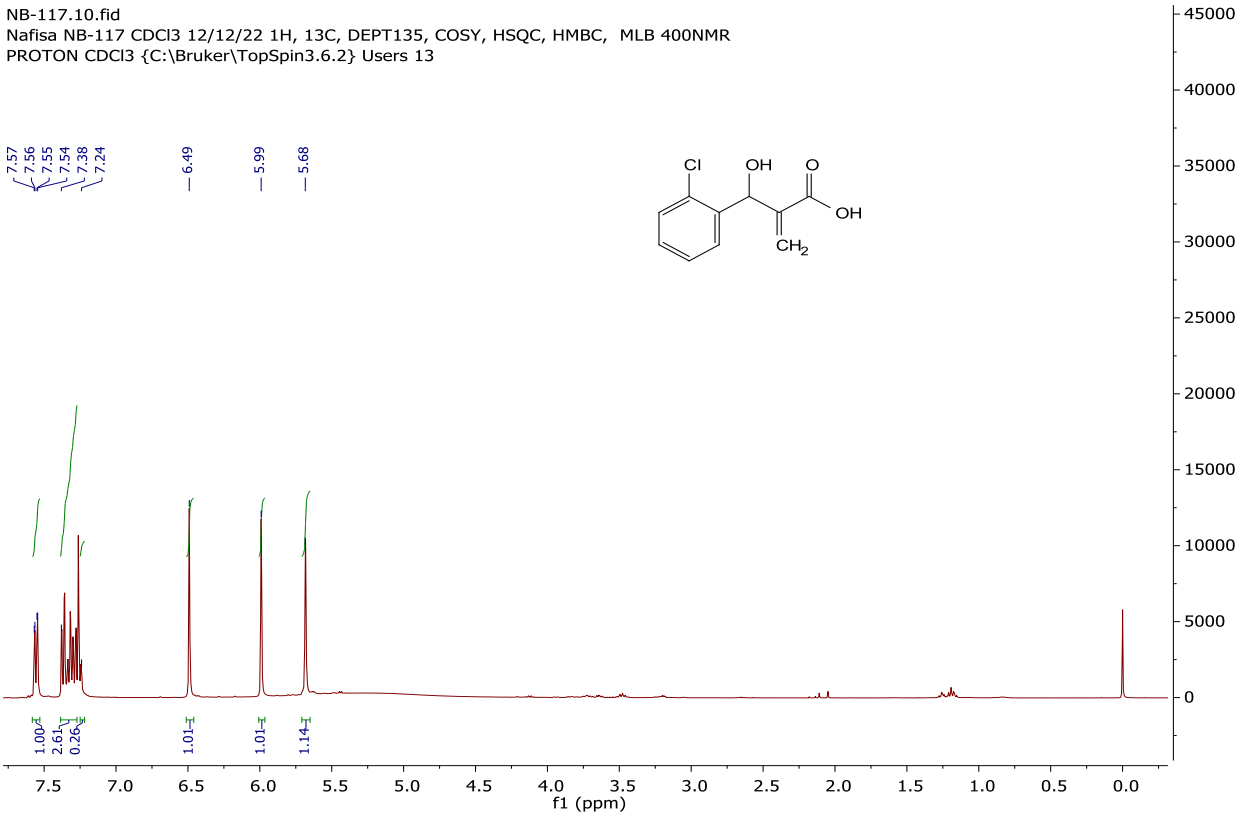
NB-117.10.fid
Nafisa NB-117 CDCl3 12/12/22 1H, 13C, DEPT135, COSY, HSQC, HMBC, MLB 400NMR
PROTON CDCl3 {C:\Bruker\TopSpin3.6.2} Users 13
7.57
7.56
7.55
7.54
7.38
7.24
6.49
5.99
5.68
1.00
2.61
0.26
1.01
1.01
1.14
f1 (ppm)

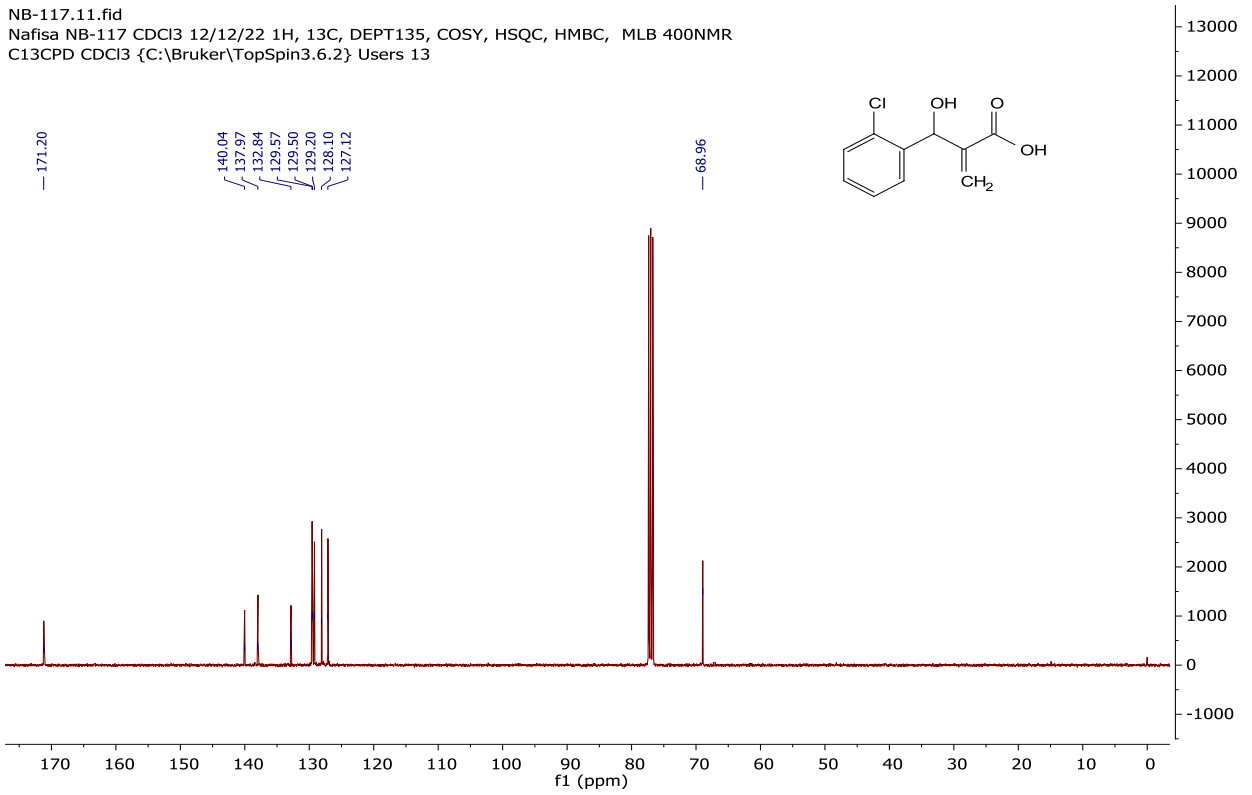
NB-117.11.fid
Nafisa NB-117 CDCl3 12/12/22 1H, 13C, DEPT135, COSY, HSQC, HMBC, MLB 400NMR
C13CPD CDCl3 {C:\Bruker\TopSpin3.6.2} Users 13
171.20
140.04
137.97
132.84
129.57
129.50
129.20
128.10
127.12
68.96
Cl
OH
O
OH
CH2
f1 (ppm)

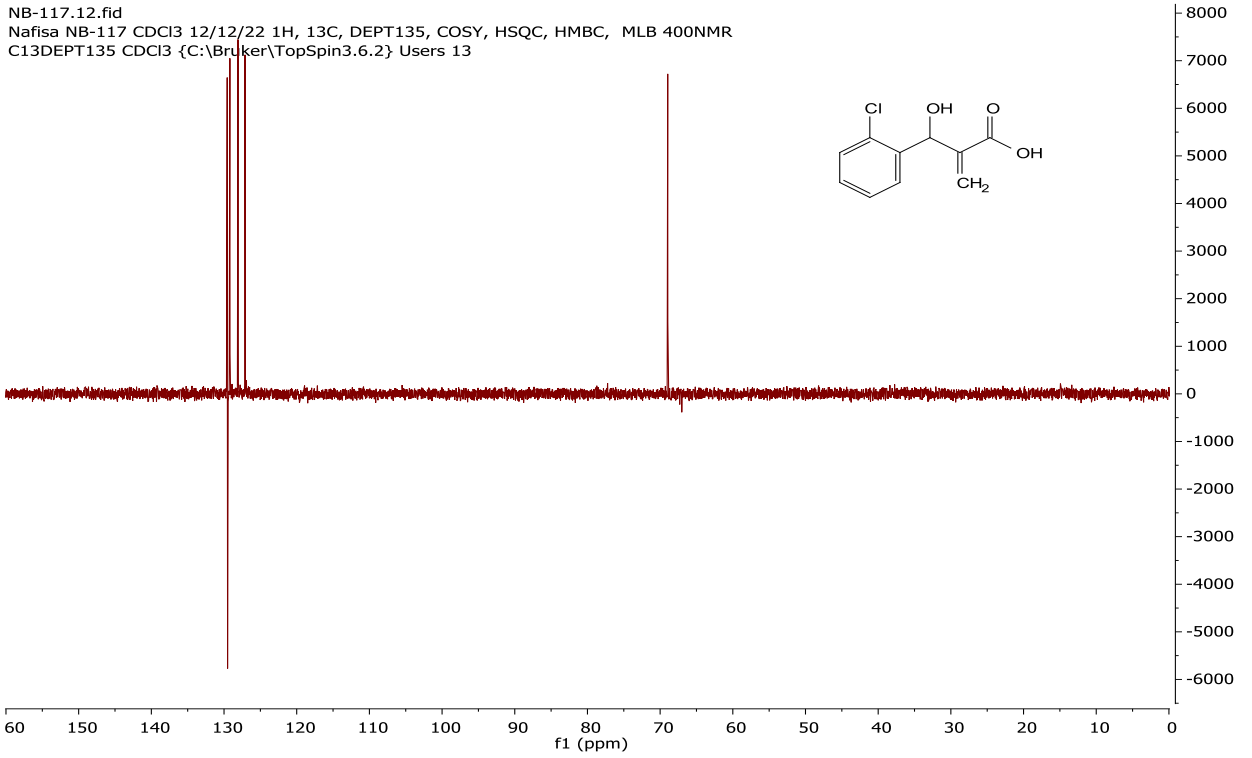
NB-117.12.fid
Nafisa NB-117 CDCl3 12/12/22 1H, 13C, DEPT135, COSY, HSQC, HMBC, MLB 400NMR
C13DEPT135 CDCl3 {C:\Bruker\TopSpin3.6.2} Users 13
Cl
OH
O
OH
CH2
f1 (ppm)

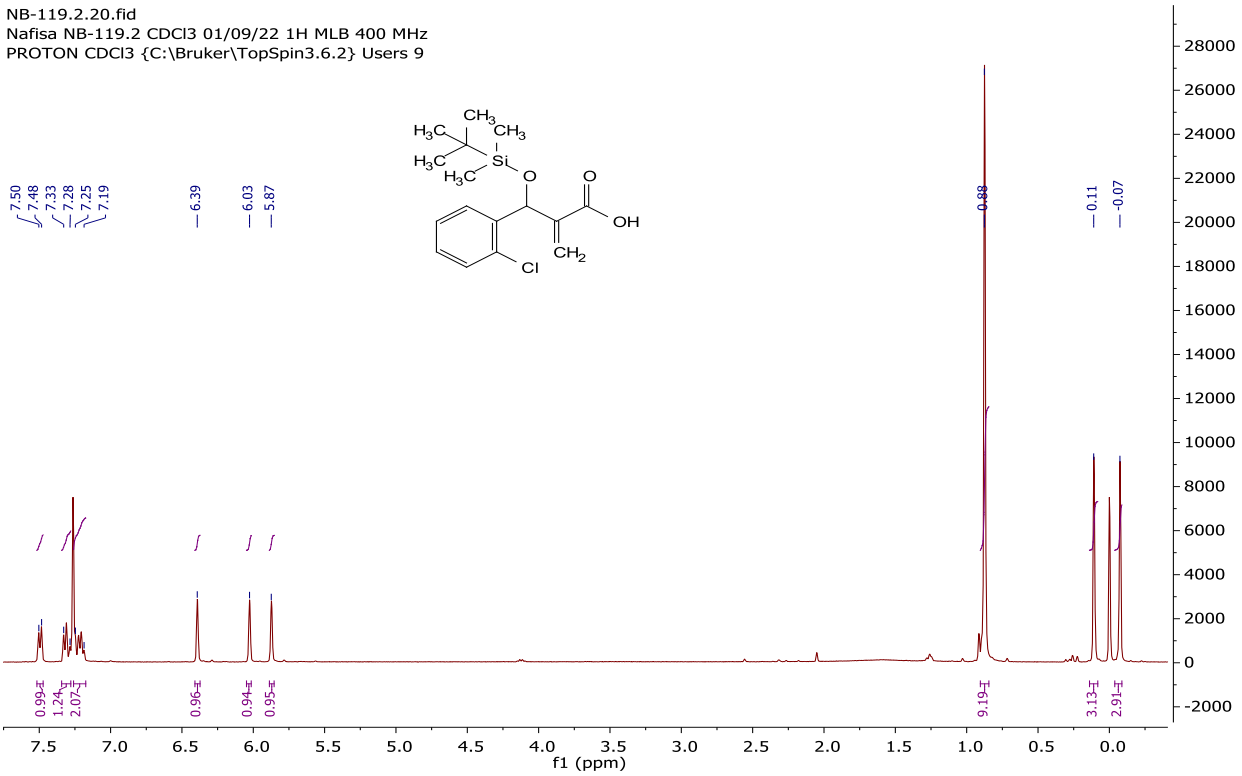
NB-119.2.20.fid
Nafisa NB-119.2 CDCl3 01/09/22 1H MLB 400 MHz
PROTON CDCl3 {C:\Bruker\TopSpin3.6.2} Users 9
7.50
7.48
7.33
7.28
7.25
7.19
6.39
6.03
5.87
0.88
0.11
-0.07
0.99
1.24
2.07
0.96
0.94
0.95
9.19
3.13
2.91
f1 (ppm)

1745830_N.BHOM_MSc dissertation-1.docx

ORIGINALITY REPORT

16%	11%	15%	8%
SIMILARITY INDEX	INTERNET SOURCES	PUBLICATIONS	STUDENT PAPERS

PRIMARY SOURCES

1	kclpure.kcl.ac.uk Internet Source	3%
2	Memory Zimuwandeyi, Fatima Kola, Andreas Lemmerer, Dean Brady, Amanda L. Rousseau, Moira L. Bode. "PADAM reactions of α-aminoaldehydes: Identity of major and minor diastereomers from the Passerini reaction", Tetrahedron, 2018 Publication	2%
3	core.ac.uk Internet Source	2%
4	Submitted to University of Witwatersrand Student Paper	2%
5	Grabowski, Matthias. "Untersuchungen zu diastereoselektiven En-In-Ringumlagerungsmetathesen und deren Anwendung in der Synthese von Lepadiforminen", Technische Universität Berlin, 2013. Publication	1%

6	Submitted to University of St Andrews Student Paper	1 %
7	Worrall, Christopher. "Atropisomeric Diaryl Ethers.", The University of Manchester (United Kingdom), 2018 Publication	1 %
8	StephenP. Andrews. "Total Synthesis of Five Thapsigargins: Guaianolide Natural Products Exhibiting Sub-Nanomolar SERCA Inhibition", Chemistry - A European Journal, 07/06/2007 Publication	1 %
9	Submitted to Imperial College of Science, Technology and Medicine Student Paper	1 %
10	theses.gla.ac.uk Internet Source	1 %
11	Omid Khalili Arjomandi, Mahboubeh Kavoosi, Hadi Adibi. " Synthesis and enzyme-based evaluation of analogues -tyrosine thiol carboxylic acid inhibitor of metallo-β-lactamase IMP-1 ", Journal of Enzyme Inhibition and Medicinal Chemistry, 2019 Publication	<1 %
12	Garduno Castro, Monserrat Herenia. "Sm(Ii)-Mediated Lactone Cyclisations in Complexity Generating Cascade Reactions.", The	<1 %

University of Manchester (United Kingdom), 2021
Publication

13	Aycock, P. Adam. "Radical Conjugate Addition of N-Heterocycles and Tertiary Amines", Emory University, 2021 Publication	<1%
14	Pathak, R.. "A concise synthesis of novel naphtho[a]carbazoles and benzo[c]carbazoles", Tetrahedron, 20060320 Publication	<1%
15	Fernandez Reina, Daniel. "Photoinduced Generation of Electrophilic Radicals: N-Arylation, N-Cyclisation and Vinylation Reactions.", The University of Manchester (United Kingdom), 2021 Publication	<1%
16	Marchese, Austin D.. "From Palladium to Nickel: The Carboiodination Reaction Forward and Back", University of Toronto (Canada), 2022 Publication	<1%
17	Negru, Mihaela. "Imine von Formyl-[2.2]paracyclophanen und ihre Anwendung in der enantioselektiven Katalyse", 09: Chemie, Pharmazie und Geowissenschaft. 09: Chemie, Pharmazie und Geowissenschaft, 2009. Publication	<1%

Exclude quotes On
Exclude bibliography On
Exclude matches < 8 words